Cell proliferation and glucose transport: the intracellular signal transduction pathways that mediate the early phase of growth factor-stimulated glucose transport

A thesis presented to the University of Glasgow

for the degree of Doctor of Philosophy

Nicola Wendy Merrall

Department of Biochemistry, University of Glasgow

ProQuest Number: 13818551

ProQuest 13818551

Summary

Growth factors stimulate glucose transport; the increase in the rate is biphasic, with the early phase occurring immediately and lasting up to two hours.

3T3-L1 fibroblasts are a murine cell line which express a single facilitative monosaccharide transporter, Glut1. Insulin and platelet-derived growth factor (PDGF) stimulate cell proliferation in 3T3-L1 fibroblasts. These growth factors and the tumour promoter, 4ß-phorbol 12-myristate, 13-acetate (PMA), all stimulate 2-deoxyglucose uptake, in a similar manner. These effects are not additive, so the effects of these ligands on the rate of glucose transport may be mediated by a similar signal transduction pathway.

The role of sn-1,2-diacylglycerol (DAG) and protein kinase C (PKC) in the early phase of insulin-, PDGF- and PMA-stimulated glucose transport was examined in 3T3-L1 fibroblasts. Insulin has no effect on either DAG accumulation or PKC activity, so neither DAG nor PKC is necessary for insulin-stimulated glucose transport. PDGF stimulates both DAG accumulation and PKC activity; however, PDGF-stimulated glucose transport is unaffected by the down-regulation or the inhibition of PKC, so PKC is not necessary for PDGF-stimulated glucose transport. PMA also stimulates both DAG accumulation and PKC activity, and PMA-stimulated glucose transport is abolished by the down-regulation and the inhibition of PKC, so PKC is necessary for PMA-stimulated glucose transport. Thus, a signal transduction pathway involving PKC is not necessary for the early phase of insulin- or PDGF-stimulated glucose transport, but it is necessary for the early phase of PMA-stimulated glucose transport.

The role of mitogen-activated protein kinase (MAPK) in the early phase of insulin-, PDGF- and PMA-stimulated glucose transport was also examined in 3T3-L1 fibroblasts. Insulin, PDGF and PMA stimulate MAPK activity with the same dependancy on PKC as for the increase in the rate of glucose transport. In addition, insulin-, PDGF- and PMA-stimulated activation of MAPK precedes the increase in the rate of glucose transport.

Therefore, given that the activation of MAPK and the increase in the rate of glucose transport have the same dependency on PKC, and that the activation of MAPK precedes the increase in the rate of glucose transport, it is possible that the early phase of growth factor-stimulated glucose transport is mediated by a signal transduction pathway involving MAPK in 3T3-L1 fibroblasts.

Xenopus laevis oocytes also only express Glut1. Insulin-like growth factor-I (IGF-I) stimulates both glucose transport and MAPK activity in *X. laevis* oocytes. Again, the activation of MAPK precedes the increase in the rate of glucose transport.

In addition, the microinjection into *X. laevis* oocytes of recombinant $p42^{mapk}$, purified MAPK kinase (MAPKK) or $p39^{mos}$ fusion protein, results in an increase in the rate of glucose transport. Since $p39^{mos}$ activates MAPKK, which in turn activates MAPK, it seems that components of a signal transduction pathway involving MAPK are able to stimulate glucose transport in *X. laevis* oocytes.

Furthermore, IGF-I-stimulated glucose transport is inhibited by the microinjection of CL100, a protein tyrosine/ threonine phosphatase that is specific for MAPK.

Therefore, given that IGF-I stimulates both glucose transport and MAPK activity, that components of a signal transduction pathway involving MAPK also stimulate glucose transport, and that inhibition of MAPK activity abolishes IGF-I-stimulated glucose transport, it is likely that IGF-I-stimulated glucose transport is mediated by a signal transduction pathway involving MAPK in *X. laevis* oocytes.

The insulin and IGF-I receptors are tyrosine protein kinases of a similar structure, and either ligand can bind to either receptor, so it is likely that insulin- and IGF-I-stimulated glucose transport are mediated by a similar signal transduction pathway.

Therefore, given that it is possible that the early phase of growth factor-stimulated glucose transport is mediated by a signal transduction pathway involving MAPK in 3T3-L1 fibroblasts, that it is likely that IGF-I-stimulated glucose transport is mediated by a signal transduction pathway involving MAPK in *X. laevis* oocytes, and that it is likely that insulin- and IGF-I-stimulated glucose transport are mediated by a similar

signal transduction pathway, it seems that the early phase of insulin-stimulated glucose transport in 3T3-L1 fibroblasts is, in fact, mediated by a pathway involving MAPK.

Furthermore, PDGF, which also binds to a tyrosine protein kinase receptor, has similar effects to insulin on the rate of glucose transport and the activation of MAPK in 3T3-L1 fibroblasts. Therefore, it is also likely that the early phase of PDGF-stimulated glucose transport is also mediated by a signal transduction pathway involving MAPK.

This thesis concludes that the early phase of growth factor-stimulated glucose transport is mediated by a signal transduction pathway involving MAPK.

Acknowledgements

Abbreviations

The abbreviations used are defined in 'Instructions to authors', Biochem J (1993) **289** 1–15. The abbreviations defined below are also used.

AP-1	activator protein-1
ATP[S]	adenosine 5'-[γ-thio]triphosphate
Ch	choline
Ch*P*	phosphocholine
DAG	*sn*-1,2-diacylglycerol
DFP	diisopropyl fluorophosphate
DMEM	Dulbecco's modified Eagle's medium
E 64	*trans*-epoxysuccinyl-L-leucylamido(4-guanidino)-butane
ECL	enhanced chemiluminescence
EGF	epidermal growth factor
ERK	extracellular signal-regulated kinase
FAK	focal adhesion kinase
FGF	fibroblast growth factor
GAP	GTPase-activating protein

Glut (*GLUT*)	facilitative monosaccharide transporter protein (gene)
GNRP	guanine nucleotide-releasing protein
Grb2	growth factor receptor bound protein-2
GSK	glycogen synthase kinase
HBG	Hanks buffered saline with BSA and glucose
HBS	Hanks buffered saline
HRP	horseradish peroxidase
IGF	insulin-like growth factor
Ins(1,4,5)P_3	D-*myo*-inositol 1,4,5-trisphosphate
IRS-1	insulin receptor substrate-1
KRP	Krebs Ringer buffered phosphate
LPA	lysophosphatidic acid
MalE	Maltose binding protein
MalE-Mos	a fusion protein consisting of MalE and p39^{mos}
MAPK	mitogen-activated protein kinase
MAPKAP kinase	MAPK-activated protein kinase
MAPKK	MAPK kinase
MAPKKK	MAPKK kinase

MARCKS	myristoylated alanine-rich C kinase substrate
MEK	MAPK/ ERK kinase
NCS	newborn calf serum
4α-PDD	4α-phorbol 12,13-didecanoate
PDGF	platelet-derived growth factor
PH	pleckstrin homology domain
PKC	protein kinase C
PLA	phospholipase A
PLC	phospholipase C
PLD	phospholipase D
PMA	4ß-phorbol 12-myristate, 13-acetate
PP1$_G$	glycogen-associated protein phosphatase-1
PtdCh	*sn*-1,2-phosphatidyl choline
PtdCh-PLC	*sn*-1,2-phosphatidyl choline-specific phospholipase C
PtdCh-PLD	*sn*-1,2-phosphatidyl choline-specific phospholipase D
PtdIns	*sn*-1,2-phosphatidyl inositol
PtdIns 3'-K	*sn*-1,2-phosphatidyl inositol 3'-kinase
PtdIns(4)P	*sn*-1,2-phosphatidyl inositol 4-phosphate

PtdIns(4,5)P_2 sn-1,2-phosphatidyl inositol 4,5-bisphosphate

PtdIns-PLC sn-1,2-phosphatidyl inositol-specific phospholipase C

PtdOH   phosphatidic acid

RasGAP   p21^{ras}-GTPase activating protein

Sglt (*SGLT*)   active sodium/ monosaccharide transporter protein (gene)

SH   Src homology domain

TAG   triacylglycerol

TBST   Tris buffered saline with Tween-20

TEMED   N, N, N', N'-tetramethylethylenediamine

TRE   phorbol ester responsive element

Contents

2   Materials and methods

3   Characterisation of the early phase of growth factor-stimulated glucose transport in 3T3-L1 fibroblasts

6   The activation of MAPK in *Xenopus laevis* oocytes

Figures

Tables

1   Introduction

1.1   Cell proliferation

1.1.1   The somatic cell cycle

The somatic cell cycle is a complex series of events which culminates in nuclear division
(mitosis) and cytoplasmic division (cytokinesis), producing two daughter cells, each with
an identical complement of chromosomes to the parent cell. The process is highly
coordinated so that cytoplasmic growth and one round of DNA replication are followed
by mitosis then cytokinesis [Johnston et al., 1977]. In mammalian cells, the cell cycle is
divided into the interphase (consisting of the S phase and two gaps of varying length:
G1 and G2), and the M phase. Cytoplasmic growth (the synthesis of new proteins,
membranes and organelles) occurs throughout the interphase. DNA replication occurs
during the S phase. Mitosis and cytokinesis occur during the M phase. In rapidly
dividing human cells, the interphase takes about 24 hours and the M phase about 30
minutes.

1.1.2   Control of the cell cycle

Reasons for control

Cells only divide in specific conditions. If conditions are inappropriate for cell division,
then, after reaching a critical point in G1, the cells exit from the cell cycle and enter a
quiescent state, G0. They remain in G0 until the correct conditions occur; thus the
length of G0 can vary considerably. This critical point is known as START in yeast and
as the restriction point in mammalian cells. Entry and exit from G0 is determined by
the presence or absence of extracellular signals. These signals are different for
unicellular and multicellular organisms.

The survival of a unicellular organism, such as the budding yeast, *Saccharomyces
cerevisiae*, depends on rapid cell division. But, one of the conditions for cell division is
that the cell must have a certain size. Hence, when cells are starved of an essential
nutrient they will not pass through START, and so they enter G0 [Johnston et al., 1977].

In addition, budding yeasts also reproduce by conjugation. Consequently, when cells are exposed to mating pheromones, they enter G0 [Reed, 1991].

The survival of a multicellular organism, such as man, depends on the survival of the organism as a whole. Again, the cells may only divide if they have a certain size. Division also requires a physiologically appropriate time and location, for example, during development or wound repair. Therefore, cell division in multicellular organisms is under greater control than in unicellular organisms, and consequently is influenced by more extracellular signals. These additional signals include growth factors [Pardee, 1974] and anchorage to the extracellular matrix [Folkman and Moscona, 1978]. In the absence of these signals, cells enter G0. Cells will also enter G0 when they touch other cells, a phenomenon known as contact inhibition. Furthermore, cells in multicellular organisms become senescent after a certain number of cell cycles.

Growth factor dependence

Growth factors are secreted by many cell types into the blood stream. Growth factors bind to specific membrane-spanning cell surface proteins which are expressed in a cell-specific manner. These receptors can be divided into groups, based on their structures, reflecting their different modes of action. Class I receptors are heteromers, each subunit having between four and six transmembrane domains. These receptors enclose anion or cation channels which open or close in response to ligand-binding [Barnard, 1992]. Class II receptors are monomers, each monomer having seven transmembrane domains. These receptors have an intracellular domain through which they bind to G proteins that are activated in response to ligand-binding [Hepler and Gilman, 1992]. Class III receptors are either monomers or formed from monomers, each monomer having a single transmembrane domain. These receptors have intrinsic intracellular protein tyrosine kinase or guanylate cyclase domains which are activated in response to ligand-binding [Yarden et al., 1986].

Growth factors are known to bind to G protein-coupled receptors and to tyrosine protein kinase receptors. Examples of growth factors which bind to G protein-coupled receptors include: the phospholipid, lysophosphatidic acid (LPA) [van Corven et al., 1989]; and the neuropeptides, bombesin [Battey et al., 1991] and α-thrombin [Vu et al., 1991]. Examples of growth factors which bind to tyrosine protein kinase receptors include: the

polypeptides, epidermal growth factor (EGF), fibroblast growth factor (FGF), insulin, insulin-like growth factor-I (IGF-I), and platelet-derived growth factor (PDGF) [Yarden et al., 1986].

The binding of a growth factor to its receptor activates signal transduction pathways that stimulate the events of cell division. Some signal transduction pathways will be discussed in later chapters.

Since growth factor receptors are expressed in a cell-specific manner, and growth factors can only bind to their own receptors, a growth factor can only affect certain cell types. Thus, by controlling which growth factors are released, a multicellular organism can control which cell types divide.

Anchorage dependence

Cells are surrounded by the extracellular matrix, a network of macromolecules secreted by members of the connective-tissue cell family {Section 3.1.2}. The extracellular matrix consists of adhesive fibrous proteins, such as fibronectin and laminin, and structural fibrous proteins, such as collagen and elastin, embedded in a polysaccharide glycosaminoglycan gel. The composition of the extracellular matrix depends on its location.

Cells bind to the adhesive proteins in the extracellular matrix and to proteins on the surface of other cells using integrins. Integrins are heterodimeric membrane-spanning proteins that are expressed in a cell-specific manner, and bind specifically to different extracellular proteins and to cytoskeletal proteins [Sastry and Horwita, 1993; Schaller and Parsons, 1993]. Since integrins are expressed in a cell-specific manner, integrins bind specifically to distinct subsets of extracellular proteins, and the composition of the extracellular matrix itself depends on its location, the interaction between extracellular proteins and integrins serves to anchor a particular cell type to a particular location.

Integrins are also involved in signal transduction. The binding of extracellular proteins to integrins induces changes in the intracellular pH, the intracellular free calcium ion concentration, tyrosine phosphorylation of cellular proteins and gene expression [Schaller and Parsons, 1993]. Since integrins have no enzymatic activity, these signals

must arise from intermediary proteins; possible candidates are the non-receptor tyrosine protein kinases: focal adhesion kinase, p125^{FAK}, and Src, p60^{src} [Zachary and Rozengurt, 1992; Schaller and Parsons, 1993].

In addition, growth factors regulate the affinity of integrins for their extracellular ligands [Sastry and Horwita, 1993] and cytoskeleton reorganisation [Ridley and Hall, 1992; Ridley et al., 1992]. Thus, signal transduction pathways may link and integrate the growth factor and anchorage dependence of the cell cycle.

Loss of control

In tumour cells and transformed cultured cells, there is no control of the cell cycle. Consequently, these cells proliferate in the absence of growth factors and anchorage, and do not undergo senescence. In the case of tumour cells, loss of control of the cell cycle usually results from a combination of gene mutations occurring spontaneously, or in response to chemical carcinogens or radiation. Since there are several controlling factors in cell division, loss of control of the cell cycle usually requires four to six mutations; one mutation is not enough. In the case of cultured cells, loss of control of the cell cycle often results from transformation of the cell by a single mutated gene, since cultured cells already contain mutations that enable them to be maintained in culture. These mutations usually occur in the genes encoding proteins that are involved in the regulation of the cell cycle. This can occur in two ways: firstly, proteins that stimulate cell proliferation (the products of proto-oncogenes) become hyperactive (the products of oncogenes) [Bishop, 1985]; or secondly, proteins that inhibit cell proliferation (the products of tumour repressor genes) become inactive [Goodrich and Lee, 1992].

1.1.3   Early events of the cell cycle

The early events of the cell cycle prepare the cell for the increase in biosynthetic activity that leads to cytoplasmic growth and DNA replication, and include: an increase in the rate of transcription of intermediate-early genes [Greenberg and Ziff, 1984; Stumpo and Blackshear, 1986]; an increase in sodium/ proton exchange [Moolenaar et al., 1984a]; an increase in the intracellular free calcium ion concentration [Berridge and Irvine, 1989]; an increase in the phosphorylation of ribosomal protein S6 [Sturgill and Wu, 1991] and increase in the rate of transport of nutrients [Jimenez de Asua and Rozengurt, 1974].

The increase in the rate of glucose transport forms the significant interest in this thesis.

The increase in the biosynthetic activity results in an increase in demand for nutrients such as amino acids, inorganic phosphate, nucleosides and monosaccharides, so an early event of G1 is an increase in the rates of transport of these nutrients [Jimenez de Asua and Rozengurt, 1974]. When quiescent Swiss 3T3 cells are exposed to serum, the rate of glucose transport increases in a biphasic manner {Figure 1.1}. The early phase occurs during the first two hours of exposure to serum, during which the increase in the rate of glucose transport is rapid, reaching a maximum of approximately two fold by 60 to 120 minutes. The late phase occurs during longer exposures to serum, during which the increase in the rate of glucose transport is rapid and maintained over several hours, reaching five to ten fold [Jimenez de Asua and Rozengurt, 1974]. The early phase is independent of protein synthesis, while the late phase is dependent on protein synthesis {Figure 1.1}.

A biphasic increase in the rate of glucose transport is also observed in response to many growth factors, for example: angiotensin II, EGF, thrombin and vasopressin in vascular smooth muscle cells [Low et al., 1992]; connective tissue-activating peptide-III and neutrophil-activating peptide-2 in 3T3-442A fibroblasts [Tai et al., 1992]; bombesin, FGF and PDGF in Swiss 3T3 fibroblasts [Takuwa et al., 1987; Kitagawa et al., 1989]; PDGF in Balb/c 3T3 fibroblasts [Rollins et al., 1988] and tumour necrosis factor-α in 3T3-L1 fibroblasts [Cornelius et al., 1990].

A biphasic increase in the rate of glucose transport is also observed in response to tumour promoters, for example: 4ß-phorbol 12-myristate, 13-acetate (PMA) in Fisher rat 3T3 fibroblasts [Flier et al., 1987].

Figure 1.1   The effect of serum on the rate of deoxyglucose uptake

After incubation of quiescent Swiss 3T3 fibroblasts with foetal calf serum and with (□) or without (o) 10 mg/ml cyclohexïmide, for the times shown, a 10 minute uptake of 2-deoxyglucose was measured [Jimenez de Asua and Rozengurt, 1974]. These results show that growth factor-stimulated glucose transport occurs in a biphasic manner and that the early phase occurs independently of protein synthesis, while the late phase is dependent on protein synthesis.
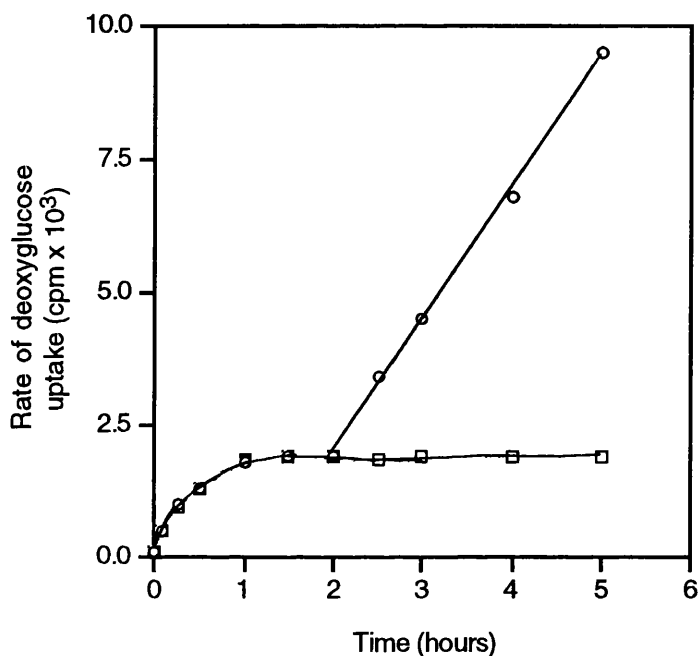
1.2   Monosaccharide transport

1.2.1   Entry of small molecules into cells

Diffusion, passive transport and active transport

Small molecules can pass through a lipid membrane in three ways: firstly, by simple diffusion; secondly, by facilitated diffusion (passive transport); and thirdly, by active transport {Figure 1.2}. The rate of simple diffusion is dependent on the size of the molecule and its relative solubility in non-polar solvents. Non-polar molecules, such as oxygen (32 Da) and small polar molecules, such as water (18 Da) diffuse rapidly across the membrane, while, larger, polar molecules, such as glucose (180 Da), diffuse slowly. Facilitated diffusion and active transport are protein-mediated; facilitated diffusion by facilitative transporter proteins or by channel proteins, and active transport by active transporter proteins. Transporter proteins undergo a conformational change after solute-binding in order to transfer that solute across the membrane. Transport across a membrane will only occur if the solute is able to bind to a transporter protein in that membrane. Channel proteins are water-filled pores that extend across the membrane; when they are open they allow solutes to pass through them. Transport across a membrane will only occur if the solute, which is usually an inorganic ion, has the correct charge and is small enough. These processes are faster than simple diffusion for larger hydrophilic solutes, such as monosaccharides, because the solute passes through the protein instead of the membrane so the size and solubility requirements of the membrane no longer apply. Facilitative transporter proteins and channel proteins, move a solute energetically downhill, across the membrane, that is, down the electrochemical gradient of the solute. However, active transporter proteins move a solute energetically uphill across the membrane, that is, up the electrochemical gradient of the solute. This is achieved by coupling solute transport to another process which is energy yielding and can drive solute uptake. Examples of such processes include the transport of a second solute down its electrochemical gradient, and the hydrolysis of ATP.

Figure 1.2   The movement of monosaccharides across membranes

Monosaccharides can pass through membranes in three ways:
a) Simple diffusion,
b) Facilitated diffusion,
c) Active transport.

The example shown is that of the movement of glucose across the plasma membrane of the epithelia of the small intestine brush border. The facilitative monosaccharide transporter located in the basolateral membrane is Glut2. The active monosaccharide transporter located in the apical membrane is Sglt1.
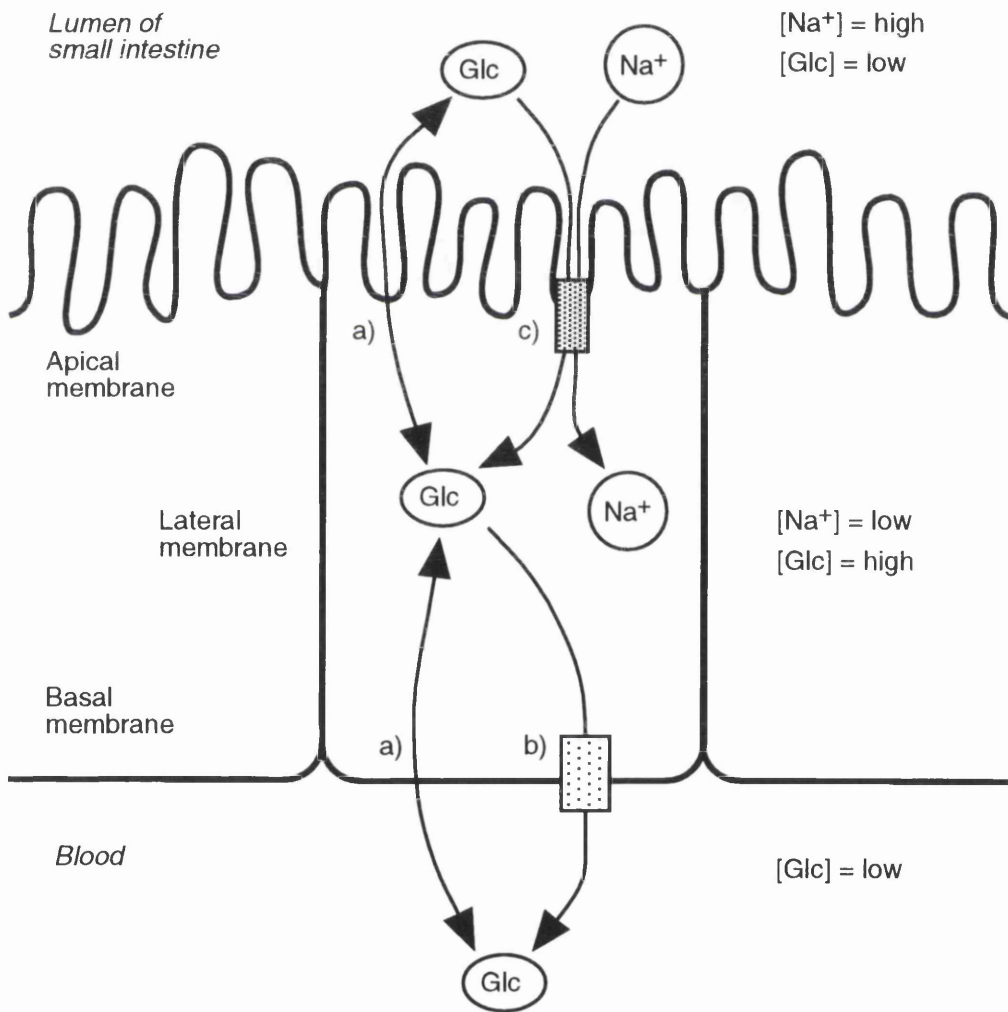
Monosaccharides

Monosaccharides, and glucose in particular, are important nutrients, providing energy for metabolic processes in many organisms. Simple diffusion of monosaccharides is ubiquitous, but is too slow to meet the full energy requirements of the cell. However, facilitated diffusion of monosaccharides, through facilitative transporter proteins is common to most cells, and active transport is common in prokaryotes and some eukaryotes.

1.2.2   Mammalian transporter proteins

The majority of monosaccharides enter mammalian cells by facilitated diffusion, but active transport of monosaccharides also occurs in certain tissues.

Facilitative transporter proteins

To date, seven different genes for mammalian, facilitative monosaccharide transporter proteins have been identified, and are named according to their order of cloning: *GLUT1* [Mueckler et al., 1985; Birnbaum et al., 1986; Asano et al., 1988], *GLUT2* [Fukumoto et al., 1988; Thorens et al., 1988; Asano et al., 1989a], *GLUT3* [Kayano et al., 1988; Nagamatsu et al., 1992], *GLUT4* [Birnbaum, 1989; Fukumoto et al., 1989; James et al., 1989], *GLUT5* and *GLUT6* [Kayano et al., 1990], and *GLUT7* [Waddell et al., 1992]. Six of the seven genes encode proteins, but *GLUT6* is a pseudo-gene, with a DNA sequence most closely related to that of *GLUT3* [Kayano et al., 1990]. Within mammals, the corresponding proteins are expressed in a tissue-specific manner {Table 1.1}, which is preserved across species. Furthermore, the expression of these transporter proteins can vary during development. For example, levels of Glut1 are very high in most foetal tissues, decreasing between 40 to 80 percent in all tissues, except the brain, after birth [Asano et al., 1988]. The levels of other transporter proteins, such as Glut2 and Glut5, increase in their respective tissues during foetal development [Davidson et al., 1992]. Since different tissues have different requirements for monosaccharides, this distribution and variance suggests that the transporter proteins have different functions.

Table 1.1   The major sites of expression of the mammalian facilitative monosaccharide transporters

The data shown was obtained by Western blotting with antibodies which recognise Glut1 [Birnbaum et al., 1986; James et al., 1989; Gould et al., 1992; Nagamatsu et al., 1992]; Glut2 [Davies et al., 1987; Thorens et al., 1988; Orci et al., 1989]; Glut3 [Gould et al., 1992; Nagamatsu et al., 1992; Shepherd et al., 1992]; Glut4 [Fukumoto et al., 1989; James et al., 1989; Zorzano et al., 1989]; Glut5 [Davidson et al., 1992]; and Glut7 [Waddell et al., 1992].

Isoform	Tissues
Glut1	Foetal tissues—cardiac and skeletal myocytes, hepatocytes, brown adipocytes; Adult tissues—erythrocytes, endothelia and epithelia of the blood-tissue barriers (placenta, brain, nerve, retina, kidney, colon); Cultured cells, transformed cells, tumour cells.
Glut2	Pancreatic ß-cells; Hepatocytes (sinusoidal membrane); Epithelia (basolateral membrane) of kidney proximal tubules and small intestine brush border.
Glut3	Brain and neurones (rodents); Brain, neurones, heart, liver and placenta (human).
Glut4	Skeletal and cardiac myocytes; Brown and white adipocytes.
Glut5	Epithelium (apical membrane) of the small intestine brush border; Adipocytes and hepatocytes (low levels in human).
Glut7	Hepatocytes (endoplasmic reticulum membrane).

Active transporter proteins

Two different genes for mammalian, active monosaccharide transporter proteins have been identified, and are named in order of their cloning: Sglt1 [Hediger et al., 1989], and Sglt2 [Wells et al., 1992]. Both encode proteins that are sodium ion/ sugar symporters. Sglt1 is expressed in the apical membranes of the epithelia in the small intestine brush border and, to a lesser extent, the kidney nephron proximal tubule, while Sglt2 is expressed in the apical membranes of the epithelium of the kidney proximal tubule [Hediger et al., 1989; Wells et al., 1992].

The facilitative transporter proteins form the significant interest in this thesis.

Structure of the facilitative transporter proteins

A model, based on analysis of the Glut1 amino acid sequence, has been proposed for the orientation of Glut1 in the plasma membrane [Mueckler et al., 1985]. There are twelve transmembrane α-helical domains arranged so that the hydrophilic amino- and carboxy-termini are both intracellular. The loops between the putative transmembrane domains are very short, usually seven to fourteen amino acid residues long, except for two longer loops, one between transmembrane domains 1 and 2 (the first loop), and another between 6 and 7 (the middle loop). All of the transporter proteins have a single asparagine-linked, heterogeneous oligosaccharide on the first loop [Cairns et al., 1984; Mueckler et al., 1985]. Many of these features have been confirmed using antibodies specific to different regions of the transporter protein [Mueckler et al., 1985; Davies et al., 1987]. It is possible that the constraints imposed by the short loops produce a bilobular structure, consisting of two separate, but close groups of transmembrane helical domains: six nearer the amino-terminal and six nearer the carboxy-terminal. This has been observed using low resolution electron microscopy for lactose permease, which is a structurally related transporter protein from *Escherichia coli* [Li and Tooth, 1987].

There is a high level of amino acid sequence identity between the human, facilitative monosaccharide transporter proteins {Table 1.2}, and the hydropathy plots are mostly superimposable. So, although Glut2 to Glut7 have been less well studied than Glut1, they are predicted to have a similar structure. A comparison of the amino acid residues for the human transporter proteins shows that 26 percent are invariant and 13 percent

Table 1.2   The sequence identity between the mammalian facilitative monosaccharide transporters

The data shown was derived from the amino acid sequences of human Glut1 (492 amino acids) [Mueckler et al., 1985], Glut2 (524 amino acids) [Fukumoto et al., 1988], Glut3 (496 amino acids) [Kayano et al., 1988], Glut4 (509 amino acids) [Fukumoto et al., 1989] and Glut5 (501 amino acids) [Kayano et al., 1990]. The human Glut7 has not been cloned, but rat Glut7 (528 amino acids) has 68% sequence identity to rat Glut2 [Waddell et al., 1992].

Isoform	Glut1	Glut2	Glut3	Glut4
Glut2	55.5			
Glut3	64.0	52.0		
Glut4	65.0	54.0	58.0	
Glut5	42.0	40.0	39.0	42.0

are conservative substitutions [Kayano et al., 1990]. These low variance amino acid residues (the 39 percent) are found mainly in the putative transmembrane domains, while the ones of high variance are found in the amino- and carboxy-termini, and also in the first loop [Kayano et al., 1990]. Glut5 is the most divergent; this is thought to be because it transports fructose rather than glucose. A comparison of the amino acid sequences for the transporter proteins between species shows that their amino acid sequences are also highly conserved (greater than 80 percent sequence identity) [Asano et al., 1988; Gould and Bell, 1990; Nagamatsu et al., 1992].

Kinetics of facilitated transport

The kinetics of facilitated transport can be described in a similar way to the kinetics of enzyme-catalysed reactions. A solute exists in an equilibrium between two compartments, as defined by a membrane; the facilitative transporter protein accelerates the attainment of that equilibrium.

$$T + S_{ext} \underset{k_{-1}}{\overset{k_1}{\rightleftarrows}} TS \xrightarrow{k_2} T + S_{int}$$
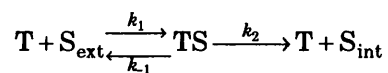
where T is the transporter protein, TS is the transporter-solute complex and S_{ext} and S_{int} are the extracellular and intracellular solutes respectively. The substrates and the products of a biochemical reaction exist in an equilibrium; the enzyme accelerates the attainment of that equilibrium.

$$E + S \underset{k_{-1}}{\overset{k_1}{\rightleftarrows}} ES \xrightarrow{k_2} E + P$$
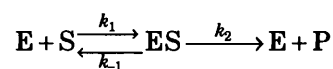
where E is the enzyme, ES is the enzyme-solute complex, S is the substrates and P is the products. However, neither transporter proteins nor enzymes have any effect on the position of the equilibrium point.

Transport is dependent on the solute binding to the transporter protein. At low concentrations of solute, the rate of transport is almost proportional to the solute concentration. At a sufficiently high solute concentration the solute-binding sites become saturated, so the rate of transport reaches a maximum value, equivalent to V_{max}, the maximum rate of an enzyme-catalysed reaction. Transporter kinetics can be described by the Michaelis-Menten equation:

$$V = V_{max} \frac{[S]}{[S] + K_m}$$

where V is the rate of transport, V_{max} is the maximum rate of transport, $[S]$ is the extracellular solute concentration, and K_m is the concentration of solute at which the transport rate is half its maximal value.

Furthermore, facilitated transport is also inhibited by competitive or non-competitive and reversible or irreversible inhibitors. Again, the effects of inhibitors on protein-mediated transport can be described in a similar way to the effects of inhibitors on enzyme-catalysed reactions.

The kinetic properties of the mammalian, facilitative monosaccharide transporter proteins have been analysed by studying their expression in bacteria [Thorens et al., 1988], cultured cells [Asano et al., 1989b] and *Xenopus laevis* oocytes [Birnbaum, 1989; Gould and Lienhard, 1989]. Only the D-enantiomers of glucose, galactose and fructose are transported [Gould and Lienhard, 1989]. D-Glucose is transported by Glut1, Glut2, Glut3, Glut4 and Glut7, D-galactose by Glut1, Glut2 and Glut3, and D-fructose by Glut2 and Glut5 {Table 1.3}. Each transporter protein has a characteristic K_m and V_{max} for each monosaccharide that it is able to transport. The influx K_m and the efflux K_m for the transport of an individual monosaccharide by a single transporter protein may be different. For example, Glut1 is asymmetric with respect to glucose, while Glut2 and Glut4 are symmetric with respect to glucose [Craik and Elliott, 1979; Taylor and Holman, 1981].

The fungal metabolite, cytochalasin B, which binds to all the mammalian transporter proteins, is a competitive inhibitor of glucose efflux mediated by all the transporter proteins [Bloch, 1973]. It is also a non-competitive inhibitor of glucose influx mediated by Glut1, Glut2, Glut3 and Glut4 [Keller et al., 1989; Colville et al., 1993], of fructose influx mediated by Glut2 and of galactose influx mediated by Glut3 [Colville et al., 1993]. However, it has no effect on fructose influx through Glut5 [Burant et al., 1992]. Phloretin is a competitive inhibitor for glucose efflux [Krupka, 1971; Basketter and Widdas, 1978].

Table 1.3   Kinetic parameters of the mammalian facilitative monosaccharide transporters

The data shown was obtained by measuring the zero-*trans* influx of 2-deoxy-D-glucose, galactose and fructose, and the equilibrium exchange of 3-*O*-methyl-D-glucose in *X. laevis* oocytes after microinjection of the mRNAs for Glut1 [Gould and Lienhard, 1989; Keller et al., 1989; Gould et al., 1991; Burant and Bell, 1992; Nishimura et al., 1993], Glut2 and Glut3 [Gould et al., 1991; Burant and Bell, 1992; Colville et al., 1993], Glut4 [Keller et al., 1989; Burant and Bell, 1992; Nishimura et al., 1993] and Glut5 [Burant et al., 1992]. ND: not determined.

Isoform	K_m (mM)			
	2-deoxy-D-glucose	3-*O*-methyl-D-glucose	D-galactose	D-fructose
Glut1	7	17–26	17	Not transported
Glut2	11–17	42	36–86	67
Glut3	1–2	11	6–8	Not transported
Glut4	5	2–4	ND	ND
Glut5	Not transported	ND	ND	6

Functions of monosaccharide transporter proteins

Monosaccharide transporter proteins are important for the homeostatic control of the blood glucose concentration in mammals. Control of the blood glucose concentration is important because, if the concentration is too low, tissues that are highly dependent on glucose (such as the brain) will be damaged (hypoglycaemia), and if it is too high, glucose will be excreted by the kidneys (hyperglycaemia). The blood glucose concentration is controlled by balancing the entry and the exit of glucose from the blood stream.

Under physiological conditions, the blood glucose concentration is between 4.4 and 6.7 mM (80 to 120 mg/ 100 ml). The rate of glucose transport through Glut1, Glut3 and Glut4 is normally at a maximum because each of these transporters has a low K_m for glucose relative to the physiological blood glucose concentration {Table 1.3}, and therefore each is normally saturated with glucose. However, the rate of glucose transport through Glut2 varies proportionally with the blood glucose concentration because it has a very high K_m for glucose relative to physiological blood glucose concentrations {Table 1.3}, and therefore it is not normally saturated with glucose.

During the absorptive state, monosaccharides are absorbed from the lumen of the small intestine into the hepatic portal vein. They enter the epithelial cells of the small intestine by passing through the apical membrane, glucose and galactose via Sglt1 and fructose via Glut5, and leave the epithelial cells by passing through the basolateral membrane, all three via Glut2 {Figure 1.1}. Consequently, the blood glucose concentration rises dramatically. The reabsorption of glucose from the proximal tubule, of the kidney, into the peritubular capillaries occurs in the same way as the absorption of dietary glucose. If the blood glucose concentration is very high, the transporter proteins will be saturated and glucose will be excreted.

In order to prevent excretion, glucose is stored as glycogen by the liver and skeletal muscles and as triacylglycerols (TAG) by adipocytes. The rate of glucose transport into the liver increases proportionally with the blood glucose concentration, since the liver expresses Glut2. The rate of glucose transport increases in adipocytes and skeletal muscle, by 20 to 30 fold and five fold respectively, in response to insulin which is released by the ß-cells of the islets of Langerhans. The insulin is released in response to

high blood glucose concentrations. The insulin-stimulated glucose transport is mainly due to an increase in the rate of transport through Glut4 {Section 1.3.2}. In addition, Glut2 may have a role in insulin secretion, its high K_m enabling the ß-cells of islets of Langerhans to sense changes in the blood glucose concentration [Holz and Habener, 1992].

In the post-absorptive state, glucose is no longer absorbed from the small intestine, the blood glucose concentration is maintained by the efflux of glucose from the liver. Glucose is formed there by glycogenolysis and gluconeogenesis. The last stage of these pathways, the dephosphorylation of glucose-6-phosphate by glucose-6-phosphatase, occurs in the lumen of the endoplasmic reticulum. Glut7, which is expressed in the membrane of the hepatic, endoplasmic reticulum, allows glucose to pass into the cytosol [Waddell et al., 1992]. Glut2, which is kinetically symmetric, allows glucose to leave the liver. Furthermore, the demand for glucose is reduced since most cells obtain energy from alternative sources; however, neurones remain dependent on glucose. During prolonged starvation, when blood glucose concentrations are lower than normal, neurones have priority access to glucose, over other cells, because the K_m, for glucose, of Glut3 is lower than that of Glut1.

Since most cells express Glut1, which is saturated under physiological conditions, the rate of glucose transport into most cells does not increase significantly in response to the higher blood glucose concentrations. However, the rate of glucose transport, through Glut1, is regulated during processes such as cell division and cell differentiation, during which the rate of metabolism increases. For example, growth factors which regulate cell division also stimulate the rate of glucose transport in a biphasic manner {Section 1.1.3}.

1.3 Regulation of monosaccharide transport

1.3.1 Mechanisms

In certain conditions, the rate of glucose transport may be regulated; for example, the rate of transport through Glut1 increases during cell division in response to growth factors {Section 1.1.3}, and the rate of transport through Glut4 increases during the

absorptive state in response to insulin {Section 1.2.2}. There are three mechanisms by which rates of transport may be regulated: firstly, by increasing the number of transporter proteins at the plasma membrane by increasing their translocation from an intracellular location [Suzuki and Kono, 1980]; secondly, by increasing the total number of transporter proteins through increased transcription, greater stability of mRNA, or increased translation; and thirdly, by increasing the activity of transporter proteins, in a manner analogous to the control of enzyme activity by an allosteric or covalent factor [Czech et al., 1992].

1.3.2   Changes in the intracellular location

Cell proliferation: the early phase

The early phase of growth factor-stimulated glucose transport {Section 1.1.3} results from the movement of existing Glut1 from an intracellular site to the plasma membrane [Yang et al., 1992; Yang and Holman, 1993]. For example, when quiescent 3T3-L1 fibroblasts are treated with insulin there is a two fold increase in Glut1 in the plasma membrane, 25 percent of the total Glut1 is present in the plasma membrane in the quiescent cells and 50 percent in insulin-treated cells [Yang et al., 1992]. Translocation of Glut1 also occurs in response to the tumour promoter, PMA, in Swiss 3T3 fibroblasts [Kitagawa et al., 1985].

Glut1 continually recycles between the plasma membrane and an intracellular site in both quiescent and growth factor-treated cells; the changes in the intracellular location result from regulation of the kinetics of endocytosis and, or exocytosis. For example, in 3T3-L1 adipocytes, insulin stimulates Glut1 exocytosis, increasing the rate constant by three fold, but only reduces the rate constant for Glut1 endocytosis slightly [Yang and Holman, 1993].

However, the mechanism by which translocation occurs is not understood and little is known about the signal transduction pathways that mediate the early phase of growth factor-stimulated glucose transport.

Blood glucose homeostasis

Insulin-stimulated glucose transport {Section 1.2.2} results primarily from the movement of Glut4 from an intracellular site to the plasma membrane [Holman et al., 1990], although, skeletal myocytes and adipocytes express both Glut1 and Glut4, and insulin stimulates the rapid movement of both transporters to the plasma membrane [Holman et al., 1990; Slot et al., 1991a,b]. The greater significance of Glut4 for insulin-stimulated glucose transport arises because 95 percent of Glut4 is in an intracellular location in the basal state; that is, it is found in small tubulo-vesicular structures located near the *trans*-Golgi reticulum, as well as near the sarcolemma and transverse tubular system in myocytes [Slot et al., 1991a,b]. Consequently, there is the potential for large increases in the plasma membrane Glut4 level. For example, when brown adipose tissue is treated with insulin there is a 40 fold increase in Glut4 levels in the plasma membrane [Slot et al., 1991b]. In contrast, 20 percent of Glut1 is found in the plasma membrane in the basal state [Yang et al., 1992]; consequently, the maximum possible increase in the plasma membrane Glut1 level is approximately five fold. Furthermore, since Glut4 accounts for 90 percent of the total glucose transporter protein in adipocytes and myocytes [Zorzano et al., 1989], a small increase in the plasma membrane Glut4 level would be equivalent to all of the Glut1 moving to the plasma membrane. However, since Glut4 probably has a higher intrinsic activity than Glut1, it may make an even greater contribution to the insulin-stimulated increase in the rate of glucose transport than can be explained by changes in the intracellular locations alone [Holman et al., 1990].

Glut4 is efficiently sequestered intracellularly in the absence of insulin. This is believed to be determined by a structural feature of Glut4, since the presence of Glut4 alone is sufficient for accurate localisation when expressed in 'non-insulin sensitive' cells such as 3T3-L1 fibroblasts or Hep2 cells [Haney et al., 1991], Chinese hamster ovary cells [Piper et al., 1992], NIH 3T3 fibroblasts [Hudson et al., 1992], PC12 cells [Hudson et al., 1993] and *X. laevis* oocytes [Thomas et al., 1993]. The precise intracellular targeting motif is disputed, with groups assigning it to either an amino-Phe sequence [Piper et al., 1992; Piper et al., 1993] or a carboxy-di-leucine sequence [Verhey and Birnbaum, 1994].

Glut4, like Glut1, recycles constitutively between the plasma membrane and an intracellular location in both quiescent and insulin-treated cells; insulin induces a

redistribution of Glut4 by altering the kinetics of endocytosis and or exocytosis [Czech and Buxton, 1993; Yang and Holman, 1993]. For example, in 3T3-L1 adipocytes insulin stimulates Glut4 exocytosis, increasing the rate constant by nine fold, but only reduces the rate constant for Glut4 endocytosis slightly [Yang and Holman, 1993]. However, the expression of Glut4 in various 'non-insulin sensitive' insulin receptor positive cell types does not lead to insulin-responsive translocation, indicating the need for the expression of additional, and as yet, unidentified gene products to produce this response [Piper et al., 1992; Thomas et al., 1993].

Again, little is known about the signal transduction pathways that mediate the insulin-stimulated increase in the rate of glucose transport in adipocytes and muscle.

1.3.3   Changes in the total transporter level

Cell proliferation: the late phase
The late phase of growth factor-stimulated glucose transport {Section 1.1.3} results from an increase in Glut1 mRNA and concomitantly in Glut1 protein [Hiraki et al., 1988; Rollins et al., 1988; Kitagawa et al., 1989; Mountjoy et al., 1989; Cornelius et al., 1990; Low et al., 1992; Tai et al., 1992]. Growth factors stimulate the rate of transcription of *GLUT1* [Hiraki et al., 1988; Rollins et al., 1988; Kitagawa et al., 1989] and possibly also increase the stability of Glut1 mRNA [Rollins et al., 1988].

GLUT1 has several regulatory elements in the 5'-untranslated region. These include: a phorbol ester responsive element (TRE), three glucocorticoid response elements and four Sp1 hexamers [Williams and Birnbaum, 1988].

The transcription of genes with a TRE increases when the transcription factor activator protein-1 (AP-1) binds to the TRE. Phorbol esters and growth factors stimulate the transcriptional activity of AP-1 [Angel and Karin, 1991]. PMA-stimulated AP-1 activity is dependent on protein kinase C (PKC). Depletion of PKC abolishes the increase in the rate of glucose transport and the level of Glut1 mRNA observed in response to PMA [Hiraki et al., 1988; Mountjoy et al., 1989]. It is likely, therefore, that PMA-stimulated *GLUT1* transcription is mediated by a signal transduction pathway involving PKC that leads to an increase in AP-1 activity. In contrast, depletion of PKC has no effect on the

increase in the rate of glucose transport and the level of Glut1 mRNA observed in response to growth factors [Hiraki et al., 1988; Rollins et al., 1988; Kitagawa et al., 1989] or transformation [Hiraki et al., 1989], suggesting that PKC is not necessary for these responses. However, AP-1 activity can be regulated independently of PKC, by a signal transduction pathway involving mitogen-activated protein kinases (MAPK) {Section 5.1.1}. MAPK is activated in response to many growth factors, and therefore, it is likely that growth factor-stimulated *GLUT1* transcription is mediated by a signal transduction pathway involving MAPK.

Transformation

Transformation of cultured cells by oncogenes results in a loss of control over the cell cycle. This leads to an increase in biosynthetic activity and an increase in demand for nutrients, including glucose. Therefore, an early event during transformation is an increase in the rate of glucose transport which also results from an increase in the level of Glut1 mRNA and therefore Glut1 protein [Birnbaum et al., 1986; Flier et al., 1987].

Transcription of *GLUT1* in response to both growth factors and transformation occurs from the same initiation site [Williams and Birnbaum, 1988], and therefore regulation of transcription of *GLUT1* during normal cell division and transformation appears to be mediated by similar pathways.

Oncogenes, which induce classical morphological transformation, such as v-*fps*, v-*ras* and v-*src*, lead to a four to ten fold increase in the rate of glucose transport; however, oncogenes which promote transformation weakly, such as c-*myc*, have no effect on the rate of glucose transport [Flier et al., 1987]. The normal cellular proteins corresponding to the first group of oncogenes, for example, p21$^{c\text{-}ras}$ and p60$^{c\text{-}src}$, are thought to be involved in the signal transduction pathways that regulate the cell cycle. This further suggests that the regulation of *GLUT1* transcription during normal cell division and transformation is mediated by similar pathways.

1.3.4   Changes in the intrinsic activity

Although, researchers agree that growth factor- and insulin-stimulated glucose transport occur primarily by translocation or by increases in the total transporter level

{Sections 1.3.2 and 1.3.3}, it is possible that there may also be an increase in the intrinsic activity of the transporter proteins [Czech et al., 1992; Yang et al., 1992]. However, the physiological importance of activation is far from clear. There are no direct methods for measuring changes in intrinsic activity, and therefore a role for intrinsic activation is instead inferred when the changes in the intracellular location or the total level of the glucose transporter proteins are not sufficient to account for the whole of the observed increases in the rate of glucose transport.

The use of different cells and techniques for measurements of glucose transporter levels also complicates the issue, and consequently the contribution of changes in the intrinsic activity of transporter proteins to growth factor and insulin-stimulated glucose transport remains uncertain. However, in certain situations it would appear that the intrinsic activity of glucose transporter proteins is regulated. 3T3-L1 fibroblasts and Chinese hamster ovary fibroblasts have similar basal rates of glucose transport. Both express only Glut1; however, there are ten times the number of Glut1 transporters in the plasma membrane of 3T3-L1 fibroblasts than in Chinese hamster ovary fibroblasts. Thus the basal rate of glucose transport appears to be suppressed in 3T3-L1 fibroblasts, perhaps as a result of an inhibitory regulator protein [Harrison et al., 1991].

The intrinsic activity of transporter proteins could be regulated by phosphorylation. Glut1 is a substrate for PKC and undergoes phosphorylation in response to PMA in both 3T3-L1 adipocytes [Gibbs et al., 1986] and human fibroblasts [Allard et al., 1987]. However, there is no change in the phosphorylation state of Glut1 in response to insulin in 3T3-L1 adipocytes [Gibbs et al., 1986] nor in response to PDGF, insulin and EGF in human fibroblasts [Allard et al., 1987], suggesting that phosphorylation has no effect on the intrinsic activity of Glut1.

1.4 Aim

The aim of this work was to establish which signal transduction pathway mediates the early phase of growth factor-stimulated glucose transport. After characterisation of the early phase of insulin and PDGF-stimulated glucose transport in 3T3-L1 fibroblasts, the roles of a signal transduction pathway involving phospholipid hydrolysis and PKC

activation and a signal transduction pathway involving MAPK activation were analysed. Finally, the role of a signal transduction pathway involving MAPK activation in IGF-I-stimulated glucose transport in *X. laevis* oocytes was also analysed.

2 Materials and methods

2.1 Materials

All reagents used were of the highest quality available and were obtained from the following suppliers:

2.1.1 General reagents

Amersham International Plc, Aylesbury, Buckinghamshire, UK
PDGF (BB homodimer, human recombinant)
enhanced chemiluminescence (ECL) Western blotting detection reagents

Bio-Rad Laboratories Ltd, Hemel Hempstead, Hertfordshire, UK
cellophane membrane backing
N, N, N', N'-tetramethylethylenediamine (TEMED)
prestained SDS-PAGE standards (myosin, ß-galactosidase, BSA and ovalbumin)

Boehringer Manheim, Lewes, Sussex, UK
ATP (519 979)

Calbiochem-Novabiochem (UK) Ltd, Nottingham, Nottinghamshire, UK
IGF-I (human recombinant, cell culture grade)
sn-1,2-diacylglycerol (DAG) kinase (*E. coli* recombinant)

Fisons, Loughborough, Leicestershire, UK
acrylamide
ammonium persulphate
chloroform
ethanoic acid
Folin and Ciocalteu's phenol reagent
glucose
glycerol
glycine
Hepes

hydrochloric acid

methanol

N, N' methylene-bis-acrylamide

potassium chloride

SDS

sodium chloride

sodium dihydrogen orthophosphate dihydrate

sodium EDTA

sodium hydrogen carbonate

trichloroacetic acid

Gibco BRL, Paisley, Lanarkshire, UK

Tris base

urea

Hayman Ltd, Witham, Essex, UK

ethanol

Kodak Ltd, Hemel Hempstead, Hertfordshire, UK

RP X-Omat liquid fixer/ replenisher

RP X-Omat liquid developer/ replenisher

X-Omat AR film

Lipid Products, Nutley, Surrey, UK

phosphatidyl serine (grade 1)

Merck Ltd (BDH), Lutterworth, Leicestershire, UK

calcium chloride hexahydrate

calcium nitrate tetrahydrate

dimethyl sulphoxide

magnesium chloride hexahydrate

magnesium sulphate heptahydrate

SG60 pre-coated tlc plates (10 x 20 cm, layer thickness of 0.25 mm)

tetra -sodium pyrophosphate decahydrate

National Diagnostics, Aylesbury, Buckinghamshire, UK

Ecoscint scintillation fluid

Premier Brands UK, Knighton Adbaston, Staffordshire, UK

Marvel powdered milk

Schleicher & Schuell, Dassel, Germany

nitrocellulose membrane (0.45 μM)

Sigma Chemical Company Ltd, Poole, Dorset, UK

BSA (A-7030)

Bromophenol blue

cyclohex imide

cytochalasin B

2-deoxy-D-glucose

digitonin

diisopropyl fluorophosphate (DFP)

dithiothreitol

trans-epoxysuccinyl-L-leucylamido(4-guanidino)-butane (E 64)

imidazole hydrochloride

insulin (porcine monocomponent)

3-*O*-methyl-D-glucose

Pepstatin A

Pipes

protein A-agarose

4ß-phorbol 12-myristate, 13-acetate

4α-phorbol 12, 13-didecanoate (4α-PDD)

sodium ß-glycerophosphate

sodium deoxycholate

sodium EGTA

sodium fluoride

sodium orthovanadate

sn-1-stearoyl-2-arachidonylglycerol

trichloroacetic acid

Triton X-100

Tween-20

Thomson & Joseph, Norwich, Norfolk, UK

tricane methene sulphate (MS 222)

Whatman International Ltd, Maidstone, UK

Whatman P81 ion-exchange chromatography paper

2.1.2   Animals

South African Xenopus Facility, Noordhoek, Republic of South Africa

Female *X. laevis* toads (wild)

2.1.3   Antibodies

Affiniti Research Products Ltd, Nottingham, Nottinghamshire, UK

mouse anti-MAPK monoclonal antibody

mouse anti-p125^{FAK} monoclonal antibody

Amersham International Plc, Aylesbury, Buckinghamshire, UK

horseradish peroxidase (HRP)-conjugated sheep anti-mouse IgG antibody

HRP-conjugated donkey anti-rabbit IgG antibody

Dupont (UK) Ltd, Stevenage, Hertfordshire, UK

^{125}I-conjugated goat anti-rabbit IgG antibody

East Acres Biologicals, Southbridge, Massachusetts, USA

rabbit anti-human Glut1 antibody

Sigma Chemical Company, Poole, Dorset, UK

rabbit anti-mouse IgG antibody

2.1.4 Cells

American Type Culture Collection, Rockville, USA

3T3-L1 fibroblasts

2.1.5 Cell culture media and reagents

Gibco BRL, Paisley, Lanarkshire, UK

Dulbecco's modified Eagle's medium (without sodium pyruvate, with 4500 mg/L glucose)
(DMEM)

10000 U/ml penicillin, 10000 U/ml streptomycin solution

trypsin

Flow Laboratories, Irvine, Ayrshire, UK

new born calf serum (NCS)

2.1.6 Cell culture plastics

AS Nunc, DK Roskilde, Denmark

50 ml centrifuge tubes

6 cm^2 cell culture plates

10 cm^2 cell culture plates

75 cm^3 cell culture flasks

6-well cell culture plates

Bibby Sterilin Ltd, Stone, Staffordshire, UK

sterile pipettes

13.5 ml centrifuge tubes

Corning Glass Works, Corning, New York, USA

6 cm^2 cell culture plates

10 cm^2 cell culture plates

75 cm^2 cell culture flasks

6-well cell culture plates

Costar, Cambridge, Massachusetts, USA

cryotubes

Sartorius AG, Göttingen, Germany

Minisart NML filters (0.2 μm)

2.1.7   Microinjection equipment

Pierce Warriner, Chester, Cheshire, UK

SpectraMesh (08-670-183, size 1000 microns)

Garnier Glass, Claremont, California, USA

glass capillary tubes (internal diameter 0.0285 inches, external diameter 0.048 inches,

length 7.09 inches)

World Precision Instruments, New Haven, Connecticut, USA

PUL-1 system

Drummond Scientific Company, Broomall, Pennsylvania, USA

manual injection pipette (model 3-00-510-X)

Narishige Europe Ltd, Sydenham, London, UK

micromanipulator (model MN-153)

2.1.8   Radioactive materials

Amersham International Plc, Aylesbury, Buckinghamshire, UK

[γ-^{32}P]ATP (PB 108)

3-O-methyl-D-[1-^{3}H]glucose

2-deoxy-D-[2,6-^{3}H]glucose

[^{3}H]thymidine

Dupont (UK) Ltd, Stevenage, Hertfordshire, UK

3-*O*-methyl-D-[1-^{3}H]glucose

2-deoxy-D-[2,6-^{3}H]glucose

^{125}I-conjugated goat anti-rabbit IgG antibody

2.2　Buffers and media

2.2.1　Cell culture media

Serum-free DMEM

100 U/ml penicillin, 100 U/ml streptomycin in DMEM.

0.5% NCS/ DMEM

100 U/ml penicillin, 100 U/ml streptomycin, 0.5% (v/v) NCS in DMEM.

10% NCS/ DMEM

100 U/ml penicillin, 100 U/ml streptomycin, 10% (v/v) NCS in DMEM.

Sterile trypsin solution for cell passage

A solution of 25% (w/v) trypsin in PBS {Section 2.2.2} was filtered through a sterile 2 µM

membrane and stored in 10 ml aliquots in sterile universal tubes at –20°C.

2.2.2　Standard buffers

Barths buffer

88 mM sodium chloride, 2.4 mM sodium hydrogen carbonate, 1.0 mM potassium

chloride, 0.82 mM magnesium sulphate heptahydrate, 0.41 mM calcium chloride

hexahydrate, 0.33 mM calcium nitrate tetrahydrate, 5.0 mM Hepes, pH 7.6.

Barths buffer was autoclaved and stored at room temperature.

DAG mass assay: Incubation buffer

250 mM imidazole pH 6.6, 250 mM sodium chloride, 62.5 mM magnesium chloride hexahydrate, 5.0 mM sodium EGTA.

Hanks buffered saline (HBS)

137 mM sodium chloride, 5.37 mM potassium chloride, 4.20 mM sodium hydrogen carbonate, 1.26 mM calcium chloride hexahydrate, 0.90 mM magnesium sulphate heptahydrate, 0.50 mM magnesium chloride hexahydrate, 0.35 mM sodium dihydrogen orthophosphate dihydrate, pH 7.4.

Hanks buffered saline with BSA and glucose (HBG)

10 mM glucose, 2% (w/v) BSA, 137 mM sodium chloride, 5.37 mM potassium chloride, 4.2 mM sodium hydrogen carbonate, 1.26 mM calcium chloride hexahydrate, 0.90 mM magnesium sulphate heptahydrate, 0.50 mM magnesium chloride hexahydrate, 0.35 mM sodium dihydrogen orthophosphate dihydrate, pH 7.4.

Homogenisation buffer

80 mM sodium ß-glycerophosphate, 20 mM EGTA, 15 mM magnesium chloride, 0.5 mM sodium vanadate.

HPFEV

50 mM Hepes, 100 mM sodium fluoride, 10 mM *tetra*-sodium pyrophosphate decahydrate, 4 mM sodium EDTA, 2 mM sodium orthovanadate, pH 7.4.

HPFEV was stored in a dark bottle at 4°C.

Krebs Ringer buffered phosphate (KRP)

1.37 mM sodium chloride, 4.7 mM potassium chloride, 5.0 mM sodium dihydrogen orthophosphate dihydrate, 1.25 mM magnesium sulphate heptahydrate, 1.25 mM calcium chloride hexahydrate, pH 7.4.

Phosphate buffered saline (PBS)

150 mM sodium chloride, 10 mM sodium dihydrogen orthophosphate dihydrate, pH 7.4.

Protein concentration assay: Reagent A

0.025% (w/v) copper sulphate pentahydrate/ 0.05% (w/v) sodium potassium tartrate/ 2.5% (w/v) sodium carbonate/ 2.5% (w/v) SDS/ 0.2 M sodium hydroxide.

Reagent A was made from equal proportions of a) 0.1% (w/v) copper sulphate pentahydrate/ 0.2% (w/v) sodium potassium tartrate/ 2.5% (w/v) sodium carbonate, b) 10% (v/v) SDS, c) 0.8 M sodium hydroxide and d) water.

Protein concentration assay: Reagent B

A 1:5 dilution of Folin and Ciocalteu's phenol reagent in water.

Protein kinase C activity assay: Intracellular buffer

5.16 mM magnesium chloride hexahydrate, 94 mM potassium chloride, 12.5 mM Pipes, 12.5 mM sodium EGTA, 8.17 mM calcium chloride hexahydrate, pH 7.4.

2.2.3   SDS-PAGE buffers

Electrode buffer

25 mM Tris-base, 192 mM glycine, 0.1% (w/v) SDS.

Sample buffer (for standard use)

93 mM Tris hydrochloride pH 6.8, 20 mM dithiothreitol, 1 mM sodium EDTA, 10% (v/v) glycerol, 2% (w/v) SDS, 0.002% (w/v) Bromophenol blue.

The dithiothreitol was added immediately before use.

Sample buffer (for phosphotyrosine-containing proteins)

93 mM Tris hydrochloride pH 6.8, 20 mM dithiothreitol, 1 mM sodium EDTA, 2.0 mM sodium pyrophosphate, 10% (v/v) glycerol, 2% (w/v) SDS, 0.002% (w/v) Bromophenol blue.

The dithiothreitol was added immediately before use.

Sample buffer (for immunoprecipitation)

8 M urea, 93 mM Tris hydrochloride, pH 6.8, 2.0 mM sodium pyrophosphate, 20 mM dithiothreitol, 10 mM sodium EDTA, 10% (v/v) glycerol, 2% (w/v) SDS, 0.002% (w/v) Bromophenol blue.

The dithiothreitol was added immediately before use.

2.2.4   Protease inhibitor stocks

Pepstatin A
1 mg/ml in DMSO.

E 64
10 mM in 2 mM sodium EDTA.

DFP
200 mM in isopropanol.

All of the protease inhibitor stocks were stored at -20°C.

2.2.5   Western blot buffers

Blot buffer
25 mM sodium dihydrogen orthophosphate dihydrate, pH 6.5.

First wash buffer
150 mM sodium chloride, 5 mM sodium dihydrogen orthophosphate dihydrate, 1 mM sodium EDTA, 0.1% (w/v) Triton X-100, pH 7.4.

Second wash buffer

790 mM sodium chloride, 5 mM sodium dihydrogen orthophosphate dihydrate, 1 mM sodium EDTA, 0.1% (w/v) Triton X-100, pH 7.4.

Towbin buffer

25 mM Tris-base, 192 mM glycine, 20% (v/v) methanol, pH 8.3.

Tris buffered saline with 0.02% Tween-20 (TBST-1)

20 mM Tris, 150 mM sodium chloride, 0.02% (v/v) Tween-20, pH 7.4.

Tris buffered saline with 0.3% Tween-20 (TBST-2)

20 mM Tris, 150 mM sodium chloride, 0.3% (v/v) Tween-20, pH 7.4.

2.3   3T3-L1 fibroblast culture

2.3.1   Growth

3T3-L1 fibroblasts were grown on cell culture flasks and plates containing 10% (v/v) NCS/ DMEM {Section 2.2.1}. The medium was replaced every 2 days. The cells were kept at 37°C in a humidified atmosphere containing 10% CO_2.

2.3.2   Passage

When the cells were subconfluent, they were removed from the plates using trypsin. The medium was replaced with 2 ml of sterile 0.25% (w/v) trypsin in PBS {Section 2.2.2}. When some cells had started to float, a Pasteur pipette was used to loosen the remainder, and the action of the trypsin was stopped by the addition of a small volume of 10% (v/v) NCS/ DMEM {Section 2.2.1}. The cells were then diluted and mixed in a larger volume of 10% (v/v) NCS/ DMEM and seeded onto new cell culture dishes; for example, the cells from a 10 cm^2 plate were seeded onto ten 10 cm^2 plates.

2.3.3   Preparation for experiment

For most experiments, quiescent, confluent cells were required; this was achieved by incubation of the cells in serum-free DMEM {Section 2.2.1} for 3 hours. For other experiments, preparation details are given with the method.

2.3.4   Long term storage

Confluent cells were removed from the plates using trypsin {Section 2.3.2}. The cells from a 75 cm^3 flask were resuspended in 5 ml of 10% (v/v) NCS/ DMEM {Section 2.2.1}, and the suspension was spun at 1000 g at room temperature for 5 minutes; the supernatant was then removed. 10% (v/v) NCS/ DMEM containing 10% (v/v) glycerol was equilibrated in 10% carbon dioxide for 1 hour, and the cell pellet was resuspended in 1 ml of this medium. Aliquots of the suspension were put into cryotubes, packed in cotton wool and frozen overnight at -80°C. The cryotubes were then transferred to liquid nitrogen for long-term storage.

Cells to be recovered from storage were thawed rapidly at 37°C, and then the contents of each cryotube were resuspended in 10 ml of 10% (v/v) NCS/ DMEM on 10 cm^2 plates.

2.4   *Xenopus laevis* maintenance and oocyte preparation

2.4.1   Maintenance

Female *X. laevis* were housed three to an aquarium (22 x 22 x 30 cm) in about 15 cm of distilled water, and had unrestricted access to the surface. The aquariums were kept in a quiet, environmentally controlled room, at a water temperature of 18°C, on a 12 hour light/ dark cycle. The toads were fed, twice a week, on a diet of chopped, raw heart. The water in the aquariums was changed the day after feeding.

2.4.2   Oocyte preparation

Anaesthesia and recovery

Female *X. laevis* were anaesthetised quickly by immersion in 0.15% (w/v) MS222 in a total of 500 ml distilled water supplemented with 25 ml of 0.5 M sodium bicarbonate to counteract the irritant effect of the low pH of MS222. Anaesthesia was complete once the toad was immobile upon being placed on her back, occurring, typically, five to ten minutes after immersion. After surgery, the toad was rinsed in distilled water and placed in an aquarium containing sufficient water to cover the bottom of the tank without covering the toad's nostrils. The exposed skin was moistened periodically. Recovery was complete once full movement had returned, occurring, typically, within one hour of surgery.

Removal of ovarian tissue

The toad was placed on her back, a small slit (about 1 cm) was made in the lower third of the abdominal wall and the inner body cavity was opened gently. An oocyte lobe was located, and a small sample of it was removed. The oocytes were inspected under the microscope, and if healthy, more of the oocyte lobe was taken out and placed into Barths medium {Section 2.2.2} on a 6 cm^2 cell culture plate. The incision was closed with stitches in the inner body wall and the outer dermis. Extracted oocyte lobes were cut into clumps about 5 mm long and placed on clean cell culture plates.

Isolation of individual oocytes

All the dissection procedures were carried out in Barths buffer under a binocular microscope using 10 x 23 magnification eyepieces. A 'swan-necked' light source was used to avoid heating the oocytes directly.

The oocytes isolated were in stages IV or V of development. Such oocytes are the largest, having a distinct boundary between the animal (dark brown) and vegetal (light green/ yellow) poles. The animal pole has uniform pigmentation.

An oocyte lobe consists of a central artery and connective tissue to which the oocytes are attached by a thin translucent stalk. Individual oocytes were removed from the connective tissue by manual dissection. The central artery was held using a pair of fine

watchmakers forceps (INOX size 5), and a second pair of forceps was used to tease out individual oocytes from the connective tissue. Damaged oocytes were discarded immediately to prevent damage to others from the release of proteases. The isolated oocytes were transferred onto a clean cell culture plate for overnight incubation in Barths buffer at 18°C. Again, damaged oocytes and debris were removed.

2.5 Protein preparation for microinjection

Brief details of the preparation of proteins for microinjection are given for completeness; however, they were not carried out by the author, but by others as acknowledged.

2.5.1 Recombinant p42^{mapk}

The cloning, expression and purification of recombinant p42^{mapk} was carried out at the University of Dundee[1]. p42^{mapk} was cloned from a Swiss 3T3 fibroblast cDNA library [Stokoe et al., 1992a]. The full length p42^{mapk} clone was expressed as a glutathione-S-transferase fusion protein in *E. coli*. The fusion protein was then purified by affinity chromatography using glutathione-Sepharose beads, and the p42^{mapk} was cleaved from glutathione-S-transferase using thrombin, producing a p42^{mapk} concentration of 0.06 mg/ml [Stokoe et al., 1992a].

The recombinant p42^{mapk} was maximally activated, to 800 U/mg, by incubation, for 2 hours at 30°C, in 50 mM Tris pH 7.3, 2 mM sodium EDTA, 2 mM sodium EGTA, 5% (v/v) glycerol, 0.3 mM sodium orthovanadate, 0.03% (w/v) Brij 35, 0.1% (v/v) 2-mercaptoethanol, 6 µM specific peptide inhibitor of cyclic AMP-dependent protein kinase containing MAPK kinase (MAPKK) (from purified rabbit skeletal muscle [Nakielny et al., 1992a]), 10 mM magnesium acetate and 0.2 mM adenosine

---

[1] The active recombinant p42^{mapk} was a gift from Professor P Cohen, Medical Research Council Protein Phosphorylation Unit, Department of Biochemistry, University of Dundee, Tayside, UK.

5'-[γ-thio]triphosphate (ATP[S]). The activated p42^{mapk} was then concentrated to an activity of 450 units/ml by centrifugation through a Centricon 30 membrane. The activity of p42^{mapk} is defined on the basis that one enzyme unit catalyses the phosphorylation of 1 nmole of myelin basic protein in 1 minute [Stokoe et al., 1992a].

2.5.2   Purified MAPKK

The purification of MAPKK from rabbit skeletal muscle after intravenous injection of insulin was carried out at the University of Dundee[2] [Nakielny et al., 1992a]. One unit of MAPKK activity is that amount which produces a 50 percent reactivation of MAPK in 1 minute [Nakielny et al., 1992a].

2.5.3   Recombinant p39$^{c\text{-}mos}$

The cloning, expression and purification of recombinant p39$^{c\text{-}mos}$ was carried out at the Imperial Cancer Research Fund Laboratories, South Mimms[3]. The proto-oncogene, c-mos, was cloned from a *X. laevis* cDNA library. The full length c-mos clone was expressed as a fusion protein with the *E. coli* maltose-binding protein (MalE-Mos), in *E coli* [Nebreda and Hunt, 1993]. The fusion protein was then purified by affinity chromatography using an amylose affinity column (amylose specifically binds to the MalE) [Yew et al., 1992].

---

[2] The purified MAPKK was a gift from Professor P Cohen, Medical Research Council Protein Phosphorylation Unit, Department of Biochemistry, University of Dundee, Dundee, Tayside, UK.

[3] The MalE-Mos fusion protein was a gift from Dr A R Nebreda, Imperial Cancer Research Fund, Clare Hall Laboratories, South Mimms, Hertfordshire, UK.

2.6   Microinjection of oocytes

Hollow needles with a diameter of approximately 0.5 µm were made from glass capillary tubes using an automatic needle puller (PUL-1). Each needle was mounted on a manual injection pipette attached to a micro-manipulator. Using a plastic pipette, oocytes were placed on a piece of SpectraMesh attached to a 6 cm^2 cell culture plate, and then, using the glass needle, 50 nl of a water, a buffer or a protein solution {Section 2.5} was injected into the vegetal pole of the oocyte {see Section 2.1.7 for equipment details}.

2.7   DNA synthesis assay

DNA synthesis in 3T3-L1 fibroblasts was assayed by measuring the amount of incorporation of [^{3}H]thymidine [Kitagawa et al., 1989] The fibroblasts were grown on 6-well cell culture plates. After reaching 50% confluence, they were incubated firstly, in 0.5% (v/v) NCS/ DMEM {Section 2.2.1} for 24 hours at 37°C, then secondly, in serum-free DMEM {Section 2.2.1} for 3 hours at 37°C, and thirdly, in serum-free DMEM containing 1 µCi/ml [^{3}H]thymidine and the ligands (as indicated in the figure legends) for 24 hours at 37°C. The incubation was terminated by washing each well twice in 2 ml of ice-cold PBS {Section 2.2.2}. The proteins were precipitated by washing the cells three times in 2 ml of ice-cold 5% (w/v) trichloroacetate and twice in 2 ml of ice-cold ethanol. Finally, the precipitate was dissolved in 1 ml of 0.3 M sodium hydroxide, and Ecoscint was added before the measurement of [^{3}H]thymidine incorporation.

2.8   Glucose transport assays

Transport of a solute is usually assayed using a mixture of the radioactive and the non-radioactive forms. In the case of glucose, a mixture of the radioactive and non-radioactive forms of an analogue is used because the use of glucose is impractical since it is completely metabolised during glycolysis and the tricarboxylic acid cycle. The two most commonly used analogues (and radioactive forms) are 2-deoxy-D-glucose (2-deoxy-D-[2,6-^{3}H]glucose) and 3-O-methyl-D-glucose (3-O-[1-^{3}H]methyl-D-glucose).

41

2-deoxyglucose undergoes only the first step of glycolysis, phosphorylation by hexokinase, forming 2-deoxyglucose-6-phosphate which is trapped inside the cell {Figure 2.1}. Therefore, uptake of 2-deoxyglucose consists of two steps, transport and phosphorylation. Since the K_m of hexokinase for glucose is lower than that of the glucose transporter protein, and ATP pools are not depleted when uptake times are short, glucose transport is usually the rate-limiting step, and so the phosphorylation step can be ignored [Kletzien and Perdue, 1974]. Therefore, deoxyglucose 'uptake' will be taken to mean deoxyglucose 'transport', unless otherwise stated. In addition, the low K_m of hexokinase results in an intracellular deoxyglucose level which is too low for significant efflux, and the equilibrium between the concentrations of extracellular and intracellular deoxyglucose is never reached. As a consequence, assays of the rate of 2-deoxyglucose uptake measure only the influx. 2-deoxyglucose influx occurs with first order kinetics (linear), until the ATP levels have decreased sufficiently to become rate-limiting.

3-O-methylglucose is another glucose analogue used for kinetic studies. It is non-metabolisable, resulting in influx and efflux, and it accumulates until equilibrium is reached {Figure 2.1}. Hence 3-O-methylglucose transport shows first order kinetics initially, then mixed order kinetics, then zero order kinetics when equilibrium has been reached. As a consequence, several different types of assay are possible, two of which are commonly used. Firstly, a zero-*trans* influx assay, which measures the rate of influx of 3-O-methylglucose into sugar-free cells. Influx follows first order kinetics, so the initial velocities can usually be used to estimate the V_{max} and K_m. Secondly, an equilibrium exchange assay, which can be used to overcome the problems where the initial influx occurs too fast for a zero-*trans* influx assay, for instance, when a transporter protein is over-expressed in a cell [Gould et al., 1991]. In such an assay, cells are incubated in various concentrations of unlabelled 3-O-methylglucose, until equilibrium is attained. The addition of labelled 3-O-methylglucose measures the rate of steady-state rate of transport. The transport values are converted to a rate constant (k_{obs}) using the first order rate equation:

$$-k_{obs}t = \ln\frac{[C_\infty - C_0] - [C_t - C_0]}{[C_\infty - C_0]}$$

where C_∞ is the radioactivity after full equilibration of the cellular water space, C_t is the

Figure 2.1   The transport of glucose analogues

a) 2-deoxyglucose undergoes the first step of glycolysis, phosphorylation by hexokinase, forming 2-deoxyglucose-6-phosphate which is trapped inside the cell.
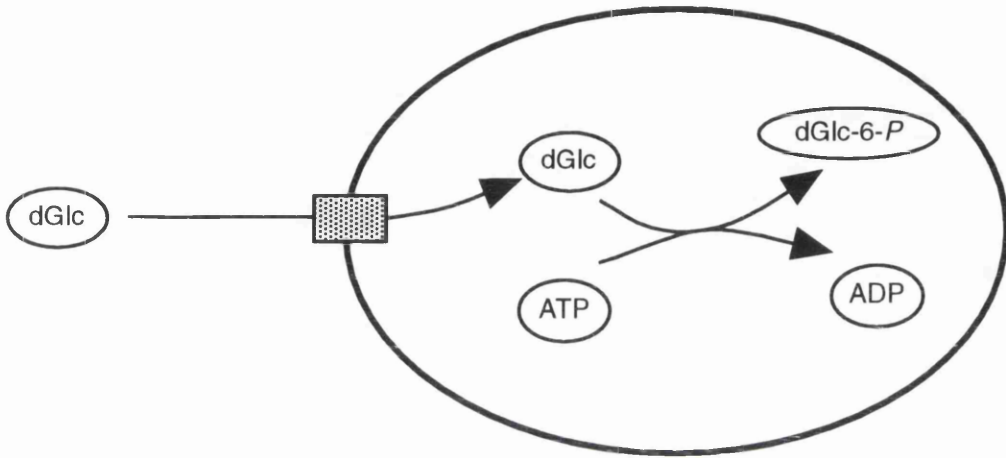
b) 3-*O*-methylglucose is not metabolised, therefore it may enter and leave the cell.
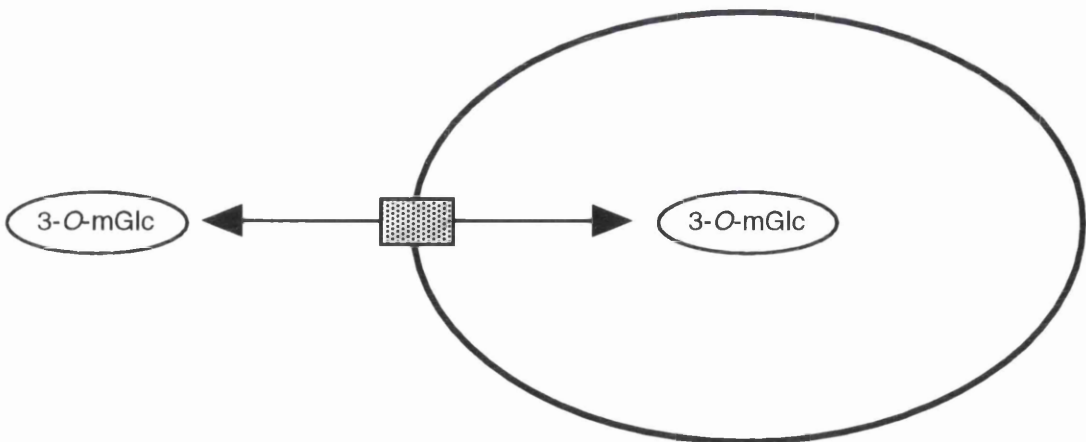
radioactivity at time t and C_0 is the radioactivity at time, 0. The rate constants obtained are used in Lineweaver-Burk plots by plotting $1/k_{obs}$ [3-O-mGlc] against $1/$[3-O-mGlc] to determine the K_m and V_{max} values.

Since a zero-*trans* influx assay measures influx and an equilibrium-exchange assay measures a combination of influx and efflux, the values for K_m and V_{max} produced by these two assays are characteristically different.

2.8.1   2-deoxyglucose uptake assay in 3T3-L1 fibroblasts

The rate of 2-deoxyglucose uptake was assayed in 3T3-L1 fibroblasts [Gibbs et al., 1988]. Quiescent 3T3-L1 fibroblasts, grown on 6-well plates, were washed three times in 3 ml of KRP {Section 2.2.2} at 37°C, then incubated in 1 ml of 1% (w/v) BSA/ KRP, for 1 hour, on a hotplate at 37°C. The ligands were present for the times indicated in the figure legends. 2-deoxyglucose uptake was started by addition of 50 µl of 2-deoxyglucose (final concentration 100 µM; 0.25 µCi/ml) and was stopped rapidly, after 3 to 5 minutes incubation at 37°C, by inverting the plates to remove the buffer, followed by immersion twice in ice-cold PBS {Section 2.2.2.}. The cells from each well were solubilised in 1 ml of 1% (w/v) Triton X-100, by a 1 hour incubation with agitation, before the addition of Ecoscint and measurement of radioactivity. The uptake values were corrected for the non-specific association of 2-deoxy-D-[2,6-^{3}H]glucose with the cells by subtracting the uptake in the presence of 10 µM cytochalasin B, a potent inhibitor of facilitated glucose transport [Bloch, 1973; Basketter and Widdas, 1978]. Cytochalasin B was present throughout the 1 hour incubation.

2.8.2   2-deoxyglucose uptake assay in *X. laevis* oocytes

The rate of 2-deoxyglucose uptake was assayed in *X. laevis* oocytes [Gould et al., 1991]. Groups of uninjected, buffer-injected or protein-injected oocytes were placed into 13.5 ml centrifuge tubes containing 450 µl of Barths buffer {Section 2.2.2} at room temperature, with the ligands present for the times indicated in the figure legends. 2-deoxyglucose uptake was started by the addition of 50 µl 2-deoxyglucose (final concentration 100 µM, 0.5 µCi per tube) and stopped rapidly, after a 1 hour incubation at room temperature, by aspiration of the buffer. The oocytes were washed three times in 3 ml of ice-cold PBS

{Section 2.2.2} containing 0.1 mM phloretin [Krupka, 1971; Basketter and Widdas, 1978], then placed into scintillation vials (one oocyte per vial) and solubilised in 0.5 ml of 1% (w/v) SDS by overnight incubation with agitation, before addition of Ecoscint and measurement of radioactivity.

2.8.3   Zero-*trans* 3-*O*-methylglucose transport assay in *X. laevis* oocytes

The rate of 3-*O*-methylglucose zero-*trans* transport was assayed in *X. laevis* oocytes [Gould et al., 1991]. Groups of uninjected, buffer-injected or protein-injected oocytes were placed into 13.5 ml centrifuge tubes containing 450 µl of Barths buffer {Section 2.2.2}, for 1 hour, at room temperature. 3-*O*-methylglucose transport was started by the addition of 50 µl 3-*O*-methylglucose (final concentration 100 µM, 1.0 µCi per tube) and stopped rapidly, after incubation of times between 0 and 8 hours, at room temperature, by aspiration of the buffer. The oocytes were washed three times in 3 ml of ice-cold PBS {Section 2.2.2} containing 0.1 mM phloretin, then placed into scintillation vials (one oocyte per vial) and solubilised by overnight incubation in 0.5 ml of 1% (w/v) SDS with agitation before the addition of Ecoscint and measurement of radioactivity.

2.9   DAG mass assay

2.9.1   Lipid extraction

Total cellular lipids were extracted by a modification of the Bligh and Dyer lipid extraction, in which cellular extracts are dissolved in a monophase and then the organic and aqueous components separated between two phases [Bligh and Dyer, 1959]. Quiescent 3T3-L1 fibroblasts, grown on 6-well plates, were washed three times in 3 ml of HBS {Section 2.2.2} at 37°C, then incubated in 1 ml of HBG {Section 2.2.2} for 1 hour on a hotplate at 37°C. The ligands were present for the times indicated in the figure legends. The incubations were stopped rapidly by aspiration of the buffer then by addition of 500 µl of ice-cold methanol to each well. The cells were triturated and the cell suspension from each well was transferred to a clean 2 ml Teflon capped glass vial. Each well was washed in a further 200 µl of ice-cold methanol and the suspension was

added to the appropriate vial. A chloroform/ methanol (1:1, v/v) mixture was formed by the addition of 700 µl of chloroform to the cell suspension, the monophase was mixed and incubated on ice for 30 minutes. A chloroform/ methanol/ distilled water (1:1:0.8, v/v/v) mixture was formed by the addition of 585 µl of distilled water, the contents of each vial mixed and incubated on ice until two separate phases were seen. The lower phase (organic) of each sample was transferred, using Hamilton syringes, to a clean glass vial and stored overnight under nitrogen.

2.9.2 Quantification

sn-1,2-diacylglycerol (DAG) in mixed micelles was converted to [^{32}P]phosphatidic acid using DAG kinase and the incorporation of ^{23}P was measured [Preiss et al., 1986; Paterson et al., 1991].

Preparation of lipid/ phosphatidyl serine/ Triton X-100 mixed micelles

720 nmoles of phosphatidyl serine was dried under vacuum in 2 ml glass tubes, then solubilised in 1.0 ml of 0.6% (w/v) Triton X-100 by sonication at 4°C until no solid matter remained (approximately 40 minutes). The solution was transferred to a larger glass tube and diluted by adding a further 1.5 ml of 0.6% (w/v) Triton X-100 to form 0.6% (w/v) Triton X-100, 288 µM phosphatidyl serine.

The lipid extracts (Section 2.9.1) were dried under vacuum then solubilised in 50 µl of 0.6% Triton X-100/ 288 µM phosphatidyl serine by sonication at 4°C for 30 minutes.

Conversion to [^{32}P]phosphatidic acid

The reaction was carried out in a total volume of 100 µl of 0.3% (w/v) Triton X-100, 144 µM phosphatidyl serine, 50 mM imidazole hydrochloride pH 6.6, 50 mM sodium chloride, 12.5 mM magnesium chloride hexahydrate, 1 mM sodium EGTA, 10 mM dithiothreitol, 0.5 mM ATP (20 µCi/ mmol [γ-^{32}P]ATP) and 5 mU DAG kinase. This was achieved by addition of 20 µl of Incubation buffer (Section 2.2.2), 10 µl of fresh 100 mM dithiothreitol and 10 µl of DAG kinase (5 mU) to each vial. The reaction was started by the addition to each vial of 10 µl of 5 µM ATP in 100 mM imidazole, pH 6.6, containing 1.25 µCi [γ-^{32}P]ATP, the contents mixed and incubated for 30 minutes at 30°C. The reaction was stopped by the addition of 470 µl of a chloroform/ methanol/ hydrochloric

acid (15:30:2, v/v) mixture, and then left to stand for 10 min at room temperature. The phases were split by the addition of 150 µl of chloroform followed by 1 ml of distilled water. The upper (aqueous) phase was removed and the lower (organic) phase was washed twice in 1.0 ml of distilled water before being dried under vacuum. The dried lipids were dissolved in 40 µl of a chloroform/ methanol (19:1, v/v) mixture and spotted onto a 10 x 20 cm Silica Gel 60 tlc plate, previously activated by heating at 120°C for 1 hour. The plates were developed with a chloroform/ methanol/ ethanoic acid (130:30:15, v/v/v) mixture, then air-dried and autoradiographed. The area of silica corresponding to [^{32}P]phosphatidic acid was scraped into a scintillation vial to which Ecoscint was added before measurement of radioactivity.

A standard curve (0 to 2000 pmoles) was constructed from 100 mM sn-1-stearoyl-2-arachidonylglycerol in chloroform. This was treated in the same manner as the samples and was used to calculate the DAG level in each sample {Figure 2.2}.

2.10   Protein kinase C activity assay

Protein kinase C (PKC) activity was assayed by phosphorylation of a synthetic peptide substrate in permeablised cells [Heasley and Johnson, 1989; Alexander et al., 1990]. Quiescent 3T3-L1 fibroblasts, grown on 6-well plates, were washed twice in 3 ml of KRP {Section 2.2.2} at 37°C then incubated in 1 ml of 1% (w/v) BSA/ KRP for 1 hour on a hotplate at 37°C. The ligands were present for the times indicated in the figure legends. The cells in each well were washed quickly in 1 ml of Intracellular buffer {Section 2.2.2} at 37°C, and then incubated, with occasional agitation, in 500 µl of Intracellular buffer containing 250 µM ATP, 1.0 µCi [γ-^{32}P] ATP, 200 µg/ml digitonin, and 200 µM PKC peptide substrate (sequence Pro-Leu-Ser-Arg-Thr-Leu-Ser-Val-Ala-Ala-Lys-Lys)[4] [House et al., 1987] for 10 minutes on a hotplate at 37°C. Reactions were stopped by the addition of 100 µl of 25% (w/v) trichloroacetic acid, the wells agitated, then incubated on

---

[4] The PKC peptide substrate was a gift from Dr F G Rowan, Strathclyde Institute for Drug Research, University of Strathclyde, Glasgow, Strathclyde, UK.

Figure 2.2   A standard curve for the DAG mass assay

sn-1-stearoyl-2-arachidonylglycerol was used to construct a standard curve (from 0 to 2000 pmoles) for the DAG mass assay {Section 2.9.2}. Each result shows the mean DAG mass level (± SD) for triplicate determinations. The SD for some of the results from this experiment are too small to be seen on the graph. A standard curve was prepared with each experiment.
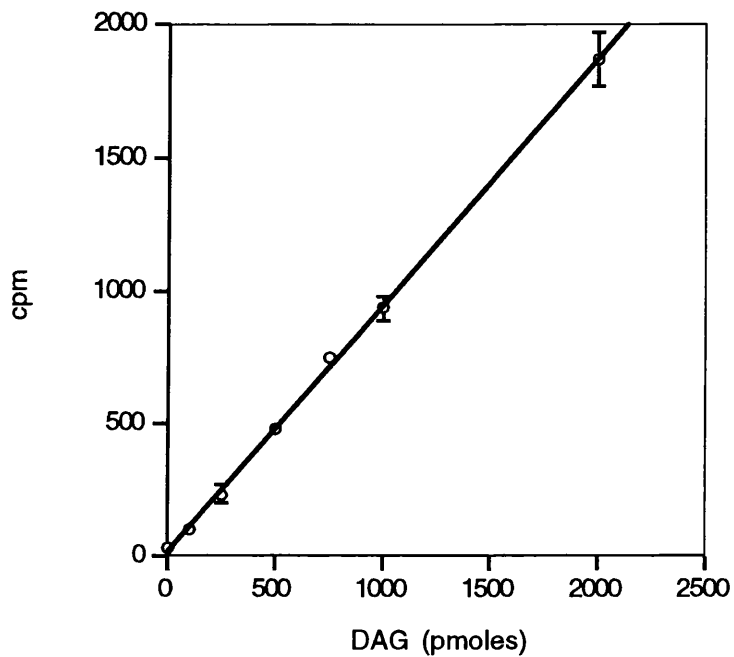
ice for 10 minutes. The cells were scraped off the plates, transferred to an Eppendorf tube and spun for 10 minutes at 4°C at 16 000 g. 100 µl of the supernatant was spotted onto 3 x 3 cm squares of P81 ion-exchange chromatography paper, then air-dried. The paper was washed three times in 75 mM orthophosphoric acid, then once in ethanol with agitation. The paper was dried and the associated radioactivity determined.

2.11   Down-regulation of protein kinase C

PKC activity was down-regulated by a long incubation in a high concentration of an active phorbol ester [Blackshear et al., 1985]. Quiescent 3T3-L1 fibroblasts, grown on 6-well plates, were incubated in sterile 1% (w/v) BSA/ serum-free DMEM {Section 2.2.1} containing 1 µM PMA or 1 µM 4α-PDD (4α-phorbol 12, 13-didecanoate) (an inactive phorbol ester) for 16 hours at 37°C. Each well was washed four times in 2 ml of 1% BSA/ serum-free DMEM at 37°C, and then three times in 3 ml of KRP {Section 2.2.2} at 37°C. The cells were then used for 2-deoxyglucose uptake assays or for the preparation of cell lysates.

2.12   Inhibition of protein kinase C activity

PKC activity was inhibited using a bisindolylmaleimide, Ro 31-8220[5] [Davis et al., 1989; Wilkinson et al., 1993]. Quiescent 3T3-L1 fibroblasts, grown on 6-well plates, were washed three times in 3 ml of KRP {Section 2.2.2} at 37°C, and then incubated in 1 ml of 1% (w/v) BSA/ KRP containing 1 µM Ro 31-8220 for 20 minutes on a hotplate at 37°C. Cells were then used for 2-deoxyglucose uptake assays.

---

[5] The PKC inhibitor, Ro 31-8220, was a gift from Dr G Lawton, Roche Products Ltd, Welwyn Garden City, Hertfordshire, UK.

2.13   Protein preparation for Western blotting

2.13.1   Preparation of 3T3-L1 fibroblast membrane proteins

Quiescent 3T3-L1 fibroblasts, grown on 10 cm^2 plates, were washed three times in 5 ml
of KRP {Section 2.2.2} at 37°C, then incubated in 3 ml of 1% (w/v) BSA/ KRP for 1 hour
on a hotplate at 37°C. The ligands were present for the times indicated in the figure
legends. The incubations were terminated by washing three times in 3 ml of ice-cold
PBS or HPFEV (for phosphotyrosine-containing proteins) {Section 2.2.2}. The cells were
scraped into 4 ml of ice-cold PBS (or HPFEV) containing 1 µg/ml Pepstatin A, 10 µM
trans-epoxysuccinyl-L-leucylamido(4-guanidino)-butane (E 64) and 200 µM diisopropyl
fluorophosphate (DFP) {Section 2.2.4}. The cell lysates were homogenised by sonication,
three times for 10 seconds with 15-second gaps, at 60 W using a Dawe sonicator with a
microtip (Lucas Dawe Ultrasonics Ltd, London, UK; model number: 7532-1), then spun
at 1000 g for 10 minutes at 4°C. The supernatants were transferred to clean centrifuge
tubes and the pellets (nuclei) discarded. The supernatants were spun at 100 000 g for
1 hour at 4°C and the resulting supernatant discarded. The pellets containing the
membrane proteins were resuspended in 200 µl PBS containing 1 µg/ml Pepstatin A,
10 µM E 64 and 200 µM DFP. The samples were snap-frozen in liquid nitrogen and
stored at -80°C.

Before use in SDS-PAGE, the protein concentration of each sample was measured
{Section 2.14}. Each sample was then diluted with 4 x SDS-PAGE sample buffer
{Section 2.2.3} containing 1 µg/ml Pepstatin A, 10 µM E 64 and 200 µM DFP.

2.13.2   Preparation of 3T3-L1 fibroblast lysates

Quiescent 3T3-L1 fibroblasts, grown on 6-well plates, were washed three times in 3 ml
of KRP {Section 2.2.2} at 37°C, then incubated in 1 ml of 1% (w/v) BSA/ KRP for 1 hour
on a hotplate at 37°C. The ligands were present for the times indicated in the figure
legends. The incubations were terminated rapidly by inverting the plates to remove the
buffer; the cells were then washed twice by immersion in ice-cold PBS {Section 2.2.2} (or
ice-cold HPFEV {Section 2.2.2} for phosphotyrosine-containing proteins). The remaining

buffer was aspirated and 750 μl of hot (70°C) SDS-PAGE sample buffer {Section 2.2.3} containing 1 μg/ml Pepstatin A, 10 μM E 64 and 200 μM DFP {Section 2.2.4} was added to each well. The DNA was sheared by drawing the lysate five times through a 21 gauge needle. The samples were transferred to Eppendorf tubes, then boiled for 5 minutes. The samples were snap-frozen in liquid nitrogen and stored at -80°C.

2.13.3   Immunoprecipitation of phosphotyrosine-containing proteins from 3T3-L1 fibroblasts

Lysate preparation

Quiescent 3T3-L1 fibroblasts, grown on 10 cm^2 plates, were washed three times in 5 ml KRP {Section 2.2.2} at 37°C then incubated in 4 ml of 1% (w/v) BSA/ KRP for 30 minutes on a hotplate at 37°C. The ligands were present for the times indicated in the figure legends. The incubations were terminated by washing three times in 4 ml ice-cold HPFEV {Section 2.2.2}. The cells were scraped into 5 ml of ice-cold 0.05% (w/v) SDS/ 2% (w/v) Triton X-100/ HPFEV containing 1 μg/ml Pepstatin A, 10 μM E 64 and 200 μM DFP {Section 2.2.4}. The lysates were spun at 100 000 *g* for 30 minutes at 4°C. The supernatants were transferred to new Eppendorf tubes, snap-frozen in liquid nitrogen and stored at -80°C.

Immunoprecipitation

The phosphotyrosine-containing proteins were immunoprecipitated by incubating the supernatants with 50 μl of a rabbit anti-phosphotyrosine antibody[6] [Pang et al., 1985] for 2 hours on ice then adding 50 μl of 50% Protein A-agarose in 1% (w/v) Triton X-100, and slowly rotating for 2 hours at 4°C. The tubes were spun for 10 seconds at 12 000 *g* and the supernatant discarded. The beads were washed three times in 1 ml of 1% (w/v) Triton X-100/ HPFEV, then once in 1 ml of 0.1% (w/v) Triton X-100/ HPFEV, then resuspended in 100 μl of 1.3 x SDS-PAGE sample buffer for immunoprecipitation {Section 2.2.3} containing 1 μg/ml Pepstatin A, 10 μM E 64 and 200 μM DFP. The

---

[6] The rabbit anti-phosphotyrosine antibody was a gift from Dr G Lienhard, Dartmouth Medical School, Hanover , New Hampshire, USA.

suspensions were incubated at room temperature for 30 minutes, then the tubes were spun for 30 seconds at 12 000 g, and the supernatant was transferred to new Eppendorf tubes, snap-frozen in liquid nitrogen and stored at -80°C.

2.13.4 Preparation of *X. laevis* oocyte lysates

Lysates were prepared from groups of five uninjected oocytes [Nebreda and Hunt, 1993]. The oocytes were placed into 13.5 ml centrifuge tubes containing 500 µl of Barths buffer {Section 2.2.2}, then incubated for 1 hour at room temperature. The ligands were present for the times indicated in the figure legends. The incubations were terminated rapidly by aspirating the buffer then washing twice in ice-cold HPFEV {Section 2.2.2}. Each group of five oocytes was homogenised in 250 µl of ice-cold Homogenisation buffer {Section 2.2.2} containing 1 µg/ml Pepstatin A, 10 µM E 64 and 200 µM DFP {Section 2.2.4}. The lysates were spun for 8 minutes at 12 000 g, and the cleared supernatant was transferred to clean Eppendorf tubes and diluted with 50 µl of 2 x SDS-PAGE sample buffer for phosphotyrosine-containing proteins {Section 2.2.3} containing 1 µg/ml Pepstatin A, 10 µM E 64 and 200 µM DFP. The samples were snap-frozen in liquid nitrogen and stored at -80°C.

2.14 Protein concentration assay

The protein concentration of 3T3-L1 fibroblast membrane proteins {Section 2.13.1} was assayed after acid precipitation [Lowry et al., 1951; Peterson, 1977]. The volume of each protein sample was brought to 1 ml using the same buffer as in the preparation, then 100 ml of 0.15% (w/v) sodium deoxycholate was added to each tube, the contents of each tube were mixed, then incubated at room temperature for 10 minutes. 100 µl of 72% (w/v) trichloroacetic acid was added to each tube, the contents of each tubes were mixed, and the precipitates were collected by spinning at 3000 g for 15 minutes at 4°C. The supernatants were discarded and the tubes drained. The pellets were resuspended in 200 µl of distilled water and 200 µl of Reagent A {Section 2.2.2} added, the contents of each tube mixed, then incubated at room temperature for 10 minutes. 100 µl of Reagent B {Section 2.2.2} was added, the contents of each tube mixed and the absorbance (A_{750}) measured after 30 minutes incubation at room temperature. The

concentration of the sample proteins was determined from a standard curve (from 0 to 20 µg) constructed from 1 mg/ml BSA and treated in the same manner as the protein samples of unknown concentration {Figure 2.3}.

2.15 Discontinuous SDS-polyacrylamide gel electrophoresis

Protein samples {Section 2.13} were analysed using a discontinuous system [Laemmli, 1970].

2.15.1 Preparation of acrylamide gels

Acrylamide stock solution

The separating and stacking gels were made using an acrylamide/ N, N'-methylene-bis-acylamide (22.6% T, 2.66% C) stock solution, where the total monomer concentration, %T, was defined as:

$$\%T = \frac{\text{mass of acrylamide} + \text{mass of crosslinker}}{\text{total volume}} \times 100$$

and the crosslinker concentration, %C, was defined as:

$$\%C = \frac{\text{mass of crosslinker}}{\text{mass of acrylamide} + \text{mass cross linker}} \times 100$$

Separating gels

The separating gels used were of the following composition: 10% (w/v) acrylamide, 0.375 M Tris-hydrochloride, 0.1% (w/v) SDS, 0.05% (w/v) ammonium persulphate, 0.05% (v/v) N, N, N', N'-tetramethylethylenediamine (TEMED).

The casting apparatus for either the Bio-Rad mini-protean II dual slab cell electrophoresis unit (mini-gel: 7 x 8 cm) or the Hoefer SE 600 vertical slab electrophoresis unit (large gel: 14 x 16 cm) was assembled according to the manufacturers instructions.

Figure 2.3   A standard curve for the Lowry protein concentration assay

BSA was used to construct a standard curve (from 0 to 20 µg) for the Lowry protein concentration assay {Section 2.13}. Each result shows the mean protein concentration (± SD) for triplicate determinations. A standard curve was prepared with each experiment.
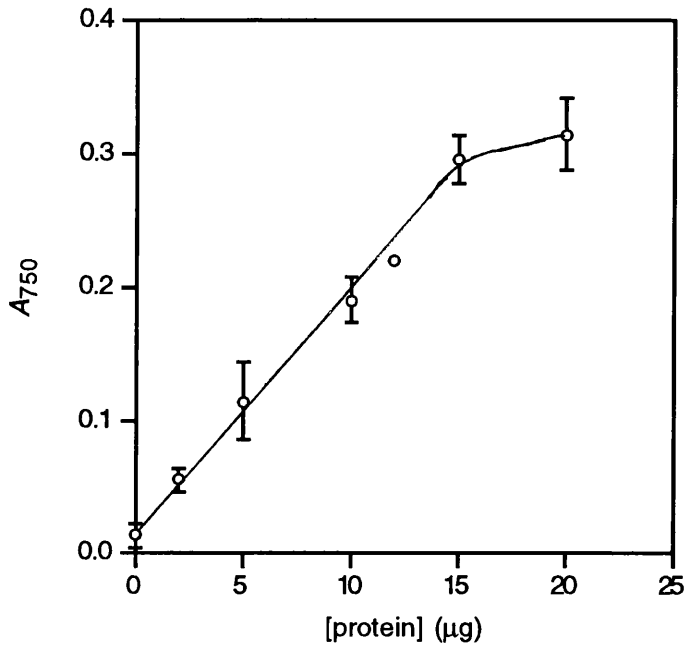
The monomer solution for the separating gel of two mini-gels was prepared by mixing 2.98 ml of distilled water, 2.5 ml of 1.5 M Tris hydrochloride pH 8.8, 4.42 ml of acrylamide stock, 50 µl of 20% (w/v) SDS. Polymerisation was initiated by the addition of 50 µl of fresh 10% (w/v) ammonium persulphate and 5 µl of TEMED, the solution mixed, then poured into the casting apparatus.

The monomer solution for the separating gel of two large gels was prepared by mixing 14.9 ml of distilled water, 12.5 ml of 1.5 M Tris hydrochloride pH 8.8, 22.1 ml of acrylamide stock and 250 µl of 20%(w/v) SDS. Polymerisation was initiated by the addition of 250 µl of fresh 10% (w/v) ammonium persulphate and 25 µl of TEMED, the solution mixed, then poured into the casting apparatus.

The monomer solution was carefully overlaid with water-saturated isobutanol to obtain a smooth surface . After polymerisation, the overlay was removed and the gel surface washed thoroughly with distilled water. Combs were placed in position.

Stacking gels

The stacking gels used were of the following composition: 5% (w/v) acrylamide, 0.125 M Tris hydrochloride, 0.1% (w/v) SDS, 0.05% (w/v) ammonium persulphate, 0.1% (w/w) TEMED.

The monomer solution for the stacking gel of two mini-gels was prepared by mixing 4.15 ml of distilled water, 2.0 ml of 0.5 M Tris hydrochloride pH 6.8, 1.77 ml of acrylamide stock and 40 µl of 20% (w/v) SDS. Polymerisation was initiated by the addition of 40 µl of fresh 10% (w/v) ammonium persulphate and 8 µl of TEMED, the solution mixed, then poured into the casting apparatus.

The monomer solution for the stacking gel of two large gels was prepared by mixing 15.6 ml of distilled water, 7.5 ml of 0.5 M Tris hydrochloride, pH 6.8, 6.6 ml of acrylamide stock and 150 µl of 20% (w/v) SDS. Polymerisation was initiated by the addition of 150 of µl fresh 10% (w/v) ammonium persulphate and 30 µl of TEMED, the solution mixed then poured into the casting apparatus.

After polymerisation, the combs were removed and the wells rinsed with distilled water.

2.15.2   Running conditions

Mini gels were subjected to electrophoresis at a constant voltage of 150 V in Electrode buffer {Section 2.2.3} using a Bio-Rad mini-protean II dual slab cell electrophoresis unit.

Large gels were subjected to electrophoresis at a constant current of 15 mA per 1.5 mm thick gel in Electrode buffer {Section 2.2.3} using a Hoefer SE 600 vertical slab electrophoresis unit.

2.15.3   Protein molecular weight standards

The molecular mass of proteins was estimated by comparing their mobility to that of pre-stained SDS-PAGE standards. The standards used were myosin (205 kDa), ß-galactosidase (116.5 kDa), BSA (80 kDa) and ovalbumin (49.5 kDa).

$$R_F = \frac{\text{distance moved by protein}}{\text{distance moved by dye front}}$$

The calculated R_F value obtained for the individual SDS-PAGE standards was plotted against log (molecular mass) to produce a calibration curve from which the molecular mass of the unknown species can be determined by interpolation.

2.16   Western blotting

2.16.1   Mini-gels

Glut1

Glut1 was examined by Western blotting [Towbin et al., 1979] after separation of proteins on 10% mini-acrylamide gels by SDS-PAGE.

The gels were equilibrated by shaking in Blot buffer {Section 2.2.5} for 30 minutes. The proteins were transferred to a nitrocellulose membrane, at a constant current of 250 mA for 3 hours, using a Bio-Rad Mini-Trans-Blot electrophoretic transfer cell. After the

transfer, the non-specific binding sites were blocked by incubation in 3% (w/v) BSA/ First wash buffer {Section 2.2.5} for 30 minutes, then the blots were rinsed in First wash buffer. The blots were incubated overnight in 3% BSA/ First wash buffer containing a 1:1000 dilution of a rabbit anti-human Glut1 antibody that also recognises mouse Glut1[7] [Davies et al., 1987], then washed several times in First wash buffer. The blots were incubated for 3 hours in 3% BSA/ First wash buffer containing 0.1 μCi/ml ^{125}I-conjugated goat anti-rabbit IgG antibody, then washed several times in Second wash buffer {Section 2.2.5}. The blots were dried between two layers of a cellophane membrane backing, then placed next to X-Omat AR film in cassettes with an intensification screen and kept at -80°C for 48 hours. The autoradiographs were developed using a X-Omat processor.

Glut2, Glut3 and Glut4

Glut2, Glut3 and Glut4 were examined by Western blotting after separation of proteins on 10% mini-acrylamide gels by SDS-PAGE.

Western blotting was carried out as above with the following exceptions. The non-specific binding sites were blocked by incubation in 5% (w/v) Marvel/ First wash buffer for 30 minutes. The antibodies were diluted in 1% Marvel/ First wash buffer. Glut2 was detected with a rabbit anti-human Glut2 antibody that also recognises mouse Glut2 [Brant et al., 1992], used at a dilution of 1:66.6; Glut3 was detected with a rabbit anti-mouse Glut3 antibody [Gould et al., 1992] used at a dilution of 1:100 and Glut4 was detected with a rabbit anti-human Glut4 antibody that also recognises mouse Glut4 [Brant et al., 1992], used at a dilution of 1:66.6.

---

[7] The rabbit anti-human Glut1 antibody was a gift from Dr S Baldwin, University of Leeds, Leeds, Yorkshire, UK.

2.16.2   Large gels

Glut1

Glut1 was examined by Western blotting [Towbin et al., 1979] after separation of proteins on 10% large acrylamide gels by SDS-PAGE.

The gels were equilibrated by shaking in Blot buffer {Section 2.2.5} for 1 hour. The proteins were transferred to a nitrocellulose membrane, at a constant current of 250 mA for 3 hours, using a Bio-Rad Trans-Blot electrophoretic transfer cell. After the transfer, the non-specific binding sites were blocked by incubation in 3% (w/v) BSA/ First wash buffer {Section 2.2.5} for 3 hours, then the blots were rinsed in First wash buffer. The blots were incubated overnight in 3% BSA/ First wash buffer containing a 1:1000 dilution of a rabbit anti-human Glut1 antibody that also recognises mouse Glut1 (from East Acres Biologicals), then washed several times in First wash buffer. The blots were incubated for 1 hour in 3% BSA/ First wash buffer containing a 1:4000 dilution of a horseradish peroxidase (HRP)-conjugated donkey anti-rabbit IgG antibody, then washed several times in Second wash buffer {Section 2.2.5}. The blots were submerged in enhanced chemiluminescence (ECL) detection solutions (according to the manufacturers instructions), drained, wrapped in cling-film and exposed to X-Omat AR film for 1 to 5 minutes. The autoradiographs were developed using a X-Omat processor.

Phosphotyrosine-containing proteins

Phosphotyosine-containing proteins were examined by Western blotting after separation of proteins on 10% large acrylamide gels by SDS-PAGE.

Western blotting was carried out as above with the following exceptions. The gels were equilibrated in Towbin buffer {Section 2.2.5} and the proteins were transferred at a constant current of 350 mA. TBST-1 and TBST-2 {Section 2.2.5} were used instead of First and Second wash buffers respectively; the antibodies were diluted in 0.2% BSA/ TBST-1. Phosphotyrosine was detected with a rabbit anti-phosphotyrosine antibody [Pang et al., 1985], used at a dilution of 1:5000, MAPK with a mouse anti-MAPK antibody, used at a dilution of 1:250 000, and p125^{FAK} with a mouse anti-p125^{FAK} antibody, used at a dilution of 1:5000. The anti-MAPK and anti-p125^{FAK} antibodies were detected using a HRP-conjugated sheep anti-mouse IgG antibody.

3 Characterisation of the early phase of growth factor-stimulated glucose transport in 3T3-L1 fibroblasts

3.1   Introduction

In order to examine the signal transduction pathways that mediate the early phase of growth factor-stimulated glucose transport, the effects of insulin and PDGF on the rate of glucose transport in 3T3-L1 fibroblasts were characterised.

3.1.1   Insulin and PDGF

Structure

Insulin and PDGF are both heterodimeric proteins. Insulin is formed from a single polypeptide, proinsulin, by the process of folding, stabilisation by disulphide bonds and proteolysis. In contrast, PDGF is formed from two homologous polypeptides encoded by distinct genes. These polypeptides combine to form three PDGF isoforms, AA, AB and BB; again the dimers are stabilised by disulphide bonds [Waterfield et al., 1983]. The amino acid sequence of the PDGF B-chain is similar to that of the transforming protein product of the Simian sarcoma virus, p28^{v-sis} [Waterfield et al., 1983].

Functions

Insulin is released by the ß-cells of the Islets of Langerhans in response to a high blood glucose concentration. It reduces the blood glucose concentration by stimulating the influx of glucose into myocytes and adipocytes {Section 1.2.2}. It also modifies the activity of many enzymes in these cells, so that the storage products, glycogen and triacylglycerol, are synthesised and not metabolised.

Insulin also stimulates the rate of proliferation of some cells, for example, BC3H-1 myocytes [Standaert et al., 1987], Chinese hamster ovary cells [Wilden et al., 1990], and Rat-1 cells [McClain, 1990].

PDGF is released from the α-granules of platelets during the platelet adherence and aggregation reactions that occur when blood vessels have been injured. It is thought to aid wound repair by stimulating: chemotaxis in monocytes, neutrophils, fibroblasts and vascular smooth muscle cells; the proliferation of fibroblasts and vascular smooth

muscle cells; and the secretion of extracellular matrix constituents [Heldin and Westermark, 1990; Heldin, 1992].

PDGF is also involved in the development of the optic nerve by stimulating the proliferation of O-2A progenitor cells, and by inhibiting their differentiation into type-2 astrocytes or oligodendrites. It is released in the optic nerve by type-1 astrocytes. It may also have other roles in development, since PDGF receptors are expressed in embryonic tissue and placenta [Heldin, 1992].

The three PDGF isoforms may have similar or different effects to each other; for example, all three isoforms stimulate cell proliferation, but only PDGF-BB stimulates chemotaxis [Heldin, 1992].

Receptor structure

Both insulin and PDGF bind to tyrosine protein kinase receptors. The insulin receptor is an heterotetrameric glycoprotein consisting of two α-subunits and two ß-subunits. It is formed from two identical polypeptides, each of which contains a collinear α- and ß-subunit. The precursor becomes the mature receptor by the process of dimerisation, stabilisation by disulphide bonds, proteolysis and glycosylation. The α-subunits are completely extracellular, while each of the ß-subunits has a single membrane-spanning region. Each α-subunit has a single cysteine-rich domain and several other cysteine residues. There are also a few cysteine residues on the extracellular region of the ß-subunit. The intracellular region of the ß-subunit has a tyrosine protein kinase domain {Figure 3.1} [Ebina et al., 1985; Ullrich et al., 1985].

There are two insulin receptor isoforms which differ by a sequence of 12 amino acids near the carboxy-terminus of the α-subunit. These arise from alternative splicing of exon 11 of the insulin receptor gene. The isoforms are expressed in a tissue-specific manner, however, it is not known whether they have different functional roles [Seino and Bell, 1989; Goldstein and Dudley, 1990].

In contrast, there are two distinct receptors for PDGF: the PDGF α-receptor and the PDGF ß-receptor [Yarden et al., 1986; Claesson-Welsh et al., 1989]. These are structurally similar glycoproteins with a molecular mass of 170 to 180 kDa. Both PDGF

Figure 3.1   Tyrosine protein kinase receptors

A schematic representation of the structure of Class I, II and III tyrosine protein kinase receptors before ligand binding, represented by a) the EGF receptor (Class I), b) the PDGF ß-receptor (Class II) and c) the insulin receptor (Class III). The carboxy-termini of Class I and II receptors and of the ß-subunit of Class III receptors are cytosolic. The carboxy-termini of the α-subunits of Class III receptors are near the plasma membrane. Cysteine-rich domains are represented by hatched boxes, other cysteine residues in the extracellular domain are represented by closed circles. Tyrosine protein kinase domains are represented by dotted boxes [Ullrich et al., 1984; Ebina et al., 1985; Ullrich et al., 1985; Ullrich et al., 1986; Yarden et al., 1986].
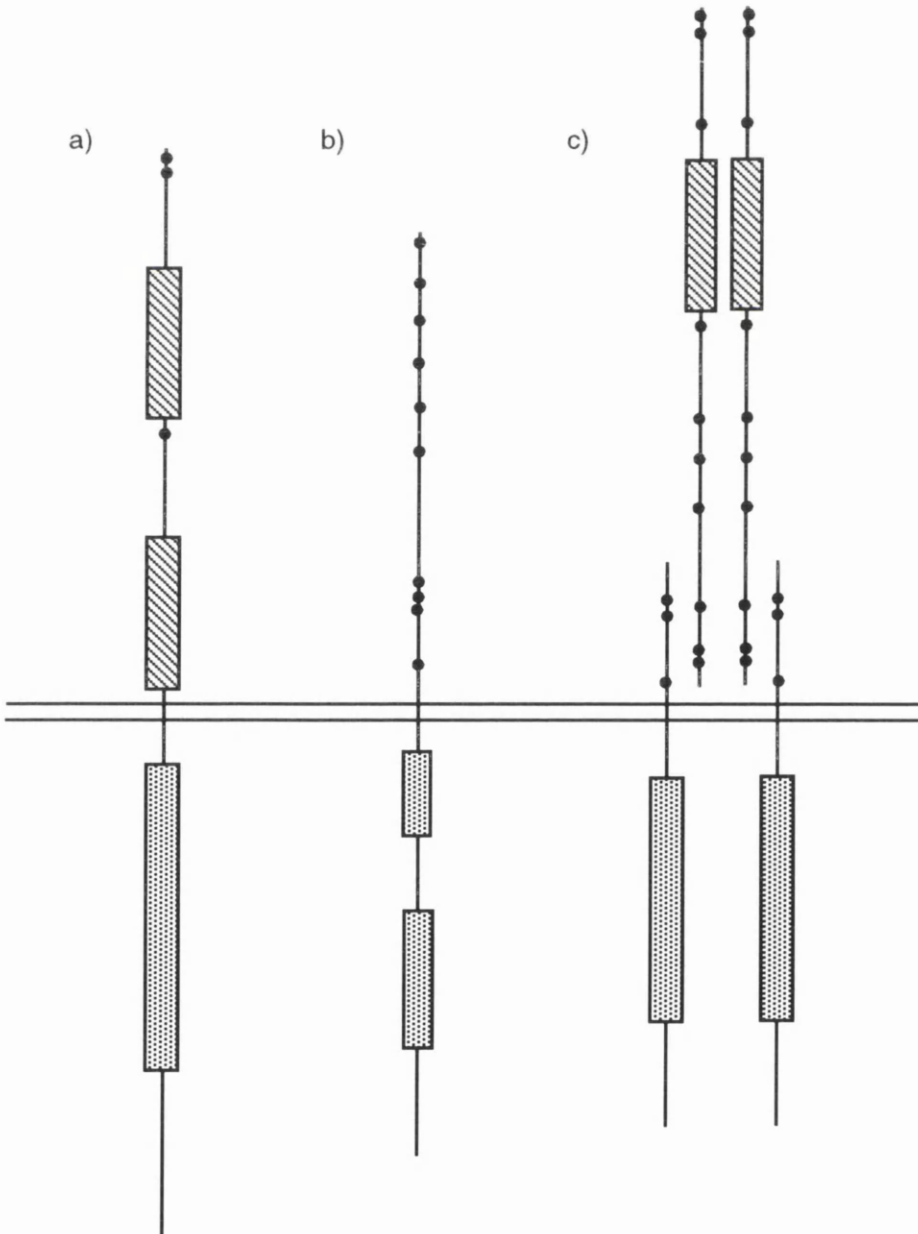
receptors have two extracellular cysteine-rich domains, a single membrane-spanning region and an intracellular tyrosine protein kinase domain, divided into two, by a sequence of approximately 100 amino acid residues known as the kinase insert region {Figure 3.1} [Yarden et al., 1986].

Ligand-binding

Most tyrosine protein kinase receptors must assemble into an oligomeric structure to permit the ligand-induced activation of the intrinsic tyrosine protein kinase. The majority of tyrosine protein kinase receptors, including both of the PDGF receptors, exist as monomers in the absence of ligand-binding. Upon ligand-binding these receptors dimerise, the two PDGF receptors forming all three combinations of receptor dimers, αα, αβ and ββ [Seifert et al., 1989]. The exact receptor dimer formed depends on the PDGF isoform: PDGF-AA forms αα, PDGF-AB forms αα and αβ, and PDGF-BB forms all three [Seifert et al., 1989; Heidaran et al., 1991]. In contrast, as described above, the insulin receptor already exists as an heterotetramer in the absence of insulin-binding, and does not dimerise further.

Following PDGF-induced receptor dimerisation, or the binding of insulin to its receptor, there is a conformational change in the receptor which activates the intrinsic tyrosine protein kinase. This catalyses the tyrosine phosphorylation of both the intracellular region of the receptor (autophosphorylation) [Herrera and Rosen, 1986] and of other substrates [White et al., 1988]. In both cases, the autophosphorylation occurs *in trans*, that is, each tyrosine protein kinase domain catalyses the phosphorylation of the other polypeptide [Kelly et al., 1991].

The tyrosine phosphorylation creates binding sites for cytosolic proteins that contain a sequence motif of approximately 100 amino acids known as a Src homology-2 (SH2) domain [Koch et al., 1991]. Different SH2 domain-containing proteins bind to different phosphotyrosine residues, the specificity arising from the amino acid sequence surrounding the phosphotyrosine residue [Songyang et al., 1993].

In the case of PDGF, the SH2 domain-containing proteins bind directly to phosphotyrosine residues in the receptor dimers. The proteins that are known to bind to the phosphotyrosine residues in the PDGF ß-receptor include: phospholipase C-γ

(PLC-γ) [Meisenhelder et al., 1989; Wahl et al., 1989], the regulatory subunit (p85) of phosphatidylinositol-3'-kinase (PtdIns-3'-K) [Kashishian et al., 1992], the p21^{ras}-GTPase activating protein (RasGAP) [Kazlauskas et al., 1990], members of the Src family of non-receptor tyrosine protein kinases (p60^{src}, p59^{fyn}, and p62^{yes}) [Kypta et al., 1990], the growth-factor receptor bound protein-2 (Grb2) [Lowenstein et al., 1992], and Syp (also known as SH2 domain-containing phosphotyrosine phosphatase-2, SH-PTP2) [Kazlauskas et al., 1993]. The phosphotyrosine residues within the PDGF ß-receptor to which some of these proteins bind have been identified {Figure 3.2}.

In the case of insulin, the SH2 domain-containing proteins do not bind directly to the insulin receptor. Instead, these proteins bind to the major substrate of the insulin receptor, insulin receptor substrate-1 (IRS-1). There are 21 potential phosphotyrosine sites in IRS-1, many of which occur in sequence motifs known to be consensus sequences for the binding of SH2 domain-containing proteins [Sun et al., 1991]. The proteins that bind to IRS-1 include: p85 [Backer et al., 1992a], Grb2 [Skolnik et al., 1993; Sun et al., 1993a], Syp [Kuhné et al., 1993; Sun et al., 1993a], and Nck [Lee et al., 1993]. PLC-γ and RasGAP do not appear to bind to IRS-1 [Lavan et al., 1992; Sun et al., 1993a]. The phosphotyrosine residues to which some of these proteins bind within IRS-1 have been identified {Figure 3.3}.

Beyond the receptor

Many of the SH2 domain-containing proteins are thought to have important roles in the signal transduction pathways that mediate the effects of ligands that bind to tyrosine protein kinase receptors [Heldin, 1991; Koch et al., 1991; Sun et al., 1993b]. The functions of some of these proteins will be discussed later.

The differences in the effects of the various polypeptide growth factors that bind to tyrosine protein kinase receptors may arise, in part, from the differences in the specificity or affinity of receptors for SH2 domain-containing proteins. This could account for the differences in the effects of the three PDGF isoforms; for example, the affinity of the PDGF ß-receptor for RasGAP is five times higher than that of the PDGF α-receptor [Heidaran et al., 1993].

Figure 3.2   The PDGF ß-receptor and the associated SH2 domain-containing proteins

A schematic representation of the specificity of interactions between the different SH2 domain-containing proteins and the known autophosphorylation sites in the PDGF ß-receptor [Kazlauskas and Cooper, 1989; Fantl et al., 1992; Kashishian et al., 1992; Rönnstrand et al., 1992; Kazlauskas et al., 1993; Mori et al., 1993; Vallus and Kazlauskas, 1993].
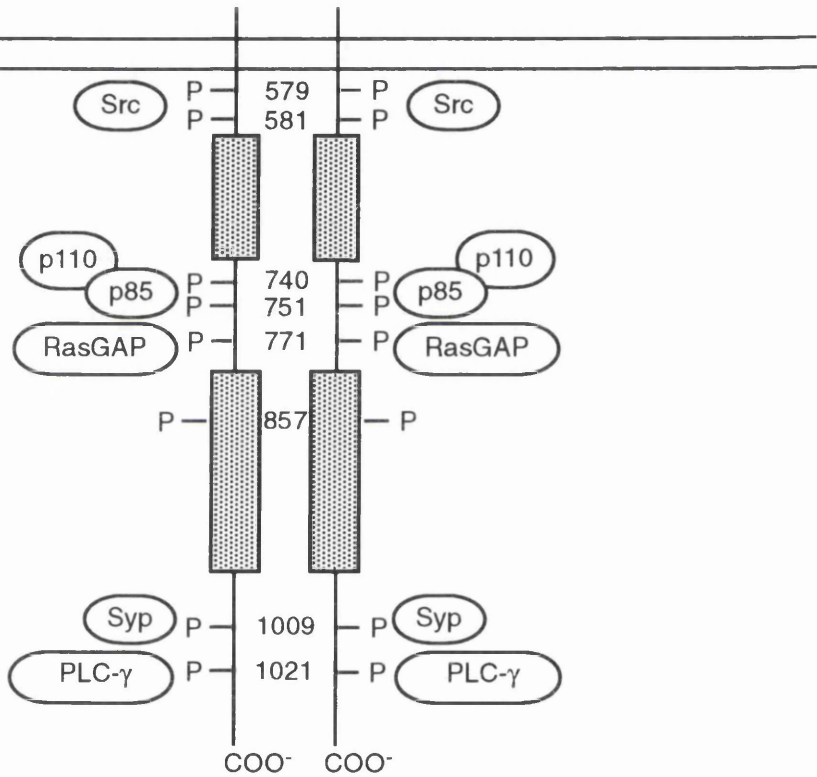
Figure 3.3   IRS-1 and the associated SH2 domain-containing proteins

A schematic representation of the specificity of interactions between the different SH2 domain-containing proteins and the known phosphorylation sites in IRS-1 [Skolnik et al., 1993; Sun et al., 1993a].
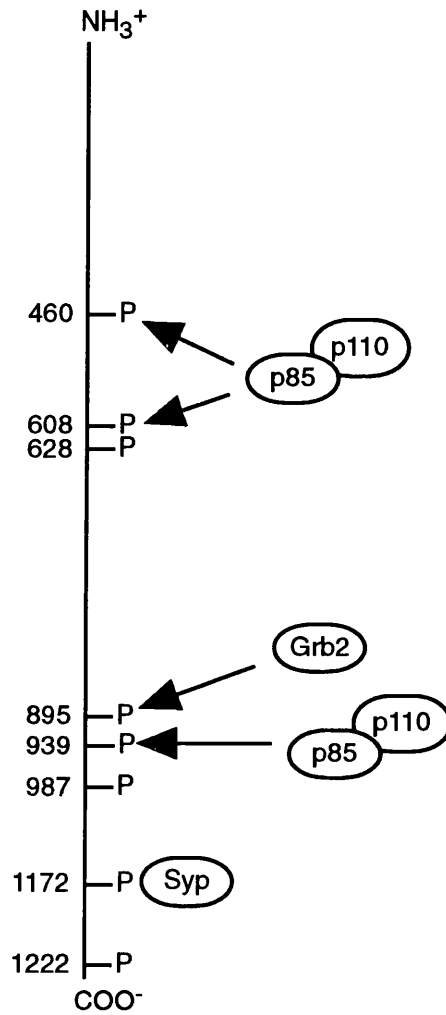
3.1.2   Fibroblasts

The connective-tissue cell family

The connective-tissue cell family includes: fibroblasts, chondroblasts, osteoblasts, adipocytes and smooth muscle cells. All the members of the connective-tissue cell family develop from fibroblasts. It is not yet clear whether there is a single type of fibroblast which is able to differentiate into many cell types, or whether there are several distinct fibroblast lineages each able to differentiate into a different cell type. Cell differentiation, like cell proliferation, is regulated by growth factors and anchorage. For example, transforming growth factor-ß induces differentiation of fibroblasts into chondrocytes, and growth hormone induces differentiation of fibroblasts into adipocytes.

The members of the connective-tissue cell family have important roles in the support and repair of most tissues and organs. Fibroblasts, chondroblasts and osteoblasts secrete the various macromolecules that form the extracellular matrix. Fibroblasts are irregular, branched cells dispersed in connective tissue throughout the body. They secrete a non-rigid, extracellular matrix rich in type I collagen. In response to growth factors, such as PDGF, which are released as a consequence of tissue injury, fibroblasts migrate to the site of injury (chemotaxis), proliferate and secrete large amounts of extracellular matrix, thus helping to repair the damaged tissue [Heldin and Westermark, 1990; Heldin, 1992].

Fibroblast cell lines

The Swiss 3T3 fibroblast cell line was isolated from mouse embryo connective tissue. These cells grow indefinitely in serial culture, but stop growing and enter G0 once they form a confluent monolayer (contact inhibition) [Todaro and Green, 1963]. If these resting cells are maintained for several weeks, some of them will develop visible lipid droplets. The lipid-accumulating cells form less than one percent of the total cell population, and are not observed among proliferating cells [Green and Kehinde, 1974; Green and Meuth, 1974]. They resemble brown or immature white adipocytes; such adipocytes have abundant cytoplasm, a central nucleus and multiple droplets of lipid, while mature white adipocytes have little cytoplasm, an eccentric nucleus and a single large, central, droplet of lipid [Green and Kehinde, 1974; Green and Meuth, 1974].

Several subclones that are able to convert with a high frequency to lipid-accumulating cells have been produced by serial selection of the cells from the lipid-rich areas of confluent, quiescent Swiss 3T3 fibroblasts (clone: Swiss 3T3-M) [Green and Kehinde, 1974].

The 3T3-L1 cell line

The cells of the subclone 3T3-L1 convert spontaneously into lipid-accumulating cells within two to four weeks of reaching confluence [Green and Kehinde, 1974]. The rate and extent of differentiation of 3T3-L1 cells increases in response to insulin [Green and Kehinde, 1975], glucocorticoids such as dexamethasone [Rubin et al., 1978], inhibitors of cyclic AMP phosphodiesterase such as 3-iso-butyl-1-methylxanthine [Rubin et al., 1978] and high concentrations of serum [Green and Meuth, 1974]. Exposure of confluent 3T3-L1 cells to mixtures of these agents induces differentiation such that more than 90 percent of the cells resemble fully mature white adipocytes within ten days [Rubin et al., 1978; Frost and Lane, 1985].

The undifferentiated form of 3T3-L1 cells synthesise collagen [Green and Meuth, 1974]. The only monosaccharide facilitative transporter protein expressed by these cells is Glut1. The rate of glucose transport increases two to five fold in response to insulin and other growth factors arising from the translocation of Glut1 {Section 1.3.2}. The rate of TAG synthesis is comparable to that observed in fibroblasts, and is insensitive to lipogenic and lipolytic agents [Green and Kehinde, 1975; Mackall et al., 1976; Ahmad et al., 1979]. The number of insulin-binding sites is comparable to that in other fibroblast cell lines [Reed et al., 1977]. Thus, the non-differentiated form of 3T3-L1 cells resembles fibroblasts.

In contrast, the differentiated form of 3T3-L1 cells expresses two monosaccharide facilitative transporter proteins, Glut1 and Glut4 [Calderhead et al., 1990a]. The rate of glucose transport increases 20 fold in response to insulin [Calderhead et al., 1990a], arising mainly from the translocation of Glut4 {Section 1.3.2} [Holman et al., 1990]. However, the rate of glucose transport increases only two to five fold in response to growth factors [Gould et al., 1994] and phorbol esters [Gibbs et al., 1991]. The expression of various enzymes required for fatty acid and TAG synthesis is higher than that in non-differentiated cells [Mackall et al., 1976; Ahmad et al., 1979]. Consequently,

the activities of these enzymes are ten to 50 fold higher and the rate of TAG synthesis itself is greater than in non-differentiated cells [Green and Kehinde, 1975; Mackall et al., 1976; Ahmad et al., 1979]. Furthermore, TAG synthesis is sensitive to lipogenic agents such as insulin [Ahmad et al., 1979], and is also sensitive to lipolytic agents such as adrenocorticotrophic hormone and ß-adrengeric agents [Rubin et al., 1977]. The number of insulin-binding sites is comparable to that in human and rat adipocytes, while the number of EGF-binding sites is comparable to that in fibroblasts [Reed et al., 1977]. Thus, the differentiated form of 3T3-L1 cells resembles adipocytes.

3.2 Results

The effects of the growth factors, insulin and PDGF, on cell proliferation and the rate of glucose transport in 3T3-L1 fibroblasts were characterised.

3.2.1 The effect of growth factors on cell proliferation

The effects of insulin and PDGF on cell proliferation in 3T3-L1 fibroblasts were established by measuring DNA synthesis by means of the incorporation of [^{3}H]thymidine {Section 2.7}. NCS was used as a positive control. Insulin, PDGF and NCS all stimulated incorporation of [^{3}H]thymidine. The results, from a representative experiment, are shown in Table 3.1; the incorporation was stimulated 3.8 fold by 1 µM insulin, 7.2 fold by 25 ng/ml PDGF and 8.3 fold by 20% NCS.

3.2.2 The effect of growth factors on the rate of glucose transport

The effect of insulin on the rate of glucose transport in 3T3-L1 fibroblasts was established by measuring the rate of 2-deoxyglucose uptake {Section 2.8.1}. The EC_{50} value was typically 5.0 nM. At a concentration of 1 µM insulin, the rate of uptake increased rapidly. The increase in the rate was evident within one minute of exposure to insulin, reaching a maximum by 60 minutes. The maximal stimulation in the rate in response to 1 µM insulin was 2.0 to 5.0 fold. A representative dose-response curve and a

Table 3.1   The effect of insulin and PDGF on DNA synthesis in 3T3-L1 fibroblasts

After incubation of quiescent 3T3-L1 fibroblasts with 1 μCi [^{3}H]thymidine and 1 μM insulin, 25 ng/ml PDGF or 20% NCS for 24 hours, [^{3}H]thymidine incorporation was measured {Section 2.7}. Each result shows the mean [^{3}H]thymidine incorporation (± SD) for six determinations. This is a representative experiment from a group of four.

	[^{3}H]thymidine incorporation (cpm per well)
Basal	5170 ± 1500
Insulin	19600 ± 3000
PDGF	37100 ± 9300
NCS	42900 ± 1100

representative time course for insulin-stimulated 2-deoxyglucose uptake are shown in Figures 3.4 and 3.5, respectively.

The effect of IGF-I on the rate of glucose transport in 3T3-L1 fibroblasts was established by measuring the rate of 2-deoxyglucose uptake {Section 2.8.1}. The EC_{50} value was typically 0.5 nM. The maximal stimulation in the rate in response to IGF-I was 4.0 to 5.0 fold. A representative dose-response curve for IGF-I-stimulated 2-deoxyglucose uptake is shown in Figure 3.6.

The effect of PDGF on the rate of glucose transport in 3T3-L1 fibroblasts was established by measuring the rate of 2-deoxyglucose uptake {Section 2.8.1}. The EC_{50} value was typically 0.5 ng/ml. At a concentration of 25 ng/ml PDGF, the rate of uptake increased rapidly. The increase in the rate was evident within one minute of exposure to PDGF and reached a maximum by 60 minutes. The maximal stimulation in the rate in response to 25 ng/ml PDGF was 2.0 to 3.5 fold. A representative dose-response curve and a representative time course for PDGF-stimulated 2-deoxyglucose uptake are shown in Figures 3.7 and 3.8, respectively.

3.2.3   The effect of a tumour promoter on the rate of glucose transport

The effect of PMA on the rate of glucose transport in 3T3-L1 fibroblasts was established by measuring the rate of 2-deoxyglucose uptake {Section 2.8.1}. At a concentration of 100 nM PMA, the rate of uptake increased rapidly. The increase in the rate was evident within one minute of exposure to PMA and reached a maximum by 60 minutes. The maximal stimulation in the rate in response to 100 nM PMA was 2.0 to 3.0 fold. A representative time-course for PMA-stimulated 2-deoxyglucose uptake is shown in Figure 3.9.

3.2.4   Identification of the facilitative monosaccharide transporter proteins expressed in 3T3-L1 fibroblasts

The presence of the monosaccharide facilitative transporter protein isoforms in 3T3-L1 fibroblasts was established by Western blotting. Membrane proteins were prepared

Figure 3.4   A dose response curve for insulin-stimulated 2-deoxyglucose uptake

After incubation of quiescent 3T3-L1 fibroblasts with insulin present in concentrations ranging from 0 to 1 µM for 60 minutes, a 3 minute uptake of 2-dexoy-D-[2,6-^{3}H]glucose was measured {Section 2.8.1}. Each result shows the mean rate of specific 2-deoxyglucose uptake (± SD) for triplicate determinations. Each result is expressed relative to the basal rate which was measured at 11.6 ± 1.7 pmoles/ min/ 10^6 cells. This is a representative experiment from a group of five; basal rates varied from 6.0 to 49 pmoles/ min/ 10^6 cells, the EC$_{50}$ value was typically 5 nM and the maximal stimulation was between 2.5 and 5.0 fold.
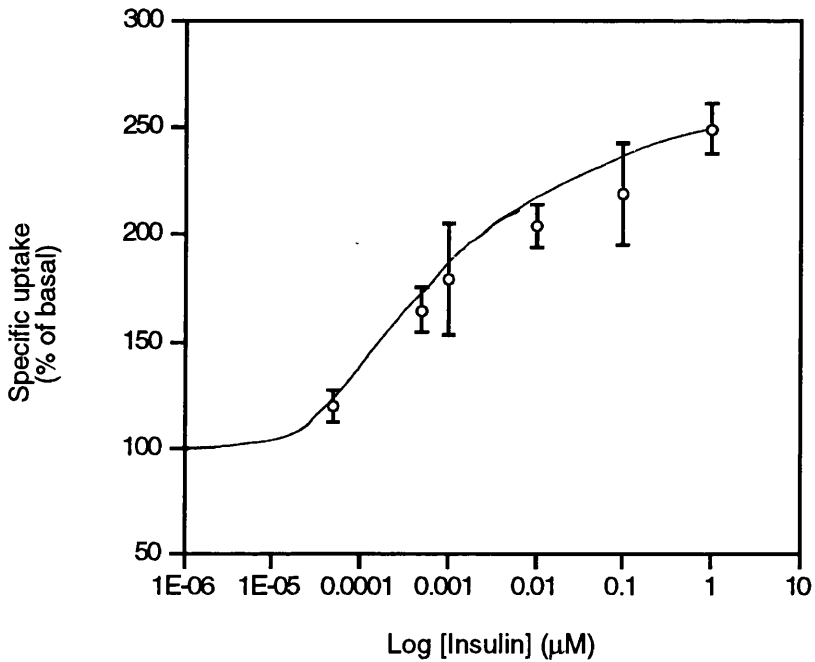
Figure 3.5   A time course for insulin-stimulated 2-deoxyglucose uptake

After incubation of quiescent 3T3-L1 fibroblasts with 1 µM insulin present for the times shown, a 3 minute uptake of 2-dexoy-D-[2,6-^{3}H]glucose was measured {Section 2.8.1}. Each result shows the mean rate of specific 2-deoxyglucose uptake (± SD) for triplicate determinations. Each result is expressed relative to the basal rate which was measured at 48.5 ± 2.6 pmoles/ min/ 10^6 cells. This is a representative experiment from a group of four; basal rates varied from 6.0 to 49 pmoles/ min/ 10^6 cells and the maximal stimulation was between 2.5 and 5.0 fold.
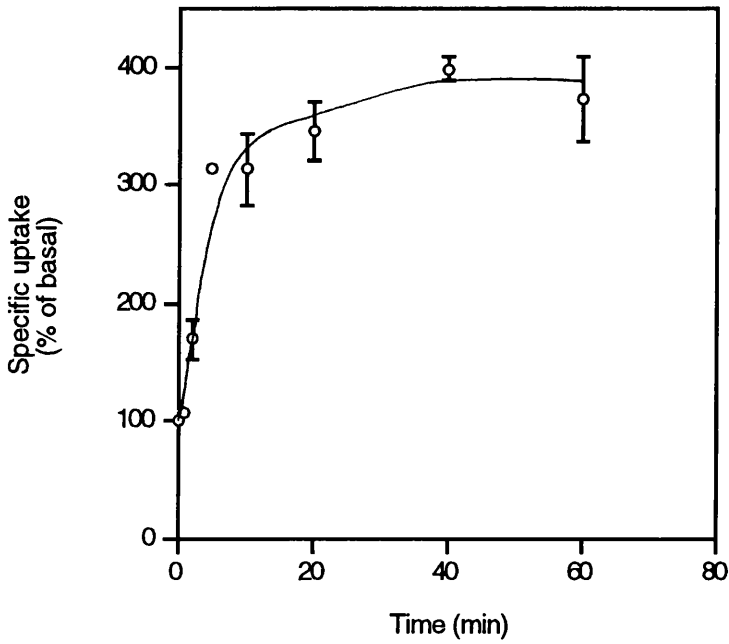
Figure 3.6   A dose response curve for IGF-I-stimulated 2-deoxyglucose uptake

After incubation of quiescent 3T3-L1 fibroblasts with IGF-I present in concentrations
ranging from 0 to 1 μM for 60 minutes, a 3 minute uptake of 2-dexoy-D-[2,6-^{3}H]glucose
was measured {Section 2.8.1}. Each result shows the mean rate of specific
2-deoxyglucose uptake (± SD) for triplicate determinations. Each result is expressed
relative to the basal rate which was measured at 6.3 ± 1.3 pmoles/ min/ 10^6 cells. This is
a representative experiment from a group of three; basal rates varied from 6.0 to 49
pmoles/ min/ 10^6 cells, the EC$_{50}$ value was typically 0.5 nM and the maximal
stimulation was between 3.4 and 5.0 fold.
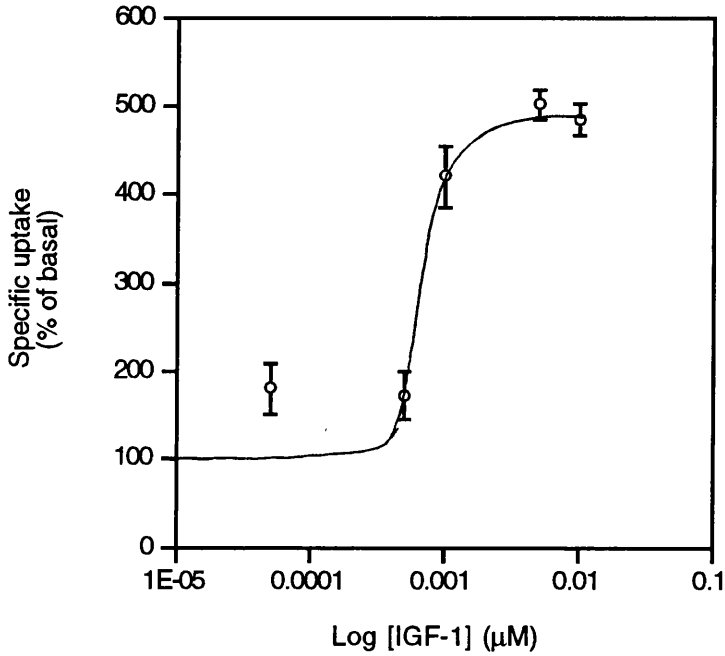
Figure 3.7   A dose-response curve for PDGF-stimulated 2-deoxyglucose uptake

After incubation of quiescent 3T3-L1 fibroblasts with PDGF present in concentrations
ranging from 0 to 25 ng/ml for 60 minutes, a 3 minute uptake of 2-dexoy-
D-[2,6-^{3}H]glucose was measured {Section 2.8.1}. Each result shows the mean rate of
specific 2-deoxyglucose uptake ($\pm$ SD) for triplicate determinations. Each result is
expressed relative to the basal rate which was measured at 8.87 $\pm$ 2.7 pmoles/ min/ 10^6
cells. This is a representative experiment from a group of three; basal rates varied from
6.0 to 49 pmoles/ min/ 10^6 cells, the EC$_{50}$ value was typically 0.5 ng/ml and the maximal
stimulation was between 2.5 and 5.0 fold.
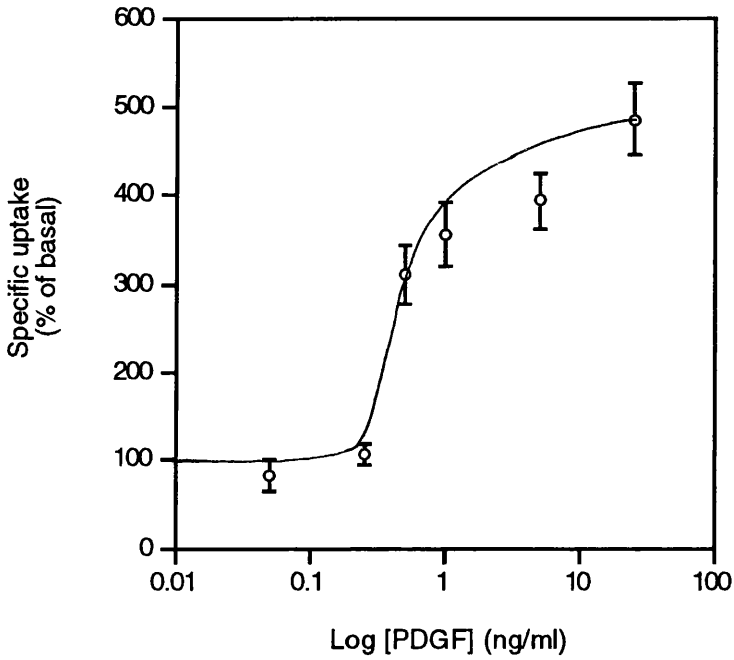
Figure 3.8   A time course for PDGF-stimulated 2-deoxyglucose uptake

After incubation of quiescent 3T3-L1 fibroblasts with 25 ng/ml PDGF present for the times shown, a 3 minute uptake of 2-deoxy-D-[2,6-^{3}H]glucose was measured {Section 2.8.1}. Each result shows the mean rate of specific 2-deoxyglucose uptake ($\pm$ SD) for triplicate determinations. Each result is expressed relative to the basal rate which was measured at 47.8 ± 1.9 pmoles/ min/ 10^6 cells. This is a representative experiment from a group of three; basal rates varied from 6.0 to 49 pmoles/ min/ 10^6 cells and the maximal stimulation was between 1.7 and 2.0 fold.
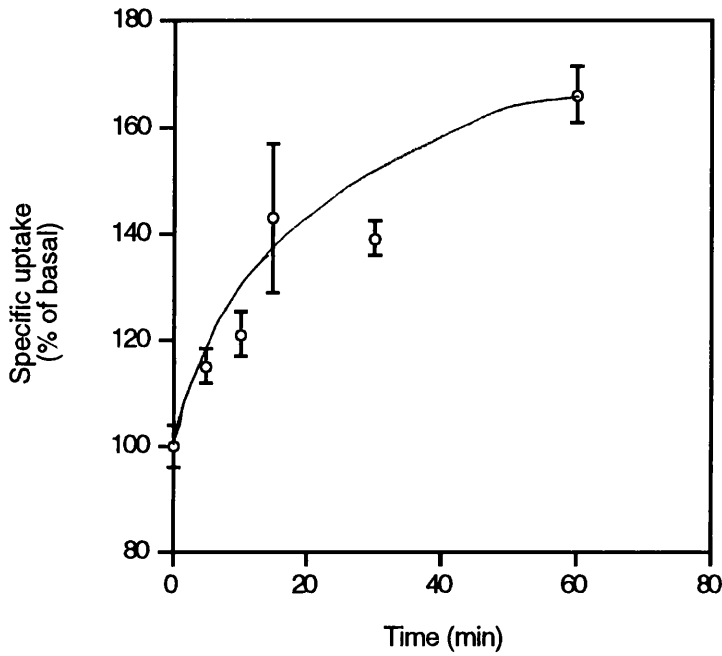
Figure 3.9   A time course for PMA-stimulated 2-deoxyglucose uptake

After incubation of quiescent 3T3-L1 fibroblasts with 100 nM PMA present for the times shown, a 3 minute uptake of 2-dexoy-D-[2,6-^{3}H]glucose was measured {Section 2.8.1}. Each result shows the mean rate of specific 2-deoxyglucose uptake ($\pm$ SD) for triplicate determinations. Each result is expressed relative to the basal rate which was measured at 20.3 $\pm$ 2.6 pmoles/ min/ 10^6 cells. This is a representative experiment from a group of three; basal rates varied from 6.0 to 49 pmoles/ min/ 10^6 cells and the maximal stimulation was between 2.5 and 3.0 fold.
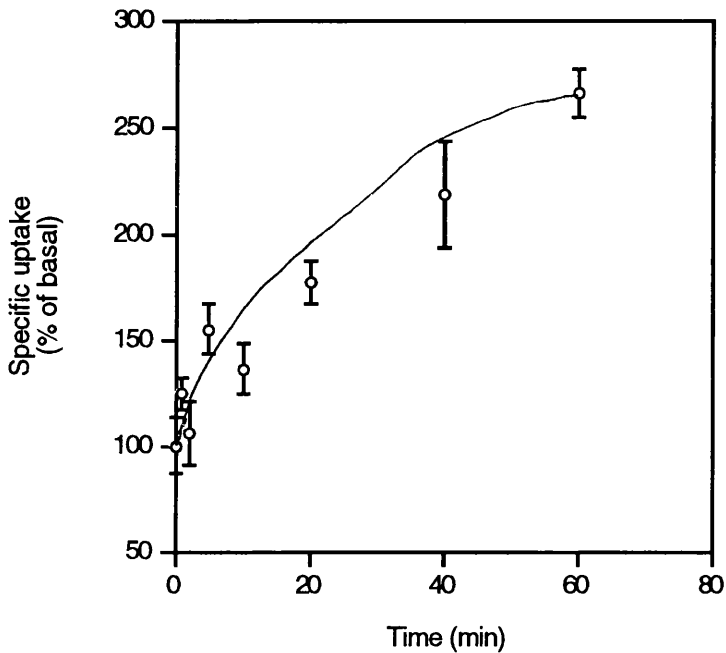
from 3T3-L1 fibroblasts {Section 2.13.1}. These membrane proteins and selected transporter protein standards were separated by SDS-PAGE {Section 2.15}, and then transferred onto nitrocellulose membranes. The membranes were probed with antibodies which recognised the different isoforms {Section 2.16.1}. The rabbit anti-Glut1 antibody was raised against the carboxy-terminal 14 amino acids of human Glut1, but the antibody also recognises mouse Glut1 [Davies et al., 1987]. The rabbit anti-Glut2 antibody was raised against a sequence of 14 amino acids in the carboxy-terminal region of human Glut2, but the it also recognises mouse Glut2 [Brant et al., 1992]. The rabbit anti-Glut3 antibody was raised against the carboxy-terminal 13 amino acids of mouse Glut3 [Gould et al., 1992]. The rabbit anti-Glut4 antibody was raised against the carboxy-terminal 16 amino acids of human Glut4, but again the antibody recognises mouse Glut4 [Brant et al., 1992]. Proteins were detected using a ^{125}I-conjugated goat anti-rabbit IgG antibody {Section 2.16.1}.

When membrane proteins from 3T3-L1 fibroblasts were probed with the anti-Glut1 antibody, the antibody recognised a broad band with an approximate, molecular mass of 50 kDa. A representative Western blot is shown in Figure 3.10.

When membrane proteins from 3T3-L1 fibroblasts and the Glut2 standard (mouse liver membrane proteins [Marchmont et al., 1981]) were probed with the anti-Glut2 antibody, the antibody recognised a narrow band with an approximate, molecular mass of 56 kDa in the lanes containing the Glut2 standard. However, bands corresponding to Glut2 were not observed in the lanes containing the 3T3-L1 fibroblast proteins, although there was a band with an approximate molecular mass of 50 kDa probably due to non-specific binding. A representative Western blot is shown in Figure 3.11a.

When membrane proteins from 3T3-L1 fibroblasts and the Glut3 standard (mouse brain membrane proteins [Gould et al., 1992]) were probed with the anti-Glut3 antibody, the antibody recognised a major band with an approximate, molecular mass of 48 kDa in the lanes containing the Glut3 standard. Other fainter bands of higher molecular mass were also observed, but these bands are not thought to be Glut3 [Gould et al., 1992]. However, bands corresponding to Glut3 were not observed in the lanes containing the 3T3-L1 fibroblast proteins. A representative Western blot is shown in Figure 3.11b.

Figure 3.10   The effect of insulin, PDGF and PMA on the total Glut1 level

After incubation of quiescent 3T3-L1 fibroblasts with 1 µM insulin, 25 ng/ml PDGF or 100 nM PMA for 60 minutes, membrane proteins were prepared {Section 2.13.1}. Approximately 60 µg of protein was loaded onto 10% (w/v) polyacrylamide mini-gels, the proteins were separated by SDS-PAGE {Section 2.15}, and then transferred onto nitrocellulose membranes. The membranes were probed with a rabbit anti-Glut1 antibody, then with a ^{125}I-conjugated goat anti-rabbit IgG antibody {Section 2.16.1}. This is a representative Western blot from a group of two membrane protein preparations.

Lane A: basal; Lane B: insulin; Lane C: vehicle (insulin); Lane D: PDGF; Lane E: vehicle (PDGF); Lane F: PMA.
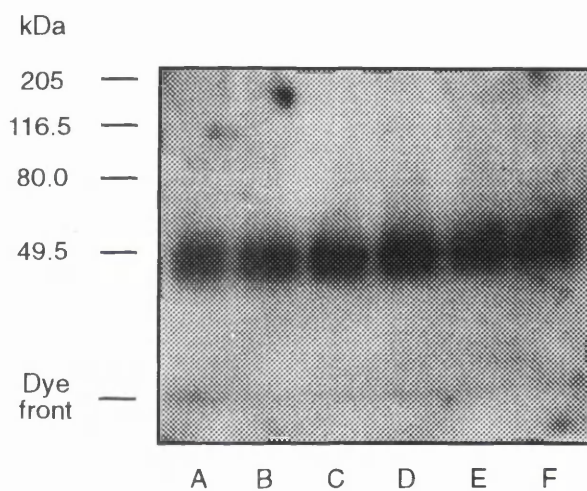
**Figure 3.11   The monosaccharide facilitative transporter isoforms expressed in 3T3-L1
fibroblasts**

Membrane proteins were prepared from quiescent 3T3-L1 fibroblasts {Section 2.13.1}.
The proteins were loaded onto 10% (w/v) polyacrylamide mini-gels, separated by SDS-
PAGE {Section 2.15}, and then transferred onto nitrocellulose membranes. The
membranes were probed with a) rabbit anti-Glut2, b) rabbit anti-Glut3 or c) rabbit
anti-Glut4 antibodies, and then with an ^{125}I-conjugated goat anti-rabbit IgG antibody
{Section 2.16.1}. The standards used were mouse liver (Glut2), mouse brain (Glut3)
and 3T3-L1 adipocyte (Glut4) membrane proteins. This is a representative experiment
from a group of two membrane protein preparations.

Lanes A and B: 30 µg and 60 µg of 3T3-L1 fibroblast membrane proteins respectively;
Lanes C and D: 30 µg and 60 µg of standard membrane proteins respectively.
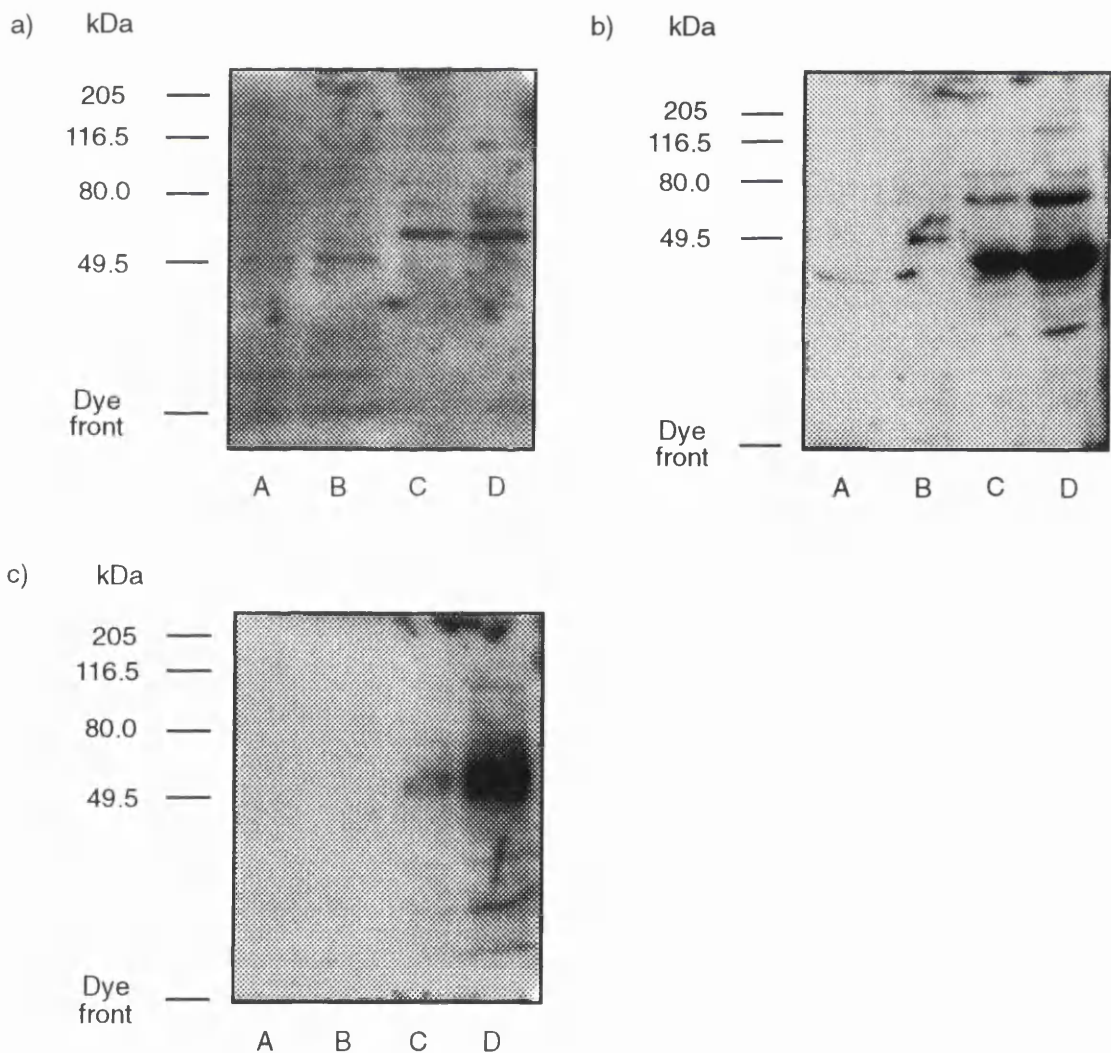
When membrane proteins from 3T3-L1 fibroblasts and the Glut4 standard (3T3-L1 adipocyte membrane proteins [Gould et al., 1989]) were probed with the anti-Glut4 antibody, the antibody recognised a band with an approximate, molecular mass of 55 kDa in the lanes containing the Glut4 standard. However, bands corresponding to Glut4 were not observed in the lanes containing the 3T3-L1 fibroblast proteins. A representative Western blot is shown in Figure 3.11c.

3.2.5   The effect of insulin, PDGF and PMA on the total Glut1 level

The effect of insulin, PDGF and PMA on the total Glut1 level in 3T3-L1 fibroblasts was established by Western blotting. Membrane proteins were prepared from 3T3-L1 fibroblasts after incubation in 1 μM insulin, 50 μM hydrochloric acid (the vehicle for insulin), 25 ng/ml PDGF, 1 mM sodium acetate, 0.15 mM sodium chloride (the vehicle for PDGF) or 100 nM PMA, for 60 minutes {Section 2.13.1}. The membrane protein samples were separated by SDS-PAGE {Section 2.15}, and then transferred onto nitrocellulose membranes. The membranes were probed with the anti-Glut1 antibody described above {Section 3.2.4} and then with an ^{125}I-conjugated goat anti-rabbit IgG antibody {Section 2.16.1}. The level of Glut1 in each sample was quantified by measurement of radioactivity.

The anti-Glut1 antibody recognised a diffuse band with a molecular mass of approximately 50 kDa in each lane containing the 3T3-L1 fibroblast proteins. A representative Western blot is shown in Figure 3.10.

The Glut1 level varied slightly in the untreated, agonist- and vehicle-treated samples. However, the results obtained by this method typically varied by ten percent, therefore it is unlikely that the relatively small differences observed in the Glut1 level are significant. The results from a representative experiment are shown in Table 3.2.

Table 3.2   The effect of insulin, PDGF and PMA on the total Glut1 level

After incubation of quiescent 3T3-L1 fibroblasts with 1 µM insulin, 25 ng/ml PDGF or
100 nM PMA for 60 minutes, membrane proteins were prepared {Section 2.13.1}.
Approximately 60 µg of protein was loaded onto 10% (w/v) polyacrylamide mini-gels, the
proteins resolved by SDS-PAGE {Section 2.15}, and then transferred onto nitrocellulose
membranes The membranes were probed with a rabbit anti-Glut1 antibody, and then
with a ^{125}I-conjugated goat anti-rabbit IgG antibody {Section 2.16.1}. The level of Glut1
in each sample was quantified by the measurement of radioactivity.

	Glut1 levels (cpm per band)
Basal	798
Insulin	767
Vehicle (insulin)	892
PDGF	1174
Vehicle (PDGF)	1144
PMA	1034

3.3 Discussion

3.3.1 The effect of growth factors on cell proliferation

Most growth factors stimulate cell growth and proliferation. Some stimulate cell differentiation. Some, such as PDGF, affect the proliferation of many cell types, while others, such as erythropoietin, affect the proliferation of a single cell type. The ability of a growth factor to affect the proliferation of a given cell type depends on which growth factor receptors are expressed by that cell.

In order to establish whether or not insulin or PDGF could stimulate proliferation of 3T3-L1 fibroblasts, DNA synthesis was measured. The incorporation of the radioactive-labelled DNA precursor [^{3}H]thymidine into DNA was assayed after a 24 hour incubation in the presence of each of the two growth factors and NCS. [^{3}H]thymidine incorporation was stimulated 3.8 fold in response to 1 μM insulin, 7.2 fold in response to 25 ng/ml PDGF, and 8.3 fold in response to 20% NCS (Table 3.1). NCS which contains many growth factors and hormones, including PDGF, was the most potent stimulant of proliferation in 3T3-L1 fibroblasts, and PDGF alone was nearly as potent; insulin alone had a lesser effect.

3.3.2 The effect of growth factors on the rate of glucose transport

The increase in the rate of growth factor-stimulated glucose transport is biphasic (Figure 1.1). The early phase of insulin- and PDGF-stimulated glucose uptake, in 3T3-L1 fibroblasts, was characterised by measuring the effects of insulin and PDGF on the rate of 2-deoxyglucose uptake. For insulin-stimulated 2-deoxyglucose uptake, the EC_{50} value was typically 5.0 nM (Figure 3.4). At a concentration of 1 μM insulin, a maximal stimulation of the rate of 2-deoxyglucose uptake of 2.0 to 5.0 fold was observed within 60 minutes (Figure 3.5). For PDGF-stimulated 2-deoxyglucose uptake, the EC_{50} value was typically 0.5 ng/ml (Figure 3.7). At a concentration of 25 ng/ml PDGF, a maximal stimulation of the rate of 2-deoxyglucose uptake of 2.0 to 3.5 fold was observed within 60 minutes (Figure 3.8). The EC_{50} values and the magnitudes of the maximal

increases in the rate of 2-deoxyglucose uptake are in agreement with work carried out by other researchers in similar cells [Allard et al., 1987].

Insulin is closely related to two other growth factors, IGF-I and IGF-II. The IGF-I receptor is similar to, but distinct from, the insulin receptor; both the receptors are Subclass III tyrosine protein kinase receptors {Figure 3.1} [Ullrich et al., 1985; Ullrich et al., 1986]. Insulin binds with high affinity to its own receptor, with low affinity to the IGF-I receptor, and with very low affinity to the IGF-II receptor. IGF-I binds with highest affinity to its own receptor, with lower affinity to the IGF-II receptor, and with lowest affinity to the insulin receptor [Ullrich et al., 1986]. Despite the structural similarities of the insulin and IGF-I receptors and the ability to bind to each other's receptors, insulin and IGF-I are thought to have different physiological roles in mammals. Insulin is known to have an important role in the regulation of blood glucose concentrations and many metabolic pathways {Section 1.2.2}, while IGF-I is thought to be important in development, both for proliferation (osteocytes and myocytes) and differentiation (adipocytes, myocytes and chondrocytes). Furthermore, during the differentiation of 3T3-L1 fibroblasts into adipocytes, the level of the insulin receptor mRNA increases, while the level of the IGF-I receptor mRNA decreases; presumably affecting the levels of the corresponding proteins. Consequently, it is likely that the observed effects of insulin on cell proliferation and the rate of glucose transport in 3T3-L1 fibroblasts occur as a consequence of insulin being able to bind to the IGF-I receptor.

This possibility was examined by comparing the dose-response curves for insulin- and IGF-I-stimulated 2-deoxyglucose uptake. If the effects of insulin are mediated by the IGF-I receptor then the EC_{50} value for insulin-stimulated 2-deoxyglucose uptake would be higher than the EC_{50} value for IGF-I-stimulated 2-deoxyglucose. For insulin the value was typically 5.0 nM {Figure 3.4} and for IGF-I the value was typically 0.5 nM {Figure 3.6}, which supports the hypothesis that insulin-stimulated glucose transport is mediated by the IGF-I receptor in 3T3-L1 fibroblasts.

There are three PDGF isoforms {Section 3.1.1}. All the work presented in this thesis was performed using PDGF-BB. PDGF-BB binds to both the PDGF α- and ß-receptor isoforms, leading to formation of all three receptor dimers {Section 3.1.1}. Preliminary

work, using PDGF-AA showed that PDGF-AA also stimulated the rate of 2-deoxyglucose uptake in 3T3-L1 fibroblasts (results not shown). PDGF-AA is thought to bind to only the PDGF α-receptor isoform [Heldin, 1992]. Therefore, it is likely that 3T3-L1 fibroblasts express this isoform. However, this has not been confirmed, nor has the presence of the PDGF ß-receptor isoform in 3T3-L1 fibroblasts. Both the PDGF receptor isoforms are expressed by NIH 3T3 fibroblasts [Heidaran et al., 1991], so it is expected that 3T3-L1 fibroblasts will also express both isoforms.

3.3.3   The effect of a tumour promoter on the rate of glucose transport

The tumour promoter PMA mimics the actions of DAG by binding to and activating PKC (Section 4.1.2), leading to cell proliferation [Nishizuka, 1984]. The early phase of PMA-stimulated glucose transport in 3T3-L1 fibroblasts was characterised by measuring the affect of PMA on the rate of 2-deoxyglucose uptake. At a concentration of 100 nM PMA, the maximal stimulation of the rate of uptake of 2.0 to 3.0 fold occurred within 60 minutes (Figure 3.9). This is similar in magnitude and timing to the early phase of insulin- and PDGF-stimulated glucose transport.

The effects of insulin, PDGF and PMA on the rate of 2-deoxyglucose uptake were not additive; that is, the incubation of 3T3-L1 fibroblasts with combinations of these ligands did not lead to significantly greater increases in the rate of uptake than incubation with any of the ligands alone (results not shown). Similar results were obtained concerning the effects of EGF, insulin, PDGF and PMA on 2-deoxyglucose uptake in human fibroblasts [Allard et al., 1987]. One interpretation of these results is that the early phases of insulin-, PDGF- and PMA-stimulated glucose transport are mediated by a common signal transduction pathway.

3.3.4   Identification of facilitative transporter proteins

The mammalian monosaccharide facilitative transporter protein isoforms are expressed in a tissue-specific manner (Table 1.1). All cultured cells express Glut1, in fact, it is the only one known to be expressed in 3T3-L1 fibroblasts. Western blotting of 3T3-L1

fibroblast membrane proteins confirmed that Glut1 is the only transporter protein expressed by these cells {Figures 3.10 and 3.11}.

3.3.5   The mechanism by which growth factors stimulate glucose transport

There are three mechanisms by which the rate of transport can be altered {Section 1.3.1}. Published work suggests that the early phase of growth factor-stimulated glucose transport occurs as a consequence of translocation of Glut1 from an intracellular location to the plasma membrane and not as a consequence of an increase in the total level of Glut1 {Section 1.3.2}. Western blotting of 3T3-L1 fibroblast membrane proteins with an antibody raised against Glut1, showed that there were only small differences in the total Glut1 level after incubation with 1 μM insulin, 25 ng/ml PDGF and 100 nM PMA {Figure 3.10 and Table 3.2}. These differences could be due to experimental variation and are not large enough to account for the 2 to 5 fold increases observed in the rate of 2-deoxyglucose uptake {Sections 3.2.2 and 3.2.3}. Hence, the early phase of the growth factor-stimulated glucose transport probably occurs because of translocation of Glut1.

3.3.6   The basal rate of 2-deoxyglucose uptake

The basal rate of 2-deoxyglucose uptake varied between 6.0 to 49 pmoles/ min/ 10^6 cells. Other researchers have recorded similar variations when using cultured cells in the basal rate of 2-deoxyglucose uptake and in the magnitude of the maximal increase in response to growth factors [Allard et al., 1987]. Recent research suggests that these variations may arise from a gradual increase in the intracellular sequestration of Glut1 as the fibroblasts become confluent [Yang et al., 1992]. For example, the majority of Glut1 is found at the cell surface in preconfluent 3T3-L1 fibroblasts, and the proportion of Glut1 at the cell surface decreases as the cells become confluent. In addition, the basal rate of 2-deoxyglucose uptake decreases and the magnitude of insulin-stimulated 2-deoxyglucose uptake increases as 3T3-L1 fibroblasts become confluent; these changes reflect the increase in intracellular sequestration of Glut1 [Yang et al., 1992].

3.3.7   Summary

Insulin and PDGF stimulate cell proliferation in 3T3-L1 fibroblasts, and these growth factors and the tumour promoter, PMA, all stimulate 2-deoxyglucose uptake in a similar manner. In each case, the increase occurs within minutes and reaches a maximum within 60 minutes of exposure to the agonist. The maximum increases in the rate of 2-deoxyglucose uptake are between 2.0 to 5.0 fold.

3T3-L1 fibroblasts express only one facilitative monosaccharide transporter isoform, Glut1. The observed increases in the rate of 2-deoxyglucose uptake probably arise from the translocation of Glut1, but not because of an increase in the total level of Glut1.

Since insulin, PDGF and PMA all have similar effects to each other on the rate of glucose transport in 3T3-L1 fibroblasts, it is possible that the intracellular signal transduction pathways that mediate these effects are similar. The effects of many ligands that bind to plasma membrane receptors are mediated by signal transduction pathways that involve DAG and PKC. The effects of PMA are also mediated by PKC. Therefore, the possibility that the early phase of insulin-, PDGF- and PMA-stimulated glucose transport is mediated by a signal transduction pathway involving phospholipids and PKC was investigated and is discussed next.

4 DAG and the activation of protein kinase C in 3T3-L1 fibroblasts

4.1 Introduction

The growth factors, insulin and PDGF, and the tumour promoter, PMA, all have similar effects on the rate of glucose transport in 3T3-L1 fibroblasts. The increase in the rate of glucose transport is evident within minutes of exposure to ligand, reaching a maximum within 60 minutes (Section 3.2.2). This increase is likely to occur as a result of translocation of Glut1 to the plasma membrane; it does not involve an increase in the total Glut1 protein level (Section 3.2.5).

Since these ligands have similar effects to each other on the rate of glucose transport in 3T3-L1 fibroblasts, it is possible that the intracellular signal transduction pathways that mediate these effects are similar. The effects of many ligands that bind to plasma membrane receptors are mediated by signal transduction pathways that involve the hydrolysis of certain phospholipids. This produces DAG which binds to and activates PKC [Asaoka et al., 1992; Liscovitch, 1992]. The effects of PMA are also mediated by PKC [Nishizuka, 1984]. Since the effects of insulin and PDGF on the rate of glucose transport are similar to those of PMA, it is possible that the effects of insulin and PDGF are also mediated by a signal transduction pathway involving DAG and PKC. Therefore, the effects of insulin and PDGF on DAG accumulation and PKC activity, and the necessity of PKC in the early phase of insulin- and PDGF-stimulated glucose transport, were investigated.

4.1.1 Phospholipid hydrolysis

Signal-activated phospholipases

Ligand-stimulated hydrolysis of phospholipids is catalysed by signal-activated phospholipases. Each signal-activated phospholipase catalyses the hydrolysis of a particular bond; for example, phospholipase A_2 (PLA$_2$) catalyses the hydrolysis of the ester bond at the sn-2 position, phospholipase C (PLC) catalyses the hydrolysis of the phosphoester bond at the sn-3 position, and phospholipase D (PLD) catalyses the hydrolysis of the bond between the phosphate group and the polar headgroup (Figure 4.1a). Consequently, the hydrolysis of a given phospholipid by different signal-activated phospholipases produces different types of products (Figure 4.1b). Furthermore, each

signal-activated phospholipase catalyses the hydrolysis of a particular group of phospholipids; for example, the phosphatidyl inositol-specific PLC (PtdIns-PLC) isozymes catalyse the hydrolysis of phosphatidyl inositols; significantly, sn-1,2-phosphatidyl inositol 4,5-bisphosphate (PtdIns(4,5)P_2) produces D-myo-inositol 1,4,5-trisphosphate (Ins(1,4,5)P_3) and DAG. The phosphatidyl choline-specific PLC (PtdCh-PLC) isozymes catalyse the hydrolysis of sn-1,2-phosphatidyl choline (PtdCh), the products being phosphocholine (ChP) and DAG. The PtdCh-specific PLD (PtdCh-PLD) isozymes also catalyse the hydrolysis of PtdCh, but the products are choline (Ch) and phosphatidic acid (PtdOH) [Exton, 1990].

Phosphatidyl inositol hydrolysis

The PtdIns-PLC family members are the most well characterised signal-activated phospholipases. The amino acid sequences of 16 distinct isozymes are known. Comparison of these sequences shows that they form three subfamilies, PLC-ß, PLC-γ and PLC-δ. The members of each subfamily have distinct catalytic properties and modes of activation [Rhee and Choi, 1992].

The PLC-ß isozymes are activated in response to ligands that bind to G protein-linked receptors, particularly those receptors which bind to the members of the Gq family {see Section 5.1.3 for a more detailed description of the activation of G proteins}. The activation of a Gq leads to activation of PLC-ß1 [Smrcka et al., 1991; Sternweis and Smrcka, 1992].

The PLC-γ isozymes are activated in response to ligands that bind to tyrosine protein kinase receptors [Rhee and Choi, 1992]. The activation of a tyrosine protein kinase leads to phosphorylation of the receptor and association of PLC-γ1, via its SH2 domains, with certain phosphotyrosine-containing sequences in the receptor {Section 3.1.1}. For example, PLC-γ1 associates with Tyr-1021 in the PDGF ß- receptor {Figure 3.2} [Rönnstrand et al., 1992].

Association of PLC-γ1 with a tyrosine protein kinase receptor is followed by its phosphorylation on residues Tyr-771, Tyr-783 and Tyr-1254. However, its catalytic activity is not altered by tyrosine phosphorylation [Rhee and Choi, 1992]. In quiescent

Figure 4.1   Phospholipids and signal-activated phospholipases

a) A typical phospholipid, consisting of a DAG moiety linked via a phosphodiester bond to a polar headgroup. Phospholipids differ from one another with respect to the structure of the polar headgroup and the composition of the fatty acids. The polar headgroup may be choline, ethanolamine, Ins(4,5)P_2, phosphatidic acid or serine. The fatty acid in the sn-1 position usually is saturated (R) and that in the sn-2 position unsaturated (R'). The sites of hydrolysis by some signal-activated phospholipases are also shown.
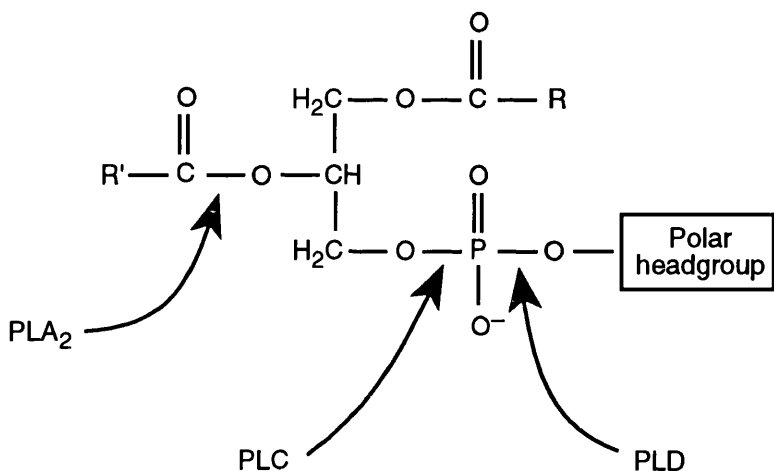
b) The products formed by PLA$_2$-, PLC- and PLD-catalysed hydrolysis of PtdCh.
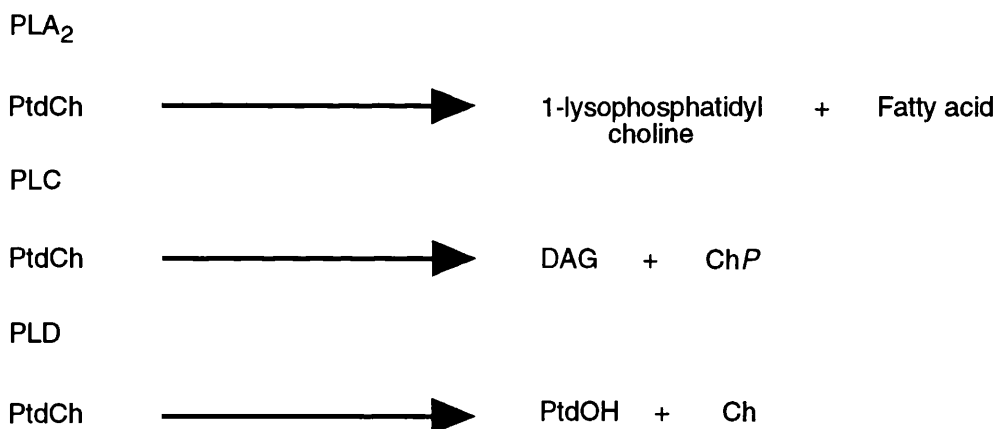
cells, PLC-γ1-catalysed hydrolysis of PtdIns(4)P and PtdIns(4,5)P_2 is inhibited by profilin, a small soluble actin-binding protein which also binds to these phospholipids with high affinity, but not to any other phospholipids [Goldschmidt-Clermont et al., 1991]. However, after tyrosine phosphorylation, PLC-γ1 can catalyse the hydrolysis of the profilin-associated phosphatidyl inositols [Goldschmidt-Clermont et al., 1991]. In addition, the association of profilin with phosphatidyl inositols inhibits the interaction of profilin with actin. Consequently, the profilin released after PLC-γ1-catalysed hydrolysis of profilin-associated phosphatidyl inositols can bind to actin, and may have a role in mediating growth factor-stimulated rearrangements of the cytoskeleton and membrane ruffling.

The products of PLC-catalysed hydrolysis of PtdIns(4,5)P_2 are Ins(1,4,5)P_3 and DAG. Ins(1,4,5)P_3 is a soluble molecule which binds to a receptor that encloses a calcium ion channel (a Class I receptor) {Section 1.1.2}. The receptor is found in the membrane of calcium ion-sequestering organelles [Taylor and Marshall, 1992]. Ins(1,4,5)P_3 opens the channel, thus stimulating the transport of calcium ions from the intracellular stores into the cytosol, leading to a rise in the intracellular, free calcium ion concentration [Moolenaar et al., 1984b; Berridge, 1993]. The activity of many intracellular proteins, including that of some PKC isozymes, is regulated by calcium ion binding. DAG, the other product of PtdIns(4,5)P_2 hydrolysis, also has a role in the stimulation of PKC activity {Section 4.1.2} [Kikkawa et al., 1989]. However, hydrolysis of PtdIns(4,5)P_2 is transient, therefore the increases in Ins(1,4,5)P_3 mass and the intracellular, free calcium ion concentration are also transient [Takuwa et al., 1987]. This is thought to be a negative feedback effect of PKC [Price et al., 1989] which catalyses the phosphorylation of PLC-ß, thus preventing its interaction with Gq [Ryu et al., 1990], and of PLC-γ1, thus preventing its tyrosine phosphorylation [Park et al., 1992].

Phosphatidyl choline hydrolysis
Many ligands stimulate a rapid, transient increase in the Ins(1,4,5)P_3 level, but a sustained increase in the DAG level. For example, in bombesin-treated Swiss 3T3 fibroblasts, the increase in Ins(1,4,5)P_3 mass reaches a maximum in five to ten seconds, and returns to the basal level by 30 seconds. The increase in the DAG level is biphasic; the first phase of DAG accumulation parallels the increase in Ins(1,4,5)P_3 mass, while the second phase arises after 30 seconds, but remains above the basal level for at least

four hours [Takuwa et al., 1987; Cook et al., 1990]. A similar profile of DAG accumulation is observed in PDGF- and vasopressin-treated Swiss 3T3 fibroblasts [Price et al., 1989] and in α-thrombin-treated IIC9 fibroblasts [Wright et al., 1988; Pessin and Raben, 1989; Ha and Exton, 1993].

Other ligands have no effect on PtdIns(4,5)P_2 hydrolysis, but stimulate a slow and sustained increase in the DAG level. Such a profile of DAG accumulation is observed in IIC9 fibroblasts in response to PDGF-BB [Ha and Exton, 1993], EGF and low concentrations of α-thrombin [Wright et al., 1988], and in EGF-treated Swiss 3T3 fibroblasts [Cook et al., 1991]. In Swiss 3T3 fibroblasts treated with the tumour promoter, PMA, there is also a slow, sustained increase in the DAG level, in the absence of PtdIns(4,5)P_2 hydrolysis [Cook et al., 1991].

The slow, sustained increase in accumulation of DAG occurs because of an increase in the hydrolysis of PtdCh. The fatty acid composition of PtdIns and PtdCh are different, PtdIns having a higher content of stearic and arachidonic acids, while PtdCh has a higher content of palmitic, oleic and linoleic acids [Patton et al., 1982]. Analysis of the molecular species of DAG produced in response to various ligands shows that the sustained increase in DAG mass arises from the hydrolysis of PtdCh [Pessin and Raben, 1989; Exton, 1990]. In addition, many ligands stimulate accumulation of Ch and of ChP, suggesting that ligand-stimulated hydrolysis of PtdCh is catalysed by both PLC and PLD {Figure 4.1}. The activation of PtdCh-PLC produces DAG directly, while the activation of PtdCh-PLD produces DAG indirectly, following the hydrolysis of PtdOH by phosphatidic acid phosphohydrolase [Cook et al., 1991]. However, in most cells PtdCh-PLD activity reaches a maximum between two to five minutes, suggesting that the majority of the DAG formed arises from another source, most likely through the activation of PtdCh-PLC [Cook and Wakelam, 1989; Exton, 1990; Cook et al., 1991; McKenzie et al., 1992].

PtdCh-PLC and PtdCh-PLD are activated in response to ligands that bind to G protein-linked receptors. The activation may involve direct coupling of the phospholipase to the receptor by a G protein [Boeckino et al., 1987]. PtdCh-PLC and PtdCh-PLD are also activated in response to ligands that bind to tyrosine protein kinase receptors. It is not known how activation of these phospholipases is coupled to these receptors, except that

tyrosine protein kinase activity is necessary [Cook and Wakelam, 1992]. In addition,

PKC may have a role in the receptor-mediated activation of PtdCh-specific

phospholipases, although this is more likely to be a positive feedback effect [Cook and

Wakelam, 1989; Price et al., 1989; Cook et al., 1991; Conricode et al., 1992]. In contrast,

PMA-stimulated PtdCh-specific phospholipase activation is likely to be mediated by

PKC, since PMA binds directly to PKC [Cook et al., 1991].

Thus, signal-activated phospholipases catalyse the hydrolysis of various phospholipids.

The PtdIns-PLC isozymes catalyse the hydrolysis of PtdIns(4,5)P_2, producing

Ins(1,4,5)P_3 and DAG, both of which are involved in the activation of PKC. However,

PKC inhibits PtdIns-PLC activity, therefore the accumulation of Ins(1,4,5)P_3 is

transient. In contrast, the accumulation of DAG is often biphasic; the first phase is

rapid but transient and corresponds to the hydrolysis of PtdIns(4,5)P_2, while the second

phase is sustained and corresponds to the hydrolysis of PtdCh, catalysed by the

PtdCh-PLC and PtdCh-PLD isozymes. The activity of these phospholipases is

potentiated by PKC {Figure 4.2}.

4.1.2   Protein kinase C

The mammalian isozymes

The mammalian PKC family contains at least twelve isozymes, nine of which have been

cloned. Comparison of the amino acid sequences shows that the isozymes comprise

three subfamilies. Furthermore, the members of each subfamily have distinct kinetic

characteristics [Bell and Burns, 1991; Asaoka et al., 1992; Dekker and Parker, 1994].

The 'classical' PKC subfamily consists of four isozymes, α, βI, βII and γ. Activation of

these isozymes is dependent on calcium ion, the normal intracellular, free calcium ion

concentration being too low for activation to occur. Activation of these isozymes also

requires the membrane phospholipid, phosphatidyl serine, a cofactor, and DAG, an

activator, which increases the affinity of these isozymes for calcium ions.

Cis-unsaturated fatty acids and lysophosphatidyl choline also enhance the activity of

these isozymes. The 'novel' PKC subfamily consists of five isozymes, δ, ε, η, θ and μ.

Activation of these isozymes occurs independently of calcium ions, but requires

phosphatidyl serine and DAG. The 'atypical' PKC subfamily consists of three isozymes,

ζ, λ and ι. These isozymes are not fully characterised; however, it is known that

Figure 4.2 Signal transduction pathways involving phospholipid hydrolysis and PKC activation

A schematic representation of the activation of PtdIns-PLC, PtdCh-PLC and PtdCh-PLD in response to ligands that bind to G protein-coupled receptors. These phospholipases are also activated in response to ligands that bind to tyrosine protein kinase receptors.
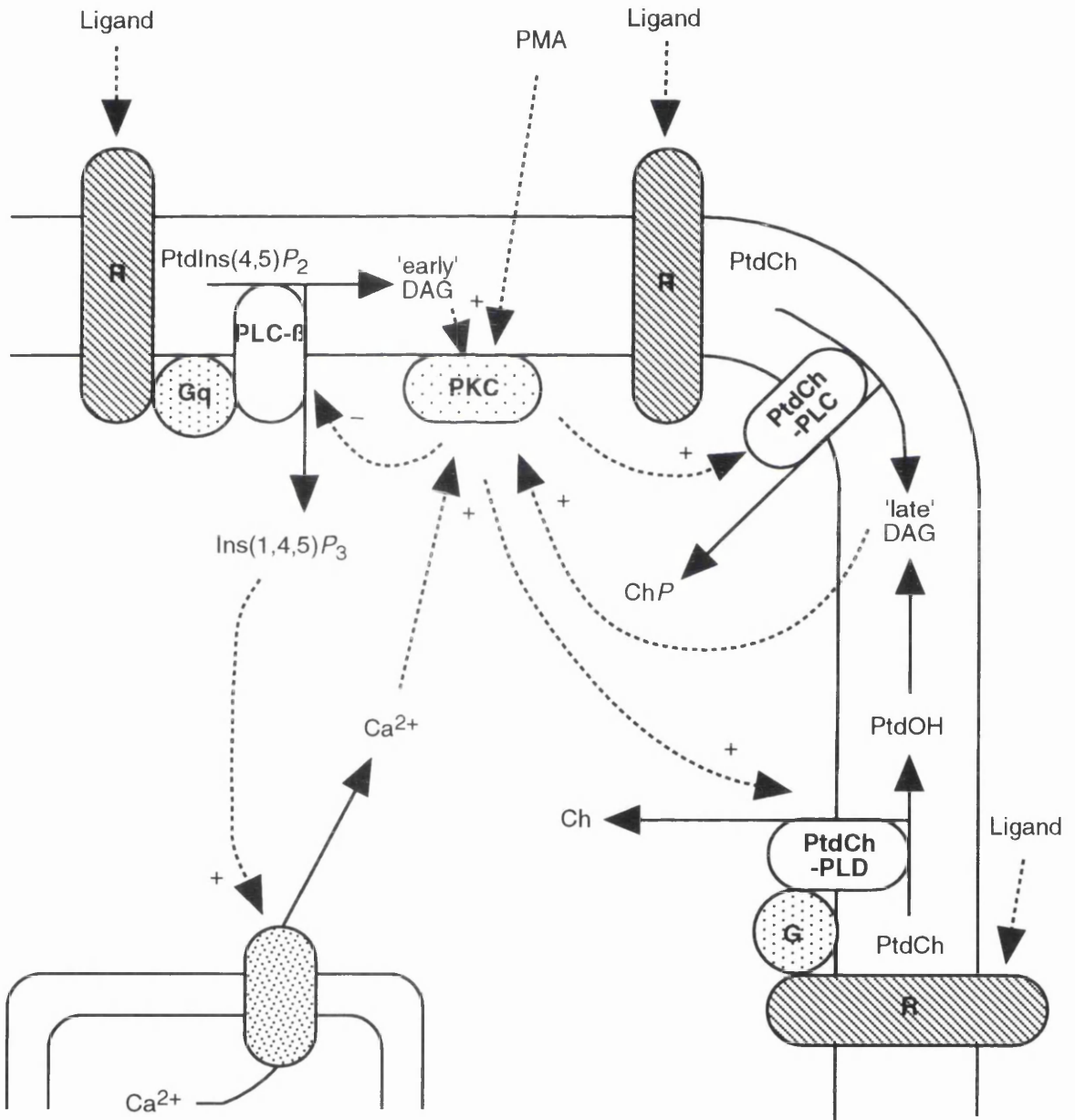
activation of the ζ-isozyme occurs independently of calcium ions and DAG. Furthermore, this isozyme is not activated in response to phorbol esters [Bell and Burns, 1991; Asaoka et al., 1992; Dekker and Parker, 1994].

PMA directly binds to and activates the 'classical' and 'novel' PKC isozymes. This activation occurs in the absence of changes in the intracellular, free calcium ion concentration [Nishizuka, 1984], and leads to a slow, sustained accumulation of DAG [Cook et al., 1991].

The PKC isozymes are expressed in a tissue-specific manner. PKC-α, PKC-δ and PKC-ζ are ubiquitous, while others are restricted to one or to a few tissues. Consequently, each cell type expresses a characteristic subset of isozymes. This suggests that there is a divergence in function between the isozymes [Asaoka et al., 1992; Dekker and Parker, 1994]. However, the combination of isozymes expressed by most cells is yet to be determined.

Different ligands activate different combinations of PKC isozymes in the same cell; for example, in α-thrombin-treated IIC9 fibroblasts PKC-α and PKC-ε are activated, but in PDGF-BB-treated IIC9 fibroblasts only PKC-ε is activated. The activation of PKC-α is transient, while that of PKC-ε is sustained. This reflects the effects of these ligands on phospholipid hydrolysis; in α-thrombin-treated IIC9 fibroblasts DAG accumulation is biphasic, while in PDGF-BB-treated IIC9 fibroblasts it is monophasic, being slow in onset and sustained. Thus, the activation of PKC-α occurs in response to hydrolysis of PtdIns, while the activation of PKC-ε occurs in response to hydrolysis of PtdCh. The difference in the patterns of isozyme activation arises from the differing requirements of the two PKC isozymes for calcium ions and the differing effects of hydrolysis of the two phospholipids on the intracellular, free calcium ion concentration [Ha and Exton, 1993].

Activation
The PKC isozymes have a carboxy-terminal catalytic domain and an amino-terminal regulatory domain. Within the regulatory domain, there is a sequence of amino acids, termed the pseudo-substrate site, which resembles the consensus phosphorylation site for PKC, but differs in that it contains an alanine residue instead of the serine/ threonine residue that is the site of phosphorylation. When the enzyme is cytosolic or

membrane-bound through interaction with phospholipid cofactors, the pseudo-substrate site interacts with the substrate-binding site in the catalytic domain with relatively high affinity, thus inhibiting interaction of the substrate-binding site with substrates, and so inhibits the kinase activity. When a lipid activators, such as DAG, binds to PKC, the affinity of the pseudo-substrate site for the substrate binding-site is lowered, thus allowing substrates to compete more effectively [Bell and Burns, 1991; Dekker and Parker, 1994].

Substrates

The myristoylated alanine-rich C kinase substrate (MARCKS), is a good substrate for PKC, but not for other kinases [Stumpo et al., 1989]. In quiescent cells, MARCKS binds to actin filaments, cross-linking them. MARCKS also binds to calmodulin but, only in the presence of calcium ions; phosphorylation of MARCKS prevents it binding to calmodulin. The binding of MARCKS to actin filaments is disrupted by both phosphorylation and calcium ion-calmodulin binding. Thus, an increase in the intracellular, free calcium ion concentration and the activation of PKC leads to the release of MARCKS from the plasma membrane and major cytoskeletal rearrangement [Aderem, 1992a,b; Blackshear, 1993].

Glycogen synthase kinase-3ß (GSK-3ß) activity is inhibited by PKC-catalysed phosphorylation [Goode et al., 1992]. GSK-3ß catalyses the phosphorylation of c-Jun, a component of the transcription factor AP-1, and so inactivates it. Therefore, PKC-catalysed phosphorylation of GSK-3ß activates c-Jun, leading to an increase in the transcriptional activity of AP-1.

However, each PKC isozyme has a different affinity for a given substrate. For example, PKC-α, PKC-ßI, PKC-ßII and PKC-γ catalyse the phosphorylation of GSK-3ß, while PKC-ε cannot significantly catalyse the phosphorylation of this enzyme [Goode et al., 1992]. Again, detailed information concerning the substrate specificity of the PKC isozymes has not yet been determined.

Thus, the response of a cell to a ligand which activates PKC-dependent signal transduction pathways depends on the ability of that ligand to activate the different

PKC isozymes, which PKC isozymes are expressed by the cell, and which substrates of the expressed PKC isozymes are also expressed.

4.1.3   The relationship with cell proliferation

The results of early work on signal transduction pathways involving phospholipid hydrolysis and PKC activation lead to the suggestion that these events may mediate cell proliferation. In many cells a given ligand stimulates DAG accumulation, PKC activity and cell proliferation, for example, bombesin, PDGF and phorbol esters in Swiss 3T3 fibroblasts [Cook and Wakelam, 1989; Cook et al., 1990; Larrodera et al., 1990], LPA and phorbol esters in HF fibroblasts [van Corven et al., 1989] and α-thrombin in Chinese hamster fibroblasts [Magnaldo et al., 1988]. Transformation of cells with oncogenes such as v-*ros*, v-*src*, v-*fms*, v-*ras* and v-*sis*, also leads to DAG accumulation [Wolfman et al., 1987].

In support of this hypothesis, the exogenous addition of the PtdCh-PLC from *Bacillus cereus* to Swiss 3T3 fibroblasts stimulates both PtdCh hydrolysis and the rate of cell proliferation [Larrodera et al., 1990]. In addition, the overexpression of PKC in Rat 6 fibroblasts results in many phenotypic changes, for example, an increase in the rate of cell proliferation and the loss of anchorage-dependence, both in the absence and presence of PMA [Housey et al., 1988]. Furthermore, the rate of cell proliferation increases in response to PMA in Swiss 3T3 fibroblasts; this effect is abolished by the depletion of PKC, and is restored by the microinjection of PKC [Pasti et al., 1986].

However, the activation of PtdIns-PLC is not necessary for growth factor-stimulated cell proliferation. For example, the mutation of the tyrosine residue in the PLC-γ binding site of the FGF receptor inhibits the FGF-stimulated hydrolysis of PtdIns(4,5)P_2 and increase in the intracellular free calcium ion concentration, but has no effect on FGF-stimulated cell proliferation. Furthermore, a major requirement for a signal transduction pathway that mediates cell proliferation is that it remains active for many hours following ligand activation [Van Obberghen-Schilling et al., 1985; Zhan et al., 1993]. Thus, the transient increase in the DAG level due to the hydrolysis of PtdIns(4,5)P_2, may be sufficient to mediate some of the early events of the cell cycle, but

it is not sufficient to stimulate or to maintain growth factor-stimulated cell proliferation [van Corven et al., 1989; Seuwen et al., 1990].

Furthermore, the activation of either PtdCh-PLC or PtdCh-PLD is also not sufficient for cell proliferation. For example, the activities of PtdCh-PLC and PtdCh-PLD increases without any effect on the rate of cell proliferation in response to carbacol, a muscarinic agonist, in Chinese hamster fibroblasts transfected with the human M1 muscarinic acetylcholine receptor [McKenzie et al., 1992]. In addition, the activation of either PtdCh-PLC or PtdCh-PLD is not necessary for growth factor-stimulated cell proliferation. For example, the rate of cell proliferation increases without any change in the activities of PtdCh-PLC or PtdCh-PLD in FGF- and PDGF-treated Chinese hamster fibroblasts [McKenzie et al., 1992].

In addition, PKC may not be necessary for growth factor-stimulated cell proliferation; for example, the rate of cell proliferation increases in Swiss 3T3 fibroblasts in response to PDGF and in HF fibroblasts in response to lysophosphatidic acid after depletion of PKC [van Corven et al., 1989].

However, PKC is probably necessary for PMA-stimulated cell proliferation, since the depletion of PKC abolishes the effect of PMA on cell proliferation in Swiss 3T3 fibroblasts [Pasti et al., 1986]. In PMA-treated T-cells, there is a sustained increase in PKC activity and an increase in the rate of cell proliferation, however, in DAG-treated T-cells, there is only a transient increase in PKC activity, with no effect on cell proliferation [Berry et al., 1990]. This suggests that only a sustained activation of PKC is sufficient to stimulate cell proliferation, indeed multiple additions of DAG stimulate T-cell proliferation [Berry et al., 1990].

Therefore, PtdIns-PLC, PtdCh-PLC and PtdCh-PLD are not necessary or sufficient to stimulate the rate of cell proliferation. In contrast, PKC is not necessary, but may be sufficient for an increase in the rate of cell proliferation. However, these effects may be sufficient to stimulate some of the early events of cell proliferation such as the early phase of growth factor-stimulated glucose transport.

4.1.4　The relationship with glucose transport

Since the early phase of growth factor-stimulated glucose transport is an early event of the cell cycle, it is possible that it could be mediated by a signal transduction pathway involving DAG and PKC. In support of this hypothesis, the addition of DAG, to primary adipocytes, stimulates the rate of glucose transport. The most effective DAGs are *sn*-1,2-ditetradecanoylglycerol, *sn*-1,2-dihexadecenoylglycerol and *sn*-1,2-dioctadecenolyglycerol [Strålfors, 1988]. In addition, 1-monooleoylglycerol, a DAG kinase inhibitor, stimulates the rates of glucose transport and of cell proliferation in Swiss 3T3 fibroblasts [Takuwa et al., 1988]. The rate of glucose transport also increases after the exogenous addition of PtdIns-PLC from *B. cereus* to primary adipocytes [Strålfors, 1988], or of PtdCh-PLC from *Clostridium perfringens* to rat epitrochlearis muscle [Henriksen et al., 1989] or BC3H-1 myocytes [Standaert et al., 1988]. However, the exogenous addition of PtdIns-PLC, from *Staphylococcus aureus* or *Bacillus thuringiensis*, to BC3H-1 myocytes has no effect on the rate of glucose transport [Standaert et al., 1988]. PMA also stimulates the rate of glucose transport in many cell types [Flier et al., 1987].

PDGF is able to activate signal transduction pathways involving phospholipid hydrolysis and PKC activation, although the precise pathway activated depends on the cell type. PDGF has no effect on the hydrolysis of PtdIns or PtdCh in Chinese hamster lung fibroblasts [McKenzie et al., 1992], but stimulates the hydrolysis of PtdCh in IIC9 fibroblasts [Wright et al., 1988; Pessin and Raben, 1989; Ha and Exton, 1993] and stimulates the hydrolysis of both PtdIns and PtdCh in Swiss 3T3 fibroblasts [Price et al., 1989]. However, it is not known whether a signal transduction pathway involving DAG and PKC mediates the early phase of PDGF-stimulated glucose transport.

Some groups claim that a signal transduction pathway involving DAG and PKC mediates the early phase of insulin-stimulated glucose transport. However, many other groups do not see any effect of insulin on these processes.

Insulin stimulates the *de novo* synthesis of phospholipids in BC3H-1 myocytes [Farese et al., 1984], but has no effect on PtdIns hydrolysis in BC3H-1 myocytes [Farese et al., 1985], rat hepatocytes [Sakai and Wells, 1986] or adipocytes [Augert and Exton, 1988].

In agreement with this, insulin has no effect on the intracellular free calcium ion concentration in BC3H-1 myocytes [Farese et al., 1985] or HF fibroblasts [Moolenaar et al., 1984b]. Insulin is reported to stimulate DAG accumulation by *de novo* synthesis and by the hydrolysis of PtdCh in BC3H-1 myocytes, rat adipocytes [Farese et al., 1985] and soleus muscle [Ishizuka et al., 1990]. However, other studies show no effect of insulin on DAG mass in rat adipocytes [Augert and Exton, 1988] or on PtdCh hydrolysis in Swiss 3T3 fibroblasts [Price et al., 1989].

Insulin is reported to stimulate the activation of PKC in BC3H-1 myocytes, rat adipocytes [Acevedo-Duncan et al., 1989; Ishizuka et al., 1989; Vila et al., 1989; Cooper et al., 1990; Egan et al., 1990], and soleus muscle [Ishizuka et al., 1990]. Insulin-stimulated glucose transport is abolished by the PKC inhibitors, staurosporine and polymixin B in rat muscle [Ishizuka et al., 1990] and by staurosporine, H-7 and sangiuamyan in rat adipocytes and BC3H-1 myocytes [Standaert et al., 1990]. However, insulin is also reported to have no effect on PKC activity in rat epitrochlearis muscle [Henriksen et al., 1989], or in HIRC-B fibroblasts, BC3H-1 myocytes, 3T3-L1 adipocytes, and H35 hepatoma cells transfected with the MARCKS protein [Blackshear et al., 1991]. Furthermore, the down-regulation of PKC has no effect on many insulin-stimulated responses in many cell types including 3T3-L1 fibroblasts, 3T3-L1 adipocytes, H35 hepatoma cells, HIRC-B cells, HIR 3.5 cells, Chinese hamster ovary T-cells, or BC3H-1 myocytes [Blackshear et al., 1985; Stumpo and Blackshear, 1986; Blackshear et al., 1990; Lai et al., 1990; Blackshear et al., 1991; Stumpo and Blackshear, 1991].

Thus, it is not clear whether a signal transduction pathway involving DAG and PKC is activated in response to insulin, and therefore whether such a signal transduction pathway mediates the early phase of insulin-stimulated glucose transport. Nor is it clear whether such a signal transduction pathway mediates the early phase of PDGF-stimulated glucose transport. In order to examine whether the early phase of growth factor-stimulated glucose transport is mediated by a signal transduction pathway involving DAG and PKC, several approaches were taken. Firstly, the effects of insulin and PDGF on DAG mass were established. Secondly, the effects of these growth factors on PKC activity were determined. Finally, the requirement of the early phase of growth factor-stimulated glucose transport for PKC was examined.

4.2   Results

4.2.1   The effect of growth factors on DAG accumulation

The effects of insulin and PDGF on DAG accumulation were established by measuring total DAG mass levels in 3T3-L1 fibroblasts. The lipids were extracted after incubation of 3T3-L1 fibroblasts in 1 µM insulin or 25 ng/ml PDGF {Section 2.9.1}. The lipid extracts were incubated with DAG kinase and [γ-^{32}P]ATP, thus catalysing the phosphorylation of DAG to produce [^{32}P]-labelled PtdOH. The lipids in each sample were separated by tlc and the [^{32}P]-labelled PtdOH was located by autoradiography. The amount of [^{32}P]-labelled PtdOH was quantified by liquid scintillation counting {Section 2.9.2}. The standard curve was linear from 0 to 2000 pmoles of *sn*-1-stearoyl-2-arachidonylglycerol {Figure 2.2}.

At a concentration of 1 µM insulin there was no change in DAG mass at any time between 15 seconds and 60 minutes of exposure to insulin. A representative time-course for the effect of insulin on the DAG mass level is shown in Figure 4.3.

At a concentration of 25 ng/ml PDGF, DAG mass increased rapidly. The increase in DAG mass was evident within 1 minute of exposure to PDGF and reached a maximum by 10 minutes, after which it declined slowly. The DAG mass was still significantly above the basal level after 60 minutes. The maximal stimulation of DAG accumulation, observed in response to 25 ng/ml PDGF, was 1.5 to 1.7 fold. A representative time course for the effect of PDGF on DAG mass levels is shown in Figure 4.4.

4.2.2   The effect of a tumour promoter on DAG accumulation

The effect of PMA on DAG accumulation was established by measuring total DAG mass levels in 3T3-L1 fibroblasts {Section 2.9}. At a concentration of 100 nM PMA, DAG mass increased rapidly. The increase in DAG mass was evident within 1 minute of exposure to PMA and was still increasing by 60 minutes. The increase in DAG mass, observed in response to 100 nM PMA at 60 minutes, was 2.8 to 3.0 fold. A representative time-course for the effect of PMA on DAG mass is shown in Figure 4.5.

Figure 4.3   A time course for insulin-stimulated DAG accumulation

After incubation of quiescent 3T3-L1 fibroblasts with 1 µM insulin present for the times shown, the lipids were extracted and the DAG mass measured (Section 2.9). Each result shows the mean DAG mass level (± SD) for triplicate determinations. Each result is expressed relative to the basal level which was measured at 223 ± 24 pmoles/ 10^6 cells. This is a representative experiment from a group of six; basal levels were between 140 and 260 pmoles/ 10^6 cells.
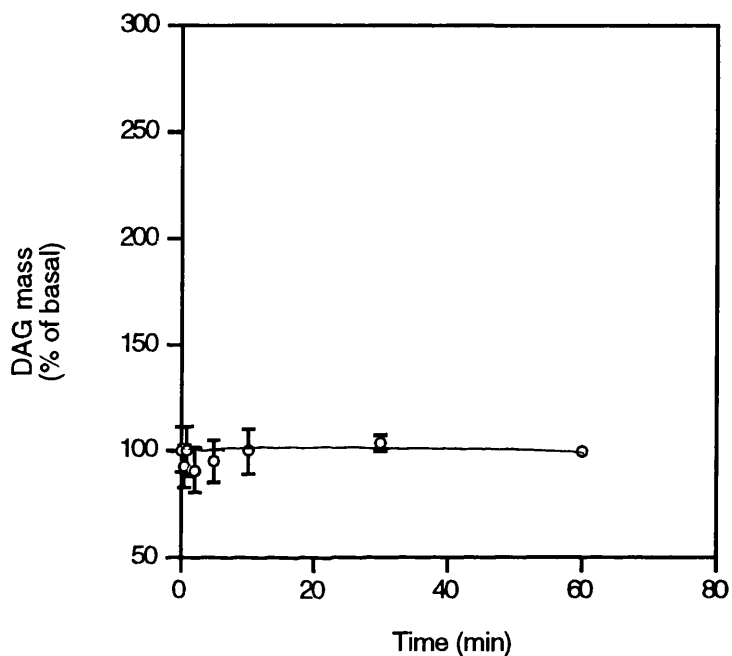
Figure 4.4   A time course for PDGF-stimulated DAG accumulation

After incubation of quiescent 3T3-L1 fibroblasts with 25 ng/ml PDGF present for the times shown, the lipids were extracted and the DAG mass measured {Section 2.9}. Each result shows the mean DAG mass level (± SD) for triplicate determinations. Each result is expressed relative to the basal level which was measured at 101 ± 13 pmoles/ 10^6 cells. This is a representative experiment from a group of seven; basal levels varied from 140 to 260 pmoles/ 10^6 cells and the maximal stimulation was between 1.5 and 1.7 fold (at 10 minutes).
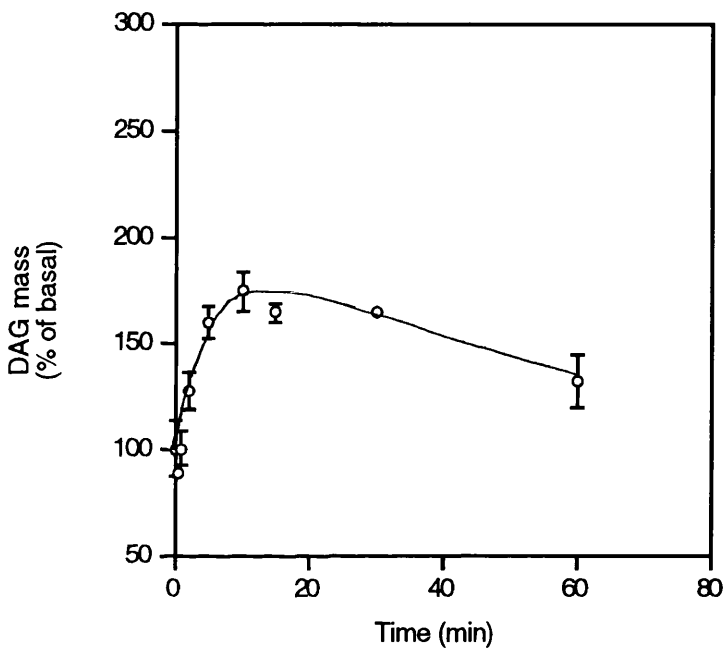
Figure 4.5   A time course for PMA-stimulated DAG accumulation

After incubation of quiescent 3T3-L1 fibroblasts with 100 nM PMA present for the times shown, the lipids were extracted and the DAG mass measured {Section 2.9}. Each result shows the mean DAG mass level (± SD) for triplicate determinations. Each result is expressed relative to the basal level which was measured at 188 ± 9.4 pmoles/ 10^6 cells. This is a representative experiment from a group of four; basal levels varied from   140 to 260 pmoles/ 10^6 cells and the maximal stimulation was between 2.8 and 3.0 fold.
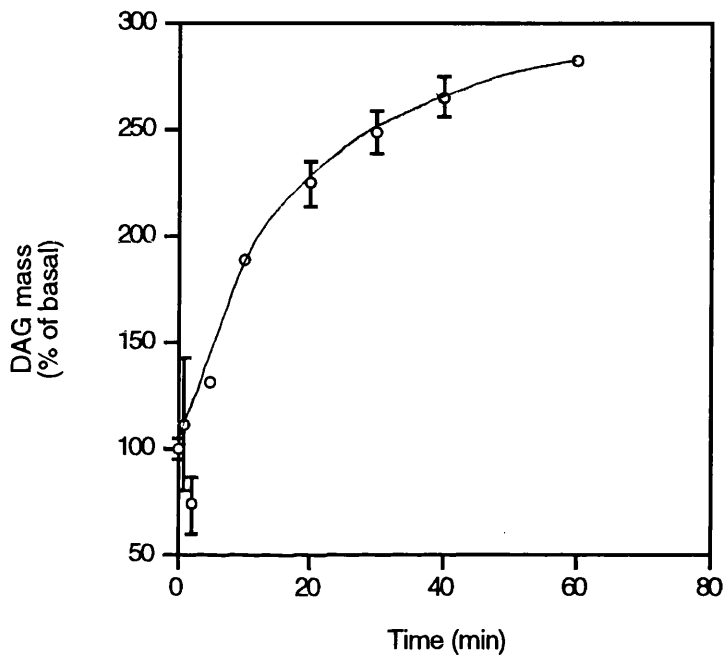
4.2.3 The effect of growth factors and a tumour promoter on PKC activity

The effects of insulin, PDGF and PMA on PKC activity were established by the measurement of incorporation of [^{32}P] into a peptide substrate of PKC {Section 2.10}. This was carried out with permeabilised 3T3-L1 fibroblasts which had been previously incubated for 16 hours in 1 μM 4α-PDD, an inactive phorbol ester, or in 1 μM PMA, an active phorbol ester {Section 2.11}. After the 16 hour incubation in 4α-PDD, there was no change in PKC activity in response to 1 μM insulin, but PKC activity increased 1.7 fold in response to 25 ng/ml PDGF and 3.8 fold in response to 100 nM PMA. After the 16 hour incubation in 1 μM PMA there was no change in PKC activity in response to 1 μM insulin, 25 ng/ml PDGF or 100 nM PMA. The results of a representative experiment are shown in Table 4.1.

4.2.4 The effect of PKC on growth factor and tumour promoter-stimulated glucose transport

The requirement of insulin-, PDGF- and PMA-stimulated glucose transport for PKC activity was established by measuring the rate of 2-deoxyglucose uptake after down-regulation or inhibition of PKC.

Down-regulation of PKC

The rate of 2-deoxyglucose uptake was measured in 3T3-L1 fibroblasts acutely treated with 1 μM insulin, 25 ng/ml PDGF or 100 nM PMA {Section 2.8.1} after a 16 hour incubation in 1 μM 4α-PDD or 1 μM PMA {Section 2.11}. After the 16 hour incubation in 1 μM 4α-PDD, the rate of 2-deoxyglucose uptake increased 1.5 to 5.0 fold in response to 1 μM insulin, 1.5 to 4.0 fold in response to 25 ng/ml PDGF and 1.5 to 4.0 fold in response to 100 nM PMA. After the 16 hour incubation in 1 μM PMA, the rate of 2-deoxyglucose uptake increased 1.5 to 2.5 fold in response to 1 μM insulin and 1.5 to 2.5 fold in response to 25 ng/ml PDGF, but there was no change in response to 100 nM PMA. Furthermore, the basal rate of 2-deoxyglucose uptake was 2.0 to 4.0 fold higher after the 16 hour incubation in 1 μM PMA than after the 16 hour incubation in 1 μM 4α-PDD. The results from a representative experiment are shown in Table 4.2.

Table 4.1   The effect of insulin, PDGF and PMA on PKC activity, after the down-regulation of PKC

After incubation of quiescent 3T3-L1 fibroblasts with 1 μM 4α-PDD or 1 μM PMA overnight {Section 2.11}, then with 1 μM insulin, 25 ng/ml PDGF or 100 nM PMA for 10 minutes, PKC activity was measured {Section 2.10}. Each result shows the mean PKC activity (± SD) for triplicate determinations. This is a representative experiment from a group of four. * p < 0.05; †: not significant.

	PKC activity (cpm incorporated/ min)	
	4α-PDD	PMA
Basal	72.0 ± 1.5	73.5 ± 2.0
Insulin	77.5 ± 3.5†	74.5 ± 1.5†
PDGF	125 ± 2.0*	73.0 ± 1.5†
PMA	274 ± 3.5*	74.5 ± 2.1†

Table 4.2   The effect of insulin, PDGF and PMA on the rate of 2-deoxyglucose uptake, after the down-regulation of PKC

After incubation of quiescent 3T3-L1 fibroblasts with 1 μM 4α-PDD or 1 μM PMA for 16 hours {Section 2.11}, then with 1 μM insulin or 25 ng/ml PDGF for 15 minutes or with 100 nM PMA for 60 minutes, a 5 minute uptake of 2-deoxy-D-[2,6-^{3}H]glucose was measured {Section 2.8.1}. Each result shows the mean rate of specific 2-deoxyglucose uptake (± SD) for triplicate determinations. This is a representative experiment from a group of five; basal rates varied from 6.0 to 21 pmoles/ min/ 10^6 cells after a 16 hour incubation in 1 μM 4α-PDD and from 31 to 80 pmoles/ min/ 10^6 cells after a 16 hour incubation in 1 μM PMA. Basal rates were between 2.4 and 5.0 fold higher after a 16 hour incubation in 1 μM PMA than in 1 μM 4α-PDD. * p < 0.05; †: not significant.

	Rate of 2-deoxyglucose uptake (pmoles/ min/ 10^6 cells)	
	4α-PDD	PMA
Basal	7.9 ± 1.3	31.5 ± 5.8
Insulin	30.4 ± 4.0*	69.5 ± 5.4*
PDGF	30.6 ± 1.7*	62.4 ± 4.4*
PMA	30.9 ± 4.4*	41.8 ± 4.6†

Inhibition of PKC

The rate of 2-deoxyglucose uptake was measured in 3T3-L1 fibroblasts treated with 1 μM insulin, 25 ng/ml PDGF or 100 nM PMA {Section 2.8.1} after a 15 minute incubation with or without Ro 31-8220, a PKC inhibitor {Section 2.12}. In control cells, the rate of 2-deoxyglucose uptake increased 3.0 to 4.6 fold in response to 1 μM insulin, 4.8 to 9.4 fold in response to 25 ng/ml PDGF and 2.0 to 3.0 fold in response to 100 nM PMA. After the 15 minute incubation in 3 μM Ro 31-8220, the rate of 2-deoxyglucose uptake increased 2.7 to 7.7 fold in response to 1 μM insulin and 4.0 to 6.8 fold in response to 25 ng/ml PDGF, but there was no change in response to 100 nM PMA. Incubation in 3 μM Ro 31-8220 had no effect on the basal rate of 2-deoxyglucose uptake. The results from a representative experiment are shown in Table 4.3.

4.2.5   The effect of PKC on the total Glut1 level

The effect of PKC on the total Glut1 protein level was established by Western blotting. Lysates were prepared from 3T3-L1 fibroblasts {Section 2.13.2} treated with 1 μM insulin, 25 ng/ml PDGF or 100 nM PMA after a 16 hour incubation in 1 μM 4α-PDD or 1 μM PMA {Section 2.11}. The proteins were separated by SDS-PAGE {Section 2.15}, then transferred onto nitrocellulose membranes. The membranes were probed with a rabbit anti-Glut1 antibody (East Acres), then with a HRP-conjugated donkey anti-rabbit IgG antibody. The sites of antibody binding were visualised using a ECL detection system {Section 2.16.2}.

When proteins from 3T3-L1 fibroblasts were probed with the anti-Glut1 antibody, the antibody recognised a broad band with a molecular mass of approximately 50 kDa. After the 16 hour incubation in 1 μM 4α-PDD, there was no change in the total Glut1 level in response to 1 μM insulin, 25 ng/ml PDGF or 100 nM PMA. After the 16 hour incubation in 1 μM PMA, there was also no change in the total Glut1 level in response to 1 μM insulin, 25 ng/ml PDGF or 100 nM PMA. However, the basal total Glut1 level was clearly higher after the 16 hour incubation in 1 μM PMA than after the 16 hour incubation in 1 μM 4α-PDD. Representative Western blots are shown in Figure 4.6.

Table 4.3   The effect of insulin, PDGF and PMA on the rate of 2-deoxyglucose uptake, after the inhibition of PKC

After incubation of quiescent 3T3-L1 fibroblasts with 1 µM Ro 31-8220 for 15 minutes (Section 2.12), then with 1 µM insulin or 25 ng/ml PDGF for 15 minutes or with 100 nM PMA for 60 minutes, a 5 minute uptake of 2-deoxy-D-[2,6-^{3}H]glucose was measured (Section 2.8.1). Each result shows the mean rate of specific 2-deoxyglucose uptake ($\pm$ SD) for triplicate determinations. This is a representative experiment from a group of three; basal rates varied from 6.1 to 28.3 pmoles/ min/ 10^6 cells. * p < 0.05; †: not significant.

	Rate of 2-deoxyglucose uptake (pmoles/ min/ 10^6 cells)	
	Control	Ro 31-8220
Basal	9.0 ± 3.9	11.1 ± 2.8
Insulin	$36.8 \pm 4.1*$	$31.6 \pm 2.0*$
PDGF	$72.6 \pm 8.3*$	$51.2 \pm 9.2*$
PMA	$29.6 \pm 7.1*$	$15.0 \pm 2.1^†$

110

Figure 4.6   The effect of PKC on the total Glut1 level

After incubation of quiescent 3T3-L1 fibroblasts with a) 1 μM 4α-PDD or b) 1 μM PMA for 16 hours {Section 2.11}, and then with A) 1 μM insulin, B) 25 ng/ml PDGF or C) 100 nM PMA present for the times shown, lysates were prepared {Section 2.13.2}. Approximately 0.03 mg of protein was loaded onto 10% (w/v) polyacrylamide large gels, the proteins were separated by SDS-PAGE {Section 2.15}, and then transferred onto nitrocellulose membranes. The membranes were probed with a rabbit anti-Glut1 antibody, then with a HRP-conjugated donkey anti-rabbit IgG antibody. The sites of antibody binding were visualised using an ECL detection system {Section 2.16.2}. These are representative Western blots from groups of two lysate preparations.

111
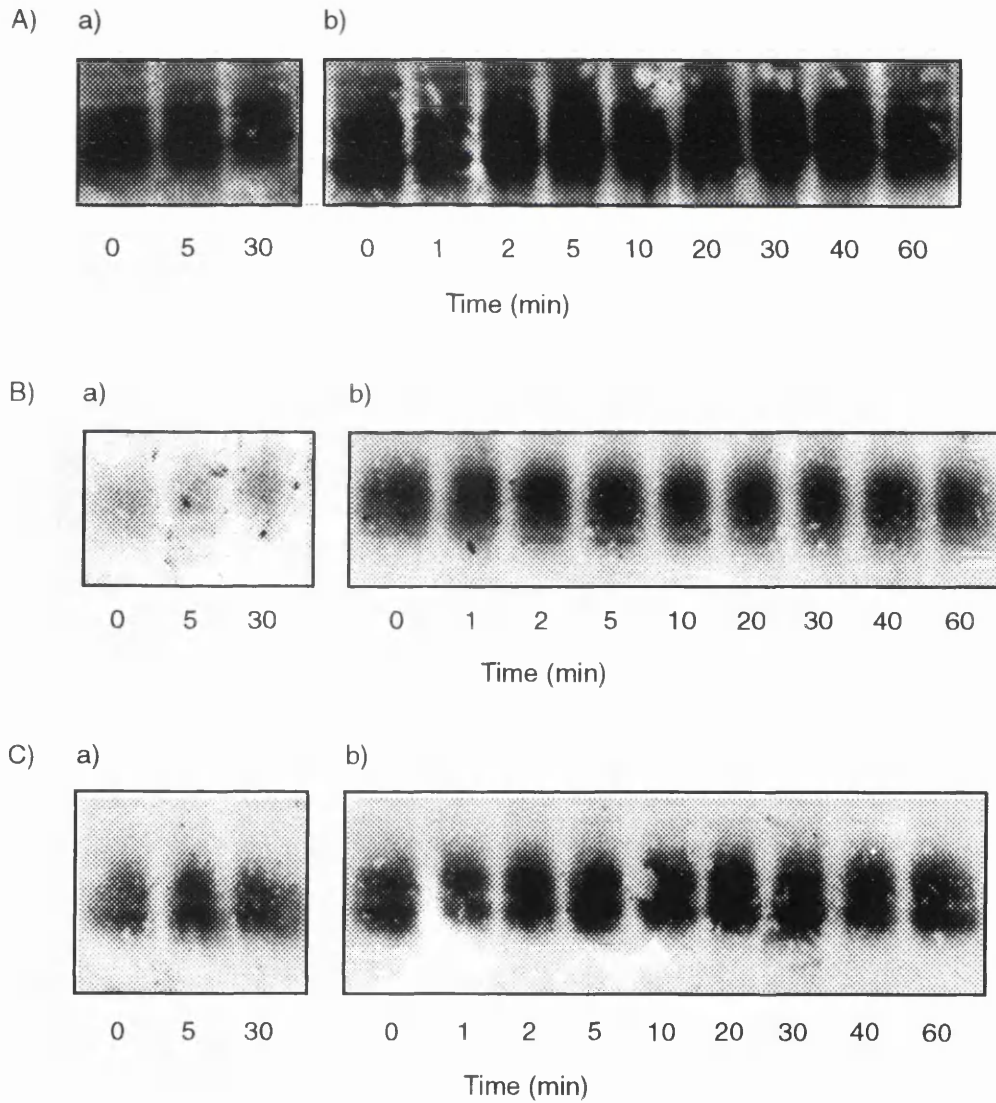
4.3 Discussion

In order to examine whether the early phase of growth factor-stimulated glucose transport is mediated by a signal transduction pathway involving DAG and PKC, several approaches were taken. Firstly, the effects of insulin and PDGF on DAG accumulation were determined. Secondly, the effects of these growth factors on PKC activity were established. Finally, the requirement of the early phase of growth factor-stimulated glucose transport for PKC was examined, using pharmacological reagents that either deplete cellular PKC or inhibit its activity.

4.3.1 The effect of growth factors and a tumour promoter on DAG accumulation

Insulin stimulated the rate of 2-deoxyglucose transport in 3T3-L1 fibroblasts, the maximum rate occurring at a concentration of 1 µM insulin {Figure 3.4}. Incubation of 3T3-L1 fibroblasts in the same concentration of insulin for times between 0 and 60 minutes had no effect on the DAG mass level {Figure 4.3}. It was possible that the passages of 3T3-L1 fibroblasts used in the experiments with insulin had lost the ability accumulate DAG in response to ligands. However, an increase in the DAG mass level occurred in cells from the same passage in response to PDGF (results not shown). Therefore these cells had a functional signal transduction pathway leading to DAG accumulation. It was also possible that these cells had become insulin-insensitive. However, an increase in 2-deoxyglucose transport in response to 1 µM insulin, with characteristics as previously described, occurred in cells from the same passage (results not shown). Therefore these cells were insulin-sensitive.

If the early phase of insulin-stimulated glucose transport is mediated by a pathway involving DAG, then there should be an increase in the DAG mass level under the same conditions that the maximal increase in the rate of 2-deoxyglucose transport occurred, that is by 60 minutes in response to 1 µM insulin {Figure 3.5}. This did not occur, suggesting that the early phase of insulin-stimulated glucose transport is not mediated by a signal transduction pathway involving DAG.

PDGF stimulated the rate of 2-deoxyglucose transport in 3T3-L1 fibroblasts, the maximal rate occurring at a concentration of 25 ng/ml PDGF {Figure 3.7}. Incubation of 3T3-L1 fibroblasts in the same concentration of PDGF also led to an increase in the DAG mass level. DAG accumulation was evident within 1 minute of exposure to PDGF and reached a maximum by 10 minutes, after which it declined slowly. The DAG mass was still significantly above the basal level after 60 minutes {Figure 4.4}. If the early phase of PDGF-stimulated glucose transport is mediated by a signal transduction pathway involving DAG, then the increase in the DAG mass level should precede the increase in the rate of 2-deoxyglucose transport. This would appear to be the case {Figure 4.7}. This suggests that the early phase of PDGF-stimulated glucose transport could potentially be mediated by a signal transduction pathway involving DAG.

PMA also stimulated the rate of 2-deoxyglucose transport in 3T3-L1 fibroblasts {Figure 3.9}. Incubation of 3T3-L1 fibroblasts in 100 nM PMA also led to an increase in the DAG mass level. DAG accumulation was evident within 1 minute of exposure to PMA and reached a maximum by 60 minutes {Figure 4.5}. If the early phase of PMA-stimulated glucose transport is mediated by a signal transduction pathway involving DAG, then the increase in the DAG mass level should precede the increase in the rate of 2-deoxyglucose transport. This would appear to be the case {Figure 4.8}. This suggests that the early phase of PMA-stimulated glucose transport could potentially be mediated by a signal transduction pathway involving DAG.

The source of the DAG formed in response to PDGF and PMA was not analysed. However, the initial rates of DAG accumulation were the similar in response to PDGF and PMA {Figures 4.4 and 4.5}. Since activation of signal-activated phospholipases occurs in a time-dependent manner [Liscovitch, 1992], it is likely that PDGF and PMA stimulated the activation of the same phospholipase or groups of phospholipases. Since PtdIns-PLC-catalysed hydrolysis of PtdIns is generally transient [Cook et al., 1990], and PMA inhibits PtdIns-PLC activity [Price et al., 1989] it would seem likely that the DAG accumulation observed in response to PDGF and PMA was formed by the hydrolysis of PtdCh and not by the hydrolysis of PtdIns.

Since PDGF is able to stimulate the hydrolysis of both PtdIns and PtdCh in some cells, further analysis is necessary to confirm this hypothesis and to establish whether the

Figure 4.7   A comparison of the time courses for PDGF-stimulated 2-deoxyglucose uptake and DAG accumulation

After incubation of quiescent 3T3-L1 fibroblasts with 25 ng/ml PDGF for the times shown, either a 3 minute uptake of 2-deoxy-D-[2,6-^{3}H]glucose was measured {Section 2.8.1} or the lipids were extracted and the DAG mass measured {Section 2.9}. Each result shows the mean rate of specific 2-deoxyglucose uptake (± SD) (o), or the mean of the DAG mass level (± SD) (□) for triplicate determinations. Each result is expressed relative to the basal levels, which were measured at 47.8 ± 1.9 pmoles 2-deoxyglucose/ min/ 10^6 cells and 101 ± 13 pmoles DAG/ 10^6 cells. These are representative experiments from groups of three and six respectively; basal levels varied from 6.0 to 49 pmoles 2-deoxyglucose/ min/ 10^6 cells and 140 to 260 pmoles DAG/ 10^6 cells.
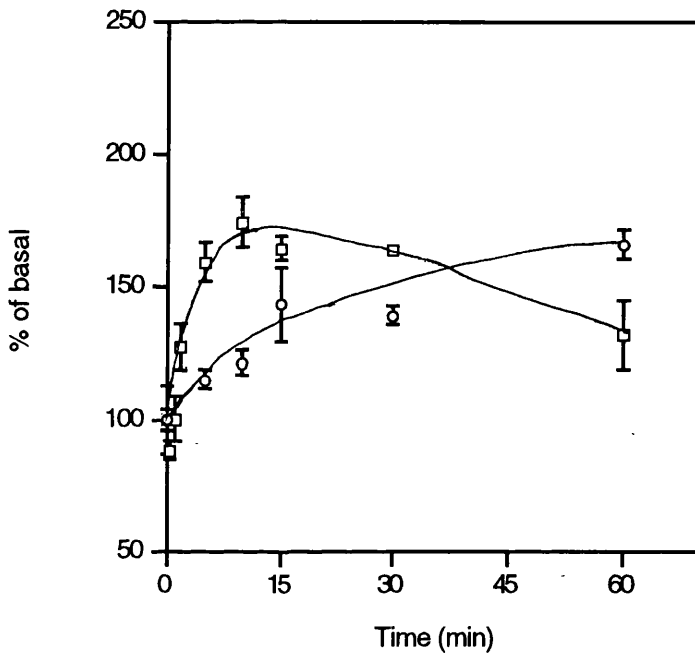
Figure 4.8   A comparison of the time courses for PMA-stimulated 2-deoxyglucose uptake and DAG accumulation

After incubation of quiescent 3T3-L1 fibroblasts with 100 nM PMA present for the times shown, either a 3 minute uptake of 2-deoxy-D-[2,6-^{3}H]glucose was measured {Section 2.8.1} or the lipids were extracted and the DAG mass measured {Section 2.9}. Each result shows the mean rate of specific 2-deoxyglucose uptake (± SD) (o), or the mean of the DAG mass level (± SD) (□) for triplicate determinations. Each result is expressed relative to the basal levels, which were measured at 20.3 ± 2.6 pmoles 2-deoxyglucose/ min/ 10^6 cells and 188 ± 9.4 pmoles DAG/ 10^6 cells. These are representative experiments from groups of three and six respectively; basal levels varied from 6.0 to 49 pmoles 2-deoxyglucose/ min/ 10^6 cells and 140 to 260 pmoles DAG/ 10^6 cells.
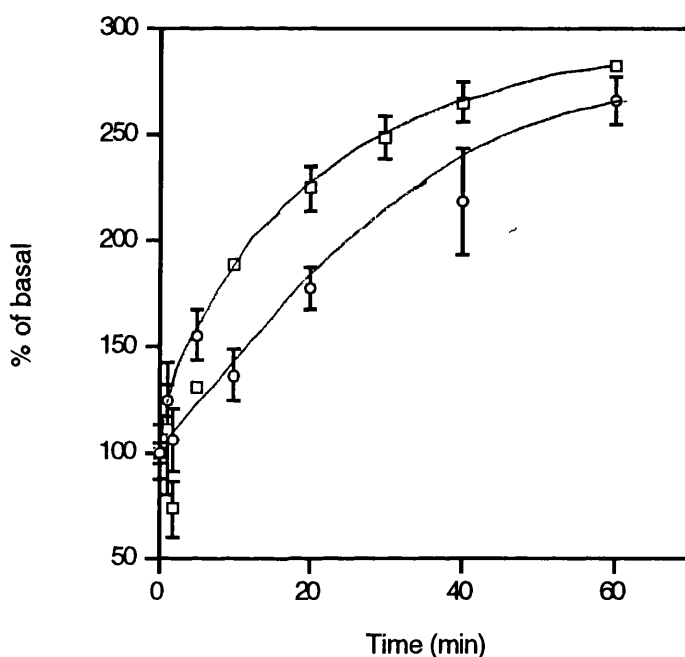
hydrolysis of PtdCh in PDGF- and PMA-treated 3T3-L1 fibroblasts is catalysed by a PLC or a PLD.

The observation that insulin did not stimulate any rapid transient increase in DAG mass in 3T3-L1 fibroblasts is in agreement with the observation that PLC-γ1 does not bind to the insulin receptor after autophosphorylation, or to IRS-1 after tyrosine phosphorylation [Sun et al., 1993a; Vallus and Kazlauskas, 1993]. This result is also in agreement with the work of several groups who have observed no effect of insulin on PtdIns hydrolysis in BC3H-1 myocytes [Farese et al., 1985], rat hepatocytes [Sakai and Wells, 1986] or rat adipocytes [Augert and Exton, 1988], or on the cytoplasmic free calcium ion concentration in BC3H-1 myocytes [Farese et al., 1985] or HF fibroblasts [Moolenaar et al., 1984b].

Farese and colleagues have reported that insulin stimulates PtdCh hydrolysis and DAG accumulation in BC3H-1 myocytes, rat adipocytes and soleus muscle [Farese et al., 1985; Ishizuka et al., 1990]. It is possible that insulin, like PDGF-BB has different effects upon PtdCh hydrolysis in different cells, so that insulin is able to stimulate PtdCh hydrolysis in some cells but not in others. However, other researchers do not observe any changes in PtdCh hydrolysis or DAG accumulation in insulin-treated rat adipocytes [Augert and Exton, 1988], thus it is unlikely that these are cell-specific differences.

4.3.2   The effect of growth factors and a tumour promoter on PKC activity

Several methods can be used to measure PKC activity. These include measurement of changes in the intracellular location of PKC (translocation), of changes in the PKC activity in different intracellular locations and of changes in the total PKC activity.

Changes in the intracellular location of PKC can be established by Western blotting of PKC in membrane and cytosolic extracts. The correlation of translocation of PKC with its activation is based upon the assumption that PKC isozymes are activated by binding to a cofactor, phosphatidyl serine, and an activator, DAG, both of which are located in the cytosolic face of the plasma membrane. Therefore cytosolic PKC is inactive while membrane PKC is active. However, association of PKC with the plasma membrane does

not necessarily reflect its activation, since PKC may be membrane bound by association with its cofactor, phosphatidyl serine, in the absence of its activator, DAG [Bell and Burns, 1991]. Consequently, changes in the intracellular location of PKC may occur without any change in the PKC activity [Halsey et al., 1987; Heidenreich et al., 1990]. Furthermore, some isozymes of PKC undergo translocation to sites other than the plasma membrane, such as the nucleus or cytoskeleton, in response to ligands [Dekker and Parker, 1994]. In addition, some isozymes of PKC are rapidly down-regulated in response to ligands [Dekker and Parker, 1994]. Therefore, measurement of the intracellular location of PKC is not a reliable indication of PKC activation.

Changes in the PKC activity in different intracellular locations can be established by measuring the phosphorylation of a substrate by membrane and cytosol extracts or by PKC partially purified from membrane and cytosolic extracts. Measurement of the PKC activity in membrane and cytosolic extracts is also based on the assumption that translocation of PKC correlates with its activation. Activation of PKC occurs by allosteric means. Therefore, disruption of the cell may allow the allosteric activators to dissociate from the kinase, and so, measurement of PKC activity in a cell extract does not measure the activation state that existed in the cell, but the amount of the enzyme present in that fraction. Therefore, measurement of the activity of PKC in various intracellular fractions is not a reliable indicator of PKC activation.

Changes in the total PKC activity also can be established by measuring the PKC activity in total cellular extracts, however, as discussed above, this approach is also flawed. The total PKC activity can also be measured i*n vivo*, for example, by measuring the phosphorylation of an endogenous specific substrate for PKC, such as MARCKS [Blackshear, 1993]. A disadvantage of this approach is that some cells such as 3T3-L1 adipocytes and H35 hepatoma cells express relatively low amounts of this protein [Blackshear et al., 1991]. This can be overcome by using cells which stably express MARCKS [Blackshear et al., 1991]. An alternative approach is to measure the phosphorylation of small synthetic peptide substrates in permeabilised cells [Heasley and Johnson, 1989; Alexander et al., 1990]. The sequence of such peptides can be based on the phosphorylation site of a substrate of PKC [House et al., 1987; Heasley and Johnson, 1989] or on the pseudo-substrate site of a PKC isozyme [Heidenreich et al., 1990]. Permeabilisation of cells allows rapid access of small peptides to the interior

without disrupting mechanisms of signal transduction [Alexander et al., 1989]. A disadvantage of this approach is that each PKC isozyme has a different substrate specificity. However, on balance, this is the best available approach to establish the effect of ligands on PKC activity.

The estimates of PKC activity presented in this thesis were made by measuring the phosphorylation of a synthetic peptide in digitonin-permeabilised cells {Section 2.10}. The peptide used for this analysis (Pro-Leu-Ser-Arg-Thr-Leu-Ser-Val-Ala-Ala-Lys-Lys) was derived from a peptide corresponding to residues one to ten of glycogen synthase [House et al., 1987]. The K_m values of rat brain PKC, rabbit muscle multifunctional calmodulin-dependent protein kinase and bovine heart cyclic AMP-dependent protein kinase for this peptide are 4.1 µM, 18 µM and 2726 µM respectively [House et al., 1987]. Therefore, this peptide is a good substrate of PKC, but not of multifunctional calmodulin-dependent protein kinase or of cyclic AMP-dependent protein kinase. Unfortunately, the affinities of the individual PKC isozymes for this peptide are unknown; this caveat should be kept in mind during the interpretation of these results.

Quiescent 3T3-L1 fibroblasts from the same passage were incubated with insulin, PDGF or PMA present at concentrations sufficient to stimulate a maximum increase in the rate of 2-deoxyglucose uptake and in the case of the latter two, to stimulate DAG accumulation. Incubations with ligand were carried out for 10 minutes, before permeabilisation and the addition of the peptide substrate. Given that increases in the rate of 2-deoxyglucose uptake and DAG accumulation were evident by 10 minutes of exposure to the ligands, this should be sufficient time to allow for any relevant activation of PKC.

The cells were also pre-incubated for 16 hours in 1 µM PMA in order to evaluate the effectiveness of a long incubation in a high concentration of phorbol ester as a method to deplete cellular PKC activity. For a control, cells were simultaneously incubated with 1 µM 4α-PDD, an inactive phorbol ester. In cells incubated with 1 µM 4α-PDD, PKC activity increased in response to 25 ng/ml PDGF and 100 nM PMA, but did not change in response to 1 µM insulin. In cells incubated with 1 µM PMA, PKC activity did not change in response to 1 µM insulin, 25 ng/ml PDGF or 100 nM PMA {Table 4.1}. These

results suggest that PDGF and PMA can stimulate PKC activity in 3T3-L1 fibroblasts, while insulin does not.

The observation that both PDGF and PMA stimulate PKC activity in 3T3-L1 fibroblasts is in agreement with the work of several other groups who observe an increase in the phosphorylation of MARCKS in response to PDGF and PMA in 3T3-L1 fibroblasts, 3T3-L1 adipocytes, BC3H-1 myocytes, and Swiss 3T3 fibroblasts [Rozengurt et al., 1983; Blackshear et al., 1985; Spach et al., 1986]. These groups also failed to observe any effect of insulin on the phosphorylation of MARCKS in these cells or in HIRC-B fibroblasts, BC3H-1 myocytes, or H35 hepatoma cells after transfection with MARCKS [Spach et al., 1986; Blackshear et al., 1991]. However, Farese and colleagues have reported that insulin stimulates PKC activity in BC3H-1 myocytes, rat adipocytes, and soleus muscle [Acevedo-Duncan et al., 1989; Ishizuka et al., 1989; Vila et al., 1989; Cooper et al., 1990; Ishizuka et al., 1990].

These differences in the activation of PKC could arise from differences in the methodology used. Firstly, Farese and colleagues correlate translocation, measured either by Western blotting or assay of PKC activity in cell extracts, with PKC activation. As discussed previously, this is a flawed approach. Indeed Farese and colleagues observed that different methods of PKC purification lead to differences in the measured PKC activity [Cooper et al., 1990]. Secondly, the differences in observed PKC activity could arise from the use of different substrate proteins in the PKC activity assays, since each PKC isozyme has a different substrate specificity. Therefore, if the activity of a PKC isozyme increases in response to insulin, it is possible that it catalyses the phosphorylation of only certain substrates. Unfortunately, the substrate specificity of each PKC isozyme is unknown.

The differences in results could also arise from the use of different cells, since the PKC isozymes are expressed in a tissue-specific manner. Unfortunately, the PKC isozymes expressed by most cells, including 3T3-L1 fibroblasts, are unknown. It is also possible that different signal transduction pathways mediate the change in the rate of glucose transport in cells that respond to insulin by increased proliferation and cells that respond to insulin with a 'classical' hormonal response (skeletal muscle and adipocyte cells). Indeed, Farese and colleagues consider BC3H-1 myocytes to be a model of such a

hormonal response. However, these cells differ considerably from skeletal muscle. Skeletal muscle expresses both Glut1 and Glut4, however, BC3H-1 myocytes express only Glut1 [Calderhead et al., 1990b]. The rate of glucose transport in skeletal muscle increases eight to ten fold in response to insulin [Henriksen et al., 1989], mainly as a consequence of translocation of Glut4 [Slot et al., 1991a], but only two to three fold in BC3H-1 myocytes as a consequence of translocation of Glut1 [Calderhead et al., 1990b]. Furthermore, insulin stimulates the proliferation of BC3H-1 myocytes [Standaert et al., 1987]. Therefore, BC3H-1 myocytes are not a good model of a 'classical' hormonal response to insulin. Thus, it is unlikely that the differences in the activation of PKC observed in 3T3-L1 fibroblasts and BC3H-1 myocytes are due to different roles of insulin in these cells.

Some groups have disputed the validity of studies using a long incubation with a high concentration of a phorbol ester to deplete cellular PKC activity, on the basis that this technique may be applicable only to certain PKC isozymes. However, PMA can bind to and stimulate the activity of all the classical and novel PKC isozymes, therefore, if such treatment can cause the degradation of one such isozyme, it is likely that it will also cause the degradation of the other classical and novel PKC isozymes. The results presented in this thesis suggest that this technique depletes cellular PKC activity. Furthermore, analysis of Western blots prepared with an anti-PKC antibody or measurement of specific phorbol ester binding show that a long incubation in a high concentration of a phorbol ester does result in depletion of cellular PKC [Blackshear et al., 1985]. In addition, many processes known to be mediated by PKC are abolished by such treatment, for example, PMA-stimulated c-*fos* induction in 3T3-L1 adipocytes [Stumpo and Blackshear, 1986] and HIRC-B cells [Stumpo and Blackshear, 1991], PMA-stimulated MARCKS protein phosphorylation in 3T3-L1 fibroblasts [Blackshear et al., 1985], and PMA-stimulated Raf-1 kinase phosphorylation in HIR 3.5 cells [Blackshear et al., 1990]. Therefore, this appears to be a valid technique for depletion of the classical and novel PKC isozymes [Blackshear et al., 1991]. However, the atypical PKC isozymes are probably unaffected by this treatment, since phorbol esters do not activate them, and probably do not bind to them. Unfortunately, little is known about the regulation of such isozymes, except that they appear to be activated independently of DAG, phosphatidyl serine and phorbol esters, and therefore are probably not activated by the signal transduction pathways described.

Therefore, the PKC isozymes that are expressed by 3T3-L1 fibroblasts and that catalyse phosphorylation of the peptide described, are activated in response to PDGF and PMA, but not in response to insulin. Furthermore, the activity of these isozymes is abolished by a long incubation in a high concentration of PMA, a technique referred to as down-regulation of PKC. However, since it is not known which PKC isozymes catalyse the phosphorylation of the peptide used in the assay presented or which are expressed by 3T3-L1 fibroblasts, it is not possible to be more precise in the interpretation of these results.

4.3.3 The effect of PKC on growth factor- and tumour promoter-stimulated glucose transport

The requirement of the early phase of insulin-, PDGF- and PMA-stimulated glucose transport for PKC activity in 3T3-L1 fibroblasts was established in two ways. The rate of 2-deoxyglucose uptake was measured in 3T3-L1 fibroblasts treated with 1 μM insulin, 25 ng/ml PDGF or 100 nM PMA, firstly, after the down-regulation of PKC and secondly, after the inhibition of PKC.

In both cases, cells from the same passage were incubated with the ligand present at concentrations sufficient to stimulate a maximal increase in the rate of 2-deoxyglucose uptake and in the case of the latter two, to stimulate DAG accumulation. Incubations with insulin and PDGF were carried out for 30 minutes, while incubations with PMA were carried out for 60 minutes, before measurement of the rate of 2-deoxyglucose uptake. Given that the maximum increase in DAG accumulation occurs by 10-minutes in response to PDGF and by 60 minutes in response to PMA, this should be sufficient time to allow for any relevant activation of PKC.

In each case, in the control cells the rate of 2-deoxyglucose uptake increased in response to insulin, PDGF and PMA. However, after down-regulation or inhibition of PKC, the rate of 2-deoxyglucose uptake increased in response to 1 μM insulin and 25 ng/ml PDGF, but did not change in response to 100 nM PMA (Tables 4.2 and 4.3). Therefore, these results suggest that PKC is not necessary for the early phase of insulin- or PDGF-stimulated glucose transport, but that it is necessary for the early phase of PMA-stimulated glucose transport.

In agreement with the results presented here, other studies of the early phase of growth factor-stimulated glucose transport have shown that the down-regulation of PKC has no effect on the rate of 3-O-methylglucose transport in response to insulin, EGF, FGF and PDGF in Swiss 3T3 fibroblasts [Kitagawa et al., 1986; Kitagawa et al., 1989], or on the rate of 2-deoxyglucose uptake in BC3H-1 myocytes [Standaert et al., 1988].

However, Farese and colleagues observe partial inhibition of insulin-stimulated glucose transport BC3H-1 myocytes, rat adipocytes and soleus muscle treated with PKC inhibitors [Ishizuka et al., 1990; Standaert et al., 1990]. Therefore, they suggest that insulin-stimulated glucose transport is mediated by a PKC-dependent pathway. In this work, the PKC inhibitors used were polymyxin B, staurosporine, H-7, and sangivamycin.

The indolocarbazole, staurosporine is a bacterial metabolite which is a non-selective protein kinase inhibitor. The IC$_{50}$ values for rat brain PKC, bovine heart cyclic AMP-dependent protein kinase and rat brain calcium/ calmodulin-dependent protein kinase for staurosporine are 0.1 µM, 0.12 µM and 0.04 µM respectively [Davis et al., 1989]. Staurosporine also inhibits the PDGF receptor tyrosine protein kinase with an IC$_{50}$ value of 0.02 µM [Secrist et al., 1990], therefore staurosporine is a general protein kinase inhibitor. Furthermore, staurosporine effects cell morphology, causing cells to round up and to detach from plate within 1 hour, consistent with staurosporine being a general protein kinase inhibitor [Susa et al., 1992]. Thus, loss of an ligand-stimulated response after treatment of cells with staurosporine does not necessarily imply that PKC is necessary for that response to occur.

H-7, is a isoquinoline-sulphonamide derivative which prevents ATP binding to PKC. However, H-7 only partially inhibits PKC activity and has no effect on some PKC mediated events [Susa et al., 1992]. Therefore, loss of an ligand-stimulated response after treatment of cells with H-7 also does not necessarily imply that PKC is necessary for that response to occur.

Ro 31-8220 is a bisindolylmaleimide derivative of staurosporine. It is a more potent inhibitor of PKC and shows a higher selectivity for PKC. The *in vitro* IC$_{50}$ values of rat brain PKC, bovine heart cyclic AMP-dependent protein kinase and rat brain calcium/ calmodulin-dependent protein kinase for Ro 31-8220 are 0.01 µM; 1.5 µM and 17 µM

respectively [Davis et al., 1989]. Ro 31-8220 can penetrate the cell and prevent PKC-mediated effects. The *in vivo* IC_{50} values of PMA-stimulated phosphorylation of pp47 in platelets and inhibition of CD3 down-regulation for Ro 31-8220 are 0.7 μM and 0.5 μM respectively [Davis et al., 1989]. Ro 31-8220 shows a slight selectivity for PKC-α over PKC-ßI, PKC-ßII, PKC-γ or PKC-ε, but not enough to differentiate between the different isozymes. The effects on PKC-δ and PKC-ζ are not yet known [Wilkinson et al., 1993].

In order to establish the dependence of a process on PKC, it is necessary to use an inhibitor specific for this enzyme, such as the bisindolylmaleimide described. Staurosporine and H-7 are not appropriate for such studies. Therefore, the results presented in this thesis suggest that PKC-α, PKC-ßI, PKC-ßII, PKC-γ and PKC-ε are not involved in the early phase of insulin- or PDGF-stimulated glucose transport in 3T3-L1 fibroblasts.

4.3.4   The basal rate of glucose transport

Down-regulation of PKC causes a significant increase in the basal rate of 2-deoxyglucose uptake {Table 4.2}. A similar increase in the basal rate of 2-deoxyglucose uptake has also been observed in 3T3-L1 adipocytes [Gibbs et al., 1991] and BC3H-1 myocytes [Standaert et al., 1988]. It is possible that PKC inhibits the basal rate of glucose transport in resting cells, and that down-regulation of PKC removes this inhibition. Therefore, incubation in a PKC inhibitor should also cause an increase in the basal rate of 2-deoxyglucose uptake. However, incubation of 3T3-L1 fibroblasts in the PKC inhibitor, Ro 31-8220 had no effect on the basal rate of 2-deoxyglucose uptake {Table 4.3}, suggesting that this is not the case.

It is also possible that depletion of PKC does not occur immediately in response to a long incubation in a high concentration of a phorbol ester and so, initially, the phorbol ester stimulates PKC activity and various PMA-stimulated effects occur, for example, an increase in the total Glut1 level. Analysis of the total Glut1 level by Western blotting of 3T3-L1 fibroblast lysates prepared from control cells and from PKC-deficient cells showed that the basal total Glut1 level was higher in PKC-deficient cells than in control cells {Figure 4.6}. This is in agreement with studies of Glut1 levels in 3T3-L1 adipocytes, where Glut1 level was approximately two fold higher after down-regulation

of PKC [Gibbs et al., 1991]. Furthermore, preliminary work showed that the increase in the basal rate of 2-deoxyglucose transport observed after down-regulation of PKC was abolished by incubating the 3T3-L1 fibroblasts in the PKC inhibitor, Ro 31-8220, before incubation in the phorbol esters (results not shown).

Therefore, the increase in the basal rate of 2-deoxyglucose uptake observed after down-regulation of PKC arises because depletion of PKC does not occur immediately on incubation in a high concentration of a phorbol ester. Consequently, during the early part of the incubation, the phorbol ester can stimulate the activation of PKC, leading to, among other things, an increase in the total Glut1 level and consequently an increase in the basal rate of glucose transport.

4.3.5   Summary

The results presented suggest that in 3T3-L1 fibroblasts PKC is not necessary for the early phase of either insulin- or PDGF-stimulated glucose transport, but that it is necessary for the early phase of PMA-stimulated glucose transport. In addition, these results show that PDGF and PMA each stimulate DAG accumulation, and PKC activity in 3T3-L1 fibroblasts, while insulin does not. Furthermore, the increase in the basal rate of 2-deoxyglucose transport observed after down-regulation of PKC occurs due to an increase in the total Glut1 level.

5   The activation of MAPK in 3T3-L1 fibroblasts

5.1 Introduction

The growth factors, insulin and PDGF, and the tumour promoter, PMA, have similar effects on the rate of glucose transport in 3T3-L1 fibroblasts {Sections 3.2.2 and 3.2.3}, therefore, it is possible that the intracellular signal transduction pathways that mediate these effects are similar. The role of signal transduction pathways involving DAG and PKC have been examined with respect to the early phase of growth factor-stimulated glucose transport. DAG and PKC appear to be unnecessary {Section 4.3}. Mitogen-activated protein kinases (MAPKs) are activated in response to many growth factors, therefore, it is possible that the early phase of growth factor-stimulated glucose transport may be mediated by a signal transduction pathway involving MAPK. Therefore, the effects of insulin and PDGF on the activation of MAPK were investigated.

5.1.1 Mitogen-activated protein kinases

The mammalian isozymes

The MAPK isozymes, also known as extracellular signal-regulated kinase (ERK), are a group of serine/ threonine protein kinases that are activated in response to many ligands [Sturgill and Wu, 1991]. These include ligands which bind to tyrosine protein kinase receptors, such as FGF, and those which bind to G protein-coupled receptors, such as thrombin [Kahan et al., 1992].

There are several mammalian MAPK isozymes, the two best characterised being, $p42^{mapk}$ (p42 MAPK or ERK2) and $p44^{mapk}$ (p44 MAPK or ERK1) [Boulton et al., 1990; Boulton et al., 1991]. The MAPK isozymes are unique in that they are the only serine/ threonine protein kinase known to require both threonine and tyrosine phosphorylation for their activation [Anderson et al., 1990]. The phosphorylation sites have been identified as Thr-183 and Tyr-185 in $p42^{mapk}$. The threonine and tyrosine residues are separated by a single glutamate residue; the Thr-Glu-Tyr motif lies 13 amino acids upstream of the Ala-Pro-Glu motif common to all protein kinases [Nishida and Gotoh, 1993]. The sequence of amino acids containing the Thr-Glu-Tyr motif and the Ala-Pro-Glu motif is highly conserved between all known MAPK isozymes [Nishida and Gotoh, 1993].

Activation of the MAPK isozymes is catalysed by a single serine/ threonine/ tyrosine protein kinase known as MAPK kinase (MAPKK) or MAPK/ ERK kinase (MEK) {Section 5.1.2} [Nakielny et al., 1992a,b; Rossomando et al., 1992; Wu et al., 1992; Kosako et al., 1993].

Substrates

MAPK catalyses the *in vitro* phosphorylation of many proteins. The consensus sequence for phosphorylation by MAPK is Pro-Xaa-Ser/ Thr-Pro, where Xaa is a neutral or basic residue [Davis, 1993]. However, other kinases, including GSK-3 and cyclin-dependent protein kinases, also preferentially catalyse the phosphorylation of serine and threonine residues in proline-rich regions [Alvarez et al., 1991].

MAPK catalyses the *in vitro* phosphorylation of several proteins that function as transcription factors [Hunter and Karin, 1992]. These include, c-Jun [Alvarez et al., 1991; Pulverer et al., 1991], c-Myc [Seth et al., 1992], p62^{TCF} (Elk-1) [Gille et al., 1992; Marais et al., 1993], NF-IL6 (C/EBPß) [Nakajima et al., 1993], and ATF-2 [Abdel-Hafiz et al., 1992].

One of the early events of the cell cycle is a rapid increase in the expression of immediate-early genes, for example c-*fos*, c-*jun* and c-*myc* [Greenberg and Ziff, 1984; Stumpo and Blackshear, 1986]. The increase in the rate of transcription of these genes occurs independently of protein synthesis, therefore, it is regulated by the modification of the activity of existing transcription factors [Almendral et al., 1988]. The growth factor-stimulated transcription of the immediate-early genes may be mediated by a MAPK signal transduction pathway, since MAPK catalyses the *in vitro* phosphorylation of several transcription factors and at least one isoform of MAPK moves rapidly to the nucleus in response to serum [Seth et al., 1992].

MAPK catalyses the phosphorylation of several protein kinases. These include the 90 kDa S6 kinases (p90^{rsk}) [Nguyen et al., 1993], MAPK-activated protein kinase-1 (MAPKAP kinase-1) [Lavoinne et al., 1991], and MAPK-activated protein kinase-2 (MAPKAP kinase-2) [Stokoe et al., 1992a].

The p90^{rsk} isozymes are a group of serine/ threonine protein kinases that catalyse the phosphorylation of the ribosomal protein S6, a component of the eukaryotic 40 S subunit [Erikson and Maller, 1986]. Phosphorylation of S6 occurs when quiescent cells re-enter the cell cycle [Sturgill and Wu, 1991], and is thought to have a role in the regulation of protein synthesis during the cell cycle [Thomas et al., 1982]. Activation of p90^{rsk} by MAPK is rapid, but transient [Ballou et al., 1991].

MAPKAP kinase-1, previously known as insulin-stimulated protein kinase-1 (ISPK1), is a mammalian skeletal muscle p90^{rsk} homologue [Lavoinne et al., 1991]. It is part of the signal transduction pathway that mediates insulin-stimulated glycogen synthesis. MAPKAP kinase-1 catalyses the phosphorylation of the regulatory subunit of the glycogen-associated protein phosphatase-1 (PP1$_G$) [Dent et al., 1990] and GSK-3ß [Sutherland et al., 1993]. The phosphorylation of PP1$_G$ leads to its activation, and therefore to the dephosphorylation and activation of glycogen synthase and the dephosphorylation and inactivation of phosphorylase kinase [Dent et al., 1990]. The phosphorylation of GSK-3ß leads to its inactivation, and therefore, also to the dephosphorylation and inactivation of glycogen synthase [Sutherland et al., 1993].

MAPKAP kinase-2 is another mammalian skeletal muscle serine/ threonine protein kinase that is a *in vitro* substrate for p42^{mapk} [Stokoe et al., 1992a]. The function of MAPKAP kinase-2 is unknown; it catalyses the phosphorylation of the heat shock proteins Hsp25, and Hsp27 [Stokoe et al., 1992b].

MAPKs catalyse the *in vitro* phosphorylation of several cytoskeletal proteins. These include microtubule-associated protein-2 [Ray and Sturgill, 1987], myelin basic protein [Erickson et al., 1990], and Tau [Drewes et al., 1992]. The phosphorylation of cytoskeletal proteins may regulate the reorganisation of the cytoskeleton which is observed during the cell cycle.

MAPKs catalyse the *in vitro* phosphorylation of several membrane proteins and membrane-associated proteins. These include the EGF receptor [Northwood et al., 1991] and the 85 kDa cytosolic PLA$_2$ [Lin et al., 1993; Nemenoff et al., 1993]. MAPK-catalysed phosphorylation of the EGF receptor is thought to regulate its internalisation and intrinsic tyrosine protein kinase activity [Northwood et al., 1991]. MAPK-catalysed

phosphorylation of PLA$_2$ is thought to stimulate its activity [Lin et al., 1993; Nemenoff et al., 1993].

Therefore, MAPK catalyses the *in vitro* phosphorylation of many proteins, including transcription factors, protein kinases, cytoskeletal proteins, and membrane proteins. Many of these could have important roles in cell proliferation.

Inactivation

The activation of the mammalian MAPK isozymes is transient under many conditions, therefore, their inactivation must be rapid. However, much less is known about the inactivation of MAPK.

Several protein tyrosine/ threonine phosphatases that are specific for MAPK have been identified recently. These phosphatases include the protein products of the human genes, *CL100* (mouse homologue, *3HC134/erp*), *HVH1* and *PAC1* [Alessi et al., 1993; Nebreda, 1994; Ward et al., 1994] These are immediate-early genes [Charles et al., 1992; Rohan et al., 1993], their expression being induced in response to the same growth factors that stimulate MAPK activity. Since, many of the potential substrates of MAPK are transcription factors, it is possible that the induction of these phosphatases could be regulated by the MAPK cascade, thus providing a negative feedback mechanism [Alessi et al., 1993; Nebreda, 1994]. In addition, PAC1, which is predominantly expressed in haematopoietic tissues, is localised to the nucleus in growth factor-stimulated cells [Rohan et al., 1993], suggesting that PAC1 may have a role in the regulation of nuclear events [Ward et al., 1994].

Other protein phosphatases can inactivate MAPK *in vitro* by the selective dephosphorylation of either the tyrosine or the threonine residue. For example, the dephosphorylation of the threonine residue by protein phosphatase 2A (PP2A) or of the tyrosine residue by a protein tyrosine phosphatase, CD45, leads to inactivation of MAPK [Anderson et al., 1990; Gómez et al., 1990]. It is not known whether this is of physiological significance.

5.1.2   MAPK kinase

Initially, it was thought that either the phosphorylation of the tyrosine and threonine residues in MAPK was catalysed by two separate protein kinases, that is a serine/ threonine protein kinase and a tyrosine protein kinase, or that the phosphorylation of one of the residues was catalysed by a single protein kinase, and the phosphorylation of the second residue occurred as a result of autophosphorylation. However, the use of kinase-inactive MAPK mutants showed that the phosphorylation of MAPK is catalysed by a single serine/ threonine/ tyrosine protein kinase, MAPKK, the only known example of a dual specificity protein kinase [Nakielny et al., 1992a,b; Rossomando et al., 1992; Wu et al., 1992; Kosako et al., 1993]. MAPKK isozymes from several organisms have been purified and cloned. The molecular masses range from 45 to 50 kDa [Nakielny et al., 1992a; Kosako et al., 1993; Zheng and Guan, 1993]. The only known substrate of MAPKK is MAPK [Nakielny et al., 1992a,b].

MAPKK is activated by serine/ threonine phosphorylation [Nakielny et al., 1992a; Rossomando et al., 1992; Kosako et al., 1993; Matsuda et al., 1993]. In mammalian cells MAPKK phosphorylation is catalysed by three serine/ threonine protein kinases, Raf-1 (p74$^{raf\text{-}1}$) [Howe et al., 1992; Kyriakis et al., 1992], MAPKK kinase (MAPKKK) [Lange-Carter et al., 1993] and Mos (p39^{mos}) [Posada et al., 1993]. The role of p74$^{raf\text{-}1}$ and MAPKKK are discussed in this chapter, p39^{mos} is not expressed in somatic cells and therefore will be discussed later {Section 6.1.2}.

The phosphorylation of MAPKK is also catalysed by MAPK [Matsuda et al., 1993], however, this occurs on different serine/ threonine residues to those which are substrates for MAPKKK, suggesting that the phosphorylation of MAPKK by MAPK has either a negative or positive-feedback role [Matsuda et al., 1993].

5.1.3   p74$^{raf\text{-}1}$

Tyrosine protein kinase receptors

The activation of p74$^{raf\text{-}1}$ and MAPK by ligands that bind to tyrosine protein kinase receptors requires Ras (p21^{ras}), a small guanine nucleotide binding protein [Thomas et al., 1992; Wood et al., 1992]. There are three mammalian Ras isoforms, H-Ras, Ki-Ras,

and N-Ras. These are all 21 kDa isoprenylated, membrane-associated proteins with a single high-affinity binding site for guanine nucleotides.

Guanine nucleotide-binding proteins cycle between an inactive GDP-bound form and an active GTP-bound form. Their activity is controlled by guanine nucleotide-releasing proteins (GNRPs) and GTPase-activating proteins (GAPs). GNRPs activate guanine nucleotide binding proteins by catalysing the release of GDP. Since the cellular concentration of GTP is higher than that of GDP, GTP preferentially binds to the empty guanine nucleotide binding site. GAPs inactivate guanine nucleotide-binding proteins by stimulating their normally low intrinsic GTPase activity so that GTP is hydrolysed to produce GDP [Hall, 1990; Bollag and McCormick, 1991].

The activity of p21^{ras} is regulated by Sos (a GNRP) [Shou et al., 1992] and RasGAP (a GAP) [Trahey and McCormick, 1987] {Figure 5.1}. Activation of tyrosine protein kinase receptors stimulates p21^{ras} activity by increasing the rate of guanine nucleotide exchange [Gibbs et al., 1990], but has no effect on the nucleotide exchange activity of Sos [Buday and Downward, 1993]. Instead, the rate of guanine nucleotide exchange is controlled by altering the intracellular location of Sos. In quiescent cells Sos, has little effect on p21^{ras} activity, because it is cytosolic, while p21^{ras} is always membrane-associated, however, after activation of a tyrosine protein kinase receptor, Sos associates with the receptor and so can stimulate p21^{ras} activity [Buday and Downward, 1993; Egan et al., 1993; Gale et al., 1993; Rozakis-Adcock et al., 1993]. The growth factor-dependent association of Sos with the receptor, is mediated by Grb2, a 25 kDa protein, consisting of one SH2 domain and two Src homology-3 (SH3) domains [Koch et al., 1991]. As previously described, after the activation of tyrosine protein kinase receptors, Grb2 binds to specific phosphotyrosine-containing sequences in the receptors or in IRS-1 via the SH2 domain {Section 3.1.1}. Grb2 also binds to Sos, the interaction occurring between the SH3 domains of Grb2 and a proline-rich region in Sos {Figure 5.2} [Buday and Downward, 1993; Egan et al., 1993; Li et al., 1993; Rozakis-Adcock et al., 1993]. Consequently, Grb2-Sos complexes move from the cytosol to the membrane and p21^{ras} activity increases in response to the activation of tyrosine protein kinase receptors [Buday and Downward, 1993; Egan et al., 1993; Gale et al., 1993; Rozakis-Adcock et al., 1993].

Figure 5.1   The activation of guanine nucleotide binding proteins

A schematic representation of receptor-mediated activation of a) p21^{ras} and b) Gq, where the GNRPs are Sos and a G protein-coupled receptor, and the GAPs are RasGAP and PLC-ß respectively.

a)
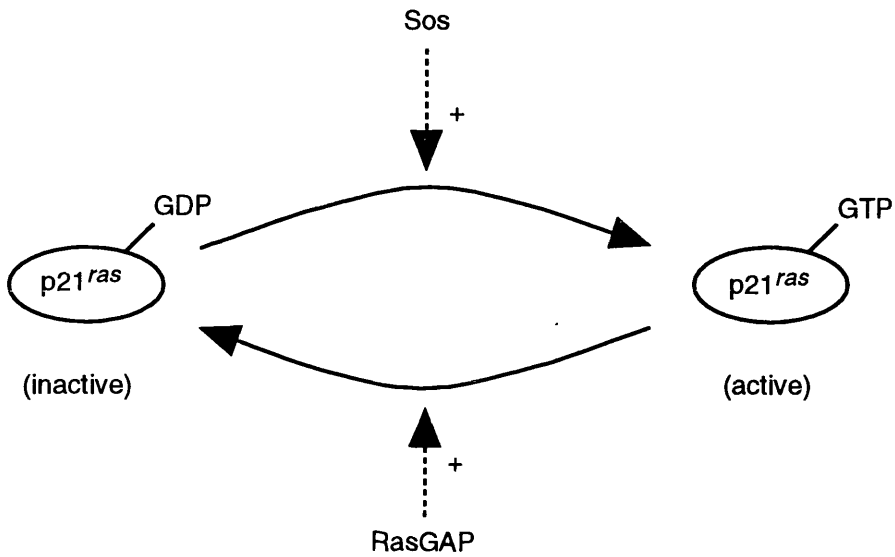
b)
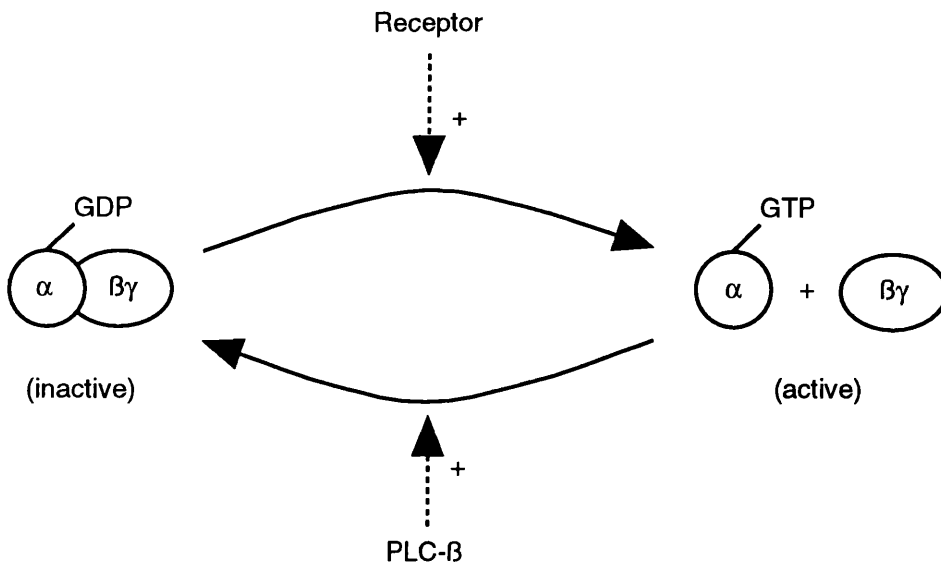
Figure 5.2   Signal transduction pathways leading to the activation of MAPK

A schematic representation of the activation of MAPK by ligands that bind to a) tyrosine protein kinase receptors and b) G protein-coupled receptors.

133
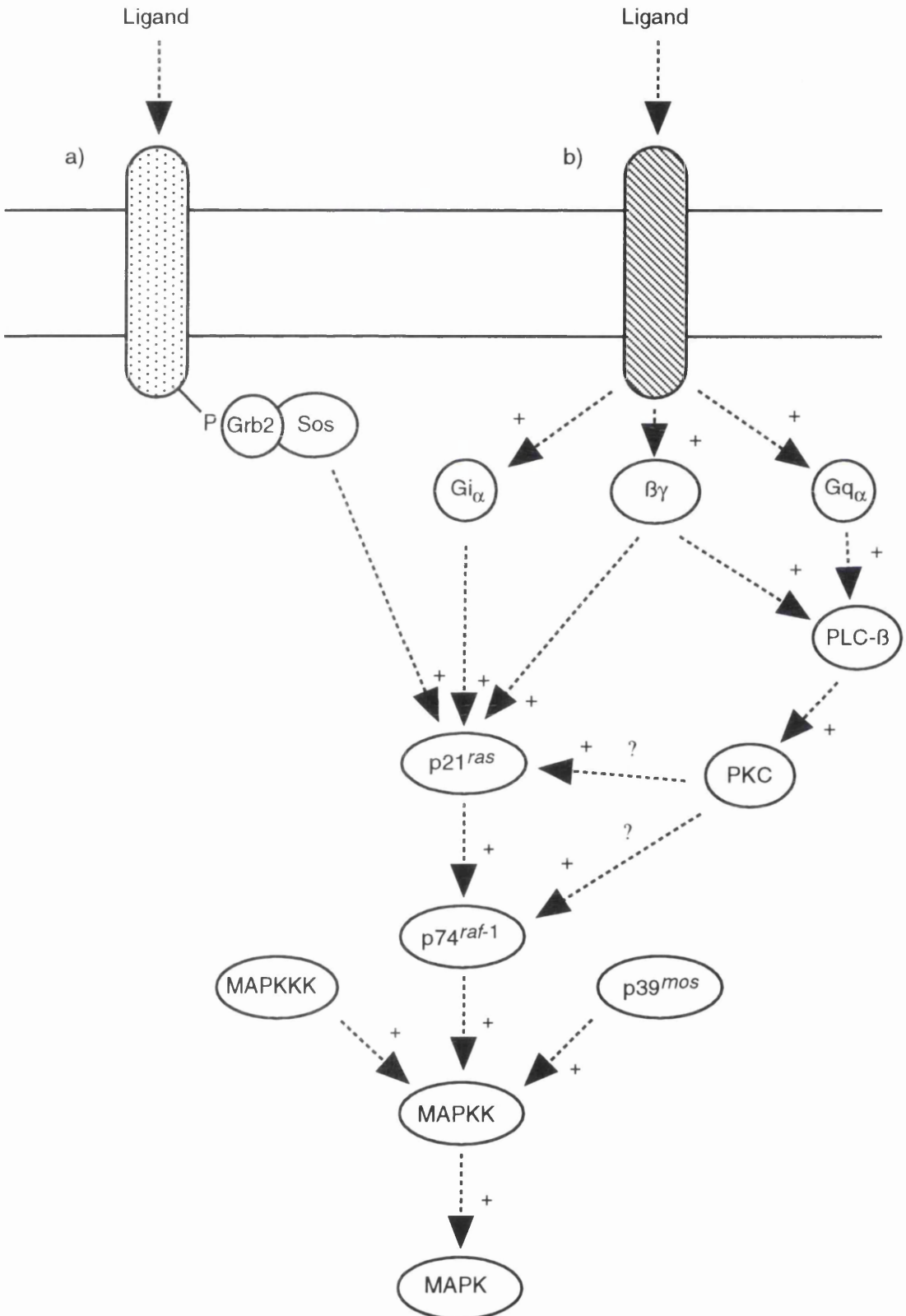
Active p21^{ras} interacts directly with the amino-terminal regulatory domain of p74^{raf-1}, but does not stimulate the kinase activity of p74^{raf-1} *in vitro* [Moodie et al., 1993; Vojtek et al., 1993; Zhang et al., 1993]. However, after its activation, p74^{raf-1} is associated with the plasma membrane, but not with p21^{ras}, suggesting that the role of p21^{ras} is to localise p74^{raf-1} to the plasma membrane where it is activated by another signal [Leevers and Marshall, 1992]. It is possible that plasma membrane-associated p74^{raf-1} is activated by hyperphosphorylation or by a conformational change in proteins with which it is associated. The hyperphosphorylation of p74^{raf-1} occurs in response to growth factors, however the kinase which catalyse the phosphorylation of p74^{raf-1} is unknown [Morrison et al., 1988; Blackshear et al., 1990; Morrison et al., 1993]. In addition, p74^{raf-1} is found in a large complex of 300 to 500 kDa, in both quiescent and activated cells. Two other proteins in this complex are the heat shock protein, hsp90, and a 50 kDa protein often found in complexes with hsp90 [Wartmann and Davis, 1994]. The hsp90-p50 complex regulates the activity of other proteins with which it also associates, such as the glucocorticoid receptor and casein kinase II, and therefore may be involved in the regulation of p74^{raf-1} activity [Wartmann and Davis, 1994].

Seven membrane-spanning domain receptors

The activation of p74^{raf-1} and MAPK in response to ligands that bind to G protein-coupled receptors occurs by p21^{ras}-dependent and -independent pathways. G proteins are another class of guanine nucleotide binding proteins that are similar to small guanine nucleotide binding proteins in that the GTP-bound form is active, while the GDP-bound form is inactive. However, G proteins are trimeric complexes, the α-subunit containing a single guanine nucleotide binding site and the GTPase. Nucleotide exchange is stimulated when a ligand binds to the G protein-coupled receptor, also causing the α-subunit to dissociate from the ßγ-subunits. Certain G protein effectors, such as PLC-ß, are thought to act as GAPs {Figure 5.1b} [Berstein et al., 1992].

The G protein-coupled receptors that stimulate p74^{raf-1} and MAPK activity bind to members of the G$_i$ and G$_q$ families. The GTP-bound α$_q$-subunit stimulates PLC-ß activity, leading to the activation of PKC [Smrcka et al., 1991; Sternweis and Smrcka, 1992]. PKC catalyses the phosphorylation of p74^{raf-1}, but it is not known whether this affects p74^{raf-1} activity [MacDonald et al., 1993]. In addition, PKC may also stimulate p21^{ras} activity, probably by stimulation of nucleotide exchange [Downward et al., 1990].

134

The GTP-bound α_i-subunit stimulates p21^{ras} activity, probably by stimulation of nucleotide exchange [van Corven et al., 1993; Winitz et al., 1993].

The ßγ-complex also stimulates the activities of PLC-ß [Carozzi et al., 1993] and p21^{ras} [Crespo et al., 1994]. The ßγ-complex is thought to bind to the pleckstrin homology (PH) domain, which is found in many proteins including the ß-adrenergic receptor kinase, PLC-ß [Parker et al., 1994], Sos and RasGAP. The ßγ-complex is thought to activate the ß-adrenergic receptor kinase by interaction with its PH domain [Shaw, 1993], therefore, it is also possible that the activities of PLC-ß and p21^{ras} are regulated in a similar manner {Figure 5.2} [Parker et al., 1994; Touhara et al., 1994].

Inhibition of p21^{ras} and p74^{raf-1}

The activity of p21^{ras} may be reduced by stimulation of the activity of RasGAP [Trahey and McCormick, 1987]. After activation of tyrosine protein kinase receptors, RasGAP binds to specific phosphotyrosine-containing sequences in the receptors {Section 3.1.1}, then undergoes tyrosine phosphorylation [Kazlauskas et al., 1990]. However, the physiological effect of growth factor-stimulated tyrosine phosphorylation of RasGAP remains uncertain [Gibbs et al., 1990].

MAPK also catalyses the *in vitro* phosphorylation of p74^{raf-1} [Lee et al., 1992], again this may have a negative or a positive-feedback role .

5.1.4   MAPK kinase kinase

MAPKKKs were initially isolated from yeasts which do not express p74^{raf-1} and p39^{mos}. Recently several mammalian MAPKKK isozymes have been cloned from mice [Lange-Carter et al., 1993; Blumer and Johnson, 1994]. Some of the mammalian MAPKKK isozymes are activated in response to growth factors; others may be activated in response to changes similar to those known to activate the yeast homologues, such as osmotic stress [Brewster, 1993].

5.1.5   The relationship with cell proliferation

MAPK is thought to have an important role in cell proliferation, in particular in control of the G0 to G1 transition. Virtually all growth factors rapidly stimulate the activity of one or more MAPK isozymes. For example, MAPK activity and cell proliferation increase in thrombin- and basic FGF-treated CCL39 cells [Kahan et al., 1992], foetal calf serum-treated Chinese hamster ovary cells [Tamemoto et al., 1992] and EGF-treated PC12 cells [Nguyen et al., 1993]. In addition, cells with defects in PMA-stimulated cell proliferation, also have defects in PMA-stimulated MAPK activity [L'Allemain et al., 1991], and growth factor-stimulated MAPK activity and cell proliferation are inhibited by the expression of dominant-negative p74^{raf-1} mutants [Kolch et al., 1991]. Furthermore, the mammalian MAPK isozymes have a high sequence identity with enzymes that are required for cell cycle control from *S. cerevisiae* and *Schizosaccharomyces pombe* [Errede and Levin, 1993].

However, MAPK is also activated by many non-proliferative signals [Wood et al., 1992] suggesting that MAPK may not be sufficient for cell proliferation. In addition, transformation does not always stimulate MAPK activity, for example, MAPK activity is not affected by the transformation of Rat 1 fibroblasts with v-*ras* or v-*raf* [Gupta et al., 1992], or of Swiss 3T3 fibroblasts with v-*myc* [Howe et al., 1992], suggesting that MAPK may not be necessary for the stimulation of cell proliferation. This also suggests that there may be cell-specific expression of some components of the signal transduction pathways that mediate the activation of MAPK.

Therefore, although the MAPK is activated in response to many growth factors that also stimulate cell proliferation it is not clear whether MAPK itself is necessary or sufficient for cell proliferation. However, MAPK may be sufficient to stimulate some of the early events of cell proliferation.

5.1.6   The relationship with glucose transport

Since the early phase of growth factor-stimulated glucose transport is an early event of the cell cycle, it is possible that it could be mediated by a signal transduction pathway involving the activation of MAPK . When this work was initiated, there was little

evidence in support or against this hypothesis. Given that MAPK appears to be important with respect to cell proliferation, it was necessary to investigate the possibility that MAPK may mediate the early phase of growth factor-stimulated glucose transport.

In order to examine whether the early phase of growth factor-stimulated glucose transport is mediated by a signal transduction pathway involving MAPK, several approaches were taken. Firstly, the effects of insulin and PDGF on tyrosine phosphorylation in 3T3-L1 fibroblasts and the requirement for PKC activity were established. Secondly, the effects of insulin and PDGF on MAPK activity in 3T3-L1 fibroblast and the requirement for PKC activity were established.

5.2   Results

5.2.1   The effect of growth factors on tyrosine phosphorylation

The effect of insulin and PDGF on tyrosine phosphorylation was established by Western blotting of cellular proteins. Lysates were prepared from 3T3-L1 fibroblasts after incubation in 1 μM insulin or 25 ng/ml PDGF {Section 2.13.2}. The proteins were separated by SDS-PAGE {Section 2.15}, and then transferred onto nitrocellulose membranes. The membranes were probed with a rabbit anti-phosphotyrosine antibody [Pang et al., 1985], and then with a HRP-conjugated donkey anti-rabbit IgG antibody. The antibody binding sites were visualised using an ECL detection system {Section 2.16.2}.

The anti-phosphotyrosine antibody recognised proteins with approximate molecular masses ranging from 30 to 200 kDa in lanes containing the untreated 3T3-L1 fibroblast lysate samples. A representative Western blot is shown in Figure 5.3.

During a 60 minute incubation in 1 μM insulin there were large increases in the tyrosine phosphorylation of proteins with approximate molecular masses of 42, 44, 120 and 166 kDa, and small increases in the tyrosine phosphorylation of a protein with an approximate molecular mass of 60 kDa and of several proteins with approximate

Figure 5.3   A time course for insulin-stimulated tyrosine phosphorylation

After incubation of quiescent 3T3-L1 fibroblasts with 1 μM insulin for the times shown, lysates were prepared {Section 2.13.2}. Approximately 30 μg of protein was loaded onto 10% (w/v) polyacrylamide large gels, the proteins were separated by SDS-PAGE {Section 2.15}, and then transferred onto nitrocellulose membranes. The membranes were probed with a rabbit anti-phosphotyrosine antibody, and then with a HRP-conjugated donkey anti-rabbit IgG antibody. The sites of antibody binding were visualised using an ECL detection system {Section 2.16.2}. This is a representative Western blot from a group of two lysate preparations.

molecular masses of 90 to 120 kDa. The tyrosine phosphorylation of the 42 and 44 kDa proteins increased within 2 minutes of exposure to insulin and reached a maximum by 5 minutes. The tyrosine phosphorylation of the 90 to 120 kDa proteins increased within 1 minute of exposure to insulin and was still elevated by 60 minutes. The tyrosine phosphorylation of the 166 kDa protein increased within 1 minute of exposure to insulin, was still elevated by 20 minutes, and then decreased. Other phosphotyrosine-containing proteins were observed, but the bands were too faint or blurred to determine if there were any changes {Figure 5.3}.

During a 60 minute incubation in 1 μM IGF-I, the changes in tyrosine phosphorylation were similar to those observed in response to insulin. A representative Western blot is shown in Figure 5.4.

During a 60 minute incubation in 25 ng/ml PDGF there were large increases in the tyrosine phosphorylation of proteins with approximate molecular masses of 42, 44, 120, 155 and 190 kDa and a small increase in the tyrosine phosphorylation of a protein with an approximate molecular mass of 170 kDa. The tyrosine phosphorylation of the 42 and 44 kDa proteins increased within 2 minutes of exposure to PDGF and reached a maximum by 5 minutes. The tyrosine phosphorylation of the 120, 155, 170 and 190 kDa proteins increased within 1 minute of exposure to PDGF, was still elevated by 30 minutes, and decreased nearly to basal levels by 60 minutes. Other phosphotyrosine-containing proteins were observed, but the bands were too faint or blurred to determine if there were any changes. A representative Western blot is shown in Figure 5.5.

The effect of insulin and PDGF on tyrosine phosphorylation was also examined by Western blotting of membrane proteins. Membrane proteins were prepared from 3T3-L1 fibroblasts after incubation in 1 μM insulin or 25 ng/ml PDGF {Section 2.13.1}. The proteins were separated by SDS-PAGE {Section 2.15}, and then transferred onto nitrocellulose membranes. The membranes were probed with the rabbit anti-phosphotyrosine antibody, and then with the HRP-conjugated donkey anti-rabbit IgG antibody. The antibody binding sites were visualised using an ECL detection system {Section 2.16.2}.

Figure 5.4   A time course for IGF-I-stimulated tyrosine phosphorylation

After incubation of quiescent 3T3-L1 fibroblasts with 1 μM IGF-I for the times shown, lysates were prepared {Section 2.13.2}. Approximately 30 μg of protein was loaded onto 10% (w/v) polyacrylamide large gels, the proteins were separated by SDS-PAGE {Section 2.15}, and then transferred onto nitrocellulose membranes. The membranes were probed with a rabbit anti-phosphotyrosine antibody, then with a HRP-conjugated donkey anti-rabbit IgG antibody. The antibody binding sites were visualised using an ECL detection system {Section 2.16.2}. This is a representative Western blot from a group of two lysate preparations.
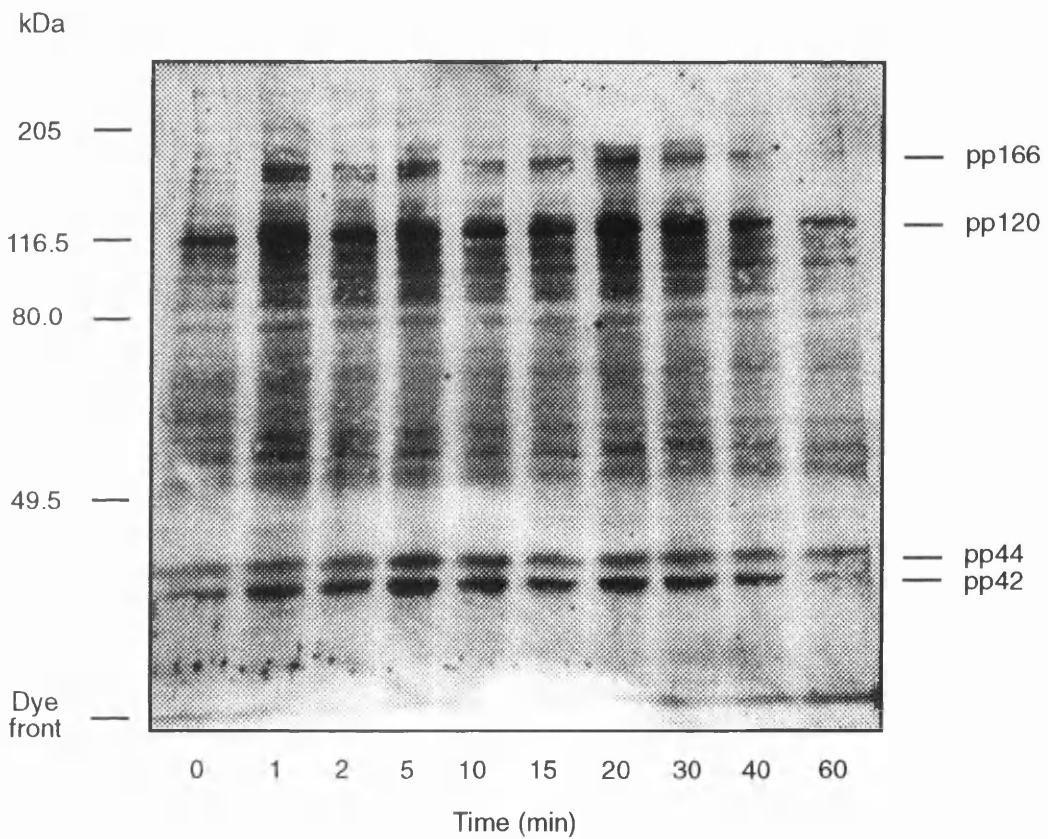
Figure 5.5   A time course for PDGF-stimulated tyrosine phosphorylation

After incubation of quiescent 3T3-L1 fibroblasts with 25 ng/ml PDGF for the times shown, lysates were prepared {Section 2.13.2}. Approximately 30 µg of protein was loaded onto 10% (w/v) polyacrylamide large gels, the proteins were separated by SDS-PAGE {Section 2.15}, and then transferred onto nitrocellulose membranes. The membranes were probed with a rabbit anti-phosphotyrosine antibody, then with a HRP-conjugated donkey anti-rabbit IgG antibody. The antibody binding sites were visualised using an ECL detection system {Section 2.16.2}. This is a representative Western blot from a group of two lysate preparations.

The anti-phosphotyrosine antibody recognised proteins with approximate molecular masses of 42, 44, and 60 kDa in lanes containing untreated 3T3-L1 fibroblast membrane protein samples. A representative Western blot is shown in Figure 5.6.

During a 10 minute incubation in 1 µM insulin there were large increases in the tyrosine phosphorylation of membrane proteins with approximate molecular masses of 20, 42, and 44 kDa and small increases in the tyrosine phosphorylation of membrane proteins with approximate molecular masses of 60 and 90 kDa. The tyrosine phosphorylation of the 42, 44, 60, 90 and 190 kDa proteins increased by 2 minutes of exposure to insulin and was still evident by 10 minutes. The tyrosine phosphorylation of the 20 kDa protein increased by 2 minutes of exposure to insulin and deceased to basal levels by 10 minutes. Other phosphotyrosine-containing proteins were observed, but the bands were too faint or blurred to determine if there were any changes {Figure 5.6}.

During a 10 minute incubation in 25 ng/ml PDGF there were large increases in the tyrosine phosphorylation of membrane proteins with approximate molecular masses of 20, 42, 44 and 190 kDa and small increases in the tyrosine phosphorylation of membrane proteins with approximate molecular masses of 60 and 155 kDa. Tyrosine phosphorylation of the 42, 44 and 190 kDa proteins increased by 2 minutes of exposure to PDGF and was still evident by 10 minutes. Tyrosine phosphorylation of the 20 kDa protein increased by 2 minutes of exposure to PDGF and deceased to basal levels by 10 minutes. Other phosphotyrosine-containing proteins were observed, but the bands were too faint or blurred to determine if there were any changes {Figure 5.6}.

5.2.2 The effect of a tumour promoter on tyrosine phosphorylation

The effect of PMA on tyrosine phosphorylation was established by Western blotting of cellular proteins. Lysates were prepared from 3T3-L1 fibroblasts after incubation in 100 nM PMA {Section 2.13.2}. The proteins were separated by SDS-PAGE {Section 2.15}, and then transferred onto nitrocellulose membranes. The membranes were probed with the rabbit anti-phosphotyrosine antibody, and then with the HRP-conjugated donkey anti-rabbit IgG antibody. The antibody binding sites were visualised using an ECL detection system {Section 2.16.2}.

Figure 5.6   The effect of PDGF and insulin on the tyrosine phosphorylation of membrane proteins

After incubation of quiescent 3T3-L1 fibroblasts with 25 ng/ml PDGF or 1 µM insulin, for the times shown, membrane proteins were prepared {Section 2.13.1}. Approximately 20 µg of protein was loaded onto 10% (w/v) polyacrylamide large gels, the proteins were separated by SDS-PAGE {Section 2.15}, and then transferred onto nitrocellulose membranes. The membranes were probed with an anti-phosphotyrosine antibody, then with a HRP-conjugated donkey anti-rabbit IgG antibody. The antibody binding sites were visualised using an ECL detection system {Section 2.16.2}. This is a representative Western blot from a group of two membrane protein preparations.

Lane A: basal; lane B: 2 minutes insulin; lane C: 10 minutes insulin; lane D: 2 minutes PDGF; lane E: 10 minutes PDGF.
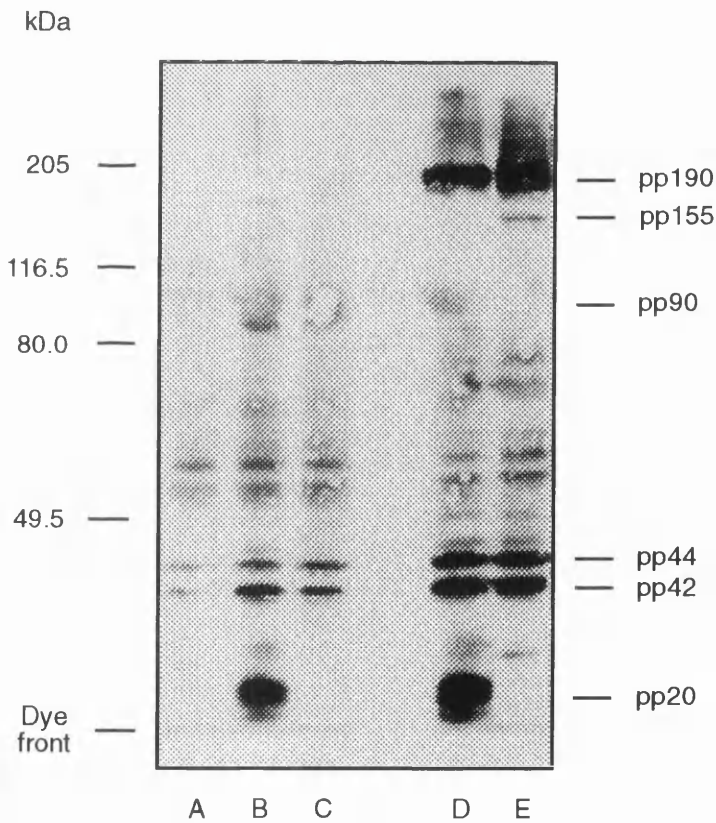
The anti-phosphotyrosine antibody recognised proteins with approximate molecular masses ranging from 30 to 200 kDa in lanes containing untreated 3T3-L1 fibroblast lysate samples. During a 60 minute incubation in 100 nM PMA there were large increases in the tyrosine phosphorylation of proteins with approximate molecular masses of 42, 44, 90 and 120 kDa and a small increase in the tyrosine phosphorylation of a protein with an approximate molecular mass of 60 kDa. The tyrosine phosphorylation of the 42 and 44 kDa proteins increased within 2 minutes of exposure to PMA and reached a maximum by 5 minutes. Other phosphotyrosine-containing proteins were observed, but the bands were too faint or blurred to determine if there were any changes. A representative Western blot is shown in Figure 5.7.

5.2.3   The effect of PKC on the pattern of tyrosine phosphorylation

The effect of PKC on the patterns of insulin-, PDGF- and PMA-stimulated tyrosine phosphorylation was established by Western blotting of cellular proteins. Lysates were prepared from 3T3-L1 fibroblasts treated with 1 μM insulin, 25 ng/ml PDGF or 100 nM PMA {Section 2.13.2}, after down-regulation of PKC {Section 2.11}. The proteins were separated by SDS-PAGE {Section 2.15}, and then transferred onto nitrocellulose membranes. The membranes were probed with the rabbit anti-phosphotyrosine antibody, and then with the HRP-conjugated donkey anti-rabbit IgG antibody. The antibody binding sites were detected using an ECL detection system {Section 2.16.2}.

Again, the anti-phosphotyrosine antibody recognised proteins with approximate molecular masses ranging from 30 to 200 kDa in lanes containing untreated 3T3-L1 fibroblast lysate samples.

The patterns of tyrosine phosphorylation observed in response to 1 μM insulin after a 16 hour incubation in 1 μM 4α-PDD or in 1 μM PMA were similar. During a 60 minute incubation in 1 μM insulin there were large increases in the tyrosine phosphorylation of proteins with approximate molecular masses of 42, 44, 120 and 166 kDa, and small increases in the tyrosine phosphorylation of a protein with an approximate molecular mass of 60 kDa and of a group of proteins with approximate molecular masses of 90 to 120 kDa. A representative Western blot is shown in Figure 5.8.

Figure 5.7   A time course for PMA-stimulated tyrosine phosphorylation

After incubation of quiescent 3T3-L1 fibroblasts with 100 nM PMA for the times shown, lysates were prepared {Section 2.13.2}. Approximately 30 µg of protein was loaded onto 10% (w/v) polyacrylamide large gels, the proteins were separated by SDS-PAGE {Section 2.15}, and then transferred onto nitrocellulose membranes. The membranes were probed with a rabbit anti-phosphotyrosine antibody, then with a HRP-conjugated donkey anti-rabbit IgG antibody. The antibody binding sites were visualised using an ECL detection system {Section 2.16.2}. This is a representative Western blot from a group of two lysate preparations.

145
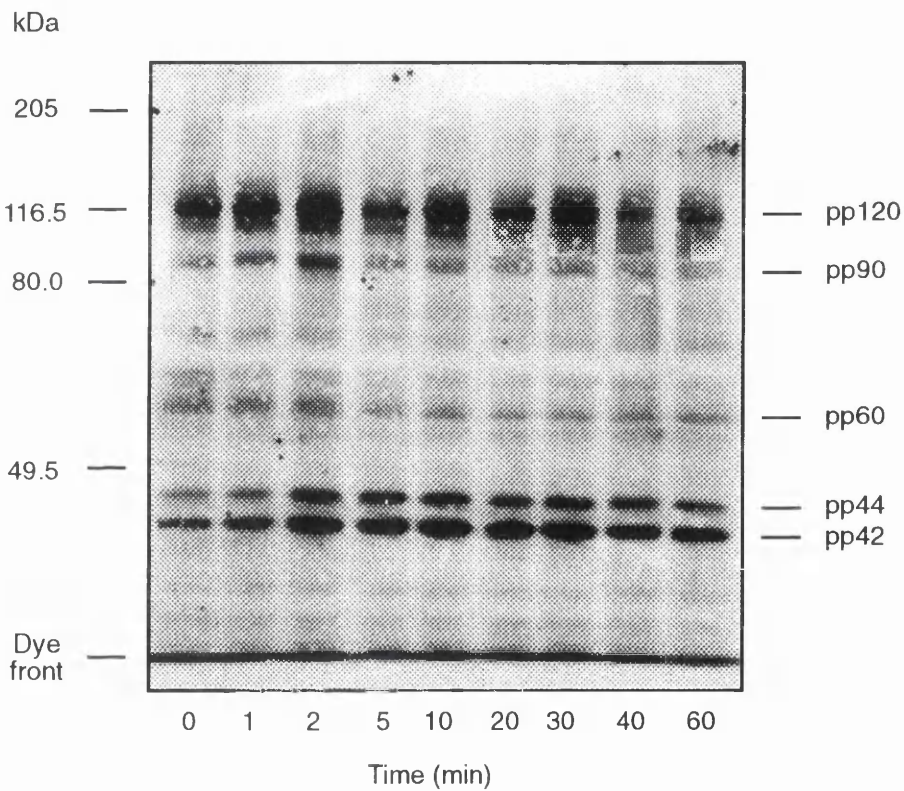
Figure 5.8   A time course for insulin-stimulated tyrosine phosphorylation, after the down-regulation of PKC

After incubation of quiescent 3T3-L1 fibroblasts with a) 1 µM 4α-PDD or b) 1 µM PMA for 16 hours {Section 2.11}, then with 1 µM insulin for the times shown, lysates were prepared {Section 2.13.2}. Approximately 30 µg of protein was loaded onto 10% (w/v) polyacrylamide large gels, the proteins were separated by SDS-PAGE {Section 2.15}, and then transferred onto nitrocellulose membranes. The membranes were probed with a rabbit anti-phosphotyrosine antibody, then with a HRP-conjugated donkey anti-rabbit IgG antibody. The sites of antibody binding were visualised using an ECL detecton system {Section 2.16.2}. This is a Western blot from a group of two lysate preparations.
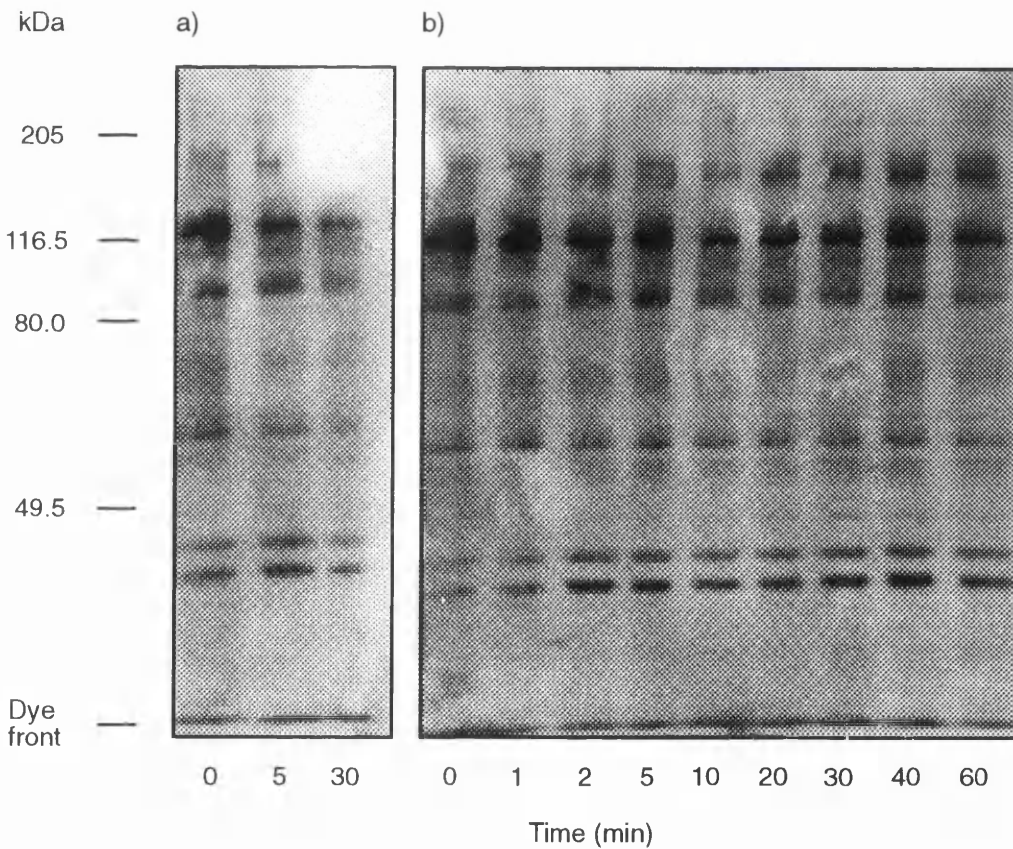
The patterns of tyrosine phosphorylation observed in response to 25 ng/ml PDGF after a 16 hour incubation in 1 μM 4α-PDD or in 1 μM PMA were similar. During a 60 minute incubation in 25 ng/ml PDGF there were large increases in the tyrosine phosphorylation of proteins with approximate molecular masses of 42, 44, 120, 155 and 190 kDa and small increases in the tyrosine phosphorylation of proteins with approximate molecular masses of 60 and 170 kDa. A representative Western blot is shown in Figure 5.9.

The patterns of tyrosine phosphorylation observed in response to 100 nM PMA after a 16 hour incubation in 1 μM 4α-PDD or in 1 μM PMA were different. After the 16 hour incubation in 1 μM 4α-PDD, there were large increases in the tyrosine phosphorylation of proteins with approximate molecular masses of 42, 44, 90 and 120 kDa and a small increase in the tyrosine phosphorylation of a protein with an approximate molecular mass of 60 kDa. After the 16 hour incubation in 1 μM PMA, there were large increases in the tyrosine phosphorylation of proteins with approximate molecular masses of 90 and 120 kDa and a small increase in the tyrosine phosphorylation of a protein with an approximate molecular mass of 60 kDa. However, there was no change in the tyrosine phosphorylation of the 42 and 44 kDa proteins. A representative Western blot is shown in Figure 5.10.

5.2.4   The effect of growth factors on MAPK activity

The effect of insulin, PDGF and PMA on the mobility of MAPK during SDS-PAGE was examined by Western blotting of cellular proteins. Lysates were prepared from 3T3-L1 fibroblasts after incubation in 1 μM insulin, 25 ng/ml PDGF or 100 nM PMA {Section 2.13.2}. The proteins were separated by SDS-PAGE {Section 2.15}, and then transferred onto nitrocellulose membranes. The membranes were probed with a mouse anti-MAPK antibody, and then with a HRP-conjugated sheep anti-mouse IgG antibody. The antibody binding sites were visualised using an ECL detection system {Section 2.16.2}.

The anti-MAPK antibody recognised proteins with approximate molecular masses of 42 kDa (p42^{mapk}) and 44 kDa (p44^{mapk}) in all 3T3-L1 fibroblast lysate samples. The electrophoretic mobility of both isozymes decreased in response to 1 μM insulin, 25 ng/ml PDGF and 100 nM PMA. However, the decrease in the mobility of p44^{mapk} was typically less pronounced than the decrease in the mobility p42^{mapk}. The decrease

Figure 5.9   A time course for PDGF-stimulated tyrosine phosphorylation, after the down-regulation of PKC

After incubation of quiescent 3T3-L1 fibroblasts with a) 1 µM 4α-PDD or b) 1 µM PMA for 16 hours {Section 2.11}, and then with 25 ng/ml PDGF for the times shown, lysates were prepared {Section 2.13.2}. Approximately 30 µg of protein was loaded onto 10% (w/v) polyacrylamide large gels, the proteins were separated by SDS-PAGE {Section 2.15}, and then transferred onto nitrocellulose membranes. The membranes were probed with a rabbit anti-phosphotyrosine antibody, then with a HRP-conjugated donkey anti-rabbit IgG antibody. The antibody binding sites were visualised using an ECL detection system {Section 2.16.2}. This is a representative Western blot from a group of two lysate preparations.
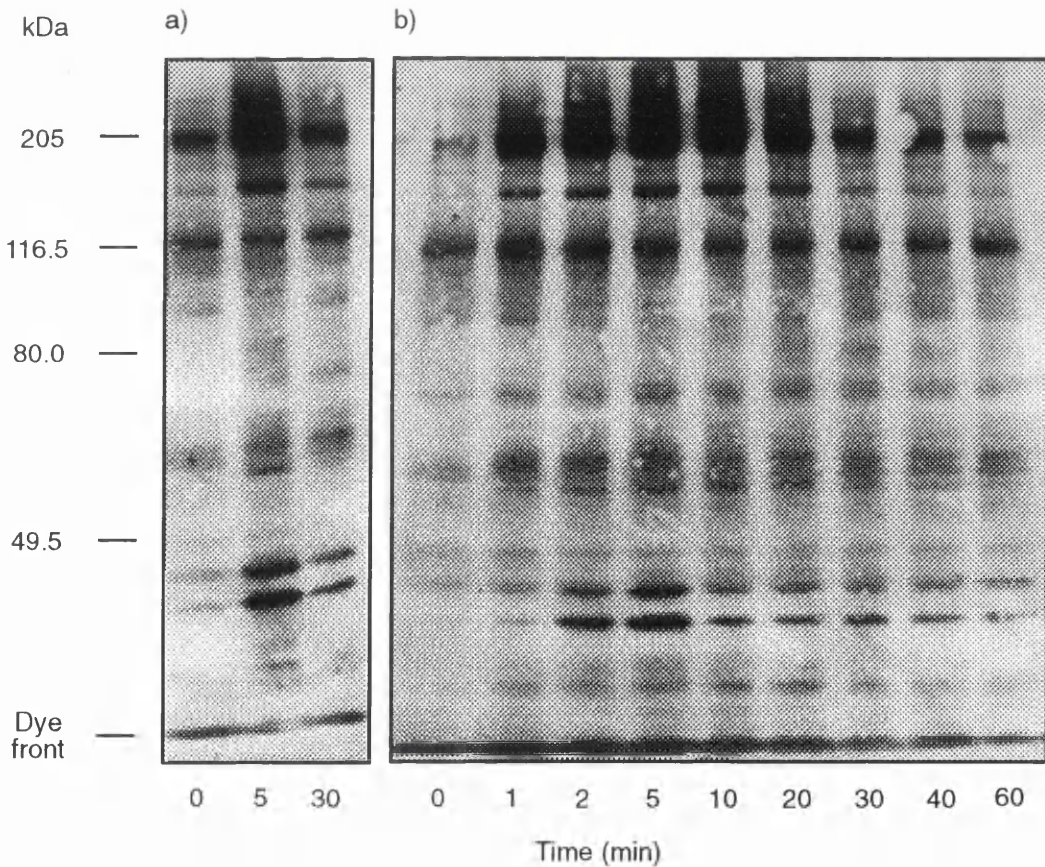
Figure 5.10   A time course for PMA-stimulated tyrosine phosphorylation, after the down-regulation of PKC

After incubation of quiescent 3T3-L1 fibroblasts with a) 1 μM 4α-PDD or b) 1 μM PMA for 16 hours {Section 2.11}, and then with 100 nM PMA for the times shown, lysates were prepared {Section 2.13.2}. Approximately 30 μg of protein was loaded onto 10% (w/v) polyacrylamide large gels, the proteins were separated by SDS-PAGE {Section 2.15}, and then transferred onto nitrocellulose membranes. The membranes were probed with a rabbit anti-phosphotyrosine antibody, then with a HRP-conjugate donkey anti-rabbit IgG antibody. The antibody binding sites were visualised using an ECL detection system {Section 2.16.2}. This is a representative Western blot from a group of two lysate preparations.

149
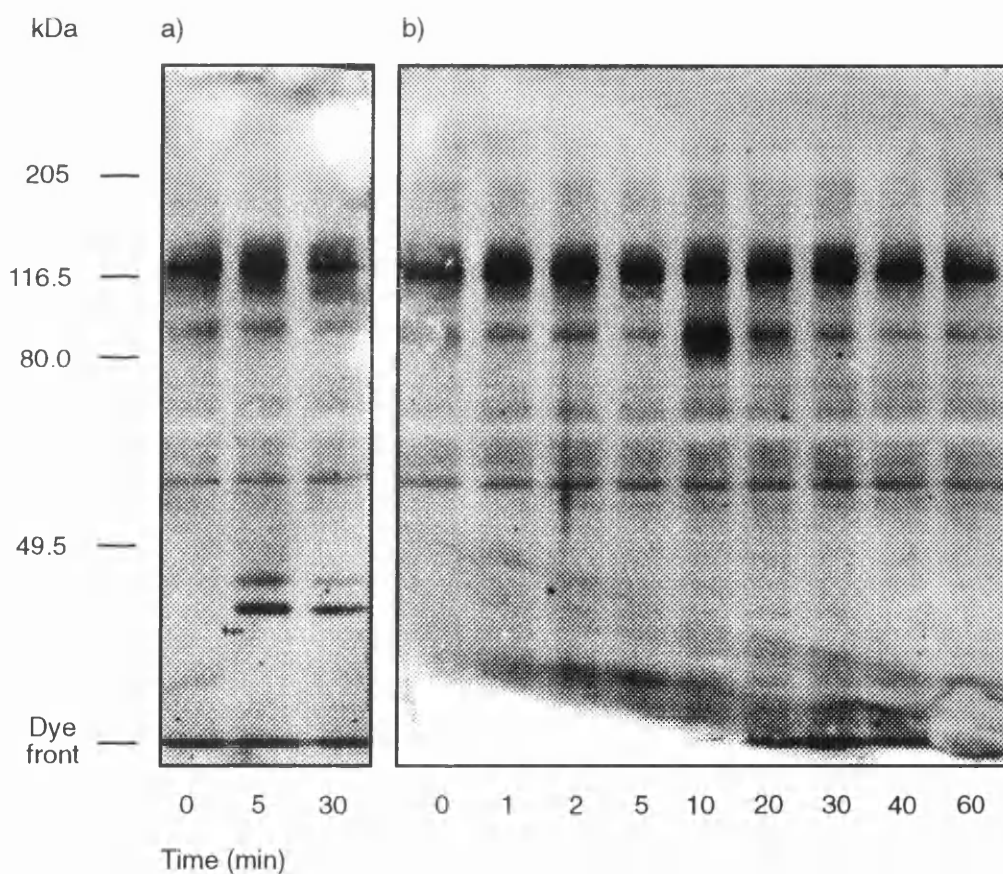
in mobility was observed within 1 minute of exposure to each of the ligands. Representative Western blots are shown in Figure 5.11.

The effect of PKC on insulin-, PDGF- and PMA-stimulated decreases in the electrophoretic mobility MAPK was established by Western blotting of cellular proteins. Lysates were prepared from 3T3-L1 fibroblasts treated with 1 µM insulin, 25 ng/ml PDGF or 100 nM PMA {Section 2.13.2}, after down-regulation of PKC {Section 2.11}. The proteins were separated by SDS-PAGE {Section 2.15}, and then transferred onto nitrocellulose membranes. The membranes were probed with the anti-MAPK antibody, and then with the HRP-conjugated donkey anti-mouse IgG antibody. The antibody binding sites were visualised using an ECL detection system {Section 2.16.2}.

After a 16 hour incubation in 1 µM 4α-PDD, the mobility of both $p42^{mapk}$ and $p44^{mapk}$ during SDS-PAGE decreased in response to 1 µM insulin, 25 ng/ml PDGF and 100 nM PMA. After a 16 hour incubation in 1 µM PMA, the mobility of both isozymes during SDS-PAGE decreased in response to 1 µM insulin and 25 ng/ml PDGF but not in response to 1 µM PMA. Representative Western blots are shown in Figure 5.12.

5.2.5   The effect of growth factors and a tumour promoter on $p125^{FAK}$

The effect of insulin, PDGF and PMA on the tyrosine phosphorylation of $p125^{FAK}$ was examined by Western blotting of immunoprecipitated phosphotyrosine proteins. Lysates were prepared from 3T3-L1 fibroblasts after incubation in 1 µM insulin, 25 ng/ml PDGF or 100 nM PMA. The phosphotyrosine proteins were immunoprecipitated using a rabbit anti-phosphotyrosine antibody {Section 2.13.3}. The immunoprecipitated proteins were separated by SDS-PAGE {Section 2.15}, and then transferred onto nitrocellulose membranes. The membranes were probed with a mouse anti-$p125^{FAK}$ antibody, and then with the HRP-conjugated sheep anti-mouse IgG antibody. The antibody binding sites were visualised using an ECL detection system {Section 2.16.2}.

The anti-$p125^{FAK}$ antibody recognised a protein with an approximate molecular mass of 120 kDa in each lane containing 3T3-L1 fibroblast lysate samples. The tyrosine phosphorylation of this protein increased in response to 1 µM insulin, 25 ng/ml PDGF and 100 nM PMA. A representative Western blot is shown in Figure 5.13.

Figure 5.11   Time courses for insulin-, PDGF- and PMA-stimulated activation of MAPK

After incubation of quiescent 3T3-L1 fibroblasts with A) 1 µM insulin, B) 25 ng/ml
PDGF or C) 100 nM PMA for the times shown, lysates were prepared {Section 2.13.2}.
Approximately 30 µg of protein was loaded onto 10% (w/v) polyacrylamide large gels,
the proteins were separated by SDS-PAGE {Section 2.15}, and then transferred onto
nitrocellulose membranes. The membranes were probed with a mouse anti-MAPK
antibody, then with a HRP-conjugated sheep anti-mouse IgG antiboby. The sites of
antibody binding were visualised using an ECL detection system {Section 2.16.2}.
These are representative Western blots from groups of two lysate preparations.

A)

p44^{mapk}
pp42^{mapk}
p42^{mapk}

0   1   2   5   10   15   20   30   40

Time (min)

B)

pp44^{mapk}
p44^{mapk}
pp42^{mapk}
p42^{mapk}

0   1   2   5   10   15   20   30   40   60

Time (min)

C)

p44^{mapk}
pp42^{mapk}
p42^{mapk}

0   1   2   5   10   20   30   40   60

Time (min)

After incubation of quiescent 3T3-L1 fibroblasts with a) 1 µM 4α-PDD or b) 1 µM PMA for 16 hours {Section 2.11}, and then with A) 1 µM insulin, B) 25 ng/ml PDGF or C) 100 nM PMA for the times shown, lysates were prepared {Section 2.13.2}. Approximately 30 µg of protein was loaded onto 10% (w/v) polyacrylamide large gels, the proteins were separated by SDS-PAGE {Section 2.15}, and then transferred onto nitrocellulose membranes. The membranes were probed with a mouse anti-MAPK antibody, then with a HRP-conjugated sheep anti-mouse IgG antibody. The antibody binding sites were visualised using an ECL detection system {Section 2.16.2}. These are representative Western blots from groups of two lysate preparations.

Figure 5.13   The effect of insulin, PDGF and PMA on the tyrosine phosphorylation of p125^{FAK}

After incubation of quiescent 3T3-L1 fibroblasts with 1 µM insulin, 25 ng/ml PDGF or 100 nM PMA for the times shown, lysates were prepared and the phosphotyrosine-containing proteins were immunoprecipitated {Section 2.13.3}. Approximately 33% of the sample (from a 10 cm plate) was loaded onto 10% (w/v) polyacrylamide mini-gels, the proteins were separated by SDS-PAGE {Section 2.15}, and then transferred onto nitrocellulose membranes. The membranes were probed with a mouse anti-p125^{FAK} antibody, then with a HRP-conjugated sheep anti-mouse IgG antibody. The antibody binding sites were visualised using an ECL detection system {Section 2.16.2}. This is a representative Western blot from a group of two lysate preparations.

Lane A: basal; lane B: 2 minutes insulin; lane C: 10 minutes insulin; lane D: 2 minutes PDGF; lane E: 10 minutes PDGF; lane F: 2 minutes PMA; lane G: 10 minutes PMA.
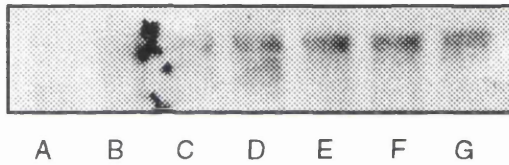
5.3   Discussion

In order to examine whether the early phase of growth factor-stimulated glucose transport is mediated by a signal transduction pathway involving MAPK, several approaches were taken. Firstly, the effects of insulin and PDGF on tyrosine phosphorylation and the requirement for PKC activity were established. Secondly, the effects of insulin and PDGF on MAPK activity and the requirement for PKC activity were established.

5.3.1   Phosphotyrosine-containing proteins

Western blotting of 3T3-L1 fibroblast lysate and membrane proteins with antibodies raised against phosphotyrosine, showed that the tyrosine phosphorylation of several proteins changed in response to all the ligands, whilst the tyrosine phosphorylation of other proteins changed in response to specific ligands only.

All ligands

Insulin, IGF-I, PDGF and PMA all stimulated an increase in the tyrosine phosphorylation of proteins with approximate molecular masses of 42 and 44 kDa in 3T3-L1 fibroblasts. The tyrosine phosphorylation was transient, increasing within 2 minutes of exposure to each ligand and reaching a maximum by 5 minutes (Figures 5.3, 5.4, 5.5 and 5.7). In addition, the tyrosine phosphorylation of proteins with approximate molecular masses of 42 and 44 kDa were increased in both membrane (Figure 5.6) and cytosolic preparations (results not shown). The molecular masses of these proteins suggest that they could be the mammalian MAPKs, p42^{mapk} and p44^{mapk} (Section 5.1.1).

Insulin, IGF-I, PDGF and PMA all also stimulated an increase in the tyrosine phosphorylation of a protein with an approximate molecular mass of 120 kDa in 3T3-L1 fibroblasts. The tyrosine phosphorylation of this protein increased within 1 minute of exposure to each ligand, was still elevated by 30 minutes, then decreased nearly to basal levels by 60 minutes (Figures 5.3, 5.4, 5.5 and 5.7). In addition, this phosphotyrosine protein was not seen in membrane samples (Figure 5.6). There are several proteins,

that have an approximate molecular mass of 120 kDa, that have a potential role in signal transduction. These include RasGAP and p125^{FAK}.

RasGAP binds to a specific phosphotyrosine sequence in the PDGF ß-receptor [Kashishian et al., 1992], and it undergoes tyrosine phosphorylation in response to PDGF [Kazlauskas et al., 1990]. However, it does not appear to bind to the insulin receptor or to IRS-1 [Sun et al., 1993a], therefore although RasGAP may be undergo tyrosine phosphorylation response to PDGF, it is unlikely to do so in response to insulin or IGF-I.

Activation of p125^{FAK} occurs in response to integrin-mediated cell adhesion [Zachary and Rozengurt, 1992] and to the neuropeptide growth factors, bombesin, endothelin and vasopressin, which bind to G protein-coupled receptors [Zachary and Rozengurt, 1992; Schaller and Parsons, 1993]. However, the mechanism by which p125^{FAK} is activated by extracellular stimuli is unclear, since, p125^{FAK} is activated by tyrosine phosphorylation, even though, the neuropeptide receptors and integrins have no intrinsic tyrosine kinase activity. There have been no previous reports of p125^{FAK} activation in response to ligands that bind to tyrosine protein kinase receptors, however, in 3T3-1 fibroblasts both insulin and PDGF stimulated the tyrosine phosphorylation of p125^{FAK} within 2 minutes of exposure to ligand {Figure 5.13}.

In Swiss 3T3 fibroblasts, PKC is not necessary for bombesin-stimulated p125^{FAK} tyrosine phosphorylation, but it is necessary for PMA stimulation [Sinnett-Smith et al., 1993]. This is surprising because the bombesin receptor is a G protein coupled receptor that activates G$_q$, then PLC-ß. However, several growth factors, for example, LPA and thrombin, which bind to G protein-coupled receptors, activate both G$_i$ and G$_q$ [Magnaldo et al., 1988; van Corven et al., 1989], therefore it is possible that bombesin stimulation of p125^{FAK} tyrosine phosphorylation is mediated by a G$_q$ independent pathway.

As there are several proteins with a similar molecular mass to p125^{FAK} that may undergo tyrosine phosphorylation in response to growth factors, it is not possible to draw definitive conclusions concerning the requirement of PKC for p125^{FAK} tyrosine phosphorylation from the Western blots presented in this thesis.

Insulin and IGF-I

When 3T3-L1 fibroblasts were incubated with insulin or IGF-I, there was an increase in the tyrosine phosphorylation of a protein with an approximate molecular mass of 166 kDa. The tyrosine phosphorylation increased within 1 minute of exposure to each ligand, was still elevated by 20 minutes, then decreased {Figures 5.3 and 5.4}. This protein could be IRS-1, which is a substrate for the tyrosine protein kinase of both the insulin and IGF-I receptors, and has an approximate molecular mass of 160 kDa in 3T3-L1 adipocytes [Yu et al., 1987] and of 180 kDa in hepatocytes [White et al., 1985]. The tyrosine phosphorylation of a membrane protein with an approximate molecular mass of 90 kDa also increased {Figure 5.6}. This protein could be the IGF-I (or insulin) receptor ß-subunit, which has an approximate molecular mass of 95 kDa, and undergoes autophosphorylation in response to ligand binding [Herrera and Rosen, 1986].

PDGF

When 3T3-L1 fibroblasts were incubated with PDGF there were increases in the tyrosine phosphorylation of proteins with approximate molecular masses of 155, 170 and 190 kDa. The tyrosine phosphorylation increased within 1 minute of exposure to PDGF, was still elevated by 30 minutes, then decreased nearly to basal levels by 60 minutes {Figure 5.5}. The tyrosine phosphorylation of membrane proteins with similar approximate molecular masses also increased {Figure 5.6}. The 190 kDa protein is likely to be the PDGF receptor, which has an approximate molecular mass of 190 kDa, and undergoes autophosphorylation in response to PDGF binding [Kelly et al., 1991]. The 155 kDa protein could be PLC-γ, which has an approximate molecular mass of 145 kDa {Section 4.1.1}. PLC-γ binds to the PDGF receptor [Meisenhelder et al., 1989; Wahl et al., 1989] and undergoes tyrosine phosphorylation in response to PDGF [Rhee and Choi, 1992].

Insulin, IGF-I and PDGF

When 3T3-L1 fibroblasts were incubated with insulin or PDGF, there was an increase in the tyrosine phosphorylation of a membrane protein with an approximate molecular mass of 20 kDa. The tyrosine phosphorylation increased within 2 minutes of exposure to PDGF or insulin, and decreased to basal levels by 10 minutes {Figure 5.6}. This protein was not observed in lysate samples. There are previous no reports of a 20 kDa phosphotyrosine protein.

When 3T3-L1 fibroblasts were incubated with insulin, IGF-I, or PDGF, there was clearly an increase in tyrosine phosphorylation of proteins with molecular masses between 60 and 120 kDa however, this region was blurred and so clear bands could not be observed. Another protein known to be a substrate for the insulin, IGF-I and PDGF receptors include Syp (p64) [Kazlauskas et al., 1993]. In addition, the regulatory subunit of PtdIns 3'-K (p85) binds to the PDGF receptor and to IRS-1 [Backer et al., 1992b; Hu et al., 1992]. There have been reports that p85 undergoes tyrosine phosphorylation in response to insulin and PDGF [Kaplan et al., 1987], however, this is disputed [Backer et al., 1992b], and it now appears that p85 only undergoes tyrosine phosphorylation when it is overexpressed [Hu et al., 1992].

The effect of PKC

When control 3T3-L1 fibroblasts (incubated for 16 hours with 1 µM 4α-PDD) were incubated with PDGF, insulin or PMA, or when PKC-depleted 3T3-L1 fibroblasts (incubated for 16 hours with 1 µM PMA) were incubated with PDGF or insulin, the time-dependent changes in tyrosine phosphorylation of all the observed proteins were similar to those observed in the absence of phorbol ester treatment {Figures 5.8, 5.9 and 5.10}. When PKC-depleted 3T3-L1 fibroblasts were incubated with PMA, the time-dependent changes in tyrosine phosphorylation of the 66 and 120 kDa were also similar to those observed in the absence of phorbol ester treatment, however, there were no changes in the tyrosine phosphorylation of the 42 and 44 kDa {Figure 5.10}.

This suggests that PKC is not necessary for PDGF- or insulin-stimulated tyrosine phosphorylation of any of the observed proteins, nor for PMA-stimulated tyrosine phosphorylation of the 66, 90 and 120 kDa proteins. However, PKC appears to be necessary for PMA-stimulated tyrosine phosphorylation of the 42 and 44 kDa proteins.

These results are in agreement with the suggestions of the identities of the various phosphotyrosine proteins. For example, insulin-stimulated tyrosine phosphorylation of the insulin receptor ß-subunit and PDGF-stimulated tyrosine phosphorylation of the PDGF ß-receptor are known only to be dependent on the intrinsic receptor tyrosine protein kinase and not on other tyrosine protein kinases.

5.3.2   MAPK

Stimulation of MAPK activity

MAPK is activated in response to many growth factors by the phosphorylation of a single threonine and a single tyrosine residue. The phosphorylation and activation of MAPK can be estimated in many ways. For example, the changes in tyrosine phosphorylation in response to various treatments can be followed by Western blotting of cellular proteins with an anti-phosphotyrosine antibody or with an anti-MAPK antibody. Phosphorylation of MAPK causes a decrease in its electrophoretic mobility [Posada et al., 1991]. Consequently, anti-MAPK Western blots of partially activated MAPK show a doublet, the band with the lower molecular mass corresponding to inactive MAPK (p42^{mapk} and p44^{mapk}) and the band with the higher molecular mass corresponding to active MAPK (pp42^{mapk} and pp44^{mapk}).

As previously described, PDGF, insulin, IGF-I and PMA stimulated increases in the tyrosine phosphorylation of two proteins with approximate molecular masses of 42 and 44 kDa in 3T3-L1 fibroblasts. The increase in tyrosine phosphorylation was rapid, tyrosine phosphorylation being evident within 2 minutes of exposure to each ligand and reaching a maximum by 5 minutes {Figures 5.3, 5.4, 5.5 and 5.7}. The molecular masses of these proteins suggest that they could be the mammalian MAPKs, p42^{mapk} and p44^{mapk}. If these phosphoproteins are the mammalian MAPKs and if the threonine and tyrosine phosphorylation of these proteins occurs in parallel, then the observed increase in the tyrosine phosphorylation of these proteins would correlate with an increase in MAPK activity. This suggests that PDGF, insulin, IGF-I and PMA stimulate a rapid increase in p42^{mapk} and p44^{mapk} activity, which reaches a maximum within 5 minutes of exposure to ligand.

When 3T3-L1 fibroblasts were incubated with PDGF, insulin or PMA, there were also decreases in the electrophoretic mobility of p42^{mapk} and of p44^{mapk}. However, the decrease in the mobility of p44^{mapk} was typically less pronounced than the decrease in the mobility of p42^{mapk}, and was best observed in response to PDGF {Figure 5.11b}. The decrease in the mobility of each MAPK isozyme was rapid, being evident within 2 minutes of exposure to each ligand and reaching a maximum by 5 minutes {Figure 5.11}. This also suggests that PDGF, insulin and PMA stimulate a rapid

increase in p42^{mapk} and of p44^{mapk} activity, which reaches a maximum within 5 minutes of exposure to ligand.

Since the time-dependent changes in tyrosine phosphorylation of the 42 kDa and 44 kDa proteins and in mobility during SDS-PAGE of p42^{mapk} and of p44^{mapk} are similar, it is most probable that the 42 and 44 kDa phosphotyrosine-containing proteins are the p42^{mapk} and of p44^{mapk} respectively.

Rapid increases in the activity of the mammalian MAPK isozymes have been observed in other cells in response to many growth factors [Kahan et al., 1992; Tamemoto et al., 1992; Nguyen et al., 1993]. In some cases the increase in MAPK activity is transient, returning to basal levels by 30 minutes, while in others the increase is sustained over several hours. For example, when PC12 cells are treated with EGF, a growth factor, the increase in MAPK activity is transient, however when they are treated with nerve growth factor, a differentiation factor, it is sustained [Nguyen et al., 1993]. In contrast, when CCL39 fibroblasts are treated with thrombin, a growth factor, the increase in MAPK activity is sustained [Kahan et al., 1992]. Therefore the role of MAPK in cell proliferation is unclear.

However, the interest in this project, is to examine whether MAPK could mediate the early phase of growth factor-stimulated glucose transport. In each experiment, the 3T3-L1 fibroblasts were incubated with ligand at a concentration sufficient to stimulate a maximum increase in the rate of 2-deoxyglucose uptake. Therefore, a concentration of each ligand sufficient to stimulate a maximal increase in the rate of 2-deoxyglucose uptake by 60 minutes, was also sufficient to stimulate a maximal increase in MAPK activity by 5 minutes. Since the apparent increase in MAPK activity precedes the increase in the rate of 2-deoxyglucose uptake, the early phase of growth factor-stimulated 2-deoxyglucose uptake could be mediated by a signal transduction pathway involving MAPK.

The effect of PKC

When control 3T3-L1 fibroblasts (incubated for 16 hours with 1 μM 4α-PDD) were incubated with PDGF, insulin or PMA, or when PKC-depleted 3T3-L1 fibroblasts were incubated with PDGF or insulin, the time-dependent changes in the tyrosine

phosphorylation of the 42 kDa and 44 kDa proteins {Figures 5.8, 5.9 and 5.10}, and in the electrophoretic mobility of p42^{mapk} and of p44^{mapk} {Figure 5.12} were similar to those observed in the absence of phorbol ester treatment. However, when PKC-depleted 3T3-L1 fibroblasts were incubated with PMA, there were no changes in the tyrosine phosphorylation of the 42 kDa and 44 kDa proteins {Figure 5.10} or in the electrophoretic mobility of p42^{mapk} and of p44^{mapk} {Figure 5.12c}.

Therefore PKC is not necessary for either insulin- or PDGF-stimulated tyrosine phosphorylation of the 42 and 44 kDa proteins, or for insulin- or PDGF-stimulated decreases in the electrophoretic mobility of p42^{mapk} and of p44^{mapk}. However, PKC is necessary for PMA-stimulated tyrosine phosphorylation of the 42 and 44 kDa proteins and decreases in the electrophoretic mobility of p42^{mapk} and of p44^{mapk}.

Since the PKC dependence of tyrosine phosphorylation of the 42 kDa and 44 kDa proteins and of the decrease in the mobility of p42^{mapk} and of p44^{mapk} are similar, tit is likely that the 42 and 44 kDa phosphoproteins are the mammalian MAPK isozymes, p42^{mapk} and p44^{mapk}. Therefore, PKC is not necessary for PDGF- or insulin-stimulated MAPK activation, but is necessary for PMA-stimulated MAPK activation. Similar results have been obtained using other cells, for example, insulin-stimulated MAPK activity in BC3H-1 myocytes is unaffected by down-regulation of PKC [Sturgill and Wu, 1991].

Since the increases in MAPK activity and the increases in the rate of 2-deoxyglucose uptake have the same dependency on PKC {Section 4.2.4}, it is possible that the early phase of 2-deoxyglucose uptake is mediated by a signal transduction pathway involving MAPK in 3T3-L1 fibroblasts.

5.3.3   Summary

Many proteins undergo tyrosine phosphorylation in response to PDGF, insulin and IGF-I. Many of these proteins have approximate molecular masses that suggest that they could be components of the signal transduction pathways stimulated by these growth factors, in particular, the tyrosine protein kinase receptors to which these growth factors bind, and substrates of these receptors. In addition, some proteins which

are not known to be substrates for the receptors also undergo tyrosine phosphorylation. These were identified as p125^{FAK}, p42^{mapk} and of p44^{mapk}.

In 3T3-L1 fibroblasts, PKC is not necessary for insulin- or PDGF-stimulated activation of MAPK, but that it is necessary for PMA-stimulated activation of MAPK. PKC is not necessary for the early phase of insulin- or PDGF-stimulated glucose transport, but that it is necessary for PMA-stimulated glucose transport {Chapter 4}. Therefore, given that the activation of MAPK and the increase in the rate of glucose transport have the same dependency on PKC, and that the activation of MAPK precedes the increase in the rate of glucose transport, it is possible that the early phase of growth factor-stimulated glucose transport is mediated by a signal transduction pathway involving MAPK. However, this does not prove that MAPK and increases in the rate glucose transport are connected.

In order to examine the role of specific proteins in an ligand-stimulated process, there are various techniques that can be used. A common technique is to use specific inhibitors, however, there are no specific inhibitors yet available for MAPK. A second technique is to express a protein in a stable or transient manner. An advantage of this technique is that the sequence of events leading to a process can be determined *in vivo* by expressing various forms of a protein, such as constitutively-active or dominant-negative mutants. However, plasmids containing the DNA sequence of the relevant proteins were not available. A third technique is to inject proteins into cells. This is probably the most technically demanding of the various methods given the small size of most cells, but, can be simplified by using larger cells such as the oocytes from the South African toad, *Xenopus laevis*. The facilities for the maintenance of *X. laevis* and for the injection of their oocytes were available. Therefore, the role of various components of the MAPK signal transduction pathway in mediating glucose transport was examined by injection of purified or recombinant proteins into *X. laevis* oocytes.

6   The activation of MAPK in *Xenopus laevis* oocytes

6.1   Introduction

The growth factors, insulin and PDGF, and the tumour promoter, PMA, all stimulate the rate of glucose transport in a similar manner in 3T3-L1 fibroblasts {Section 3.3}. These effects are not additive, therefore, the effects of these ligands on the rate of glucose transport may be mediated by a similar signal transduction pathway. Signal transduction pathways involving DAG and PKC do not appear to mediate the early phase of growth-factor stimulated glucose transport in 3T3-L1 fibroblasts {Section 4.3}. However, there is circumstantial evidence that a signal transduction pathway involving MAPK may mediate the early phase of growth factor-stimulated glucose transport {Section 5.3}.

The increase in MAPK activity precedes the increase in the rate of glucose transport in response to insulin or PDGF. In addition PKC is not necessary for insulin or PDGF-stimulated MAPK activation or glucose transport {Section 5.3}. However, this does not prove that a signal transduction pathway involving MAPK mediates growth factor-stimulated glucose transport. Therefore, the effects of MAPK on glucose transport were examined by injecting components of a signal transduction pathway involving MAPK into *X. laevis* oocytes.

6.1.1   Oocytes

Meiosis

Meiosis is a complex series of events which consists of a single nuclear division and two cytoplasmic divisions, producing four daughter cells, each with half the chromosome number of the parent cell. The daughter cells are either female gametes (eggs), or male gametes (sperm). Like mitosis, meiosis can be divided into phases, which separate into two division cycles, each of which consists of an interphase and a meiotic division.

Egg development takes several years. The first stages of meiosis occur in embryonic cells, producing the oocyte, which arrests between G2 and the M phase of its first meiotic cycle; at this point, DNA replication has occurred, but nuclear division has not [Maller, 1990]. During the G2 arrest, all the materials required for the construction of

the early embryo (other than DNA) are synthesised, hence the mature oocyte is a large cell. The G2 arrest is broken by progesterone, which is released at the time of ovulation. The oocyte then completes the first meiotic cycle and proceeds through the second meiotic cycle as far as the metaphase of meiosis II. The second arrest is broken by fertilisation. Meiosis is then quickly completed and followed by a rapid sequence of mitotic cell divisions in which the single giant cell cleaves to generate an embryo consisting of thousands of smaller cells. In *X. laevis*, the first division takes about 90 minutes, while the next 11 cleavage division occur more or less synchronously at 30 minute intervals, producing 4096 cells within about 7 hours. The prior accumulation of materials in the egg eliminates the time normally required for cell growth in each cycle, so that practically no growth occurs, although DNA is synthesised to create the necessary number of nuclei [Maller, 1990].

Comparison with mitosis

The activation of G0-arrested somatic cells and G2-arrested oocytes leads to different cell cycle stage-specific responses. For example, growth factors stimulate transcription in G0-arrested somatic cells, while hormones stimulate transcriptional shut-down in G2-arrested oocytes. However, many of the earliest events occurring during re-entry into the somatic or meiotic cell cycles are similar. For example, there are rapid changes in phospholipid metabolism, a transient elevation of free intracellular calcium, a rise in the intracellular pH, and an alteration of the cytoskeleton in both cases [Ruderman, 1993]. Therefore, both somatic cells and oocytes provide valid systems to study re-entry into the cell cycle.

6.1.2   The activation of MAPK

X. laevis homologues

A comparison of the mammalian MAPK amino acid sequences with sequences from other species shows that highly similar proteins are found in many species, including amphibians (*X. laevis*), insects (*Drosophila melanogaster*), budding yeast (*S. cerevisiae*) and fission yeast (*S. pombe*) [Nishida and Gotoh, 1993].

There are two *X. laevis* MAPK isozymes, with approximate molecular masses of 42 and 44 kDa [Posada et al., 1991]. The 42 kDa MAPK isozyme is activated by

phosphorylation on Thr-188 and Tyr-190 [Posada and Cooper, 1992]. The *X. laevis* MAPKK is a 45 kDa protein that activates MAPK by dual threonine and tyrosine phosphorylation [Matsuda et al., 1992]. *X. laevis* MAPKK may be activated by p39^{mos} [Posada et al., 1993] and MAPKKK [Matsuda et al., 1993]. p39^{mos} is involved in the release of oocytes from G2 arrest [Yew et al., 1992].

Release from G2 arrest

p39^{mos} is necessary for progesterone-induced oocyte maturation [Sagata et al., 1988]. It is absent from immature oocytes, its expression being induced within 1 hour of exposure to progesterone [Sagata et al., 1989]. It remains active until 30 minutes after fertilisation, when it is degraded by proteolysis [Watanabe et al., 1991].

p39^{mos} activates MAPKK leading to the activation of MAPK [Posada et al., 1993]. MAPK exists in the immature oocyte and is activated during oocyte maturation about 2 hours after progesterone treatment and remains active until approximately 30 minutes after fertilisation [Ferrell et al., 1991].

Insulin and IGF-I also stimulate the release of oocytes from G2 arrest [El-Etr et al., 1979]. p21^{ras} is necessary for insulin- and IGF-I-induced maturation [Korn et al., 1987], but it is not necessary for progesterone-induced maturation [Dominguez et al., 1991]. Addition of p21^{v-ras} to oocytes activates MAPK and MAPKK, suggesting that insulin and IGF-I both stimulate a signal transduction pathway involving MAPK in *X. laevis* oocytes [Hattori et al., 1992]. *X. laevis* oocytes express few if any insulin receptors, the effects of both insulin and IGF-I being mediated by the IGF-I receptor [Janicot et al., 1991].

6.1.3   Oocytes and glucose transport

X. laevis oocytes express low levels of a Glut1 homologue [Hainaut et al., 1991]. Insulin and IGF-I stimulate the rate of glucose transport in G2-arrested oocytes. The EC$_{50}$ values for insulin- and IGF-I-stimulated glucose transport are 200 to 250 nM and 3 to 3.5 nM respectively. There is a lag, of 20 to 30 minutes following exposure to insulin or IGF-I, during which the rate of glucose transport remains at the basal level. Then the rate of glucose transport increases rapidly reaching a maximum of three to four fold by

60 minutes and remains constant for several hours [Janicot and Lane, 1989]. However, the rate of glucose transport returns to the basal level before the onset of maturation [Hainaut et al., 1991].

Since, the rate of glucose transport through Glut1 is regulated by growth factors that bind to tyrosine protein kinase receptors in mammalian somatic cells and in *X. laevis* oocytes, it is possible that these effects are mediated by a similar signal transduction pathway. It is possible that a signal transduction pathway involving MAPK mediates the early phase of growth factor-stimulated glucose transport in somatic cells, however, it is difficult to examine this thoroughly in these cells. Therefore, in order to examine whether growth factor-stimulated glucose transport could be mediated by a signal transduction pathway involving MAPK, several approaches were taken. The effect of IGF-I on endogenous *X. laevis* oocyte MAPK activity, and the effect of components of a signal transduction pathway involving MAPK on the rate of glucose transport in *X. laevis* oocytes were examined.

6.2   Results

6.2.1   The effect of IGF-I on MAPK activity

The effect of IGF-I on the mobility of MAPK during SDS-PAGE was examined by Western blotting of cellular proteins. Lysates were prepared from *X. laevis* oocytes after incubation with 250 nM IGF-I {Section 2.13.4}. The proteins were separated by SDS-PAGE {Section 2.15}, and then transferred onto nitrocellulose membranes. The membranes were probed with a mouse anti-MAPK antibody, and then with a HRP-conjugated sheep anti-mouse IgG antibody. The antibody-binding sites were visualised using an ECL detection system {Section 2.16.2}.

The anti-MAPK antibody recognised two proteins with approximate molecular masses of 42 and 44 kDa in all the oocyte lysate samples. The mobility during SDS-PAGE of both proteins decreased in response to 1 µM IGF-I. The decrease in mobility was observed at 2 minutes and 10 minutes of exposure to IGF-I. The effect of incubation with IGF-I for other times was not examined. A representative Western blot is shown in Figure 6.1.

Figure 6.1   The effect of IGF-I on MAPK

After incubation of *X. laevis* oocytes with 250 nM IGF-I for the times shown, lysates were prepared {Section 2.13.4}. The lysate from two oocytes was loaded onto 10% (w/v) polyacrylamide mini-gels, the proteins were separated by SDS-PAGE {Section 2.15}, and then transferred onto nitrocellulose membranes. The membranes were probed with a mouse anti-MAP kinase antibody, and then with a HRP-conjugated sheep anti-mouse IgG antibody. The antibody binding sites were visualised using an ECL detection system {Section 2.16.2}. This is a representative Western blot from a group of two lysate preparations.

pp44^{mapk}
p44^{mapk}
pp42^{mapk}
p42^{mapk}

0   2   10

Time (min)
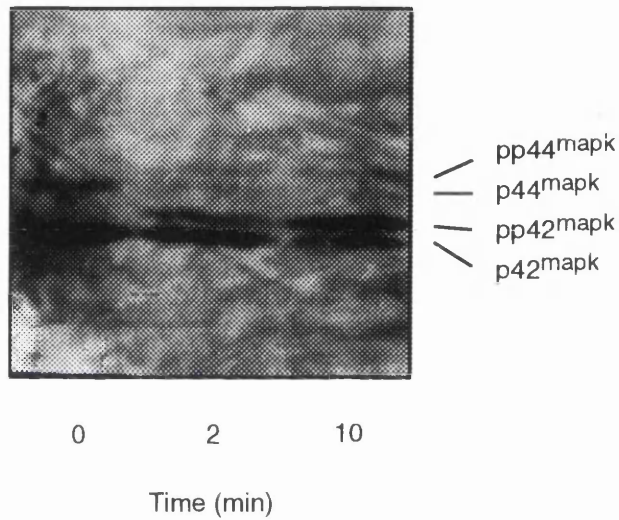
6.2.2 The effect of p42^{mapk} on the rate of glucose transport

The effect of MAPK on the rate of glucose transport in *X. laevis* oocytes was examined by measuring the rates of 2-deoxyglucose uptake {Section 2.8.2} and zero-*trans* 3-*O*-methylglucose transport {Section 2.8.3}, after the microinjection {Section 2.6} of a recombinant p42^{mapk}. Before injection, the p42^{mapk} was activated by thiophosphorylation by incubating with ATP[S] and MAPKK {Section 2.5.1}.

2-deoxyglucose uptake

After injection of 50 nl of 450 U/ml p42^{mapk} and incubation for 15, 30 and 120 minutes the rate of 2-deoxyglucose uptake increased 2.2 to 2.8 fold. After injection of 50 nl of Buffer A and incubation for 60 minutes, there was no change in the rate of 2-deoxyglucose uptake, while after injection of 50 nl of Buffer B and incubation for 60 minutes, there was a slight, but insignificant increase in the rate of 2-deoxyglucose uptake. After a 60 minute incubation with 250 nM IGF-I, the rate of 2-deoxyglucose uptake increased 2.8 to 3.5 fold. The results from a representative experiment are shown in Table 6.1.

After injection of 50 nl of 450 U/ml p42^{mapk} and a incubation with 250 nM IGF-I for 60 minutes, the rate of 2-deoxyglucose uptake increases 2.2 to 3.5 fold. After injection of 50 nl of 450 U/ml p42^{mapk} and a incubation with 10 µM cycloheximide for 60 minutes, the rate of 2-deoxyglucose uptake increased 2.2 to 2.8 fold. The results from a representative experiment are shown in Table 6.2.

Zero-trans 3-O-methylglucose transport

After injection of 50 nl of Buffer B or 450 U/ml MAPK and incubation for 60 minutes the amount of 3-*O*-methylglucose transported was such that the oocyte water space was completely equilibrated by 8 hours (results not shown). During the first 2 hours, the kinetics of transport were first order; the rate constant over this period was approximately 2 fold higher after the injection of p42^{mapk}, than after the injection of Buffer B. The results from a representative experiment are shown in Figure 6.2.

Table 6.1   The effect of p42^{mapk} on the rate of 2-deoxyglucose uptake

After incubation of *X. laevis* oocytes with 250 nM IGF-I for 60 minutes at room temperature, or after injection of *X. laevis* oocytes with 50 nl of water (basal), Buffer A, Buffer B or thiophosphorylated recombinant MAPK (450 U/ml) and incubation for the times shown at room temperature, a 60 minute uptake of 2-dexoy-D-[2,6-^{3}H]glucose was measured {Section 2.8.2}. Each result shows the mean rate of specific 2-deoxyglucose uptake (± SD) for eight oocytes. This is a representative experiment from a group of four; basal rates were 0.2 to 0.5 pmoles/ min/ oocyte and the maximal stimulation in response to IGF-I was between 2.5 and 3.5 fold, and to MAPK was between 2.2 and 2.8 fold. * p < 0.05

Buffer A: 50 mM Tris hydrochloride (pH 7.3), 2 mM sodium EDTA, 2 mM sodium EGTA, 5% (v/v) glycerol, 0.2 mM sodium vanadate, 0.03% (w/w) Brij 35, 0.1% (v/v) ß-mercaptoethanol, 6 mM specific peptide inhibitor of cyclic AMP-dependent protein kinase.

Buffer B: 10 mM magnesium acetate, 0.2 mM ATP[S] and MAPKK in Buffer A.

	Rate of 2-deoxyglucose uptake (pmoles/ min/ oocyte)
Basal (60 minutes water)	0.42 ± 0.03
60 minutes IGF-I	1.26 ± 0.09*
60 minutes Buffer A	0.46 ± 0.03
60 minutes Buffer B	0.66 ± 0.03
15 minutes MAPK	1.23 ± 0.08*
30 minutes MAPK	1.20 ± 0.06*
120 minutes MAPK	1.17 ± 0.02*

Table 6.2   The effect of p42^{mapk} and MAPKK on the rate of 2-deoxyglucose uptake

After incubation of *X. laevis* oocytes with 250 nM IGF-I or 10 µg/ml cyclohexImide for 60 minutes at room temperature, or after injection of *X. laevis* oocytes with 50 nl of water (basal), thiophosphorylated recombinant MAPK (450 U/ml), or rabbit skeletal muscle MAPKK (1.4 U per oocyte) and incubation for the times shown at room temperature, a 60 minute uptake of 2-dexoy-D-[2,6-^{3}H]glucose was measured {Section 2.8.2}. Each result shows the mean rate of specific 2-deoxyglucose uptake (± SD) for eight oocytes. This is a representative experiment from a group of three; basal rates were 0.2 to 0.5 pmoles/ min/ oocyte and the maximal stimulation in response to IGF-I was between 2.5 and 3.5 fold, to MAPK was between 2.2 and 2.8 fold, and to MAPKK was between 2.0 and 3.0 fold. * p < 0.05

	Rate of 2-deoxyglucose uptake (pmoles/ min/ oocyte)
Basal (60 minutes water)	0.24 ± 0.03
60 minutes IGF-I	0.60 ± 0.05*
120 minutes MAPK	0.54 ± 0.05*
60 minutes MAPK and IGF-I	0.57 ± 0.06*
60 minutes MAPK and cyclohexImide	0.53 ± 0.03*
60 minutes MAPKK	0.61 ± 0.05*

Figure 6.2   The effect of p42^{mapk} on 3-O-methylglucose transport

After injection of $X.$ $laevis$ oocytes with 50 nl of Buffer A ($\circ$) or thiophosphorylated recombinant MAPK($\square$) (450 units/ml), then incubation for the 60 minutes at room temperature, 3-O-methyl-D-[1-^{3}H]glucose transport, for the times shown, was measured {Section 2.8.3}. Each result shows the mean rate of specific 3-O-methylglucose transport ($\pm$ SD) for five oocytes. This is a representative experiment from a group of three; basal rates were between 0.2 and 0.5 pmoles/ min/ oocytes.

Buffer A: 50 mM Tris hydrochloride (pH 7.3), 2 mM sodium EDTA, 2 mM sodium EGTA, 5% (v/v) glycerol, 0.2 mM sodium vanadate, 0.03% (w/w) Brij 35, 0.1% (v/v) ß-mercaptoethanol, 6 mM specific peptide inhibitor of cyclic AMP-dependent protein kinase.
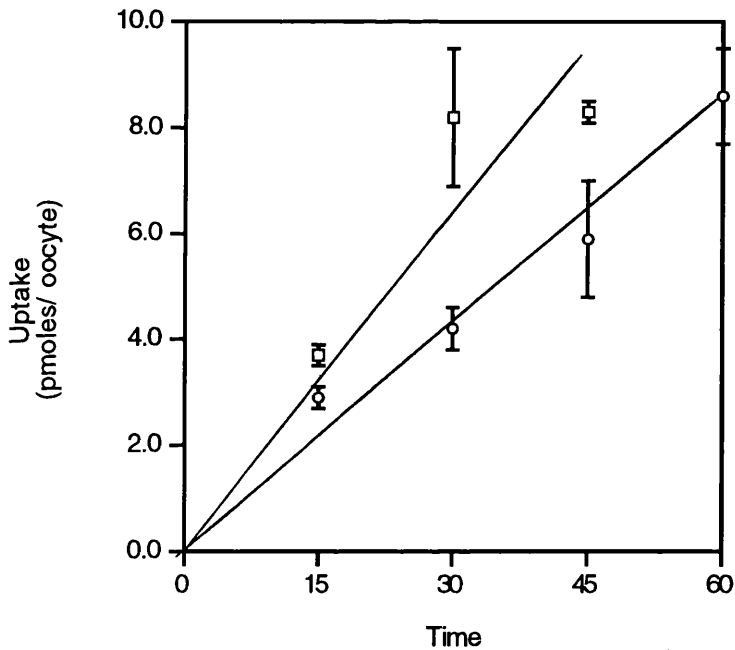
6.2.3   The effect of MAPKK on the rate of glucose transport

The effect of MAPKK on the rate of glucose transport in *X. laevis* oocytes was examined by measuring the rate of 2-deoxyglucose uptake {Section 2.8.2}, after injection of a MAPKK purified from rabbit skeletal muscle {Sections 2.5.2 and 2.6}. After injection of 50 nl of 44 800 U/ml MAPKK and incubation for 60 minutes the rate of 2-deoxyglucose uptake increased 2.5 to 3.0 fold. The results from a representative experiment are shown in Table 6.2.

6.2.4   The effect of MalE-Mos on the rate of glucose transport

The effect of Mos on the rate of glucose transport in *X. laevis* oocytes was examined by measuring the rate of 2-deoxyglucose uptake {Section 2.8.2}, after injection of a MalE-Mos fusion protein {Sections 2.5.3 and 2.6}.

After injection of 50 nl of 250 μg/ml MalE-Mos and incubation for 30, 60, 120 and 180 minutes the rate of 2-deoxyglucose uptake increased 2.0 to 2.8 fold. After injection of 50 nl of Buffer C and incubation for 60 minutes, there was no change in the rate of 2-deoxyglucose uptake. After a 60 minute incubation with 250 nM IGF-I, the rate of 2-deoxyglucose uptake increased 2.8 to 3.5 fold. The results from a representative experiment are shown in Table 6.3.

6.3   Discussion

In order to examine whether growth factor-stimulated glucose transport could be mediated by a signal transduction pathway involving MAPK, the effect of IGF-I on endogenous *X. laevis* oocyte MAPK activity, and the effect of components of a signal transduction pathway involving MAPK on the rate of glucose transport in *X. laevis* oocytes were examined.

Table 6.3   The effect of MalE-Mos on the rate of 2-deoxyglucose uptake

After incubation of *X. laevis* oocytes with 250 nM IGF-I for 60 minutes at room temperature, or injection of *X. laevis* with 50 nl of water, Buffer C or MalE-Mos (250 μg/ml) and incubation for the times shown at room temperature, a 60 minute uptake of 2-dexoy-D-[2,6-^{3}H]glucose was measured (Section 2.8.2). Each result shows the mean rate of specific 2-deoxyglucose uptake ($\pm$ SD) for eight oocytes. This is a representative experiment from a group of three; basal rates were 0.2 to 0.5 pmoles/ min/ oocyte and the maximal stimulation in response to IGF-I was between 2.8 and 3.5 fold, and to MalE-Mos was between 2.0 to 2.8 fold. * $p < 0.05$

Buffer C: 50 mM NaCl, 20 mM Tris, pH 7.5

	Rate of 2-deoxyglucose uptake (pmoles/ min/ oocyte)
Basal (60 minutes water)	0.42 ± 0.07
60 minutes IGF-I	1.31 ± 0.09*
60 minutes Buffer C	0.46 ± 0.04
30 minutes MalE-Mos	0.70 ± 0.02*
60 minutes MalE-Mos	0.81 ± 0.12*
120 minutes MalE-Mos	1.05 ± 0.09*
180 minutes MalE-Mos	1.15 ± 0.09*

6.3.1   The effect of IGF-I on MAPK activity

The phosphorylation and activation of MAPK were examined by Western blotting of cellular proteins with an anti-MAPK antibody. As previously described, anti-MAP kinase Western blots of partially activated MAPK show a doublet, the band with the lower molecular mass corresponding to inactive MAPK and the band with the higher molecular mass corresponding to active MAPK {Section 5.3.2}.

When *X. laevis* oocytes were incubated with IGF-I there was a decrease in the mobility during SDS-PAGE of *X. laevis* p42^{mapk} and p44^{mapk}. The decrease in mobility was observed from 2 to 10 minutes after exposure to IGF-I {Figure 6.1}. This suggests that IGF-I stimulates a rapid increase in MAPK activity in *X. laevis* oocytes. The effects of longer incubations with IGF-I were not examined, therefore these results do not show the length of time for which p42^{mapk} and p44^{mapk} were active. MAPK is also activated in by progesterone in G2-arrested oocytes. However, progesterone-stimulated MAPK activation does not occur until 2 hours after progesterone treatment [Ferrell et al., 1991]. This difference probably occurs because progesterone-stimulated MAPK activation is dependent upon p39^{mos} [Posada et al., 1993], which is not present in immature oocytes and therefore must be synthesised, before MAPK activation can occur, while the effects of IGF-I are dependant on p21^{ras} [Korn et al., 1987], which is expressed by the oocyte.

6.3.2   The effect of MAPK on the rate of glucose transport

The ability of MAPK to stimulate glucose transport in *X. laevis* oocytes was examined by measuring the rate of 2-deoxyglucose uptake after injection of a recombinant MAPK. The recombinant MAPK was activated by phosphorylation by incubating with MAPKK prior to microinjection. In order for the MAPK to have the maximum possible activity, thiophosphate was included in the incubation buffer. Thiophosphate groups are more resistant to *in vivo* dephosphorylation than are phosphate groups, therefore, thiophosphorylation in effect constitutively activates MAPK. The thiophosphorylated, recombinant MAPK had a specific activity similar to that of MAPK isolated from mammalian tissues (results not shown).

Since *X. laevis* oocytes express very low levels of the Glut1 homologue, the rate of glucose transport is quite low in comparison to cultured mammalian cells. Therefore, when measuring the rate of glucose transport, a short uptake time, for example 5 minutes, would not be accurate. Consequently, it is not possible to easily carry out accurate kinetic studies, that is determine the K_m and V_{max}. Instead, the uptakes were measured over 60 minutes. Therefore, the oocytes incubated for 15 minutes with MAPK were then incubated for 60 minutes with 2-deoxyglucose, a total of 75 minutes with MAPK.

The rate of 2-deoxyglucose uptake increased after incubation with MAPK, the maximal increase, of 2.8 fold, occurring after 75 minutes, then decreasing slightly but remaining significantly above the basal rate for at least 180 minutes {Table 6.1}. The effects on 2-deoxyglucose uptake of two buffers was also examined. The rate of 2-deoxyglucose uptake did not change after microinjection of Buffer A, but increased slightly, although not significantly after microinjection of Buffer B. Buffer B had the same composition as Buffer A, with the additions of magnesium acetate, ATP[S] and MAPKK. Thus, only Buffer B was capable of activating MAPK. Therefore, the small increase in the rate of 2-deoxyglucose uptake in oocytes after microinjection of Buffer B was probably due to the activation of endogenous oocyte MAPK by the MAPKK in Buffer B {Table 6.1}.

Since 2-deoxyglucose undergoes phosphorylation by hexokinase, 2-deoxyglucose uptake consists of both transport and phosphorylation {Section 2.8}. It has been assumed that transport is the rate-limiting step in these experiments. In contrast, 3-O-methylglucose is not metabolised, and therefore undergoes only transport. Therefore, in order confirm that the effect of p42^{mapk} on 2-deoxyglucose uptake was on the transport step and not the phosphorylation step, the effect of p42^{mapk} on 3-O-methylglucose transport was also determined. The rate constant for zero-*trans* 3-O-methylglucose transport was approximately 2 fold higher after injection of p42^{mapk}, than after injection of Buffer A. Therefore, the effect of MAPK was on the transport process and not on phosphorylation {Figure 6.2}. In addition, the effect of p42^{mapk} on the rate of 2-deoxyglucose uptake was not an artefact caused by excess levels of p42^{mapk}, since the amount injected into the oocytes was only 25 to 50 percent of the endogenous MAPK activity [Gotoh et al., 1991].

In addition, the effects of IGF-I and MAPK on the rate of glucose transport were not additive (Table 6.2), therefore, IGF-I and MAPK may increase the rate of glucose transport by a common mechanism. Furthermore, the microinjection of CL100, a protein tyrosine/ threonine phosphatase that is specific for MAPK [Alessi et al., 1993], into $X.$ $laevis$ oocytes inhibited p42^{mapk}- and IGF-I-stimulated glucose transport , while an inactive mutant had no effect [Arbuckle et al., 1994].

Therefore, given that IGF-I stimulates both glucose transport and MAPK activity, that the injection of a recombinant p42^{mapk} also stimulates 2-deoxyglucose uptake, and that inhibition of MAPK activity abolishes IGF-I-stimulated glucose transport, it is likely that IGF-I-stimulated glucose transport may be mediated by a signal transduction pathway involving MAPK in $X.$ $laevis$ oocytes.

6.3.3   The effect of MAPKK on the rate of glucose transport

The ability of MAPKK to stimulate glucose transport in $X.$ $laevis$ oocytes was examined by measuring the rate of 2-deoxyglucose uptake after microinjection of a MAPKK purified from rabbit skeletal muscle after intravenous injection of insulin [Nakielny et al., 1992a]. The MAPKK was purified in an active form, therefore, thiophosphorylation was not necessary. The purified MAPKK stimulated the rate of 2-deoxyglucose uptake by 2 to 3 fold (Table 6.2). Therefore, it is likely that the slight increase in the rate of 2-deoxyglucose uptake observed after injection of Buffer B was due to the MAPKK in this buffer. The residual level of MAPKK in Buffer B was 20 fold lower than the amount used for the microinjection of oocytes, thus explaining the small effect of Buffer B.

Therefore, the enzyme that activates MAPK also stimulates glucose transport.

6.3.4   The effect of p39^{mos} on the rate of glucose transport

The ability of p39^{mos} to stimulate glucose transport in $X.$ $laevis$ oocytes was also examined by measuring the rate of 2-deoxyglucose uptake after injection of a fusion protein consisting of the maltose-binding protein from $E.$ $coli$ and p39^{c-mos} (MalE-Mos). This fusion protein has p39^{mos} activity, being able to stimulate MAPK activity in $X.$

laevis oocyte extracts [Nebreda and Hunt, 1993], and able to activate MAPKK *in vitro* [Posada et al., 1993]. MalE-Mos stimulated the rate of 2-deoxyglucose uptake 2.0 to 2.8 fold after incubation with for 90 to 240 minutes {Table 6.3}. MalE-Mos also stimulates MAPK activity within 10 minutes in oocyte extracts in a dose-dependant manner [Nebreda and Hunt, 1993], suggesting that MalE-Mos-stimualted 2-deoxyglucose uptake is mediated by MAPK. In addition, the effect of MalE-Mos on 3-*O*-methylglucose transport was examined. Again, MalE-Mos stimulated the rate of 3-*O*-methylglucose transport (results not shown), confirming that the effect of MalE-Mos was on transport and not a subsequent step.

Therefore, an enzyme that activates MAPKK also stimulates glucose transport.

6.3.5   The effect of other serine/ threonine protein kinases on the rate of glucose transport

The effect of the some of the *in vitro* MAPK substrates {Section 5.1.1} on the rate of 2-deoxyglucose uptake was examined. MAPKAP kinase-1 and MAPKAP kinase-2, purified from rabbit skeletal muscle[1], were injected into *X. laevis* oocytes. The rate of 2-deoxyglucose uptake did not change, in response to either of these kinases, after incubations of one to four hours. Unfortunately, it is not possible to determine whether the kinases remained active after microinjection into the oocyte. However, since both MAPKAP kinase-1 and MAPKAP kinase-2 are skeletal muscle proteins, it is not improbable that their physiological roles are restricted to myocytes and that they are not normally expressed in other cells.

---

[1] MAPKAP kinase-1 and MAPKAP kinase-2 were gifts from Professor P Cohen, Medical Research Council Protein Phosphorylation Unit, Department of Biochemistry, University of Dundee, Dundee, Tayside, UK.

6.3.6 Summary

IGF-I stimulates both glucose transport and MAPK activity in *X. laevis* oocytes. The activation of MAPK precedes the increase in the rate of glucose transport.

In addition, the microinjection of recombinant p42^{mapk}, purified MAPKK or p39^{mos} fusion protein, results in an increase in the rate of glucose transport. Since p39^{mos} activates MAPKK, which in turn activates MAPK, it seems that components of a signal transduction pathway involving MAPK are able to stimulate glucose transport.

Furthermore, IGF-I stimulated glucose transport is inhibited by the microinjection of CL100 (a protein tyrosine/ threonine phosphatase that is specific for MAPK).

Therefore, given that IGF-I stimulates both glucose transport and MAPK activity, that components of a signal transduction pathway involving MAPK also stimulate the rate of glucose transport, and that inhibition of MAPK activity abolishes IGF-I-stimulated glucose transport, it is likely that IGF-I-stimulated glucose transport is mediated by a signal transduction pathway involving MAPK in *X. laevis* oocytes.

7 Discussion

3T3-L1 fibroblasts express only Glut1. The growth factors, insulin and PDGF, and the tumour promoter, PMA, all stimulate the rate of glucose transport in a similar manner. These effects are not additive, therefore, the effects of these ligands on the rate of glucose transport may be mediated by a similar signal transduction pathway.

Insulin has no effect on either DAG accumulation or PKC activity in 3T3-L1 fibroblasts, so neither DAG nor PKC is necessary for the early phase of insulin-stimulated glucose transport. PDGF stimulates both DAG accumulation and PKC activity; however, PDGF-stimulated glucose transport is unaffected by the down-regulation or the inhibition of PKC, so PKC is not necessary for the early phase of PDGF-stimulated glucose transport. PMA also stimulates both DAG accumulation and PKC activity, and PMA-stimulated glucose transport is abolished by the down-regulation and the inhibition of PKC, so PKC is necessary for the early phase of PMA-stimulated glucose transport. Therefore, a signal transduction pathway involving PKC is not necessary for the early phase of insulin- or PDGF-stimulated glucose transport in 3T3-L1 fibroblasts, but it is necessary for the early phase of PMA-stimulated glucose transport.

Insulin, PDGF and PMA stimulate MAPK activity in 3T3-L1 fibroblasts. Insulin has no effect on either DAG accumulation or PKC activity, so neither DAG nor PKC is necessary for insulin-stimulated activation of MAPK. PDGF stimulates both DAG accumulation and PKC activity: however, PDGF-stimulated activation of MAPK is unaffected by the down-regulation or the inhibition of PKC, so PKC is not necessary for PDGF-stimulated activation of MAPK. PMA also stimulates both DAG accumulation and PKC activity, and PMA-stimulated activation of MAPK is abolished by the down-regulation and the inhibition of PKC, so PKC is necessary for PMA-stimulated activation of MAPK. Therefore, a signal transduction pathway involving PKC is not necessary for insulin- or PDGF-stimulated activation of MAPK in 3T3-L1 fibroblasts, but it is necessary for PMA-stimulated activation of MAPK.

In addition, insulin-, PDGF- and PMA-stimulated activation of MAPK precedes the increase in the rate of glucose transport.

Therefore, given that the activation of MAPK and the increase in the rate of glucose transport have the same dependency on PKC, and that the activation of MAPK precedes

the increase in the rate of glucose transport, it is possible that the early phase of growth factor-stimulated glucose transport is mediated by a signal transduction pathway involving MAPK in 3T3-L1 fibroblasts.

X. laevis oocytes also express only Glut1. IGF-I stimulates both glucose transport and MAPK activity. Again, the activation of MAPK precedes the increase in the rate of glucose transport.

In addition, the microinjection into *X. laevis* oocytes of recombinant p42^{mapk}, purified MAPKK or p39^{mos} fusion protein, results in an increase in the rate of glucose transport. Since p39^{mos} activates MAPKK, which in turn activates MAPK, it seems that components of a signal transduction pathway involving MAPK are able to stimulate glucose transport.

Furthermore, IGF-I stimulated glucose transport in *X. laevis* oocytes is inhibited by the microinjection of CL100 (a protein tyrosine/ threonine phosphatase that is specific for MAPK).

Therefore, given that IGF-I stimulates both glucose transport and MAPK activity, that components of a signal transduction pathway involving MAPK also stimulate the rate of glucose transport, and that inhibition of MAPK activity abolishes IGF-I-stimulated glucose transport, it is likely that IGF-I-stimulated glucose transport is mediated by a signal transduction pathway involving MAPK in *X. laevis* oocytes.

The insulin and IGF-I receptors are both tyrosine protein kinases with a similar structure, and either ligand can bind to either receptor, so it is likely that insulin- and IGF-I-stimulated glucose transport are mediated by a similar signal transduction pathway.

Therefore, given that it is possible that the early phase of insulin-stimulated glucose transport is mediated by a signal transduction pathway involving MAPK in 3T3-L1 fibroblasts, that it is likely that IGF-I-stimulated glucose transport is mediated by a signal transduction pathway involving MAPK in *X. laevis* oocytes, and that it is likely that insulin- and IGF-I-stimulated glucose transport are mediated by a similar signal

transduction pathway, it seems that the early phase of insulin-stimulated glucose transport in 3T3-L1 fibroblasts is, in fact, mediated by a pathway involving MAPK.

Furthermore, PDGF, which also binds to a tyrosine protein kinase receptor, has similar effects to insulin on the rate of glucose transport and the activation of MAPK in 3T3-L1 fibroblasts. Therefore, it is also likely the early phase of PDGF-stimulated glucose transport is also mediated by a signal transduction pathway involving MAPK.

There are few, if any, published studies concerning the role of MAPK in the early phase of growth factor-stimulated glucose transport. However, several recent studies have examined the role of signal transduction pathways involving MAPK in insulin-stimulated glucose transport in 'insulin-responsive' tissues. These studies have used the differentiated form of 3T3-L1 fibroblasts; these cells have a phenotype characteristic of adipocytes {Section 3.1.2}. Importantly, they express both Glut1 and Glut4, and the rate of glucose transport increases 15 to 20 fold in response to insulin [Calderhead et al., 1990a], arising primarily from the translocation of Glut4 [Holman et al., 1990].

In one study [Inoue et al., 1993], when 3T3-L1 adipocytes were treated with ML-9, reported to be an inhibitor of myosin light chain kinase, insulin-stimulated glucose transport and translocation to the plasma membrane of both Glut1 and Glut4 were inhibited. However, further analysis showed that, in fact, the activity of myosin light chain kinase had been unaffected by the ML-9. The study concluded that ML-9 inhibits the activation of MAPK instead, and that insulin stimulation of glucose transport through both Glut1 and Glut4 is mediated by a signal transduction pathway involving MAPK.

Other recent studies also suggest that a signal transduction pathway involving MAPK may mediate the effect of growth factors on glucose transport through Glut1. In contrast, however, they suggest that the effect of insulin on glucose transport through Glut4 is not mediated by the same pathway.

Firstly, EGF and PDGF stimulated the rate of glucose transport by approximately two fold in 3T3-L1 adipocytes, while insulin stimulated the rate by approximately 20 fold. EGF, PDGF and insulin all stimulated the translocation of Glut1, but only insulin

stimulated the translocation of Glut4. Since the differences between the effects of EGF, PDGF and insulin were not due to cell-specific expression, the stimulation of glucose transport through Glut1 and Glut4 must have been mediated by different signal transduction pathways. Furthermore, it was suggested that since EGF, PDGF and insulin all stimulate MAPK activity, glucose transport through Glut1, but not through Glut4, is mediated by a signal transduction pathway involving MAPK [Fingar and Birnbaum, 1994a; Gould et al., 1994].

Secondly, expression of a constitutively active Raf-1, $p35^{raf-1}$, in 3T3-L1 adipocytes resulted in an elevated Glut1 level, while the Glut4 level and intracellular distribution remained normal [Fingar and Birnbaum, 1994b]. After microinjection with a dominant negative $p21^{ras}$ mutant, N17Ras, insulin-stimulated Glut1 translocation was abolished, while insulin-stimulated Glut4 translocation remained unaffected [Hausdorff et al., 1994]. Thus, given that $p21^{ras}$ and $p74^{raf-1}$ both appear to be involved in the regulation of glucose transport through Glut1 and not through Glut4, and that both activate the kinase cascade leading to the activation of MAPK, it is likely that a signal transduction pathway involving MAPK mediates glucose transport through Glut1, but not through Glut4.

This thesis concludes that the early phase of growth factor-stimulated glucose transport is mediated by a signal transduction pathway involving MAPK.

References

Abdel-Hafiz, H. A. M., Heasley, L. E., Kyriakis, J. M., Avruch, J., Kroll, D. J., Johnson, G. L. and Hoeffler, J. P. (1992) Mol. Endocrinol. **6**, 2079–2089

Acevedo-Duncan, M., Cooper, D. R., Standaert, M. L. and Farese, R. V. (1989) FEBS Lett. **244**, 174–176

Aderem, A. (1992a) Cell **71**, 713–716

Aderem, A. (1992b) Trends Biochem. Sci. **17**, 438–443

Ahmad, P. M., Russell, T. R. and Ahmad, F. (1979) Biochem. J. **182**, 509–514

Alessi, D. R., Smythe, C. and Keyse, S. M. (1993) Oncogene **8**, 2015–2020

Alexander, D. R., Hexham, J. M., Lucas, S. C., Graves, J. D., Cantrell, D. A. and Crumpton, M. J. (1989) Biochem. J. **260**, 893–901

Alexander, D. R., Graves, J. D., Lucas, S. C., Cantrell, D. A. and Crumpton, M. J. (1990) Biochem. J. **268**, 303–308

Allard, W. J., Gibbs, E. M., Witters, L. A. and Lienhard, G. E. (1987) Biochim. Biophys. Acta **929**, 288–295

Almendral, J. M., Sommer, D., MacDonald-Bravo, H., Burckhard, J., Perera, J. and Bravo, R. (1988) Mol. Cell. Biol. **8**, 2140–2148

Alvarez, E., Northwood, I. C., Gonzalez, F. A., Latour, D. A., Seth, A., Abate, C., Curran, T. and Davis, R. J. (1991) J. Biol. Chem. **266**, 15277–15285

Anderson, N. G., Maller, J. L., Tonks, N. K. and Sturgill, T. W. (1990) Nature **343**, 651–653

Angel, P. and Karin, M. (1991) Biochim. Biophys. Acta **1072**, 129–157

Arbuckle, M. I., Brant, A. M., Campbell, I. W., Jess, T. J., Kane, S., Livingstone, C. D., Martin, S., Merrall, N. W., Porter, L., Reid, R., Seatter, M. J. and Gould, G. W. (1994) Biochem. Soc. Trans. **22**, in the press

Asano, T., Shibasaki, Y., Kasuga, M., Kanazawa, Y., Takaku, F., Akanuma, Y. and Oka, Y. (1988) Biochem. Biophys. Res. Commun. **154**, 1204–1211

Asano, T., Shibasaki, Y., Lin, J.-L., Akanuma, Y., Takaku, F. and Oka, Y. (1989a) Nucleic Acids Res. **17**, 6386

Asano, T., Shibasaki, Y., Ohno, S., Taira, H., Lin, J.-L., Kasuga, M., Kanazawa, Y., Akanuma, Y., Takaku, F. and Oka, Y. (1989b) J. Biol. Chem. **264**, 3416–3420

Asaoka, Y., Nakamura, S.-I., Yoshida, K. and Nishizuka, Y. (1992) Trends Biochem. Sci. **17**, 414–417

Augert, G. and Exton, J. H. (1988) J. Biol. Chem. **263**, 3600–3609

Backer, J. M., Schroeder, G. G., Kahn, C. R., Myers, M. G., Wilden, P. A., Cahill, D. A. and White, M. F. (1992a) J. Biol. Chem. **267**, 1367–1374

Backer, J. M., Myers, M. G., Shoelson, S. E., Chin, D. J., Sun, X.-J., Miralpeix, M., Hu, P., Margolis, B., Skolnik, E. Y., Schlessinger, J. and White, M. F. (1992b) EMBO J. **11**, 3469–3479

Ballou, L. M., Luther, H. and Thomas, G. (1991) Nature **349**, 348–350

Barnard, E. A. (1992) Trends Biochem. Sci. **17**, 368–374

Basketter, D. A. and Widdas, W. F. (1978) J. Physiol. **278**, 398–401

Battey, J. F., Way, J. M., Corjay, M. H., Shapira, H., Kusano, K., Harkins, R., Wu, J. M., Slattery, T., Mann, E. and Feldman, R. I. (1991) Proc. Natl. Acad. Sci. U.S.A **88**, 395–399

Bell, R. M. and Burns, D. J. (1991) J. Biol. Chem. **266**, 4661–4664

Bell, G. I., Burant, C. F., Takeda, J. and Gould, G. W. (1993) J. Biol. Chem. **268**, 19161–19164

Berridge, M. J. (1993) Nature **361**, 315–325

Berridge, M. J. and Irvine, R. F. (1989) Nature **341**, 197–204

Berry, N., Ase, K., Kishimoto, A. and Nishizuka, Y. (1990) Proc. Natl. Acad. Sci. U.S.A **87**, 2294–2298

Berstein, G., Blank, J. L., Jhon, D.-Y., Exton, J. H., Rhee, S. G. and Ross, E. M. (1992) Cell **70**, 411–418

Birnbaum, M. J. (1989) Cell **57**, 305–315

Birnbaum, M. J., Haspel, H. C. and Rosen, O. M. (1986) Proc. Natl. Acad. Sci. U.S.A **83**, 5784–5788

Bishop, M. J. (1985) Cell **42**, 23–38

Blackshear, P. J. (1993) J. Biol. Chem. **268**, 1501–1504

Blackshear, P. J., Witters, L. A., Girard, P. R., Kuo, J. F. and Quamo, S. N. (1985) J. Biol. Chem. **260**, 13304–13315

Blackshear, P. J., Haupt, D. M., App, H. and Rapp, U. R. (1990) J. Biol. Chem. **265**, 12131–12134

Blackshear, P. J., Haupt, D. M. and Stumpo, D. J. (1991) J. Biol. Chem. **266**, 10946–10952

Bligh, E. G. and Dyer, W. J. (1959) Can. J. Biochem. Physiol. **37**, 911–917

Bloch, R. (1973) Biochemistry **12**, 4799–4801

Blumer, K. J. and Johnson, G. L. (1994) Trends Biochem. Sci. **19**, 236–240

Bocckino, S. B., Blackmore, P. F., Wilson, P. B. and Exton, J. H. (1987) J. Biol. Chem. **262**, 15309–15315

Bollag, G. and McCormick, F. (1991) Annu. Rev. Cell Biol. **7**, 601–632

Boulton, T. G., Yancopoulos, G. D., Gregory, J. S., Slaughter, C., Moomaw, C., Hsu, J. and Cobb, M. H. (1990) Science **249**, 64–67

Boulton, T. G., Nye, S. H., Robbins, D. J., Ip, N. Y., Radziejewska, E., Morgenbesser, S. D., DePinho, R. A., Panayotatos, N., Cobb, M. H. and Yancopoulos, G. D. (1991) Cell **65**, 663–675

Brant, A. M., McCoid, S., Thomas, H. M., Baldwin, S. A., Davies, A., Parker, J. C., Gibbs, E. M. and Gould, G. W. (1992) Cell. Signalling **4**, 641–650

Brewster, J. L. (1993) Science **259**, 1760–1763

Buday, L. and Downward, J. (1993) Cell **73**, 611–620

Burant, C. F. and Bell, G. I. (1992) Biochemistry **31**, 10414–10420

Burant, C. F., Takeda, J., Brot-Laroche, E., Bell, G. I. and Davidson, N. O. (1992) J. Biol. Chem. **267**, 14523–14526

Cairns, M. T., Elliot, D. A., Scudder, P. R. and Baldwin, S. A. (1984) Biochem. J. **221**, 179–188

Calderhead, D. M., Kitagawa, K., Tanner, L. I., Holman, G. D. and Lienhard, G. E. (1990a) J. Biol. Chem. **265**, 13800–13808

Calderhead, D. M., Kitagawa, K., Lienhard, G. E. and Gould, G. W. (1990b) Biochem. J. **269**, 597–601

Carozzi, A., Camps, M., Gierschik, P. and Parker, P. J. (1993) FEBS Lett. **315**, 340–342

Charles, C. H., Abler, A. S. and Lau, L. F. (1992) Oncogene **7**, 187–190

Claesson-Welsh, L., Eriksson, A., Westermark, B. and Heldin, C.-H. (1989) Proc. Natl. Acad. Sci. U.S.A **86**, 4917–4921

Colville, C. A., Seatter, M. J., Jess, T. J., Gould, G. W. and Thomas, H. M. (1993) Biochem. J. **290**, 701–706

Conricode, K. M., Brewer, K. A. and Exton, J. H. (1992) J. Biol. Chem. **267**, 7199–7202

Cook, S. J. and Wakelam, M. J. O. (1989) Biochem. J. **263**, 581–587

Cook, S. J. and Wakelam, M. J. O. (1992) Rev. Physiol. Biochem. Pharmacol. **119**, 13–45

Cook, S. J., Palmer, S., Plevin, R. and Wakelam, M. J. O. (1990) Biochem. J. **265**, 617–620

Cook, S. J., Briscoe, C. P. and Wakelam, M. J. O. (1991) Biochem. J. **280**, 431–438

Cooper, D. R., Ishizuka, T., Watson, J. E., Standaert, M. L., Nair, G. and Farese, R. V. (1990) Biochim. Biophys. Acta **1054**, 95–102

Cornelius, P., Marlowe, M., Lee, M. D. and Pekala, P. H. (1990) J. Biol. Chem. **265**, 20506–20516

Craik, J. D. and Elliott, K. R. F. (1979) Biochem. J. **182**, 503–508

Crespo, P., Xu, N., Simonds, W. F. and Gutkind, S. J. (1994) Nature **369**, 418–420

Czech, M. P. and Buxton, J. M. (1993) J. Biol. Chem. **268**, 9187–9190

Czech, M. P., Clancy, B. M., Pessino, A., Woon, C.-W. and Harrison, S. A. (1992) Trends Biochem. Sci. **17**, 197–201

Davidson, N. O., Hausman, A. M. L., Ifkovits, C. A., Buse, J. B., Gould, G. W., Burant, C. F. and Bell, G. I. (1992) Am. J. Physiol. **262**, C795–C800

Davies, A., Meeran, K., Cairns, M. T. and Baldwin, S. A. (1987) J. Biol. Chem. **262**, 9347–9352

Davis, P. D., Hill, C. H., Keech, E., Lawton, G., Nixon, J. S., Sedgwick, A. D., Wadsworth, J., Wetmacott, D. and Wilkinson, S. E. (1989) FEBS Lett. **259**, 61–63

Davis, R. J. (1993) J. Biol. Chem. **268**, 14553–14556

Dekker, L. V. and Parker, P. J. (1994) Trends Biochem. Sci. **19**, 73–77

Dent, P., Lavoinne, A., Nakielny, S., Caudwell, F. B., Watt, P. and Cohen, P. (1990) Nature **348**, 302–308

Dominguez, I., Marshall, M. S., Gibbs, J. B., Garcia de Herreros, A., Cornet, M. E., Graziani, G., Diaz-Meco, M. T., Johansen, T., McCormick, F. and Moscat, J. (1991) EMBO J. **10**, 3215–3220

Downward, J., Graves, J. D., Warne, P. H., Rayter, S. and Cantrell, D. A. (1990) Nature **346**, 719–723

Drewes, G., Lichtenberg-Kraag, B., Döring, F., Mandelkow, E.-M., Biernat, J., Goris, J., Dorée, M. and Mandekow, E. (1992) EMBO J. **11**, 2131–2138

Ebina, Y., Ellis, L., Jarnagin, K., Edery, M., Graf, L., Clauser, E., Ou, J.-h., Masiarz, F., Kan, Y. W., Goldfine, I. D., Roth, R. A. and Rutter, W. J. (1985) Cell **40**, 747–758

Egan, J. J., Saltis, J., Wek, S. A., Simpson, I. A. and Londos, C. (1990) Proc. Natl. Acad. Sci. U.S.A **87**, 1052–1056

Egan, S. E., Giddings, B. W., Brooks, M. W., Buday, L., Sizeland, M. A. and Weinberg, R. A. (1993) Nature **363**, 45–51

El-Etr, M., Schorderet-Slatkine, S. and Baulieu, E.-E. (1979) Science **205**, 1397–1399

Erickson, A. K., Payne, D. M., Martino, P. A., Rossomando, A. J., Shabanowitz, J., Weber, M. J., Hunt, D. F. and Sturgill, T. W. (1990) J. Biol. Chem. **265**, 19728–19735

Erikson, E. and Maller, J. L. (1986) J. Biol. Chem. **261**, 350–355

Errede, B. and Levin, D. E. (1993) Curr. Opin. Cell Biol. **5**, 254–260

Exton, J. (1990) J. Biol. Chem. **265**, 1–4

Fantl, W. J., Escobedo, J. A., Martin, G. A., Turck, C. W., del Rosario, M., McCormick, F. and Williams, L. T. (1992) Cell **69**, 413–423

Farese, R. V., Barnes, D. E., Davis, J. S., Standaert, M. L. and Pollet, R. J. (1984) J. Biol. Chem. **259**, 7094–7100

Farese, R. V., Davis, J. S., Barnes, D. E., Standaert, M. L., Babischkin, J. S., Hock, R., Rosic, N. K. and Pollet, R. J. (1985) Biochem. J. **231**, 269–278

Ferrell, J. E., Wu, M., Gerhart, J. C. and Martin, G. S. (1991) Mol. Cell. Biol. **11**, 1965–1971

Fingar, D. C. and Birnbaum, M. J. (1994a) Endocrinology **134**, 728–735

Fingar, D. C. and Birnbaum, M. J. (1994b) J. Biol. Chem. **269**, 10127–10132

Flier, J. S., Mueckler, M. M., Usher, P. and Lodish, H. F. (1987) Science **235**, 1492–1495

Folkman, J. and Moscona, A. (1978) Nature **273**, 345–349

Frost, S. C. and Lane, M. D. (1985) J. Biol. Chem. **260**, 2646–2652

Fukumoto, H., Seino, S., Imura, H., Seino, Y., Eddy, R., L., Fukushima, Y., Byers, M. G., Shows, T. B. and Bell, G. I. (1988) Proc. Natl. Acad. Sci. U.S.A **85**, 5434–5438

Fukumoto, H., Kayano, T., Buse, J. B., Edwards, Y., Pilch, P. F., Bell, G. I. and Seino, S. (1989) J. Biol. Chem. **264**, 7776–7779

Gale, N. W., Kaplan, S., Lowenstein, E. J., Schlessinger, J. and Bar-Sagi, D. (1993) Nature **363**, 88–92

Gibbs, E. M., Allard, W. J. and Lienhard, G. E. (1986) J. Biol. Chem. **261**, 16597–16603

Gibbs, E. M., Lienhard, G. E. and Gould, G. W. (1988) Biochemistry **27**, 6681–6685

Gibbs, J. B., Marshall, M. S., Scolnick, E. M., Dixon, R. A. F. and Vogel, U. S. (1990) J. Biol. Chem. **265**, 20437–20442

Gibbs, M. E., Calderhead, D. M., Holman, G. D. and Gould, G. W. (1991) Biochem. J. **275**, 145–150

Gille, H., Sharrocks, A. D. and Shaw, P. E. (1992) Nature **358**, 414–417

Goldschmidt-Clermont, P. J., Kim, J. W., Machesky, L. M., Rhee, S. G. and Pollard, T. D. (1991) Science **251**, 1231–1233

Goldstein, B. J. and Dudley, A. L. (1990) Mol. Endocrinol. **4**, 235–244

Gómez, N., Tonks, N. K., Morrison, C., Harmar, T. and Cohen, P. (1990) FEBS Lett. **271**, 119–122

Goode, N., Hughes, K., Woodgett, J. R. and Parker, P. J. (1992) J. Biol. Chem. **267**, 16878–16882

Goodrich, D. W. and Lee, W.-H. (1992) Nature **360**, 177–179

Gotoh, Y., Nishida, E., Matsuda, S., Shiina, N., Kosako, H., Shiokawa, K., Akiyama, T., Ohta, K. and Sakai, H. (1991) Nature **349**, 251–254

Gould, G. W. and Lienhard, G. E. (1989) Biochemistry **28**, 9447–9452

Gould, G. W. and Bell, G. I. (1990) Trends Biochem. Sci. **15**, 18–23

Gould, G. W., Lienhard, G. E., Tanner, L. I. and Gibbs, E. M. (1989) Arch. Biochem. Biophys. **268**, 264–275

Gould, G. W., Thomas, H. M., Jess, T. J. and Bell, G. I. (1991) Biochemistry **30**, 5139–5145

Gould, G. W., Brant, A. M., Kahn, B. B., Shepherd, P. R., McCoid, S. C. and Gibbs, E. M. (1992) Diabetologica **35**, 304–309

Gould, G. W., Merrall, N. W., Martin, S., Jess, T. J., Campbell, I. W., Calderhead, D. M., Gibbs, E. M., Holman, G. D. and Plevin, R. J. (1994) Cell. Signalling in the press *6 3/5 - 309*

Green, H. and Kehinde, O. (1974) Cell **1**, 113–116

Green, H. and Kehinde, O. (1975) Cell **5**, 19–27

Green, H. and Meuth, M. (1974) Cell **3**, 127–133

Greenberg, M. E. and Ziff, E. B. (1984) Nature **311**, 433–438

Gupta, S. K., Gallego, C., Johnson, G. L. and Heasley, L. E. (1992) J. Biol. Chem. **267**, 7987–7990

Ha, K.-S. and Exton, J., H. (1993) J. Biol. Chem. **268**, 10534–10539

Hainaut, P., Kowalski, A., Le Marchand-Brustel, Y., Giorgetti, S., Gautier, N. and Van Obberghen, E. (1991) Mol. Cell Endocrinol. **75**, 133–139

Hall, A. (1990) Science **249**, 635–640

Halsey, D. L., Girard, P. R., Kuo, J. F. and Blackshear, P. J. (1987) J. Biol. Chem. **262**, 2234–2243

Haney, P. M., Slot, J. W., Piper, R. C., James, D. E. and Mueckler, M. (1991) J. Cell Biol. **114**, 689–699

Harrison, S. A., Buxton, J. M. and Czech, M. P. (1991) Proc. Natl. Acad. Sci. U.S.A **88**, 7839–7843

Hattori, S., Fukuda, M., Yamashita, T., Nakamura, S., Gotoh, Y. and Nishida, E. (1992) J. Biol. Chem. **267**, 20346–20351

Hausdorff, S. F., Fingar, D. C. and Birnbaum, M. J. (1994) Biochem. Soc. Trans. **22**, in the press

Heasley, L. E. and Johnson, G. L. (1989) J. Biol. Chem. **264**, 8646–8652

Hediger, M. A., Turk, E. and Wright, E. M. (1989) Proc. Natl. Acad. Sci. U.S.A **86**, 5748–5752

Heidaran, M. A., Pierce, J. H., Yu, J.-C., Lombardi, D., Artrip, J. E., Fleming, T. P., Thomason, A. and Aaronson, S. A. (1991) J. Biol. Chem. **266**, 20232–20237

Heidaran, M. A., Beeler, J. F., Yu, J.-C., Ishibashi, T., LaRochelle, W. J., Pierce, J., H. and Aaronson, S. A. (1993) J. Biol. Chem. **268**, 9287–9295

Heidenreich, K. A., Toledo, S. P., Brunton, L. L., Watson, M. J., Daniel-Issakani, S. and Strulovici, B. (1990) J. Biol. Chem. **265**, 15076–15082

Heldin, C.-H. (1991) Trends Biochem. Sci. **16**, 450–452

Heldin, C.-H. (1992) EMBO J. **11**, 4251–4259

Heldin, C.-H. and Westermark, B. (1990) Cell Reg. **1**, 555–566

Henriksen, E. J., Rodnick, K. J. and Holloszy, J. O. (1989) J. Biol. Chem. **264**, 21536–21543

Hepler, J. R. and Gilman, A. G. (1992) Trends Biochem. Sci. **17**, 383–387

Herrera, R. and Rosen, O. M. (1986) J. Biol. Chem. **261**, 11980–11985

Hiraki, Y., Rosen, O. M. and Birnbaum, M. J. (1988) J. Biol. Chem. **263**, 13655–13662

Hiraki, Y., Garcia de Herreros, A. and Birnbaum, M. J. (1989) Proc. Natl. Acad. Sci. U.S.A **86**, 8252–8256

Holman, G. D., Kozka, I. J., Clark, A. E., Flower, C. J., Saltis, J., Habberfield, A. D., Simpson, I. A. and Cushman, S. W. (1990) J. Biol. Chem. **265**, 18172–18179

Holz, G. G. and Habener, J. R. (1992) Trends Biochem. Sci. **17**, 388–393

House, C., Wettenhall, R. E. H. and Kemp, B. E. (1987) J. Biol. Chem. **262**, 772–777

Housey, G. M., Johnson, M. D., Hsiao, W. L. W., O'Brian, C. A., Murphy, J. P., Kirschmeier, P. and Weinstein, I. B. (1988) Cell **52**, 343–354

Howe, L. R., Leevers, S. J., Gómez, N., Nakielny, S., Cohen, P. and Marshall, C. J. (1992) Cell **71**, 335–342

Hu, P., Margolis, B., Skolnik, E. Y., Lammers, R., Ullrich, A. and Schlessinger, J. (1992) Mol. Cell. Biol. **12**, 981–990

Hudson, A. W., Ruiz, M. L. and Birnbaum, M. J. (1992) J. Cell Biol. **116**, 785–797

Hudson, A. W., Fingar, D. C., Seider, G. A., Griffiths, G., Burke, B. and Birnbaum, M. J. (1993) J. Cell Biol. **122**, 579–588

Hunter, T. and Karin, M. (1992) Cell **70**, 375–387

Inoue, G., Kuzuya, H., Hayashi, T., Okamoto, M., Yoshimasa, Y., Kosaki, A., Kono, S., Okamoto, M., Maeda, I., Kubota, M. and Imura, H. (1993) J. Biol. Chem. **268**, 5272–5278

Ishizuka, T., Cooper, D. R. and Farese, R. V. (1989) FEBS Lett. **257**, 337–340

Ishizuka, T., Cooper, D. R., Hernandez, H., Buckley, D., Standaert, M. L. and Farese, R. V. (1990) Diabetes **39**, 181–190

James, D. E., Strube, M. and Mueckler, M. (1989) Nature **338**, 83–87

Janicot, M. and Lane, M. D. (1989) Proc. Natl. Acad. Sci. U.S.A **86**, 2642–2646

Janicot, M., Flores-Riveros, J. R. and Lane, M. D. (1991) J. Biol. Chem. **266**, 9382–9391

Jimenez de Asua, L. and Rozengurt, E. (1974) Nature **251**, 624–626

Johnston, G. C., Singer, R. A. and McFarlane, E. S. (1977) J. Bact. **132**, 723–730

Kahan, C., Seuwen, K., Meloche, S. and Pouysségur, J. (1992) J. Biol. Chem. **267**, 13369–13375

Kaplan, D. R., Whitman, M., Schaffhausen, B., Pallas, D. C., White, M., Cantley, L. and Roberts, T. M. (1987) Cell **50**, 1021–1029

Kashishian, A., Kazlauskas, A. and Cooper, J. A. (1992) EMBO J. **11**, 1373–1382

Kayano, T., Fukumoto, H., Eddy, R. L., Fan, Y.-S., Byers, M. G., Shows, T. B. and Bell, G. I. (1988) J. Biol. Chem. **263**, 15245–15248

Kayano, T., Burant, C. F., Fukumoto, H., Gould, G. W., Fan, Y.-s., Eddy, R. L., Byers, M. G., Shows, T. B., Seino, S. and Bell, G. I. (1990) J. Biol. Chem. **265**, 13276–13282

Kazlauskas, A. and Cooper, J. A. (1989) Cell **58**, 1121–1133

Kazlauskas, A., Ellis, C., Pawson, T. and Cooper, J. A. (1990) Science **247**, 1578–1581

Kazlauskas, A., Feng, G.-S., Pawson, T. and Valius, M. (1993) Proc. Natl. Acad. Sci. U.S.A **90**, 6939–6942

Keller, K., Stube, M. and Mueckler, M. (1989) J. Biol. Chem. **264**, 18884–18889

Kelly, J. D., Haldeman, B. A., Grant, F. J., Murray, M. J., Seifert, R. A., Bowen-Pope, D. F., Cooper, J. A. and Kazlauskas, A. (1991) J. Biol. Chem. **266**, 8987–8992

Kikkawa, U., Kishimoto, A. and Nishizuka, Y. (1989) Annu. Rev. Biochem. **58**, 31–44

Kitagawa, K., Nishino, H. and Iwashima, A. (1985) Biochem. Biophys. Res. Commun. **128**, 1303–1309

Kitagawa, K., Nishino, H. and Iwashima, A. (1986) Biochim. Biophys. Acta **887**, 100–104

Kitagawa, T., Tanaka, M. and Akamatsu, Y. (1989) Biochim. Biophys. Acta **980**, 100–108

Kletzien, R. F. and Perdue, J. F. (1974) J. Biol. Chem. **249**, 3366–3374

Koch, C. A., Anderson, D., Moran, M. F., Ellis, C. and Pawson, T. (1991) Science **252**, 668–674

Kolch, W., Heidecker, G., Lloyd, P. and Rapp, U. R. (1991) Nature **349**, 426–428

Korn, L. J., Siebel, C. W., McCormick, F. and Roth, R. A. (1987) Science **236**, 840–843

Kosako, H., Nishida, E. and Gotoh, Y. (1993) EMBO J. **12**, 787–794

Krupka, R. M. (1971) Biochemistry **10**, 1143–1148

Kuhné, M. R., Pawson, T., Lienhard, G. E. and Feng, G.-S. (1993) J. Biol. Chem. **268**, 11479–11481

Kypta, R. M., Goldberg, Y., Ulug, E. T. and Courtneidge, S. A. (1990) Cell **62**, 481–492

Kyriakis, J. M., App, H., Zhang, X.-f., Banerjee, P., Brautigan, D. L., Rapp, U. R. and Avruch, J. (1992) Nature **358**, 417–421

L'Allemain, G., Sturgill, T. W. and Weber, M. J. (1991) Mol. Cell. Biol. **11**, 1002–1008

Laemmli, U. K. (1970) Nature **227**, 680–685

Lai, W. S., Stumpo, D. J. and Blackshear, P. J. (1990) J. Biol. Chem. **265**, 16556–16563

Lange-Carter, C. A., Pleiman, C. M., Gardner, A. M., Blumer, K. J. and Johnson, G. L. (1993) Science **260**, 315–319

Larrodera, P., Cornet, M. E., Diaz-Meco, M. T., Lopez-Barahona, M., Diaz-Laviada, I., Guddal, P. H., Johansen, T. and Moscat, J. (1990) Cell **61**, 1113–1120

Lavan, B. E., Kuhné, M. R., Garner, C. W., Anderson, D., Reedijk, M., Pawson, T. and Lienhard, G. E. (1992) J. Biol. Chem. **267**, 11631–11636

Lavoinne, A., Erikson, E., Maller, J. L., Price, D. J., Avruch, J. and Cohen, P. (1991) Eur. J. Biochem. **199**, 723–728

Lee, C.-H., Li, W., Nishimura, R., Zhou, M., Batzer, A. G., Myers, M. G., White, M. F., Schlessinger, J. and Skolnik, E. Y. (1993) Proc. Natl. Acad. Sci. U.S.A **90**, 11713–11717

Lee, R.-m., Cobb, M. H. and Blackshear, P. J. (1992) J. Biol. Chem. **267**, 1088–1092

Leevers, S. J. and Marshall, C. J. (1992) EMBO J. **11**, 569–574

Li, J. and Tooth, P. (1987) Biochemistry **26**, 4816–4823

Li, N., Batzer, A., Daly, R., Yajnik, V., Skolnik, E., Chardin, P., Bar-Sagi, D., Margolis, B. and Schlessinger, J. (1993) Nature **363**, 85–88

Lin, L.-L., Wartmann, M., Lin, A. Y., Knopf, J. L., Seth, A. and Davis, R. J. (1993) Cell **72**, 269–278

Liscovitch, M. (1992) Trends Biochem. Sci. **17**, 393–399

Low, B. C., Ross, I. K. and Grigor, M. R. (1992) J. Biol. Chem. **267**, 20740–20745

Lowenstein, E. J., Daly, R. J., Batzer, A. G., Li, W., Margolis, B., Lammers, R., Ullrich, A., Skolnik, E. Y., Bar-Sagi, D. and Schlessinger, J. (1992) Cell **70**, 431–442

Lowry, O. H., Rosebrough, N. J., Farr, A. L. and Randall, R. J. (1951) J. Biol. Chem. **193**, 265–275

MacDonald, S. G., Crews, G. M., Wu, L., Driller, J., Clark, R., Erikson, R. L. and McCormick, F. (1993) Mol. Cell. Biol. **13**, 6615–6620

Mackall, J. C., Student, A. K., Polakis, E. and Lane, M. D. (1976) J. Biol. Chem. **251**, 6462–6464

Magnaldo, I., Pouysségur, J. and Paris, S. (1988) Biochem. J. **253**, 711–719

Maller, J. L. (1990) Biochemistry **29**, 3157–3166

Marais, R., Wynne, J. and Treisman, R. (1993) Cell **73**, 381–393

Marchmont, R. J., Ayad, S. R. and Houslay, M. D. (1981) Biochem. J. **195**, 645–652

Matsuda, S., Kosako, H., Takenaka, K., Moriyama, K., Sakai, H., Akiyama, T., Gotoh, Y. and Nishida, E. (1992) EMBO J. **11**, 973–982

Matsuda, S., Gotoh, Y. and Nishida, E. (1993) J. Biol. Chem. **268**, 3277–3281

McClain, D. A. (1990) Diabetes Care **13**, 302–316

McKenzie, F. R., Seuwen, K. and Pouysségur, J. (1992) J. Biol. Chem. **267**, 22759–22769

Meisenhelder, J., Suh, P.-G., Rhee, S. G. and Hunter, T. (1989) Cell **57**, 1109–1122

Moodie, S. A., Willumsen, B. M., Weber, M. J. and Wolfman, A. (1993) Science **260**, 1658–1661

Moolenaar, W. H., Tertoolen, L. G. J. and de Laat, S. W. (1984a) Nature **312**, 371–374

Moolenaar, W. H., Tertoolen, L. G. J. and de Laat, S., W. (1984b) J. Biol. Chem. **259**, 8066–8069

Mori, S., Rönnstrand, L., Yokote, K., Engström, Å., Courtneidge, S. A., Claesson-Welsh, L. and Heldin, C.-H. (1993) EMBO J. **12**, 2257–2264

Morrison, D. K., Kaplan, D. R., Rapp, U. and Roberts, T. M. (1988) Proc. Natl. Acad. Sci. U.S.A **85**, 8855–8859

Morrison, D. K., Heidecker, G., Rapp, U. R. and Copeland, T. D. (1993) J. Biol. Chem. **268**, 17309–17316

Mountjoy, K. G., Housey, G. M. and Flier, J. S. (1989) Mol. Endocrinol. **3**, 2018–2027

Mueckler, M., Caruso, C., Baldwin, S. A., Panico, M., Blench, I., Morris, H. R., Allard, W. J., Lienhard, G. E. and Lodish, H. F. (1985) Science **229**, 941–945

Nagamatsu, S., Kornhauser, J. M., Burant, C. F., Seino, S., Mayo, K. E. and Bell, G. I. (1992) J. Biol. Chem. **267**, 467–472

Nakajima, T., Kinoshita, S., Sasagawa, T., Sasaki, K., Naruto, M., Kishimoto, T. and Akira, S. (1993) Proc. Natl. Acad. Sci. U.S.A **90**, 2207–2211

Nakielny, S., Campbell, D. G. and Cohen, P. (1992a) FEBS Lett. **308**, 183–189

Nakielny, S., Cohen, P., Wu, J. and Sturgill, T. (1992b) EMBO J. **11**, 2123–2129

Nebreda, A. R. (1994) Trends Biochem. Sci. **19**, 1–2

Nebreda, A. R. and Hunt, T. (1993) EMBO J. **12**, 1979–1986

Nemenoff, R. A., Winitz, S., Qian, N.-X., Van Putten, V., Johnson, G. L. and Heasley, L. E. (1993) J. Biol. Chem. **268**, 1960–1964

Nguyen, T. T., Scimeca, J.-C., Filloux, C., Peraldi, P., Carpentier, J.-L. and Van Obberghen, E. (1993) J. Biol. Chem. **268**, 9803–9810

Nishida, E. and Gotoh, Y. (1993) Trends Biochem. Sci. **18**, 128–131

Nishimura, H., Pallardo, F. V., Seidner, G. A., Vannucci, S., Simpson, I. A. and Birnbaum, M. J. (1993) J. Biol. Chem. **268**, 8514–8520

Nishizuka, Y. (1984) Nature **308**, 693–698

Northwood, I. C., Gonzalez, F. A., Wartmann, M., Raden, D. L. and Davis, R. J. (1991) J. Biol. Chem. **266**, 15266–15276

Orci, L., Thorens, B., Ravazzola, M. and Lodish, H. F. (1989) Science **245**, 295–297

Pang, D. T., Sharma, B. R. and Shafer, J. A. (1985) Archives of Biochemistry and Biophysics **242**, 176–186

Pardee, A. R. (1974) Proc. Natl. Acad. Sci. U.S.A **71**, 1286–1290

Park, D. J., Min, H. K. and Rhee, S. G. (1992) J. Biol. Chem. **267**, 1496–1501

Parker, P. J., Hemmings, B. A. and Gierschik, P. (1994) Trends Biochem. Sci. **19**, 54–55

Pasti, G., Lacal, J.-C., Warren, B. S., Aaronson, S. A. and Blumberg, P. M. (1986) Nature **324**, 375–377

Paterson, A., Plevin, R. and Wakelam, M. J. O. (1991) Biochem. J. **280**, 829–830

Patton, G. M., Fasulo, J. M. and Robins, S. J. (1982) J. Lipid Res. **23**, 190–196

Pessin, M. S. and Raben, D. M. (1989) J. Biol. Chem. **264**, 8729–8738

Peterson, G. L. (1977) Anal. Biochem. **83**, 346–356

Piper, R. C., Tai, C., Slot, J. W., Hahn, C. S., Rice, C. M., Huang, H. and James, D. E. (1992) J. Cell Biol. **117**, 729–743

Piper, R. C., Tai, C., Kulesza, P., Pang, S., Warnock, D., Baenziger, J., Slot, J. W., Geuze, H. J., Puri, C. and James, D. E. (1993) J. Cell Biol. **121**, 1221–1232

Posada, J. and Cooper, J. A. (1992) Science **255**, 212–215

Posada, J., Sanghera, J., Pelech, S., Aebersold, R. and Cooper, J. A. (1991) Mol. Cell. Biol. **11**, 2517–2528

Posada, J., Yew, N., Ahn, N. G., Vande Woude, G. F. and Cooper, J. A. (1993) Mol. Cell. Biol. **13**, 2546–2553

Preiss, J., Loomis, C. R., Bishop, W. R., Stein, R., Niedel, J. E. and Bell, R. M. (1986) J. Biol. Chem. **261**, 8597–8600

Price, B. D., Morris, J. D. H. and Hall, A. (1989) Biochem. J. **264**, 509–515

Pulverer, B. J., Kyriakis, J. M., Avruch, J., Nikolakaki, E. and Woodgett, J. R. (1991) Nature **353**, 670–674

Ray, L. B. and Sturgill, T. W. (1987) Proc. Natl. Acad. Sci. U.S.A **84**, 1502–1506

Reed, B. C., Kaufmann, S. H., Mackall, J. C., Student, A. K. and Lane, M. D. (1977) Proc. Natl. Acad. Sci. U.S.A **74**, 4876–4880

Reed, S. I. (1991) Curr. Opin. Gen. Dev. **1**, 391–396

Rhee, S. G. and Choi, K. D. (1992) J. Biol. Chem. **267**, 12393–12396

Ridley, A. J. and Hall, A. (1992) Cell **70**, 389–399

Ridley, A. J., Paterson, H. F., Johnston, C. L., Diekmann, D. and Hall, A. (1992) Cell **70**, 401–410

Rohan, P. J., Davis, P., Moskaluk, C. A., Kearns, M., Krutzsch, H., Siebenlist, U. and Kelly, K. (1993) Science **259**, 1763–1767

Rollins, B. J., Morrison, E. D., Usher, P. and Flier, J. S. (1988) J. Biol. Chem. **263**, 16523–16526

Rönnstrand, L., Mori, S., Arridsson, A.-K., Eriksson, A., Wernstedt, C., Hellman, U., Claesson-Welsh, L. and Heldin, C.-H. (1992) EMBO J. **11**, 3911–3919

Rossomando, A., Wu, J., Weber, M. J. and Sturgill, T. W. (1992) Proc. Natl. Acad. Sci. U.S.A **89**, 5221–5225

Rozakis-Adcock, M., Fernley, R., Wade, J., Pawson, T. and Bowtell, D. (1993) Nature **363**, 83–85

Rozengurt, E., Rodriguez-Pena, M. and Smith, K. A. (1983) Proc. Natl. Acad. Sci. U.S.A **80**, 7244–7248

Rubin, C. S., Lai, E. and Rosen, O. M. (1977) J. Biol. Chem. **252**, 3554–3557

Rubin, C. S., Hirsch, A., Fung, C. and Rosen, O. M. (1978) J. Biol. Chem. **253**, 7570–7578

Ruderman, J. V. (1993) Curr. Opin. Cell Biol. **5**, 207–213

Ryu, S. H., Kim, U.-H., Wahl, M. I., Brown, A. B., Carpenter, G., Huang, K.-P. and Rhee, S. G. (1990) J. Biol. Chem. **265**, 17941–17945

Sagata, N., Oskarsson, M., Copeland, T., Brumbaugh, J. and Vande Woude, G. F. (1988) Nature **335**, 519–525

Sagata, N., Daar, I., Oskarsson, M., Showalter, S. D. and Vande Woude, G. F. (1989) Science **245**, 643–645

Sakai, M. and Wells, W. W. (1986) J. Biol. Chem. **261**, 10058–10062

Sastry, S. K. and Horwita, A. F. (1993) Curr. Opin. Cell Biol. **5**, 819–831

Schaller, M. D. and Parsons, J. T. (1993) Trends Cell Biol. **3**, 258–262

Secrist, J. P., Sehgal, I., Powis, G. and Abraham, R. T. (1990) J. Biol. Chem. **265**, 20394–20400

Seifert, R. A., Hart, C. E., Phillips, P. E., Forstrom, J. W., Ross, R., Murray, M. J. and Bowen-Pope, D. F. (1989) J. Biol. Chem. **264**, 8771–8778

Seino, S. and Bell, G. I. (1989) Biochem. Biophys. Res. Commun. **159**, 312–316

Seth, A., Gonzalez, F. A., Gupta, S., Raden, D. L. and Davis, R. J. (1992) J. Biol. Chem. **267**, 24796–24804

Seuwen, K., Kahan, C., Hartmann, T. and Pouysségur, J. (1990) J. Biol. Chem. **265**, 22292–22299

Shaw, G. (1993) Biochem. Biophys. Res. Commun. **195**, 1145–1151

Shepherd, P. R., Gould, G. W., Colville, C. A., McCoid, S. C., Gibbs, E. M. and Kahn, B. B. (1992) Biochem. Biophys. Res. Commun. **188**, 149–159

Shou, C., Farnsworth, C. L., Neel, B. G. and Feig, L. A. (1992) Nature **358**, 351–354

Sinnett-Smith, J., Zachary, I., Valverde, A. M. and Rozengurt, E. (1993) J. Biol. Chem. **268**, 14261–14268

Skolnik, E. Y., Lee, C.-H., Batzer, A., Vicentini, L. M., Zhou, M., Daly, R., Myers, M. J., Backer, J. M., Ullrich, A., White, M. F. and Schlessinger, J. (1993) EMBO J. **12**, 1929–1936

Slot, J. W., Geuze, H. J., Gigengack, S., James, D. E. and Lienhard, G. E. (1991a) Proc. Natl. Acad. Sci. U.S.A **88**, 7815–7819

Slot, J. W., Geuze, H. J., Gigengack, S., Lienhard, G. E. and James, D. E. (1991b) J. Cell Biol. **113**, 123–135

Smrcka, A. V., Hepler, J. R., Brown, K. O. and Sternweis, P. C. (1991) Science **251**, 804–807

Songyang, Z., Shoelson, S. E., Chaudhuri, M., Gish, G., Pawson, T., Haser, W. G., King, F., Roberts, T., Ratnofsky, S., Lechleider, R. J., Neel, B. G., Birge, R. B., Fajardo, J. E., Chou, M. M., Hanafusa, H., Schaffhausen, B. and Cantley, L. C. (1993) Cell **72**, 767–778

Spach, D. H., Nemenoff, R. A. and Blackshear, P. J. (1986) J. Biol. Chem. **261**, 12750–12753

Standaert, M. L., Mojsilovic, L., Farese, R. V. and Pollet, R. J. (1987) Endocrinology **121**, 941–947

Standaert, M. L., Farese, R. V., Cooper, D. R. and Pollet, R. J. (1988) J. Biol. Chem. **263**, 8696–8705

Standaert, M. L., Buckley, D. J., Ishizuka, T., Hoffman, J. M., Cooper, D. R., Pollet, R. J. and Farese, R. V. (1990) Metab. **39**, 1170–1179

Sternweis, P. C. and Smrcka, A. V. (1992) Trends Biochem. Sci. **17**, 502–506

Stokoe, D., Campbell, D. G., Nakielny, S., Hidaka, H., Leevers, S. J., Marshall, C. and Cohen, P. (1992a) EMBO J. **11**, 3985–3994

Stokoe, D., Engel, K., Campbell, D. G., Cohen, P. and Gaestel, M. (1992b) FEBS Lett. **313**, 307–313

Strålfors, P. (1988) Nature **335**, 554–556

Stumpo, D. J. and Blackshear, P. J. (1986) Proc. Natl. Acad. Sci. U.S.A **83**, 9453–9457

Stumpo, D. J. and Blackshear, P. J. (1991) J. Biol. Chem. **266**, 455–460

Stumpo, D. J., Graff, J. M., Albert, K. A., Greengard, P. and Blackshear, P. J. (1989) Proc. Natl. Acad. Sci. U.S.A **86**, 4012–4016

Sturgill, T. W. and Wu, J. (1991) Biochim. Biophys. Acta **1092**, 350–357

Sun, X. J., Rothenberg, P., Kahn, C. R., Backer, J. M., Araki, E., Wilden, P. A., Cahill, D. A., Goldstein, B. J. and White, M. F. (1991) Nature **352**, 73–77

Sun, X. J., Crimmins, D. L., Myers, M. G., Miralpeix, M. and White, M. F. (1993a) Mol. Cell. Biol. **13**, 7418–7428

Sun, X. J., Skolnik, E., Myers, M. G., Neel, B., Schlesinger, J. and White, M. F. (1993b) Exp. Clin. Endocrinol. **101**, 101–103

Susa, M., Vulevic, D., Lane, H. A. and Thomas, G. (1992) J. Biol. Chem. **267**, 6905–6909

Sutherland, C., Leighton, I. A. and Cohen, P. (1993) Biochem. J. **296**, 15–19

Suzuki, K. and Kono, T. (1980) Proc. Natl. Acad. Sci. U.S.A **77**, 2542–2545

Tai, P.-k. K., Liao, J.-F., Hossler, P. A., Castor, C. W. and Carter-Su, C. (1992) J. Biol. Chem. **267**, 19579–19586

Takuwa, N., Takuwa, Y., Bollag, W. E. and Rasmussen, H. (1987) J. Biol. Chem. **262**, 182–188

Takuwa, N., Takuwa, Y. and Rasmussen, H. (1988) J. Biol. Chem. **263**, 9738–9745

Tamemoto, H., Kadowaki, T., Tobe, K., Ueki, K., Izumi, T., Chatani, Y., Kohno, M., Kasuga, M., Yazaki, Y. and Akanuma, Y. (1992) J. Biol. Chem. **267**, 20293–20297

Taylor, C. W. and Marshall, I. C. B. (1992) Trends Biochem. Sci. **17**, 403–407

Taylor, L. P. and Holman, G. D. (1981) Biochim. Biophys. Acta **642**, 325–335

Thomas, G., Martin-Pérez, J., Siegmann, M. and Otto, A. M. (1982) Cell **30**, 235–242

Thomas, H. M., Takeda, J. and Gould, G. W. (1993) Biochem. J. **290**, 707–715

Thomas, S. M., DeMarco, M., D'Arcangelo, G., Halegoua, S. and Brugge, J. S. (1992) Cell **68**, 1031–1040

Thorens, B., Sarkar, H. K., Kaback, H. R. and Lodish, H. F. (1988) Cell **55**, 281–290

Todaro, G. J. and Green, H. (1963) J. Cell Biol. **17**, 299–313

Touhara, K., Inglese, J., Pitcher, J. A., Shaw, G. and Lefkowitz, R. J. (1994) J. Biol. Chem. **269**, 10217–10220

Towbin, H., Staehelin, T. and Gordon, J. (1979) Proc. Natl. Acad. Sci. U.S.A **76**, 4350–4354

Trahey, M. and McCormick, F. (1987) Science **238**, 542–545

Ullrich, A., Coussens, L., Hayflick, J. S., Dull, T. J., Gray, A., Tam, A. W., Lee, J., Yarden, Y., Libermann, T. A., Schlessinger, J., Downward, J., Mayes, E. L. V., Whittle, N., Waterfield, M. D. and Seeburg, P. H. (1984) Nature **309**, 418–425

Ullrich, A., Bell, J. R., Chen, E. Y., Herrera, R., Petruzzelli, L. M., Dull, T. J., Gray, A., Coussens, L., Liao, Y.-C., Tsubokawa, M., Mason, A., Seeburg, P. H., Grunfeld, C., Rosen, O. M. and Ramachandran, J. (1985) Nature **313**, 756–761

Ullrich, A., Gray, A., Tam, A. W., Yang-Feng, T., Tsubokawa, M., Collins, C., Henzel, W., Le Bon, T., Kathuria, S., Chen, E., Jacobs, S., Francke, U., Ramachandran, J. and Fujita-Yamaguchi, Y. (1986) EMBO J. **5**, 2503–2512

Vallus, M. and Kazlauskas, A. (1993) Cell **73**, 321–334

van Corven, E. J., Groenink, A., Jalink, K., Eichholtz, T. and Moolenaar, W. H. (1989) Cell **59**, 45–54

van Corven, E. J., Hordijk, P. L., Medema, R. H., Bos, J. L. and Moolenaar, W. H. (1993) Proc. Natl. Acad. Sci. U.S.A **90**, 1257–1261

Van Obberghen-Schilling, E., Chambard, J. C., Paris, S., L'Allemain, G. and Pouysségur, J. (1985) EMBO J. **11**, 2927–2932

Verhey, K. J. and Birnbaum, M. J. (1994) J. Biol. Chem. **269,**

Vila, M. d. C., Cooper, D. R., Davis, J. S., Standaert, M. L. and Farese, R. V. (1989) FEBS Letts **244**, 177–180

Vojtek, A. B., Hooenberg, S. M. and Cooper, J. A. (1993) Cell **74**, 205–214

Vu, T.-K. H., Hung, D. T., Wheaton, V. I. and Coughlin, S. R. (1991) Cell **64**, 1057–1068

Waddell, I. D., Zomerschoe, A. G., Voice, M. W. and Burchell, A. (1992) Biochem. J. **289**, 173–177

Wahl, M. I., Olashaw, N. E., Nishibe, S., Rhee, S. G., Pledger, W. J. and Carpenter, G. (1989) Mol. Cell. Biol. **9**, 2934–2943

Ward, Y., Gupta, S., Jensen, P., Wartmann, M., Davis, R. J. and Kelly, K. (1994) Nature **367**, 651–654

Wartmann, M. and Davis, R. J. (1994) J. Biol. Chem. **269**, 6695–6701

Watanabe, N., Hunt, T., Ikawa, Y. and Sagata, N. (1991) Nature **352**, 247–248

Waterfield, M. D., Scrace, G. T., Whittle, N., Stroobant, P., Johnsson, A., Wasteson, Å., Westermark, B., Heldin, C.-H., Huang, J. S. and Deuel, T. F. (1983) Nature **304**, 35–39

Wells, R. G., Pajor, A. M., Kanai, Y., Turk, E., Wright, E. M. and Hediger, M. A. (1992) Am. J. Physiol. **263**, F459–F465

White, M. F., Maron, R. and Kahn, C. R. (1985) Nature **318**, 183–186

White, M. F., Shoelson, S. E., Keutmann, H. and Kahn, C. R. (1988) J. Biol. Chem. **263**, 2969–2980

Wilden, P. A., Backer, J. M., Kahn, C. R., Cahill, D. A., Schroeder, G. J. and White, M. F. (1990) Proc. Natl. Acad. Sci. U.S.A **87**, 3358–3362

Wilkinson, S. E., Parker, P. J. and Nixon, J. S. (1993) Biochem. J. **294**, 335–337

Williams, S. A. and Birnbaum, M. J. (1988) J. Biol. Chem. **263**, 19513–19518

Winitz, S., Russell, M., Qian, N.-X., Gardner, A., Dwyer, L. and Johnson, G. L. (1993) J. Biol. Chem. **268**, 19196–19199

Wolfman, A., Wingrove, T. G., Blackshear, P. J. and Macara, I. G. (1987) J. Biol. Chem. **262**, 16546–16552

Wood, K. W., Sarnecki, C., Roberts, T., M. and Blenis, J. (1992) Cell **68**, 1041–1050

Wright, T. M., Rangan, L. A., Shin, H. S. and Raben, D. M. (1988) J. Biol. Chem. **263**, 9374–9380

Wu, J., Rossomando, A. J., Horng-Her, J., Weber, M. J. and Sturgill, T. W. (1992) Biochem. Soc. Trans. **20**, 675–677

Yang, J. and Holman, G. D. (1993) J. Biol. Chem. **268**, 4600–4603

Yang, J., Clark, A. E., Kozka, I. J., Cushman, S. W. and Holman, G. D. (1992) J. Biol. Chem. **267**, 10393–10399

Yarden, Y., Escobedo, J. A., Kuang, W.-J., Yang-Feng, T. L., Daniel, T. O., Tremble, P. M., Chen, E. Y., Ando, M. E., Harkins, R. N., Francke, U., Fried, V. A., Ullrich, A. and Williams, L. T. (1986) Nature **323**, 226–232

Yew, N., Mellini, M. L. and Vande Woude, G. F. (1992) Nature **355**, 649–652

Yu, K.-T., Khalaf, N. and Czech, M. P. (1987) J. Biol. Chem. **262**, 7865–7873

Zachary, I. and Rozengurt, E. (1992) Cell **71**, 891–894

Zhan, X., Hu, X., Friesel, R. and Maciag, T. (1993) J. Biol. Chem. **268**, 9611–9620

Zhang, X.-f., Settleman, J., Kyriakis, J. M., Takeuchi-Suzuki, E., Elledge, S. J., Marshall, M. S., Bruder, J. T., Rapp, U. R. and Avruch, J. (1993) Nature **364**, 308–313

Zheng, C.-F. and Guan, K.-L. (1993) J. Biol. Chem. **268**, 11435–11439

Zorzano, A., Wilkinson, W., Kotliar, N., Thoidis, G., Wadzinkski, B. E., Ruoho, A. E. and Pilch, P. F. (1989) J. Biol. Chem. **264**, 12358–12363